Quantitative Three-dimensional Echocardiography

Kwantitatieve driedimensionale echocardiografie

Boudewijn J. Krenning

Quantitative Three-dimensional Echocardiography

Kwantitatieve driedimensionale echocardiografie

Proefschrift

ter verkrijging van de graad van doctor aan de
Erasmus Universiteit Rotterdam
op gezag van de
rector magnificus

Prof.dr. S.W.J. Lamberts

en volgens besluit van het College voor Promoties.
De openbare verdediging zal plaatsvinden op
woensdag 28 november 2007 om 9.45 uur

door

Boudewijn Jurriaan Krenning

geboren te Rotterdam

ERASMUS UNIVERSITEIT ROTTERDAM

Promotiecommissie

Promotoren: Prof.dr. J.R.T.C. Roelandt
Prof.dr.ir. A.F.W. van der Steen

Overige leden: Prof.dr.ir. N. Bom
Prof.dr.ir. N. de Jong
Dr. O. Kamp

Copromotor: Dr. M.L. Geleijnse

Contents

Chapter 1

Introduction

Echocardiography is the most important non-invasive diagnostic tool for the clinical management of cardiac patients[1]. Measurement of left ventricular volume and function are the most common clinical referral questions to the echocardiography laboratory because of its value in clinical decision-making, assessment of therapeutic effects and determination of prognosis. Therefore, an accurate, fast and easy measurement of left ventricular volume and function is important. Two-dimensional echocardiography remains the most widely used method, but the advantages of three-dimensional echocardiography over two-dimensional echocardiography are increasingly recognised. Using two-dimensional echocardiography, only a limited number of cross-sections of the heart are available for analysis, while three-dimensional echocardiography allows reconstruction or real-time acquisition of a single dataset encompassing the complete heart. From this dataset an indefinite number of cross-sections and viewing planes can be analyzed, avoiding the geometric assumptions of left ventricular shape and the foreshortened image acquisition of the left ventricular cavity.

Over the years, several methods for acquisition of three-dimensional echocardiographic data have been used (Table). In the 1990's, dynamic three-dimensional echocardiographic images were created from a number of individual two-dimensional cross-sections of the heart, which were acquired using either an external (e.g. freehand scanning device) or internal reference system (e.g. a rotational system, in which the transducer is rotated stepwise or continuously around its central axis). All recorded cross-sections were then reconstructed into a volume dataset. Disadvantages were long acquisition and reconstruction times, motion artefacts (from patient breathing and transducer movement by examiner), and large gaps between image planes resulting in interpolation errors. Researchers at the Erasmus University developed a fast-rotating ultrasound transducer, which enables the acquisition of a full three-dimensional dataset of the heart in 10 seconds. Unlike

Table. Approaches for three-dimensional echocardiography

A. Reconstruction techniques
External reference system / non-systematic image acquisition
• Mechanical arm[8, 9]
• Acoustic (spark gap) locator[10]
• Optical or electromagnetic sensor[11, 12]
Internal reference system / systematic image acquisition
• Linear transducer motion[13]
• Fan-like transducer motion[14]
• Stepwise[15, 16] or continuous rotational transducer motion[17, 18]
B. Real-time volumetric techniques[2]

Adapted from: Three-dimensional echocardiography of the heart and coronary arteries (Editor: JRTC Roelandt)

other mechanical acquisition systems, which can only collect images over a limited number of rotations, this transducer acquires images over as many rotations as required. The size of the transducer is slightly larger than a standard transducer for two-dimensional echocardiography. Major advantages of this system are a short acquisition time and availability of all two-dimensional echocardiographic imaging techniques, such as second harmonic imaging.

A further development was real-time three-dimensional echocardiography, which is based on the matrix-transducer technology and first introduced by von Ramm et al. at Dukes (it is Duke and not Dukes) University[2]. This method is based on a two-dimensional grid of miniature ultrasound elements, which acquire a three-dimensional pyramidal dataset in real-time, without the need for off-line reconstruction. These systems are currently the standard for three-dimensional echocardiographic examinations. The impressive evolution of dynamic three-dimensional echocardiography in the past 17 years is illustrated by the number of world-wide PubMed publications on this topic (Figure). A increase of its applications can be expected with further technical improvements. Currently, software developments for data analysis increase the clinical applicability, including (semi-)automatic analysis of the left ventricular endocardial contour.
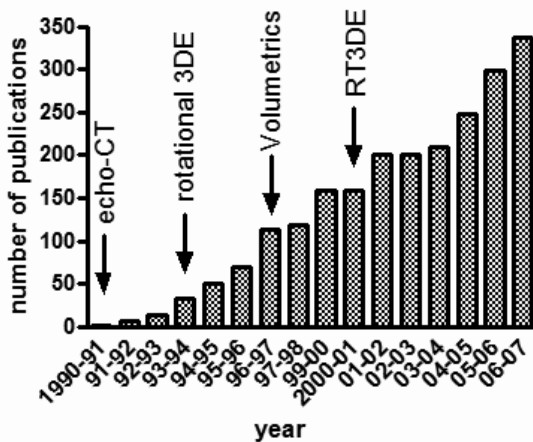
Figure 1. Annual number of publications in PubMed on three-dimensional echocardiography.

The aim of the first part of the thesis was to evaluate the feasibility and clinical applicability of the fast-rotating ultrasound transducer. For determination of left ventricular function, the fast-rotating transducer may be an excellent tool for rapid evaluation, without the necessity of an expensive high-end ultrasound system with multiple and complex applications.

Chapter two focuses on the technical details of the fast-rotating ultrasound transducer.

Chapter three describes a validation study using the fast-rotating ultrasound transducer, for analysis of left ventricular function with magnetic resonance imaging as the reference technique.

In *chapter four,* we evaluate the clinical applicability of the fast-rotating ultrasound transducer in patients undergoing hemodialysis. These patients have rapid changes in volume load of the heart and three-dimensional echocardiography may potentially improve accuracy for serial measurements of left ventricular performance, compared to two-dimensional echocardiography.

Cardiac resynchronization therapy is an additional treatment for selected patients with severe heart failure and ventricular dyssynchrony. When used in combination with optimal medical therapy, it has shown to reduce symptoms and improve cardiac function by restoring the mechanical sequence of ventricular activation and contraction. In *chapter five*, the feasibility of the fast-rotating transducer is evaluated for the determination of dyssynchrony in heart failure patient, including determination of the best pacing site for resynchronization therapy.

Part two of the thesis concerns the analysis of left ventricular function using three-dimensional echocardiography.

Numerous studies[3, 4] have focused on the advantages and improved accuracy of three-dimensional echocardiography over two-dimensional imaging for measurement of left ventricular volume and function by obviating geometric assumptions.

In *chapter six*, an overview of methods for acquisition of three-dimensional echocardiographic images is shown, including earlier studies on left ventricular volume and function assessment with three-dimensional echocardiography.

Several online and off-line analytic software programs for left ventricular volume quantification by real-time three-dimensional echocardiography are available, which use a wide spectrum of endocardial contour tracing algorithms, ranging from manual to fully automated algorithms. *Chapter seven* shows a comparison in accuracy between two different computer algorithms for calculation of left ventricular volume and function. The first algorithm determines a geometric model for the left ventricle through manual definition of the mitral annulus, aortic valve and apex, after which semi-automated border detection is performed in a limited number of cross-sections. In contrast, the second more recent algorithm performs semi-automated contour detection in the complete dynamic three-dimensional dataset ('full volume reconstruction'). Thus, significantly more data is used to determine the endocardial cavity contour for left ventricular reconstruction.

Ultrasound contrast, consisting of gasfilled microbubbles, is used for improvement of endocardial border definition by enhancement of ultrasound backscatter of the bloodpool compared to the surrounding myocardium. A higher accuracy for assessment of left ventricular function has been shown in two-dimensional echocar-

diography, particularly in patients with a suboptimal acoustic window. In *chapter eight* we evaluate whether the use of contrast enhancement improves accuracy of left ventricular function analysis by real-time three-dimensional echocardiography.

In part three of the thesis, the current status of three-dimensional stress echocardiography is described. Two-dimensional dobutamine stress echocardiography is a well-established method for the diagnosis and of prognostic value in patients with suspected coronary artery disease[5]. *Chapter nine* and *ten* present an overview of diagnostic dobutamine stress echocardiography studies and a methodological analysis to explain the wide range in diagnostic variability of dobutamine stress echocardiography.

In several recent publications the advantages of real-time three-dimensional echocardiography[6, 7] are described. The faster acquisition time and low operator dependency improve the diagnostic accuracy. The results of these studies are described in a review article on real-time three-dimensional dobutamine stress echocardiography in *chapter 11*.

However, some critical remarks are appropriate, particularly with respect to the current technical limitations of three-dimensional echocardiography. These are described in *chapter 12*. Finally, we performed two studies to assess the value of ultrasound contrast during real-time three-dimensional stress echocardiography. The study presented in *chapter 13* was performed to examine the role of ultrasound contrast for the improvement of segmental image quality and inter-observer agreement of wall motion analysis during real-time three-dimensional stress echocardiography. In *chapter 14*, we evaluate the diagnostic accuracy of contrast enhanced real-time three-dimensional stress echocardiography for the diagnosis of coronary artery disease in comparison with coronary arteriography findings as a reference.

References

1. Roelandt JRTC, Erbel R. Cardiac Ultrasound. In: Camm AJ, Luscher TH, Serruys PW, editors. The ESC textbook of cardiovascular medicine. Oxford: Blackwell Publishing Ltd.; 2006. p. 37-93.

2. von Ramm OT, Smith SW. Real time volumetric ultrasound imaging system. J Digit Imaging 1990;3(4):261-6.

3. Jenkins C, Chan J, Hanekom L, Marwick TH. Accuracy and feasibility of online 3-dimensional echocardiography for measurement of left ventricular parameters. J Am Soc Echocardiogr 2006;19(9):1119-28.

4. Nosir YF, Lequin MH, Kasprzak JD, van Domburg RT, Vletter WB, Yao J, et al. Measurements and day-to-day variabilities of left ventricular volumes and ejection fraction by three-dimensional echocardiography and comparison with magnetic resonance imaging. Am J Cardiol 1998;82(2):209-14.

5. Geleijnse ML, Fioretti PM, Roelandt JR. Methodology, feasibility, safety and diagnostic accuracy of dobutamine stress echocardiography. J Am Coll Cardiol 1997;30(3):595-606.

6. Aggeli C, Giannopoulos G, Misovoulos P, Roussakis G, Christoforatou E, Kokkinakis C, et al. Real-time three-dimensional dobutamine stress echocardiography for coronary artery disease diagnosis - validation with coronary angiography. Heart 2006.

7. Matsumura Y, Hozumi T, Arai K, Sugioka K, Ujino K, Takemoto Y, et al. Non-invasive assessment of myocardial ischaemia using new real-time three-dimensional dobutamine stress echocardiography: comparison with conventional two-dimensional methods. Eur Heart J 2005;26(16):1625-32.

8. Dekker DL, Piziali RL, Dong E, Jr. A system for ultrasonically imaging the human heart in three dimensions. Comput Biomed Res 1974;7(6):544-53.

9. Sawada H, Fujii J, Aizawa T, Kato K, Onoe M, Kuno Y, et al. [Three dimensional reconstruction of the human left ventricle from multiple cross-sectional echocardiograms: comparison with biplane cineventriculography using Simpson's rule]. J Cardiogr 1985;15(2):439-47.

10. King DL, King DL, Jr., Shao MY. Three-dimensional spatial registration and interactive display of position and orientation of real-time ultrasound images. J Ultrasound Med 1990;9(9):525-32.

11. Moritz W, Shreve P. Magnetic position and orientation tracking system. IEEE Trans Aerospace Elec Sys 1979;AES-15:709-18.

12. Legget ME, Leotta DF, Bolson EL, McDonald JA, Martin RW, Li XN, et al. System for quantitative three-dimensional echocardiography of the left ventricle based on a magnetic-field position and orientation sensing system. IEEE Trans Biomed Eng 1998;45(4):494-504.

13. Wollschlager H, Zeiher AM, Klein HP, Kasper W, Wollschlager S, Geibel A, et al. [Transesophageal echo computer tomography (ECHO-CT): a new method of dynamic 3-D reconstruction of the heart]. Biomed Tech (Berl) 1989;34 Suppl:10-1.

14. Kuroda T, Kinter TM, Seward JB, Yanagi H, Greenleaf JF. Accuracy of three-dimensional volume measurement using biplane transesophageal echocardiographic probe: in vitro experiment. J Am Soc Echocardiogr 1991;4(5):475-84.

15. Roelandt JR, ten Cate FJ, Vletter WB, Taams MA. Ultrasonic dynamic three-dimensional visualization of the heart with a multiplane transesophageal imaging transducer. J Am Soc Echocardiogr 1994;7(3 Pt 1):217-29.

16. Buck T, Schon F, Baumgart D, Leischik R, Schappert T, Kupferwasser I, et al. Tomographic left ventricular volume determination in the presence of aneurysm by three-dimensional echocardiographic imaging. I: Asymmetric model hearts. J Am Soc Echocardiogr 1996;9(4):488-500.

17. Djoa KK, de Jong N, van Egmond FC, Kasprzak JD, Vletter WB, Lancee CT, et al. A fast rotating scanning unit for real-time three-dimensional echo data acquisition. Ultrasound Med Biol 2000;26(5):863-9.

18. Voormolen MM, Krenning BJ, Lancee CT, ten Cate FJ, Roelandt JR, van der Steen AF, et al. Harmonic 3-D echocardiography with a fast-rotating ultrasound transducer. IEEE Trans Ultrason Ferroelectr Freq Control 2006;53(10):1739-48.

Chapter 2

Harmonic 3D echocardiography with a fast rotating ultrasound transducer

MM Voormolen
BJ Krenning
CT Lancee
FJ ten Cate
JRTC Roelandt
AFW van der Steen
N de Jong

Abstract

Although the advantages of three-dimensional (3-D) echocardiography have been acknowledged, its application for routine diagnosis is still very limited. This is mainly due to the relatively long acquisition time. Only recently has this problem been addressed with the introduction of new real-time 3-D echo systems. This paper describes the design, characteristics, and capabilities of an alternative concept for rapid 3-D echocardiographic recordings. The presented fast-rotating ultrasound (FRU)-transducer is based on a 64-element phased array that rotates with a maximum speed of 8 Hz (480 rpm). The large bandwidth of the FRU-transducer makes it highly suitable for tissue and contrast harmonic imaging. The transducer presents itself as a conventional phased-array transducer; therefore, it is easily implemented on existing 2-D echo systems, without additional interfacing. The capabilities of the FRU-transducer are illustrated with in-vitro volume measurements, harmonic imaging in combination with a contrast agent, and a preliminary clinical study.

Introduction

Over the last 20 years the application of threedimensional (3-D) echocadiography has been explored extensively. The reconstruction of unconventional 2-D views from a 3-D dataset has been seen as a welcome addition to the possibilities of echocardiography[1]. Also, the examination of volume-rendered 3-D recordings, the socalled surgical view, has proven very useful for the preparation of surgical interventions [2]. In addition, many studies have validated the increased accuracy obtained with the quantification of cardiac structures from 3-D data as compared to 2-D data[3].

In spite of its advantages, 3-D echocardiography is still mainly used for research purposes. Most 3-D echocardiographic techniques developed in the past are based on the stepwise displacement of a phased array[4–6].With these techniques, only one position is covered during a cardiac cycle. The subsequent cycle then is used to move to the next location. This relatively slow process prolongs the acquisition time beyond the feasible duration of a single breath hold, which in turn calls for respiratory and electrocardiogram (ECG) gating. For a densely sampled 3-D recording, the process described above requires an acquisition time of several minutes. The recordings often suffer from motion artefacts as a result of the lengthy acquisition time. Although the acquisition of a 3-D dataset does not consume more time than alternative techniques, such as magnetic resonance imaging (MRI), it is still considered a drawback. As long as standard 2-D examinations are performed in the same amount of time as a single 3-D recording, it will not likely be widely accepted in daily clinical practice.

Real-time 3-D echocardiography solves the problem of lengthy acquisition times; however, first-generation realtime 3-D echo systems suffered from insufficient image quality[7]. The recently introduced second-generation systems from Philips (Eindhoven, The Netherlands) and General Electric (Milwaukee, WI) possess an improved image quality. These commercially available systems have resulted in the increased use of 3-D echocardiography for routine diagnosis[8].

State-of-the-art 2-D echo systems cover two spatial dimensions and time with sufficient spatial and temporal resolution. Therefore, the key to fast acquisition of a 3-D dataset is an effective coverage of the third spatial dimension. With stepwise, displaced phased arrays, more frames are discarded during motion and gating than used for the actual 3-D dataset. However, a phased array moved in a continuous, uniform motion would be able to make use of the full frame rate. This paper describes the design, characteristics, and capabilities of a continuous, rotating, phased-array transducer intended for rapid 3-D echocardiographic recordings.

Materials and Methods

In the first part of this paper, the transducer's design and its consequences for the acquisition morphology will be described. The rotation speed of the transducer is not stored with the echo data but is extracted from it. The technique to recover the rotation speed from the data is explained in a subsequent section. The process needed for the reconstruction and quantification of a scanned volume will be discussed. The optimization of the rotation speed for the clinical setting is described.

The Fast-Rotating Ultrasound Transducer

The fast-rotating ultrasound (FRU)-transducer consists of three major parts: a high precision drive, a slip-ring device, and a phased array. Fig. 1 shows the latest prototype of the transducer[9]. Key features of the transducer are its wide bandwidth, allowing harmonic imaging, and its ergonomic design (width: 53 mm, height: 33 mm, length: 147 mm, and weight: 350 g).

The drive of the transducer consists of a direct current (DC) motor, a gear, an encoder, and a controller (see Fig. 1). The DC motor, gear, and chain wheel trans-

Figure. 1. The latest prototype of the fast-rotating ultrasound (FRU)-transducer. The upper panel shows the construction of the transducer with some key components annotated. The lower panel shows the transducer with its housing. Note the LEDs on the housing, which are used to indicate whether the phased array is located in one of its two fixed positions (0° and 90°).

mission combination produce a maximum torque of 85 mNm, which is well above the torque required to drive the slipring and the array. The encoder and controller provide a feedback regulation for a highly constant rotation speed, which can be controlled manually. For the acquisition of a 3-D dataset, the rotation speed is set between 4 and 8 Hz (240 and 480 rpm). In addition, the array can be positioned at two fixed stationary and perpendicular angles (0° and 90°) that are indicated with LED's on the housing of the transducer (see Fig. 1). Using a footswitch, these positions can be alternated for alignment of the transducer prior to the acquisition of a 3-D dataset (e.g., by checking the four and two chamber views before a left ventricular acquisition).

The slip-ring device is custom made (Kaydon, Reading, Berkshire, UK) and contains 82 contacts, of which 64 are used for the array elements and 16 as distributed signal ground. No measurable noise generation from the slip-ring device could be detected within the frequency range used for imaging.
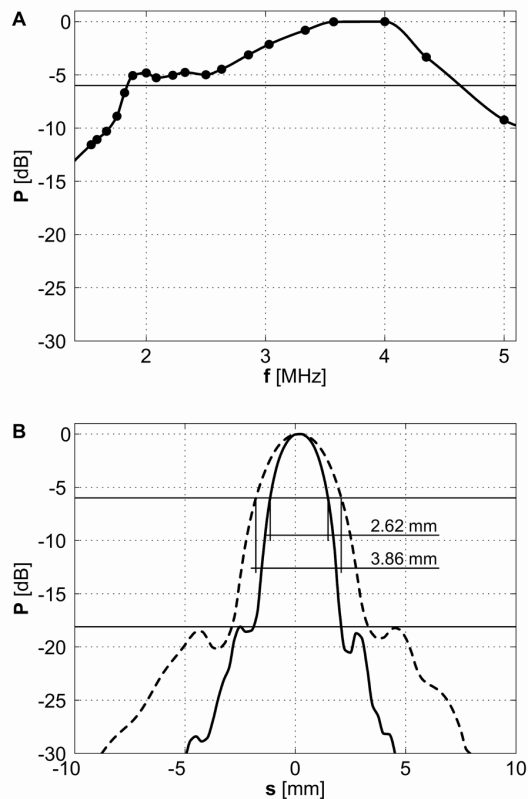
Figure. 2. Panel A shows a normalized fundamental (dashed line) and harmonic (solid line) beam profiles in lateral direction for an excitation frequency of 1.8 MHz, a pulse length of 2.5 cycles, and a nonderated mechanical index (MI) of 1.7 MI. Panel B shows the transmit sensitivity of the transducer.

The transducer's array, custom made by Delft Instruments, Delft, The Netherlands, contains 64 elements with a pitch of 0.21 mm and is tapered into an octagonal shape, approximating a circle with a radius of 7 mm. It has a fractional bandwidth of 86% with a center frequency of 3.2 MHz (see Fig. 2(A)). The fixed focus of the acoustic lens in the elevation direction is set at 60 mm. Fig. 2(B) gives the lateral transmit beam profiles at the focal distance for an excitation frequency of 1.8 MHz and a pulse length of 2.5 cycles. At –6 dB a fundamental beam width of 3.86 mm and a harmonic beam width of 2.62 mm were found. The side lobe levels of both the fundamental and harmonic profile were equal to –18.1 dB.

The transducer is connected to a General Electric/ VingMed (Horten, Norway) Vivid 5 system like a conventional phased array, but it could be used with any scanner as no additional interfacing is required.

Morphology of the Acquisition

The typical acquisition time for a full 3-D dataset is approximately 10 seconds, which allows for a dataset to be recorded within a single breath hold. With a standard frame rate of about 100 frames per second (fps), a typical dataset consists of approximately 1000 harmonic B-mode images. The frames are first stored in the scanner and later transferred to a computer for processing. The ECG signal is stored with the frames. No ECG gating is used, and exclusion of irregular cardiac cycles is carried out after the acquisition.

The continuous rotation of the array results in nonuniformly sampled 4-D datasets (three spatial dimensions and time). First, the individual frames of the recording have a curved morphology in space, as shown in Fig. 3(A). Second, the frames will sample the volume in an interleaved manner. This is most clearly illustrated in the spherical coordinate system, which is the native coordinate system of the acquisition (see Fig. 3(B)). In the spherical coordinate system, the frames are divided into halves by the imaging (or rotation) axis of the transducer. By definition, this is a consequence of the limited range of the elevation angle ($-1/2\pi$ to $1/2\pi$ rad), which represents the steering angle of the individual ultrasonic beams in the spherical domain. When a frame is acquired from right to left, the steering angle from the right half of the frame will run down. However, for the beams of the left half, the steering angle will run up. This results in inclined and intersecting rows of ultrasonic beams from the two frame halves (see Fig. 3(D)). The intersecting nature of the frame halves also can be observed in the cartesian coordinate system, but less clearly due to the curvature of the frames (see Fig. 3(C)).

From Fig. 3(C), it also can be seen that the sample density increases toward the rotation axis. The uniformity of the sampling could be improved by optimizing the scanning in the 2-D sector. In the cartesian coordinate system, which is used for visualization, there is no uniform sampling along any axis (see Fig. 3(C)). For volume rendered reviewing of recorded datasets, the data, therefore, are interpolated with

the use of a uniform cartesian grid. Reconstruction can, of course, be performed only with the availability of an accurately determined rotation speed.
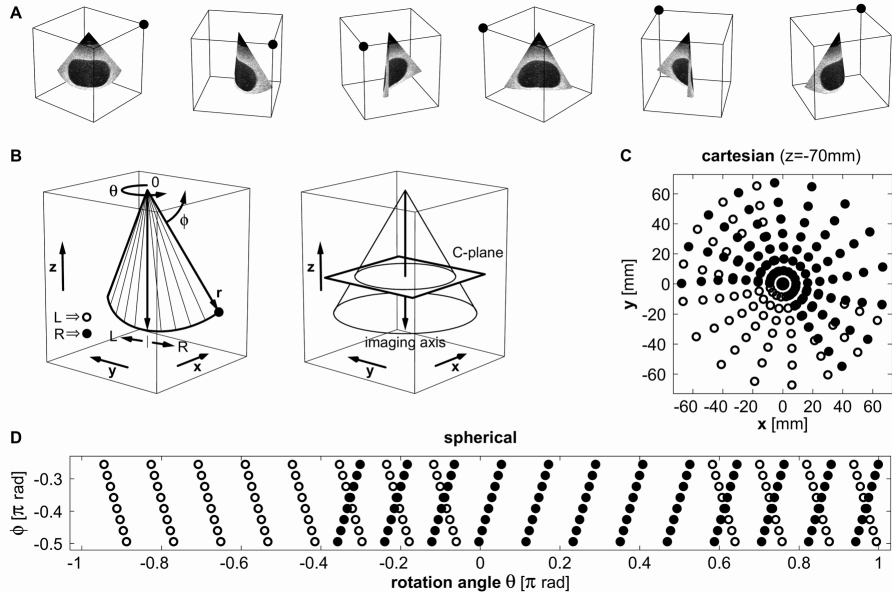
Figure. 3. Panel A shows a typical 2-D image recorded with the FRU-transducer from a cavity phantom in perspective. The consecutive frames repeat the same image, but each time rotated 60 clockwise. The sequence gives a good appreciation of the curved shape of the frame. The first part of panel B shows a curved frame and its relation to the spherical and cartesian coordinate system. The second part depicts the conical shape of the volume sampled by the FRU-transducer and the position of a C-plane. In addition, panel B shows how a frame is divided by the imaging axis into a left and a right half, indicated with *L* and *R*. Panel C shows the position of the ultrasonic beams from a number of frames in the cartesian coordinate system. Beams from the left half of the frames are indicated with an open dot and those from the right half with a closed dot (see also panel B). Panel D shows the more orderly position of the same beams in the spherical coordinate system.

Determination of the Rotation Speed

To avoid additional interfacing between the echo system and the transducer, the rotation speed is extracted from the recorded harmonic B-mode data in two steps. A first estimate of the rotation speed is obtained by correlating all frames of the dataset with an arbitrary reference frame from the same dataset. The correlation value is calculated as the sum of absolute difference between the frames. An example of the resulting correlation signal is shown in Fig. 4(A). The correlation result reveals a periodic signal with a periodicity related to the rotation speed. Fourier analysis of the correlation signal gives the first estimate of the rotation speed.

The accuracy of the first estimate of the rotation speed is limited to approximately 10 MHz due to noise and the interference of cardiac motion. To improve this
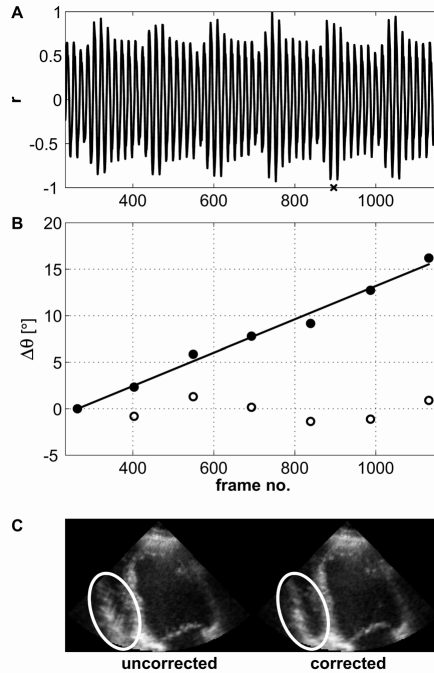
Figure. 4. Panel A shows an example of a normalized frame-to-frame correlation signal *r* with the reference frame indicated by the cross on the x-axis. The value at the reference frame is a linear interpolation of the values of its neighboring frames and, therefore, is not equal to 1. Approximately 50 rotations are shown for a recording that was made with a frame rate of 106.1 fps. An example of the second order rotation speed estimation is shown in panel B. The regression (solid line) of the angular errors $\triangle$ calculated (solid dots) resulted in a rotation speed correction of 5.3 MHz. The residual angular error after correction of the rotation speed also is shown (open dots). Panel C shows two reconstructed long axis images of the left ventricular acquisition in question. For the image on the right, the second order rotation speed correction was used, but the left image did not use the second order correction. The circled area of the image on the left clearly shows the artefacts resulting from inaccuracies in the rotation speed used.

accuracy, the rotation speed is corrected in a second step. Enddiastolic C-planes are reconstructed from each recorded cardiac cycle. The C-plane of the first cardiac cycle is used as a reference for correlation with the C-planes of subsequent cycles. By maximizing the correlation between the planes, by rotating them around the rotation axis, the angular correction for each C-plane can be found. Fig. 4(B) gives an example of the result from a C-plane correlation.

The correlation result of the C-planes shows a linear increase of the angular error due to the insufficient accuracy of the first rotation speed estimation. Using the regression of the C-plane correlation, the accuracy of the rotation speed can be increased an order of a magnitude beyond the first estimate. Typically, the residual angular error after the second order rotation speed estimation is not larger than a

few degrees (see Fig. 4(B)), which is only a fraction of the optimal angular resolution (see also Appendix A). Fig. 4(C) gives an example of the artefacts resulting from in-accuracies in the first estimate of the rotation speed. As can be seen from Fig. 4(C), the artefacts are resolved when the second order estimate is used.

Reconstruction

Following the determination of an accurate rotation speed, 4-D datasets can be constructed from the recorded frames. Datasets constructed from an acquisition of one cardiac cycle result in a sparse sampling of the time-volume space. To obtain a denser sampling of the time-volume space, a number of cardiac cycles are fused, which is also referred to as multibeat fusion.

Although the multibeat fusion results in a densely sampled 4-D dataset of the scanned volume, the dataset still has a nonuniform structure. A suitable interpola-tion technique is used to resample the data into a uniformly spaced cartesian grid.

Fig. 5 gives an example of the above techniques. The improved image quality obtained with the use of multibeat fusion is clearly depicted in Fig. 5.
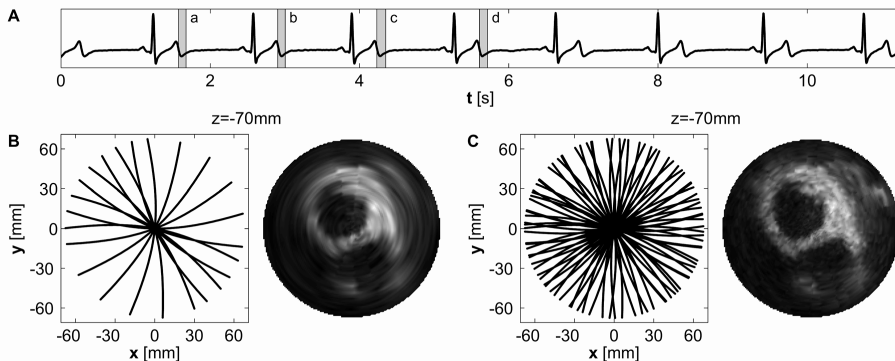
Figure. 5. In panel A the time intervals of four corresponding cardiac segments are indicated when each cardiac cycle is divided into 12 segments of equal width. If only segment *a* is used for reconstruction, a sparse sampling of the volume is obtained. Panel B depicts both the sampling of the rotation angle and the reconstruction of the corresponding C-plane for this case (*z* is the axial direction of the transducer; see also Figure. 3). The individual frames recorded within the time interval of the segment are indicated with solid lines. Panel C shows the same results when all four segments are used. The denser sampling of the volume and the improved resolution of reconstructed images clearly can be appreciated.

Optimization of the Rotation Speed

For successful reconstruction, the acquired frames should be distributed adequately over the rotation angle. This distribution depends, in the first place, on the rotation speed and the frame rate. With the use of multibeat fusion, the distribution also is dependent on the heart rate and the number of cardiac segments (i.e., the number

of time intervals in which the cardiac cycle is subdivided, typically 16). For a recording of a stationary volume with an arbitrary rotation speed, the minimum sampling interval of the rotation angle is the angle between two consecutive frames. For a cardiac recording, even this minimal resolution is not assured. It is not even unlikely that the frames from the cardiac segments used will end up in the same quadrant of the rotation angle. To prevent this from happening, an optimized rotation speed needs to be used for a given frame rate, heart rate, and number of cardiac segments. Appendix A gives the details of the calculation of such an optimized rotation speed. The calculation is based on the use of a candidate rotation frequency in which the continuity of the frame distribution over the rotation angle is assured. By correcting this candidate rotation speed toward an equiangular distribution, an optimized rotation speed is obtained. Table I gives a number of examples of the calculation for some randomly selected clinical settings.

Table 1. Randomly Selected Examples of the Rotation Frequency Calculations.

heart rate [bpm]	f_{Frame} [Hz]	$f_{Candidate}$ [Hz]	$N_{Rotation}$	$f_{Rotation}$ [Hz]	Resolution (°)	deviation (%)
47	98.7	6.6894	3	6.6920	8.18	6.4
51	98.7	7.2417	3	7.2402	8.78	3.2
64	93.4	5.6266	3	5.6252	7.20	4.1
73	104.8	6.4677	3	6.4644	7.35	7.0
81	104.8	5.7412	3	5.7394	6.54	4.6
89	104.8	6.2554	3	6.2572	7.20	2.9
97	106.1	5.1319	3	5.1319	5.81	2.0
104	106.1	7.4427	4	7.4427	6.32	1.8
120	93.4	6.3683	3	6.3683	8.18	1.4
142	104.8	7.6666	4	7.6634	6.55	3.5

Heart rates are from a wide range, commonly used frame rates and an intended reconstruction with 16 cardiac segments. The angular position of the first ultrasonic beam from each frame is defined as the angular position of the frame itself. The deviation then is specified as the standard deviation of the difference between the maximum resolution and the achieved inter-frame resolution. The mean difference between the maximum resolution and the achieved resolution always will be zero with a given number of frames and, therefore, is not included.

Quantification

Quantification tools are based on manual or semiautomatic tracing of an anatomical feature in a stack of 2-D images. This is necessary due to the fact that currently there are no fully automatic quantification algorithms available. In addition, computers are equipped with 2-D monitors that essentially can be used only to view two spatial dimensions plus time. Therefore, the recorded 4-D dataset needs to be resliced in order to obtain the 2-D image set required by the selected quantification

tool. In the case of left ventricular (LV) volume measurement this could mean a set of long and/or short axis images.

Results

The capabilities of the FRU-transducer are illustrated in three examples: in-vitro volume measurements, harmonic imaging in combination with contrast, and a preliminary clinical study.

In-Vitro Evaluation

Two geometrical agar units were made with cavities in the shape of a sphere and a beam. Each unit consisted of two halves. From the units, five different phantoms were constructed: a sphere, a beam, half a sphere, half a beam and a mixed combination of half a sphere and half a beam (or "mushroom"). Another agar phantom was made that had a LV shape.

Recordings of the phantoms were made with a rotation speed of 6 Hz (360 rpm) and a frame rate of 67.5 fps. One to two seconds of each recording were used to reconstruct the phantoms. After reconstruction, the phantom cavities were extracted with an advanced threshold-based method. For this method, depth dependent bimodal histogram thresholding, a closing procedure with a diamond structuring element of size three and volume extraction using a connectivity of six were used[10]. The extracted volumes were compared with the actual volume of the phantom cavity.

The result of one of the agar phantom reconstructions is depicted in Fig. 6. The reconstructions of the six different phantoms showed an average volume error of approximately 1% (see Table II).

Table 2. Results of the In-Vitro Volume Measurement Evaluation.

phantom	volume (ml)		deviation (%)
	actual	reconstructed	
sphere	135.5	136.9	1.0
beam	133	131.5	1.1
½ sphere	68.5	67.6	1.3
½ beam	63	62.5	0.7
'mushroom'	131.5	132	0.4
LV	131	128.7	1.8

Contrast Harmonic Imaging

A commercially available tissue mimicking flow phantom (Model 524, ATS Laboratories Inc., Bridgeport, CT) was used to explore the harmonic capabilities of the FRUtransducer in combination with the use of contrast agents. Backscatter power
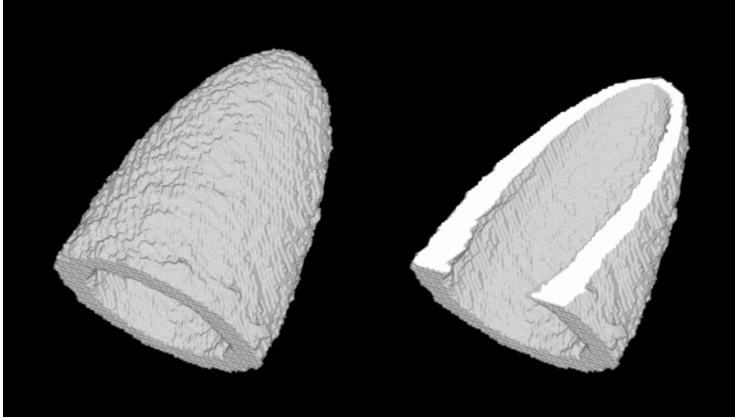
Figure. 6. Rendered reconstruction of the LV-shaped agar phantom.

spectra from a tissue and a contrast region of interest (ROI) were calculated from recorded radio frequency data. The spectra and the extracted contrast to tissue ratio from these spectra were used to determine the efficacy of harmonic imaging over fundamental imaging[11].

The contrast to tissue ratio (CTR) was defined as the ratio of the scattered power caused by the contrast to that of the tissue. The contrast and tissue ROI were selected as shown in Fig. 7(A). Optison contrast agent (Amersham Health, Princeton, NJ) was used at a dilution of 1 over 2000 in Isoton II (Beckman Coulter, Fullerton, CA) and was flowing at a constant rate of 90 ml/minute through the phantom. The ROI's were insonified with a pulse comprising a derated peak negative pressure of 150 kPa, a transmit frequency of 1.74 MHz, and a pulse length of 2.5 cycles. With these settings, an increase of more than 8 dB in the CTR was found at the second harmonic compared to the fundamental frequency (see Figs. 7(B) and (C)).
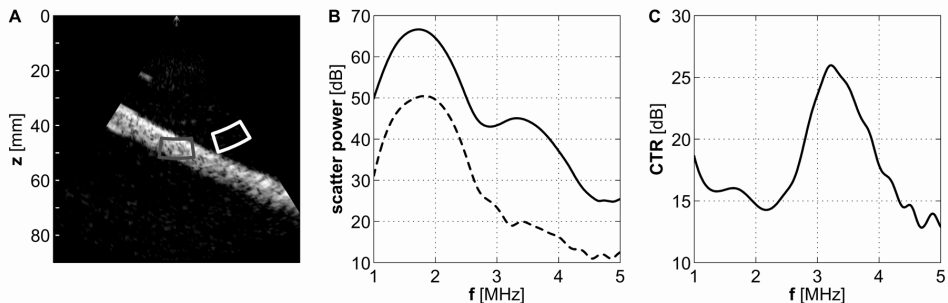
Figure. 7. In panel A, a B-mode image from the tissue-mimicking phantom with contrast in the flow area is shown. The gray and white solid lines indicate the ROI used for the power spectra calculations. The power spectra obtained from the tissue (dashed line) and contrast (solid line) region at a transmission frequency of 1.74 MHz are depicted in panel B. The difference of these power spectra, defined as the CTR, is shown in panel C.
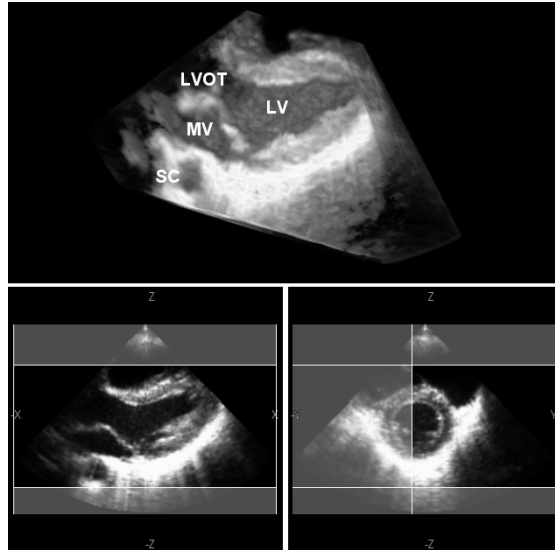
Figure. 8. The upper panel depicts a volume-rendered reconstruction of a left ventricular patient recording. The two lower panels show a reconstructed long and short axis image, respectively. The shaded regions in the lower panels annotate the cut away areas of the volumerendered image in the upper panel. LV, left ventrical; MV, mitral valve; LVOT, left ventricular outflow tract; SC, sinus coronaries.

Clinical Recordings

Fig. 8 shows a rendered patient recording of the left ventricle. The image shows the LV cavity, the mitral valve, and the aortic outlet tract. In addition, two reconstructed 2-D images of the LV short and long axis are shown.

From another patient, the LV volume and ejection fraction was determined. Quantification of the recorded echo data was performed with 4-D LV analysis software from TomTec (Munich, Germany) featuring a semiautomated border detection algorithm. End diastolic and end systolic volumes were determined using seven slices per volume with equiangular intervals. Fig. 9 shows the analysis result. An end-diastolic and end-systolic surface rendering of the endocardial border is shown along with the obtained time-volume curve. From the time-volume curve, an end-diastolic volume of 131 ml, an end-systolic volume of 66 ml, and an ejection fraction of 50% were extracted. An MRI recording of the same patient on the same day resulted in an end-diastolic volume of 131 ml, an end-systolic volume of 62 ml, and an ejection fraction of 53%.
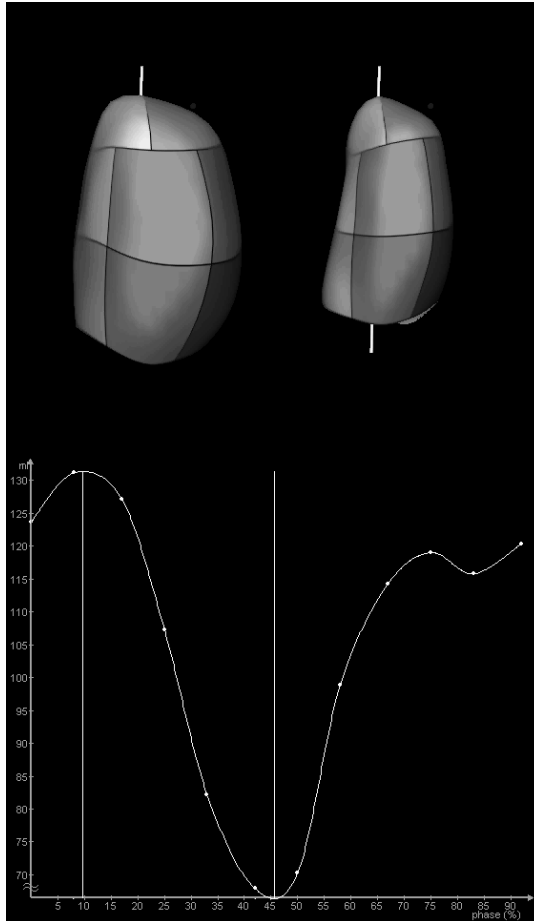
Figure. 9. The upper panel shows an end-diastolic and end-systolic surface rendered tracing result from a patient recording. The corresponding time-volume curve is shown in the lower panel. From the time-volume curve, the end-diastolic volume (131 ml), the endsystolic volume (66 ml), and the ejection fraction (50%) are derived.

Discussion

A novel transducer design, based on the continuous rotation of a phased array, for rapid 3-D echo has been presented. The short acquisition time, of approximately 10 seconds, makes it highly suitable for echocardiographic application and avoids the need for respiratory gating. In addition, its wide bandwidth allows for tissue and contrast harmonic imaging.

Although the need for fast 3-D echocardiography has been widely recognized, only one other research group has reported on a similar concept as presented

here[12-14]. Their transducer uses a fast-rotating array that is oscillating within its rotation angle range of 720 . Although its rotation speed matches that of the FRU-transducer, the oscillatory motion results in an even more complex sampling of the time-volume space. Studies in which this transducer has been used have been limited to fundamental imaging, so no record exists on its harmonic imaging capabilities.

Another concept for fast 3-D echocardiography is the use of matrix array transducers, which are currently available with the Philips Sonos 7500 scanner (Eindhoven, The Netherlands) and its x4 xMATRIX transducer as well as the General Electric Vivid 7 scanner (Milwaukee,WI) with its 3 V transducer. At the current state-of-the-art, it is very difficult for matrix transducers to both deal with the complex technology involved and also match the image quality of contemporary, phased-array transducers. Although it has been reported that second generation matrix array transducers show a big improvement of image quality compared to its predecessors[8,15], this relatively young technique still provides suboptimal image quality, especially when it comes to harmonic imaging[16,17]. In addition, advanced 2-D imaging techniques, such as contrast superharmonic imaging[18], can be implemented with the FRU-transducer in a straightforward manner and extended for use in 3-D applications. With the use of multibeat fusion, an acquisition with the FRU-transducer requires 10 seconds maximally. In principal, the matrix approach has the advantage of real-time acquisition and display; but in clinical practice, the field-of-view of real-time scanning is too limited. For a so-called full-volume recording with the Philips scanner, the acquisition is extended to four cardiac cycles, after which the data can be viewed and analyzed offline. In this respect, there is no difference between our approach and matrix-array transducers. Ultimately, the FRU-transducer also provides a cost-effective alternative to matrix-array transducers.

Although the results show feasibility of the clinical application of the FRU-transducer, a full evaluation of its clinical capabilities will be conducted in the near future. This will include the determination of the LV function compared with other techniques such as MRI and the use of contrast agents for improved 3-D assessment of the heart.

With the availability of fast 3-D echocardiographic acquisition, quantification of the recorded data has become the most time-consuming element in the diagnostic use of 3-D datasets. This is mainly due to the lack of tracing algorithms that do not need an expert to initialize the algorithm and review the tracing result. Improved image quality and border delineation will be a welcome contribution toward fully automatic quantification tools. The unique harmonic capabilities of the presented transducer could be beneficial for this purpose. Therefore, future efforts will be aimed at the use of tissue and contrast harmonic images from the FRU-transducer for such algorithms.

Conclusions

A continuous rotating array transducer has been presented suitable for fast acquisition of 3-D datasets within a clinical setting without the use of respiratory or ECG gating.

Its harmonic capabilities provide unique possibilities for tissue and contrast harmonic 3-D imaging, which could be beneficial for quantification algorithms. The concept is easily integrated in state-of-the-art, 2-D echo systems due to its innovative and cost-effective design.

Appendix A

The sampling of the rotation angle in a fused cardiac cycle, when using multibeat fusion is determined by four parameters: the rotation speed $f_{Rotation}$, the heart rate, the frame rate f_{Frame}, and the segmentation of the cardiac cycle. To determine an optimized rotation speed, we first look for a rotation speed from which the frames of corresponding and consecutive segments fill up the rotation angle as taken from a continuous sequence of frames. For a given heart rate, frame rate, and number of segments, we can calculate the average number of frames within each cardiac cycle $N_{F/C}$ and the average number of frames within each segment $N_{F/S}$. With n being the number of complete rotations covered within the time between two corresponding and consecutive cardiac segments, we can calculate candidate rotation speeds $f_{Candidate}$ for our solution with the following formula:

$$f_{Candidate} = \frac{n \cdot f_{Frame}}{[N_{F/C}] - [N_{F/S}]} \quad \text{with} \quad 4 \le f_{Candidate} \le 8 \text{ Hz and } n \in \{1,2,3,...\}$$

From the range of possible rotation speeds and the typical frame rate of approximately 100 fps, it appears that an adequate sampling of the rotation angle can be reached when a number of rotations are merged (see also Fig. 5). When, for instance, three rotations are merged, the first frame of the second rotation should start at exactly one-third or two-thirds of the angle between the first and the second frame of the set. If this is the case, the sequence will repeat itself after three full rotations, and the frames of the fourth rotation will be at the same angular position as those of the first rotation. The candidate rotation speeds usually will not meet the above requirement but can be corrected to approximate it. With a given number of merged rotations $N_{Rotation}$, which is limited by the duration of the recording, we can calculate the number of frames per rotation of the preferred rotation speed $N'_{F/R}$ from the number of frames per rotation of the candidate rotation speed $N_{F/R}$ as follows:

$$N'_{F/R} = [N_{F/R}] \pm \frac{m}{N_{Rotation}} \quad \text{with} \quad N_{F/R} = \frac{f_{Frame}}{f_{Candidate}} \,, \quad m \in \{1,2,3,...\} \quad \text{and}$$

$$m < N_{Rotation}$$

To avoid that the frame sequence will repeat itself before the number of rotations to merge m has to agree to the following additional requirement when $N_{Rotation}$ is larger than 1:

$$i \cdot m \neq j \cdot N_{Rotation} \quad \text{with} \quad i,j \in \{1,2,3,...\} \quad \text{and} \quad i < N_{Rotation}$$

By selecting the preferred number of frames per rotation that deviates the least from the number of frames per rotation of the candidate rotation speed, we then can calculate the rotation speed:

$$f_{Rotation} = f_{Candidate} \cdot \left(1 - \frac{\left(N'_{F/R} - N_{F/R}\right) N_{Rotation}}{\left(\left(\left\lceil \frac{N_{F/R} \cdot N_{Rotation}}{[N_{F/S}]} \right\rceil - 1\right) \cdot n + N_{Rotation}\right) \cdot N_{F/R}} \right)$$

With this solution, it is assured that the frames of the first and the last segments used will assume their ideal angular position. By using the rotation speed resulting from the candidate needing the smallest correction, the frames from intermediate segments only will deviate minimally from their ideal position (see Table I).

Acknowledgments

References

1. N. G. Pandian, J. Roelandt, N. C. Nanda, L. Sugeng, Q. L. Cao, J. Azevedo, S. L. Schwartz, M. A. Vannan, A. Ludomirski, G. Marx, and M. Vogt, "Dynamic three-dimensional echocardiography: Methods and clinical potential," *Echocardiography*, vol. 11, pp. 237–259, 1994.

2. J. R. T. C. Roelandt, "Three-dimensional echocardiography: The future today!," *Comput. Graph.*, vol. 24, pp. 715–729, 2000.

3. B. J. Krenning, M. M. Voormolen, and J. R. Roelandt, "Assessment of left ventricular function by three-dimensional echocardiography," *Cardiovasc. Ultrasound.*, vol. 1, 12, 2003.

4. A. Delabays, N. G. Pandian, Q. L. Cao, L. Sugeng, G. Marx, A. Ludomirski, and S. L. Schwartz, "Transthoracic real-time three-dimensional echocardiography using a fan-like scanning approach for data acquisition: Methods, strengths, problems, and initial clinical experience," *Echocardiography*, vol. 12, pp. 49–59, 1995.

5. J. Roelandt, A. Salustri, B. Mumm, and W. Vletter, "Precordial three-dimensional echocardiography with a rotational imaging probe: Methods and initial clinical experience," *Echocardiography*, vol. 12, pp. 243–252, 1995.

6. D. Papavassiliou, N. R. Doelling, M. K. Bowman, H. Yeung, J. Rock, B. Klas, K. Chung, and D. A. Fyfe, "Initial experience with an internally rotating transthoracic three-dimensional echocardiographic probe and image acquisition on a conventional echocardiogram machine," *Echocardiography*, vol. 15, pp. 369–376, 1998.

7. K. Sheikh, S. W. Smith, O. von Ramm, and J. Kisslo, "Realtime, three-dimensional echocardiography: Feasibility and initial use," *Echocardiography*, vol. 8, pp. 119–125, 1991.

8. R. S. von Bardeleben, H. P. Kuhl, S. Mohr-Kahaly, and A. Franke, "Second-generation real-time three-dimensional echocardiography. Finally on its way into clinical cardiology?," *Z. Kardiol.*, vol. 93, Suppl. 4, pp. IV56–IV64, 2004.

9. K. K. Djoa, N. de Jong, F. C. van Egmond, J. D. Kasprzak, W. B. Vletter, C. T. Lancee, A. F. van der Steen, N. Bom, and J. R. Roelandt, "A fast rotating scanning unit for realtime three-dimensional echo data acquisition," *Ultrasound Med. Biol.*, vol. 26, pp. 863–869, 2000.

10. M. Sonka, V. Hlavac, and R. Boyle, *Image Processing, Analysis, and Machine Vision*. 2nd ed. Pacific Grove, CA: PWS Pub., 1999.

11. M. M. Voormolen, A. Bouakaz, B. J. Krenning, C. T. Lancee, F. J. ten Cate, and N. de Jong, "Feasibility of 3-D harmonic contrast imaging," *Ultrasonics*, vol. 42, pp. 739–743, 2004.

12. R. Canals, G. Lamarque, and P. Chatain, "Volumetric ultrasound system for left ventricle motion imaging," *IEEE Trans. Ultrason., Ferroelect., Freq. Contr.*, vol. 46, pp. 1527–1538, 1999.

13. L. D. Nguyen and C. Leger, "Four-dimensional reconstruction of the left ventricle using a fast rotating classical phased array scan head: Preliminary results," *J. Amer. Soc. Echocardiogr.*, vol. 15, pp. 593–600, 2002.

14. L. D. Nguyen, C. Leger, D. Debrun, F. Therain, J. Visser, and E. Busemann Sokole, "Validation of a volumic reconstruction in 4-d echocardiography and gated SPECT using a dynamic cardiac phantom," *Ultrasound Med. Biol.*, vol. 29, pp. 1151–1160, 2003.

15. K. Arai, T. Hozumi, Y. Matsumura, K. Sugioka, Y. Takemoto, H. Yamagishi, M. Yoshiyama, H. Kasanuki, and J. Yoshikawa, "Accuracy of measurement of left ventricular volume and ejection fraction by new real-time three-dimensional echocardiography in patients with wall motion abnormalities secondary to myocardial infarction," *Amer. J. Cardiol.*, vol. 94, pp. 552–558, 2004.

16. K. L. Chan, X. Liu, K. J. Ascah, L. M. Beauchesne, and I. G. Burwash, "Comparison of real-time 3-dimensional echocardiography with conventional 2-dimensional echocardiography in the assessment of structural heart disease," *J. Amer. Soc. Echocardiogr.*, vol. 17, pp. 976–980, 2004.

17. R. Schnabel, A. V. Khaw, R. S. von Bardeleben, C. Strasser, T. Kramm, J. Meyer, and S. Mohr-Kahaly, "Assessment of the tricuspid valve morphology by transthoracic real-time 3-Dechocardiography," *Echocardiography*, vol. 22, pp. 15–23, 2005.

18. A. Bouakaz, B. J. Krenning, W. B. Vletter, F. J. ten Cate, and N. de Jong, "Contrast superharmonic imaging: A feasibility study," *Ultrasound Med. Biol.*, vol. 29, pp. 547–553, 2003.

Chapter 3

Rapid and accurate measurement of left ventricular function with a new second-harmonic fast-rotating transducer and semi-automated border detection

BJ Krenning
MM Voormolen
RJ van Geuns
WB Vletter
CT Lancée
N de Jong
FJ ten Cate
AFW van der Steen
JRTC Roelandt

Abstract

Measurement of left ventricular (LV) volume and function are the most common clinical referral questions to the echocardiography laboratory. A fast, practical and accurate method would offer important advantages to obtain this important information.

Objective
To validate a new practical method for rapid measurement of LV volume and function.

Design
We developed a continuous fast-rotating transducer, with second-harmonic capabilities, for three-dimensional echocardiography (3DE). 15 cardiac patients underwent both 3DE and magnetic resonance imaging (MRI, reference method) on the same day. 3DE image acquisition was performed during a 10s breath-hold with a frame rate of 100 frames/s and a rotational speed of 6 rotations/s. The individual images were postprocessed with Matlab software using multi-beat data fusion. Subsequently, with these images 12 datasets per cardiac cycle were reconstructed each comprising 7 equidistant cross-sectional images for analysis in the new TomTec 4DLV analysis software, which uses a semi-automated border detection (ABD) algorithm. The ABD requires an average analysis time of 15 min. per patient.

Results
A strong correlation was found between LV end-diastolic volume ($r = 0.99$; $y = 0.95x – 1.14$ ml; SEE = 6.5 ml), LV end-systolic volume ($r = 0.96$; $y = 0.89x + 7.91$ ml; SEE = 7.0 ml) and LV ejection fraction ($r = 0.93$; $y = 0.69x + 13.36$; SEE = 2.4 %). Inter- and intra-observer agreement for all measurements was good.

Conclusion
The fast-rotating transducer with new ABD software is a dedicated tool for rapid and accurate analysis of LV volume and function.

Introduction

Left ventricular (LV) volumes and function have major diagnostic and prognostic importance in patients with heart disease[1,2] and are the most common referral questions to the echocardiography laboratory. A fast, practical and accurate method is a prerequisite to obtain this important information for patient management. Three-dimensional echocardiography (3DE) allows accurate calculation of left ventricular ejection fraction without geometric assumptions of its shape.[3-6] Recent transducer and software developments may now allow fast acquisition and semi-automated analysis, enabling the routine clinical application of three-dimensional echocardiography.[7,8]

This study was performed to assess both the feasibility and accuracy of a new continuous fast-rotating phased-array transducer for left ventricular volume and ejection fraction calculation using commercially available quantification software. MRI was used as the reference method.

Material and methods

Study patients

Seventeen male patients (mean age 52 years, range 29 – 74 years) with a history of myocardial infarction and various degrees of wall motion abnormalities were included. All 15 patients were in sinus rhythm. Two patients suffered from ischemic cardiomyopathy. None of the patients had to be excluded because of insufficient image quality. However, two patients were excluded because of incomplete visualization of the LV in the echocardiographic window due to LV dilatation. The mean heart rate (SD) during echocardiographic examination was 57 (13) bpm. Both studies were completed in each subject within 4 hours, and MRI was performed before 3DE examination. All patients gave informed consent.

Three-dimensional echocardiography

Instrumentation
We used a new third generation prototype transthoracic, fast-rotating 64-element array transducer with a center frequency of 3 MHz. Besides decreased transducer size and technical improvements, this transducer features the capability of second harmonic imaging (Figure 1). The transducer continuously rotates around its central axis with a maximum rotation speed of 480 rotations per minute and is connected to a commercially available ultrasound system (GE Vingmed Vivid 5, Horton, Norway).[9,10] Interfaces are present for motor control, image synchronisation and data processing. Unlike other mechanical 3D-acquisition systems, which can only collect images over a limited number of rotations, this transducer acquires im-
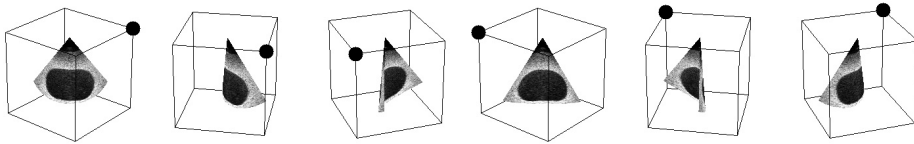
Figure 1: Image of the most recent prototype of the continuous fast-rotating transducer used in this study. Below, a 2D phantom image displayed in perspective from different angles. As shown, continuous rotation results in a curved shape of the original images.

ages over as many rotations as required.[5,7,11-15] A slip-ring, consisting of a static and rotating part, maintains electrical contact between the rotating array and the static part of the transducer. Therefore, any cable twisting and subsequent need for rotation inversion is not present. Because this transducer is capable of using standard 2D-ultrasound capabilities, a high frame rate at a wide sector angle of 90° can be chosen, which is necessary to capture the full LV in most patients. The size of the transducer is nearly the same as a standard 2D transducer. The typical frame rate for a 3D acquisition is approximately 100 frames/s..

Image acquisition
Patients are studied in the left lateral decubitus position with the transducer in the apical position and the image plane rotating around the LV long axis. The depth settings are adjusted to visualize the entire LV and part of the left atrium. Gain and power settings are optimised for endocardial border visualization. The image acquisition is made during a single end-expiratory breath hold of approximately 10 s., in second harmonic imaging mode (transmit frequency: 2 MHz). The ECG is simultaneously recorded for the 3D reconstruction process.

Imaging processing and analysis

Image data are transferred via a network connection to a dedicated PC for processing and analysis. With custom designed software, based on MatLab (The Math-Works Inc., Natick MA, USA), the original 2D images are post-processed (Figure 2A). Using the ECG, the echo data are located in their correct spatial and temporal position.[16,17] To obtain an adequate density of the spatial and temporal sampling multi-beat data fusion is employed.[16,17] Twelve 3D-datasets were reconstructed by
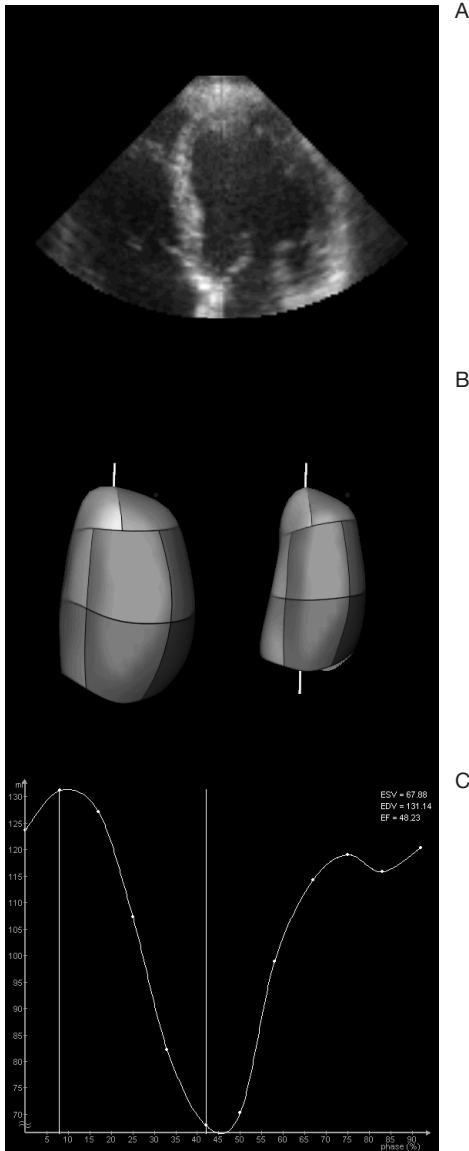
Figure 2: (A) An original image of the apical long axis view showing the image quality during fast rotation. (B) Endocardial surface rendered image of the endocardial border. (C) Volume-Time Curve; dots show measured data points.

dividing the cardiac cycle in 12 equidistant time-intervals, irrespective of its length. Due to the continuous rotation of the transducer-array, the original 2D imaging planes have a curved shape and are not suited for automated contour analysis with currently available software. Therefore, seven equidistant cross-sectional images are re-sampled from the 12 datasets and used for further contour analysis. This resulted in a rotational interval of 27° between the cross-sectional images.[17]

Subsequently, all re-sampled cross-sectional images are imported into the TomTec© 4D LV-analysis software (TomTec© Imaging Systems, Munich, Germany). Their orientation in 3D space is determined by manually marking the mitral valve, aortic root and apex. An elliptical model is then placed over one of the images of each of the 7 cross-sectional positions. Contrast and gain settings can be adjusted for optimal endocardial border visualization. After this, the software automatically performs endocardial border detection in all images of each cross-sectional position in the 12 datasets. A spatio-temporal spline model is used to generate smooth contours for both the temporal and spatial domain. Two investigators verified and corrected the results from the automated border detection independently. This was done blinded to MRI results. The first investigator analyzed the 3DE images twice, blinded for the results of the first analysis.

The analysis program displays a reconstruction of the LV as a dynamic surface rendered image, in which LV wall motion is shown in three dimensions (Figure 2B). From an automatically plotted time-volume curve (Figure 2C), LV end-diastolic (LVEDV) and end-systolic volume (LVESV) were determined by the maximal and minimal volume and ejection fraction (LVEF) was calculated.

Magnetic Resonance Imaging and analysis

All patients are studied in a supine position, with a 4-channel quadrature body phased array coil placed over the thorax, in a 1.5T whole body MR imaging system (General Electric, Milwaukee WI, USA; Signa CV/*i,* with an amplitude of 40 mTm^{-1} and a slew rate of 150 Tm^{-1}s^{-1}). For quantitative analysis approximately 10 to 12 cine short-axis series (slice thickness 8 mm, gap 2 mm) covering the heart from base to apex where acquired using a breath-hold cardiac triggered steady state free precession sequence (FIESTA) with a TR and TE of 3.5 and 1.3 ms respectively and a flip angle of 45 degrees. Additional imaging parameters were: Field of View of 340 x 255 mm, a matrix of 160x128 and a temporal resolution of 28 ms. The whole protocol could be performed within 30 minutes.

Quantitative analysis was performed using standardized software (MassPlus, General Electric, Milwaukee WI, USA). With this software endocardial contours were semi-automatic traced on all end-diastolic and systolic images to calculate the LV volumes and EF using Simpson's rule. Review of the automated tracing was performed by an investigator, blinded to the 3DE data.

Statistical analysis

Data are presented as mean (SD). A linear regression analysis was performed for the comparison of results obtained by 3DE and MRI. The first measurement of the first observer was used for comparison with MRI. The 3DE measurements from two independent observers were compared mutually to assess inter-observer variability. To assess intra-observer variability, the two blinded measurements by the first observer were compared. In addition, the limits of agreement were calculated for all comparisons and expressed as the mean ± 2 times SD[18]. To determine whether there is a statistically significant difference between the populations of each comparison, a paired t-test was performed. Data were tested for normality with the Kolmogorow-Smirnov test with Lilliefors significance correction. A probability level of p< 0.05 was considered significant.

Results

LVEDV measurements for MRI ranged from 127 to 241 ml and from 122 to 239 ml for 3DE. LVESV measurements from MRI ranged from 58 to 144 ml and from 60 to 144 ml for 3DE. The mean (SD) for LVEDV measurements were 186 (41) ml and 177 (40) ml (P < 0.001), for MRI and 3DE respectively. The mean (SD) for LVESV measurements were 99 (28) ml and 96 (25) ml (P = NS), for MRI and 3DE respectively. The Kolmogorow-Smirnov tests for normality were not significant, indicating a normal distribution of data. The time for data analysis averaged 15 (5) min. per patient.

Comparison between 3DE and MRI

Results of the regression analysis and the limits of agreement calculation for LVEDV, LVESV and LVEF are shown in Figure 3. A strong correlation was observed between MRI and 3DE for both LVEDV (r = 0.99; y = 0.95x – 1.14 ml; SEE = 6.5 ml) and LVESV measurements (r = 0.96; y = 0.89x + 7.91 ml; SEE = 7.0 ml). The limits of agreement analysis demonstrated a mean difference of -9.7 ± 13.1 ml for LVEDV and -3.0 ± 14.7 ml for LVESV. A good correlation was also observed for calculated LVEF (r = 0.93; y = 0.69x + 13.36; SEE = 2.4 %), with a mean difference of -1.7 ± 7.2%.

Intra-observer variability

The two independent measurements from the first observer show an excellent correlation for LVEDV (r = 1.00; y = 0.97x + 4.3 ml; SEE = 3.2 ml), LVESV (r = 1.00; y = 1.00x – 0.2 ml; SEE = 2.3 ml) and LVEF (r = 0.99; y = 1.04x – 2.4%; SEE = 1.2%). The limits of agreement analysis demonstrated a mean difference of -1.4 ± 6.6 ml for LVEDV, -0.1 ± 4.4 ml for LVESV and -0.3 ± 2.4% for LVEF. No significant difference was present between the two measurements.
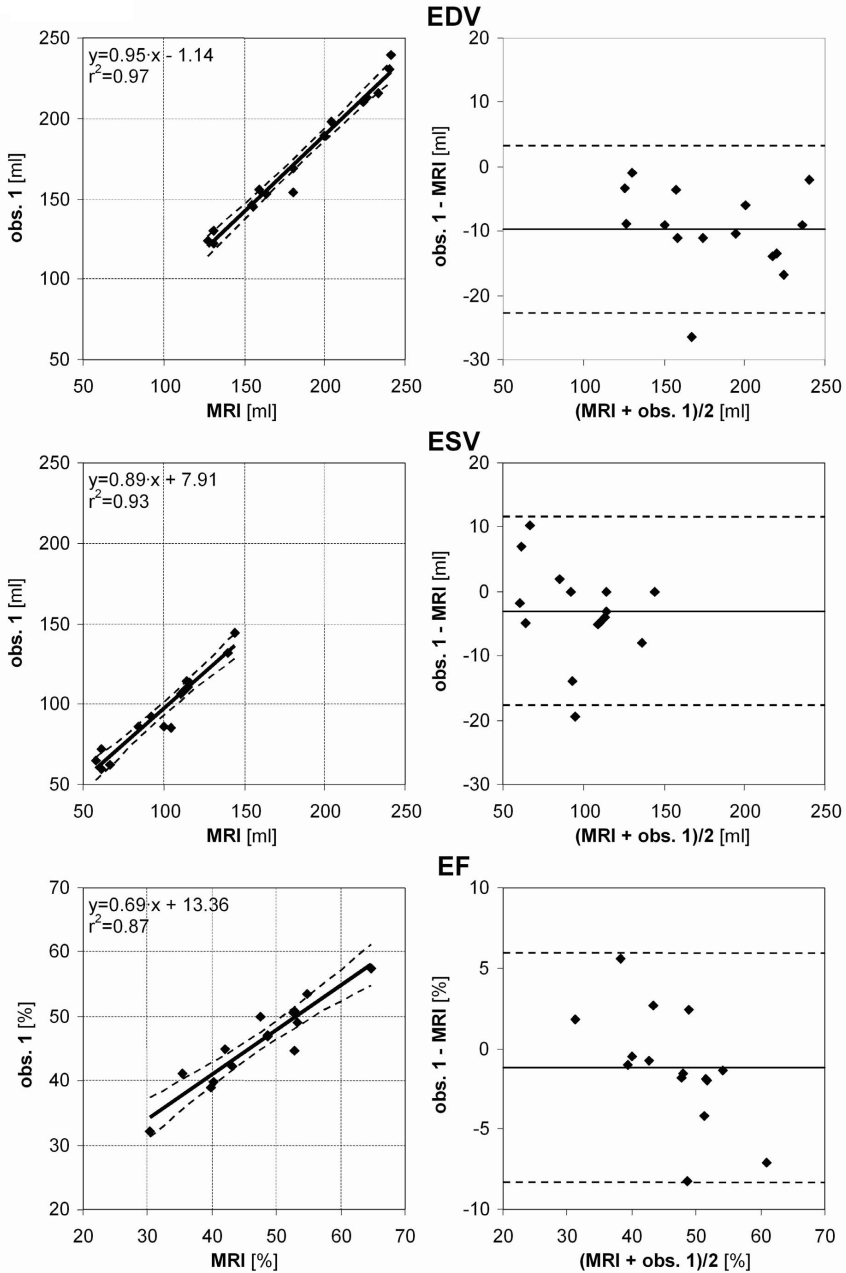
Figure 3: Relation between 3DE and MRI measurements of LVEDV, LVESV and LVEF. The left panels show the regression line between the two methods. Dashed lines delimit 95% confidence interval. The right panels show plots of the difference between MRI and 3DE, as a function of the average calculated volumes. Solid and dashed lines represent mean ± 2 SDs of the difference, respectively. (LVEDV = left ventricular end-diastolic volume, LVEF = left ventricular ejection fraction, LVESV = left ventricular end-systolic volume).
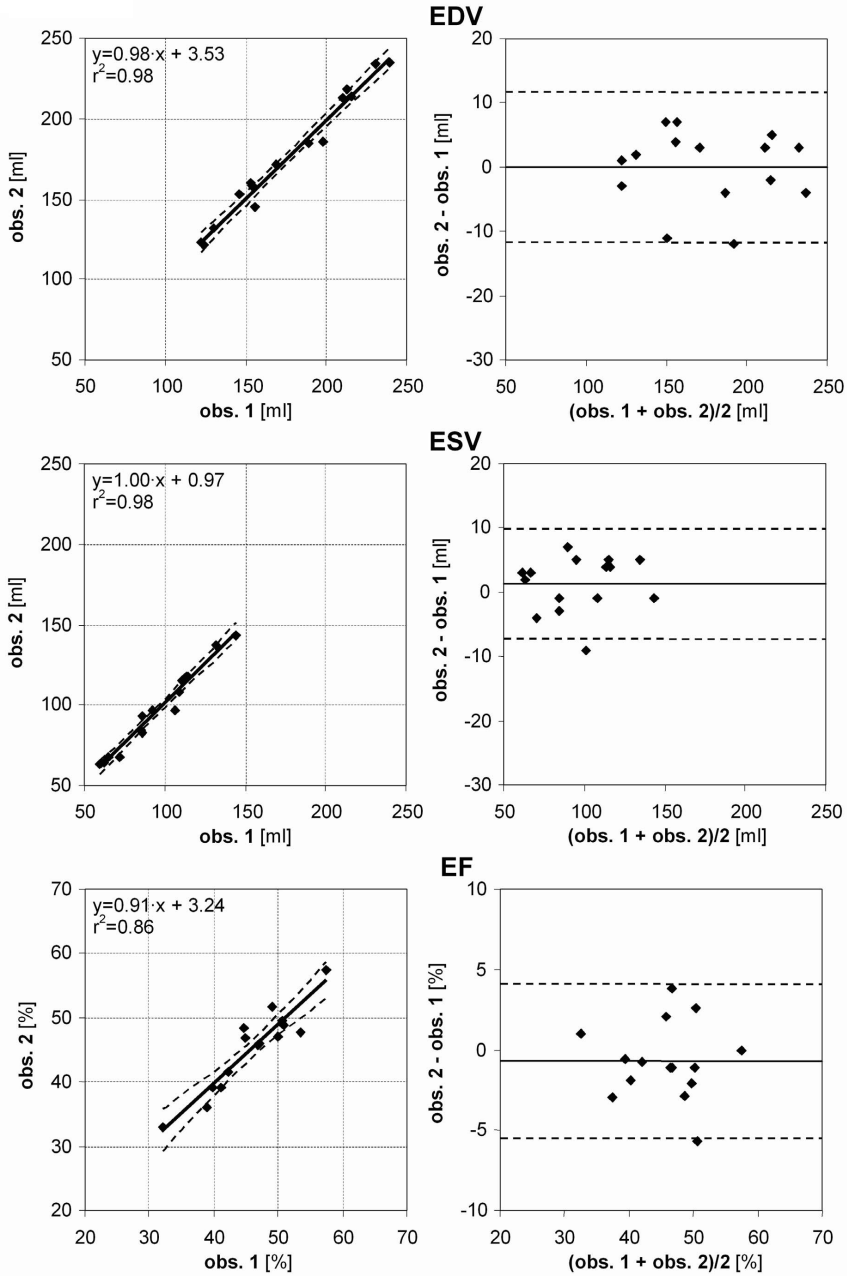
Figure 4: Interobserver variability for 3DE measurements of LVEDV, LVESV and LVEF. The left panels show the regression line between measurements obtained by two different observers. Dashed lines delimit 95% confidence interval. The right panels show plots of the differences between both measurements by two observers as a function of the average measurement. Solid and dashed lines represent mean ± 2 SDs of the difference, respectively. (LVEDV = left ventricular end-diastolic volume, LVEF = left ventricular ejection fraction, LVESV = left ventricular end-systolic volume).

Inter-observer variability

The linear regression and limits of agreement calculation for LVEDV, LVESV and LVEF from the 3D echocardiographic data by two independent observers are shown in Figure 4. These results show a good correlation and only a small mean difference for LVEDV (r = 0.99; y = 0.98x + 3.53; SEE = 6.0 ml) and LVESV (r = 0.99; y = 1.00x + 0.97; SEE = 4.5 ml). The results of the linear regression analysis for LVEF was acceptable (r = 0.93; y = 0.91x + 3.24; SEE = 2.4 %). The limits of agreement analysis demonstrated a mean difference of -0.1 ± 11.7 ml for LVEDV, 1.3 ± 8.7 ml for LVESV and -0.7 ± 4.8% for LVEF. No significant difference was present between the two observers.

Discussion

This study demonstrates that 3DE with a continuous fast-rotating ultrasound transducer and TomTec© 4DLV analysis software provides an accurate method for determination of LV volume and function. This technique allows the acquisition on data during 10s of suspended respiration, which makes it clinically feasible. We found a strong overall correlation between MRI and 3DE in a group of patients with a wide range of LV volumes who underwent MRI and 3DE examination on the same day. Further, analysis of inter- and intra-observer variability also showed a good correlation.

The MRI measurements for LVEDV in our study were higher then those of 3DE. However, almost all 3DE studies tend to underestimate LV volumes when compared to MRI[19]. One explanation for this underestimation may be a difference in tracing method. TomTec© 4DLV software requires long-axis images for endocardial border detection, while the MRI software uses short-axis cross-sections with a disk-summation method to obtain a LV volume. Using the latter method, a part of the aortic root or left atrium can be included in the volume of the reconstructed disk in the most basal cross-section. This error can theoretically be reduced by increasing the number of disks (and subsequent decrease of slice thickness), resulting in an increased review time.

Second, the endocardial contour tracing may have an important influence on volume determination[20]. MRI tracings were performed excluding the trabeculae, while 3DE tracings are performed on the endocardial border, mostly including tarbeculae. During diastole, individual trabeculae are difficult to visualize due to their small size. In systole, however, the trabeculae form a compact layer, clearly distinguishable from the blood-pool. This may explain differences in LVEDV.

In this study, we used 7 equidistant long-axis cross-sections for endocardial border detection, resulting in a good agreement compared to MRI. Several studies calculated the optimal rotational interval for LV volumes mostly based on endocardial border tracing of short axis slices of the LV or intersecting long and short

axis images.[21,22] Tanabe et al. showed that as few as 4-6 axial slices can accurately quantify LV volumes using a similar apical rotational technique in non-beating canine heart specimens with irregular shapes.[4] Because currently available software most often uses long axis border tracing, further studies are needed to determine the optimal rotational interval for this tracing method in normal and remodelled or asymmetric human ventricles with a low error in volume calculation. Also, the method described should be compared with available methods used in daily echocardiographic practice, such as acoustic quantification[23,24] and new electronic real-time (matrix) ultrasound systems.[8,25-28] Theoretically, major advantages of our system are the availability of all conventional 2D echocardiography features (such as harmonic imaging and Doppler capabilities and 90 degree sector angle imaging) and the compatibility with multiple commercially available ultrasound systems. Also, new echocardiographic techniques, such as super-harmonic imaging, may be easier to implement in our transducer.[29]

LV volume and function analysis is the most frequent referral question for echocardiography. A recent meta-analysis showed that 2DE can only provide a moderately accurate assessment of LV systolic function.[30] In literature, a 95%-confidence interval for LVEF<±10% is suggested to be important in patients with borderline LV dysfunction (LVEF 30-50%) for adequate diagnosis and risk stratification. 3DE can serve as an additional imaging technology for more accurate LVEF assessment in these patients. A routine 2D examination can then be completed with a fast 3D LV function analysis.

Conclusion: The results of this study demonstrate that the fast-rotating transducer in combination with TomTec© 4DLV analysis software provides a dedicated tool for accurate measurement of LV volume and function.

References

1. White HD, Norris RM, Brown MA, *et al.* Left ventricular end-systolic volume as the major determinant of survival after recovery from myocardial infarction. *Circulation* 1987;**76**:44-51.
2. Hall SA, Cigarroa CG, Marcoux L, *et al.* Time course of improvement in left ventricular function, mass and geometry in patients with congestive heart failure treated with beta- adrenergic blockade. *J Am Coll Cardiol* 1995;**25**:1154-61.
3. Siu SC, Rivera JM, Guerrero JL, *et al.* Three-dimensional echocardiography. In vivo validation for left ventricular volume and function. *Circulation* 1993;**88**:1715-23.
4. Tanabe K, Belohlavek M, Jakrapanichakul D, *et al.* Three-Dimensional Echocardiography: Precision and Accuracy of Left Ventricular Volume Measurement Using Rotational Geometry with Variable Numbers of Slice Resolution. *Echocardiography* 1998;**15**:575-580.
5. Nosir YF, Fioretti PM, Vletter WB, *et al.* Accurate measurement of left ventricular ejection fraction by three- dimensional echocardiography. A comparison with radionuclide angiography. *Circulation* 1996;**94**:460-6.
6. Shiota T, McCarthy PM, White RD, *et al.* Initial clinical experience of real-time three-dimensional echocardiography in patients with ischemic and idiopathic dilated cardiomyopathy. *Am J Cardiol* 1999;**84**:1068-73.
7. Belohlavek M, Tanabe K, Jakrapanichakul D, *et al.* Rapid three-dimensional echocardiography : clinically feasible alternative for precise and accurate measurement of left ventricular volumes. *Circulation (Online)* 2001;**103**:2882-2884.
8. Kuhl HP, Schreckenberg M, Rulands D, *et al.* High-resolution transthoracic real-time three-dimensional echocardiography: quantitation of cardiac volumes and function using semi-automatic border detection and comparison with cardiac magnetic resonance imaging. *J Am Coll Cardiol* 2004;**43**:2083-90.
9. Djoa KK, de Jong N, van Egmond FC, *et al.* A fast rotating scanning unit for real-time three-dimensional echo data acquisition. *Ultrasound Med Biol* 2000;**26**:863-9.
10. Voormolen MM, Bouakaz A, Krenning BJ, *et al.* A New Transducer for 3D Harmonic Imaging Proceedings of the IEEE International Ultrasonics Symposium. Munich, 2002:1261-1264.
11. Kupferwasser I, Mohr-Kahaly S, Stahr P, *et al.* Transthoracic three-dimensional echocardiographic volumetry of distorted left ventricles using rotational scanning. *J Am Soc Echocardiogr* 1997;**10**:840-52.
12. Acar P, Maunoury C, Antonietti T, *et al.* Left ventricular ejection fraction in children measured by three- dimensional echocardiography using a new transthoracic integrated 3D- probe. A comparison with equilibrium radionuclide angiography. *Eur Heart J* 1998;**19**:1583-8.
13. Nosir YF, Stoker J, Kasprzak JD, *et al.* Paraplane analysis from precordial three-dimensional echocardiographic data sets for rapid and accurate quantification of left ventricular volume and function: a comparison with magnetic resonance imaging. *Am Heart J* 1999;**137**:134-43.
14. Kim WY, Sogaard P, Kristensen BO, *et al.* Measurement of left ventricular volumes by 3-dimensional echocardiography with tissue harmonic imaging: a comparison with magnetic resonance imaging. *J Am Soc Echocardiogr* 2001;**14**:169-79.
15. Nguyen LD, Leger C. Four-dimensional reconstruction of the left ventricle using a fast rotating classical phased array scan head: preliminary results. *J Am Soc Echocardiogr* 2002;**15**:593-600.

16. Lancee CT, van Egmond FC, de Jong N, *et al.* Data Processing for a Fast Rotating Phased Array Real-time 3D Acquisition Unit Proceedings of IEEE Ultrasonics Symposium. San Juan, 2000:1597-1600.

17. Voormolen MM, Krenning BJ, Lancee CT, *et al.* Quantitative Harmonic 3D Echocardiography with a Fast Rotating Ultrasound Transducer Proceedings of IEEE Ultrasonics Symposium. Honolulu, 2003:122-125.

18. Bland JM, Altman DG. Statistical methods for assessing agreement between two methods of clinical measurement. *Lancet* 1986;**1**:307-10.

19. Krenning BJ, Voormolen MM, Roelandt JR. Assessment of left ventricular function by three-dimensional echocardiography. *Cardiovasc Ultrasound* 2003;1:12

20. Mannaerts HF, Van Der Heide JA, Kamp O, *et al.* Quantification of left ventricular volumes and ejection fraction using freehand transthoracic three-dimensional echocardiography: comparison with magnetic resonance imaging. *J Am Soc Echocardiogr* 2003;**16**:101-9.

21. Nosir YF, Vletter WB, Kasprzak JD, *et al.* Optimal rotational interval for 3-dimensional echocardiography data acquisition for rapid and accurate measurement of left ventricular function. *J Am Soc Echocardiogr* 2000;**13**:715-22.

22. Siu SC, Rivera JM, Handschumacher MD, *et al.* Three-dimensional echocardiography: the influence of number of component images on accuracy of left ventricular volume quantitation. *J Am Soc Echocardiogr* 1996;**9**:147-55.

23. Yvorchuk KJ, Davies RA, Chan KL. Measurement of left ventricular ejection fraction by acoustic quantification and comparison with radionuclide angiography. *Am J Cardiol* 1994;**74**:1052-6.

24. Perez JE, Waggoner AD, Barzilai B, *et al.* On-line assessment of ventricular function by automatic boundary detection and ultrasonic backscatter imaging. *J Am Coll Cardiol* 1992;**19**:313-20.

25. Schmidt MA, Ohazama CJ, Agyeman KO, *et al.* Real-time three-dimensional echocardiography for measurement of left ventricular volumes. *Am J Cardiol* 1999;**84**:1434-9.

26. Qin JX, Jones M, Shiota T, *et al.* Validation of real-time three-dimensional echocardiography for quantifying left ventricular volumes in the presence of a left ventricular aneurysm: in vitro and in vivo studies. *J Am Coll Cardiol* 2000;**36**:900-7.

27. Lee D, Fuisz AR, Fan PH, *et al.* Real-time 3-dimensional echocardiographic evaluation of left ventricular volume: correlation with magnetic resonance imaging--a validation study. *J Am Soc Echocardiogr* 2001;**14**:1001-9.

28. Ota T, Kisslo J, von Ramm OT, *et al.* Real-time, volumetric echocardiography: usefulness of volumetric scanning for the assessment of cardiac volume and function. *J Cardiol* 2001;**37** Suppl 1:93-101.

29. Bouakaz A, Krenning BJ, Vletter WB, *et al.* Contrast superharmonic imaging: a feasibility study. Ultrasound Med Biol. 2003;29:547-53

30. McGowan JH, Cleland JG. Reliability of reporting left ventricular systolic function by echocardiography: a systematic review of 3 methods. *Am Heart J* 2003;**146**:388-97.

Chapter 4

Feasibility of three-dimensional echocardiographic analysis of left ventricular function during hemodialysis

BJ Krenning
MM Voormolen
WB Vletter
FJ Ten Cate
AFW van der Steen
N de Jong
EHY Ie
JRTC Roelandt

Abstract

The effects of hemodialysis (HD) on left ventricular (LV) function have been studied by various echocardiographic techniques (M-mode, 2D-echocardiography). These studies are hampered by a low accuracy of measurements because of geometric assumptions regarding LV shape. Three-dimensional echocardiography (3DE) overcomes this limitation.

Methods
We tested the feasibility of 3DE assessment of LV function during HD. Conventional biplane Simpson rule (BSR) and single plane area length method (SPM) for LV function analysis were used as a reference.

Results
12 HD patients were studied and in 10 (83%) a total of 80 3D datasets were acquired. In three patients, one dataset (4%) was of insufficient quality and excluded from analysis. Correlation between SPM, BSR and 3DE for calculation of end-diastolic (EDV, r = 0.89 and r = 0.92, respectively), end-systolic volume (ESV, r = 0.92 and r = 0.93, respectively) and for ejection fraction (EF, r = 0.90 and r = 0.88, respectively) was moderate. Limits-of-agreement results for EDV and ESV were poor with confidence intervals larger than 30 ml. Both 2DE methods underestimated end-diastolic and end-systolic volume, while overestimating ejection fraction.

Conclusion
3DE is feasible for image acquisition during HD, which opens the possibility for accurate and reproducible measurement of LV function during HD. This may improve the assessment of the acute effect of HD on LV performance, and guide therapeutic strategies aimed at preventing intradialytic hypotension.

Introduction

Intradialytic hypotension is an important complication of hemodialysis (HD). Although its pathogenesis is not completely understood, it is clear that the decrease in blood volume due to ultrafiltration is the most important initiating factor. Hypotension results from a decreased product of stroke volume (SV), heart rate (HR) and systemic vascular resistance. The continuing volume withdrawal during HD is a hemodynamic challenge which may lead to an inability to generate sufficient cardiac output (CO). However, there is a large inter- and intra-individual variability regarding the incidence of intradialytic hypotension. Therefore, to better understand the interplay between progressive volume withdrawal and changes in LV performance during HD, studies have been conducted using various echocardiographic techniques, including M-mode echocardiography[1,2], two-dimensional echocardiography (2DE)[3,4] and Doppler-imaging[5,7]. Nevertheless, the acute effect of HD on cardiac function remains poorly understood, due to conflicting results. A number of factors influence cardiac function measurements, such as loading conditions[7,8]. Earlier LV performance studies may have been hampered by a low accuracy of measurements. M-mode and 2D echocardiography are limited by geometric assumptions as to volume and function calculation. 3D echocardiography (3DE) overcomes this limitation, and has recently become a feasible method for rapid and accurate measurement of LV function in a clinical rather than research setting[9]. In this study, we therefore evaluate the feasibility of 3DE assessment of LV function during HD. Also, we compared our 3D results with conventional two-dimensional methods for LV function analysis.

Methods

Patients
Twelve patients on chronic intermittent HD entered the study. Two patients were excluded because of insufficient 3D echocardiographic image quality. The remaining 10 patients had a mean age of 56 ± 15 years. All patients were in sinus rhythm and were dialysed three times a week according to a standard dialysis program, which had been unchanged for three months or longer. No medication was discontinued for this study. Four patients had a history of cardiac disease (2 coronary interventions, 1 myocardial infarction, 1 angina pectoris). The mean heart rate (SD) during echocardiographic examination was 68 ± 10 bpm. All patients gave informed verbal consent.

Hemodialysis
All dialysis treatments used Fresenius 4008 machines (Fresenius Medical Care, Bad Homburg, Germany), biocompatible membranes (Hemophane or Polysulphone) and

bicarbonate-buffered dialysate (Fresenius Medical Care SK-F213). The duration of the dialysis procedure was 4 h in all patients. During the first 30 minutes patients were connected to the dialysis machine with only blood flow (recirculation) but no HD or ultrafiltration (UF) taking place. The mean amount of fluid withdrawn was 2617 ± 1088 ml.

Three-dimensional echocardiography
We used a new prototype transthoracic, fast-rotating 64-element array transducer with a center frequency of 3 MHz. Technical aspects have been described elsewhere[10]. In short, this transducer features the capability of second harmonic imaging and continuously rotates around its central axis with a maximum rotation speed of 480 rotations per minute. The transducer is connected to a commercially available ultrasound system (GE Vingmed Vivid 5, Horton, Norway). A validation study using cardiac magnetic resonance imaging as a reference showed a strong correlation and good inter- and intra-observer agreement[11].

Image acquisition

3DE was performed before HD, 5 minutes after patient connection to the HD system, during recirculation without UF (after 30 minutes), every hour during HD with UF, and 15 minutes after HD. In total, 8 acquisitions were performed in each patient. Patients were studied in a partial left lateral decubitus position during HD. The transducer was placed in the apical position with the image plane rotating around the LV long axis. The depth settings were adjusted to visualize the entire LV and part of the left atrium. Gain and power settings were optimized for endocardial border visualization. The image acquisition was made, in second harmonic imaging mode (transmit frequency: 2 MHz) during a single end-expiratory breath hold of approximately 10 seconds and the ECG was simultaneously recorded for the 3D reconstruction process.

Three-dimensional imaging processing and analysis

Imaging processing and analysis was performed as previously described[11]. Image data were transferred via a network connection to a dedicated PC for processing and analysis. With custom designed software, based on MatLab (The MathWorks Inc., Natick MA, USA), the original 2D images are post-processed into a 3D datasets. Subsequently, TomTec© 4D LV-analysis software (TomTec© Imaging Systems, Munich, Germany) was used for further analysis. Eight equidistant cross-sectional image planes were used for analysis. The orientation of these images in 3D space was determined by manually marking the mitral valve, aortic root and apex. Con-

trast and gain settings were adjusted for optimal endocardial border visualization. Subsequently, the software automatically performed endocardial border detection in all images. One investigator verified the results from the automated border detection and corrected if necessary.

The analysis program displays a reconstruction of the LV as a dynamic surface rendered image, in which LV wall motion is shown in three dimensions (see Figure 1). From an automatically plotted volume-time curve, LV end-diastolic (EDV) and end-systolic volume (ESV) was determined by the maximal and minimal volume and ejection fraction (EF) was calculated.

Two-dimensional image processing and analysis
From the 3D dataset, two perpendicular images were extracted representing the apical two-dimensional four- and two-chamber views. Manual endocardial bor-
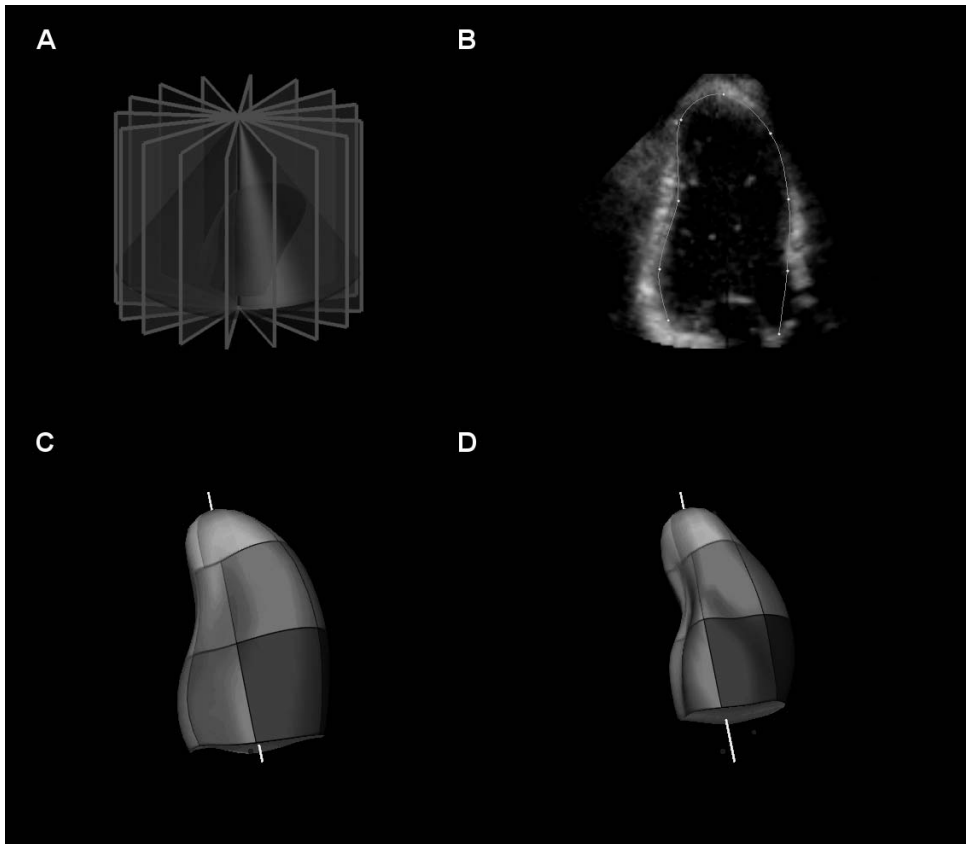
Figure 1:
(A) The LV is divided into 8 equidistant cross-sectional images which are used for contour analysis.
(B) An original image of an apical long axis view during fast rotation. (C) Reconstruction of the LV in end diastole, and (D) end systole.

der delineation was performed with MatLab using custom designed software. Two common algorithms for 2DE ventricular volume calculation were used, as recommended by the American Society of Echocardiography[12]: 1) The disc summation method or biplane Simpson rule (BSR), based on orthogonal planes from apical two- and four-chamber views. Volumes were computed using the formulation: (a and b represent diameters of discs, see Figure 2).
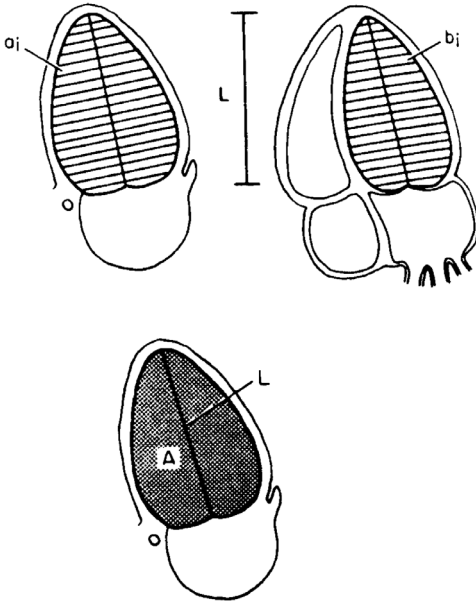
Figure 2:

Top panel: Biplane Simpson Rule for calculating LV volume, based on orthogonal planes from apical 2- and 4-chamber view. *Bottom panel*: Single Plane Area Length method, based on a single apical view. (Reprinted from Reference 12, with permission from The American Society of Echocardiography).

The single plane area length method by calculation of LV end-diastolic and end-systolic volumes and ejection fractions from the four-chamber view. Volumes were computed using the formulation: (Figure 2).

Inter- and intraobserver variability

To assess inter-observer variability for 2DE, the first two acquisitions of each patient were independently analyzed by another observer blinded to previous results. For assessment of intra-observer variability, the first observer repeated analysis in

a random order. Both were blinded to 3DE results. Data on inter- and intra-observer variability for 3DE were available from a previous validation study[11].

Statistical analysis

Results for EDV, ESV and EF are represented as mean and standard deviation (SD). Data was tested for normality with the Shapiro-Wilk test. A repeated measures ANOVA was used for analysis of differences within the variations. Post-hoc testing was performed with the paired t-test. Regression and limits of agreement analysis was performed for 3DE and 2DE measurements according to the method of Bland and Altman[13]. Results for inter- and intraobserver variations are represented as mean ± SD for the difference between the two measurements. A value of p < 0.05 was considered to be significant.

Results

Successful image acquisition was achieved in 10/12 patients (83%). A total of 80 3D datasets were acquired in these 10 patients. In three patients, one dataset (4%) was of insufficient quality and excluded from analysis. One patient suffered from symptomatic hypotension during HD, although no intervention was required. The time for data analysis averaged 15 ± 5 minutes per 3D-dataset.

Table. Comparison of LV volume and function measurement by 3DE and 2DE methods

		R	Regression equation	SEE	Mean diff ± SD	T-test vs 3DE (P-value)
Single plane method	EDV (ml)	0.89	y = 0.88x – 0.86	23.12	-16.2 ± 22.7	<0.05
	ESV (ml)	0.92	y = 0.80x + 1.33	15.43	-15.3 ± 16.7	<0.02
	EF (%)	0.90	y = 0.93x + 5.55	4.87	3.1 ± 4.6	NS
Biplane Simpson	EDV (ml)	0.92	y = 0.85 – 3.04	18.91	-21.9 ± 19.4	<0.01
	ESV (ml)	0.93	y = 0.82x – 1.57	14.20	-16.8 ± 15.4	<0.01
	EF (%)	0.88	y = 0.92x + 4.60	5.27	1.7 ± 5.0	NS

Results of regression analysis and Bland-Altman analysis comparing LV volume and function with 3D-echocardiography (3DE) and two 2D-echocardiography (2DE) methods (see text for details).

The test for normality was not significant, indicating that the data did not significantly deviate from the normal distribution. Repeated measures ANOVA showed a significant difference between the measurement methods (F=10.5; p<0.02) but no significant difference between the moment of measurement (F=0.57, p<0.78). Because a significant effect in time was not found, the data was averaged for further analysis.

Correlation between the 2DE methods and 3DE for EDV (r<0.92), ESV (r<0.93) and EF (r<0.90) was moderate (see Figure 3). However, the limits-of-agreement
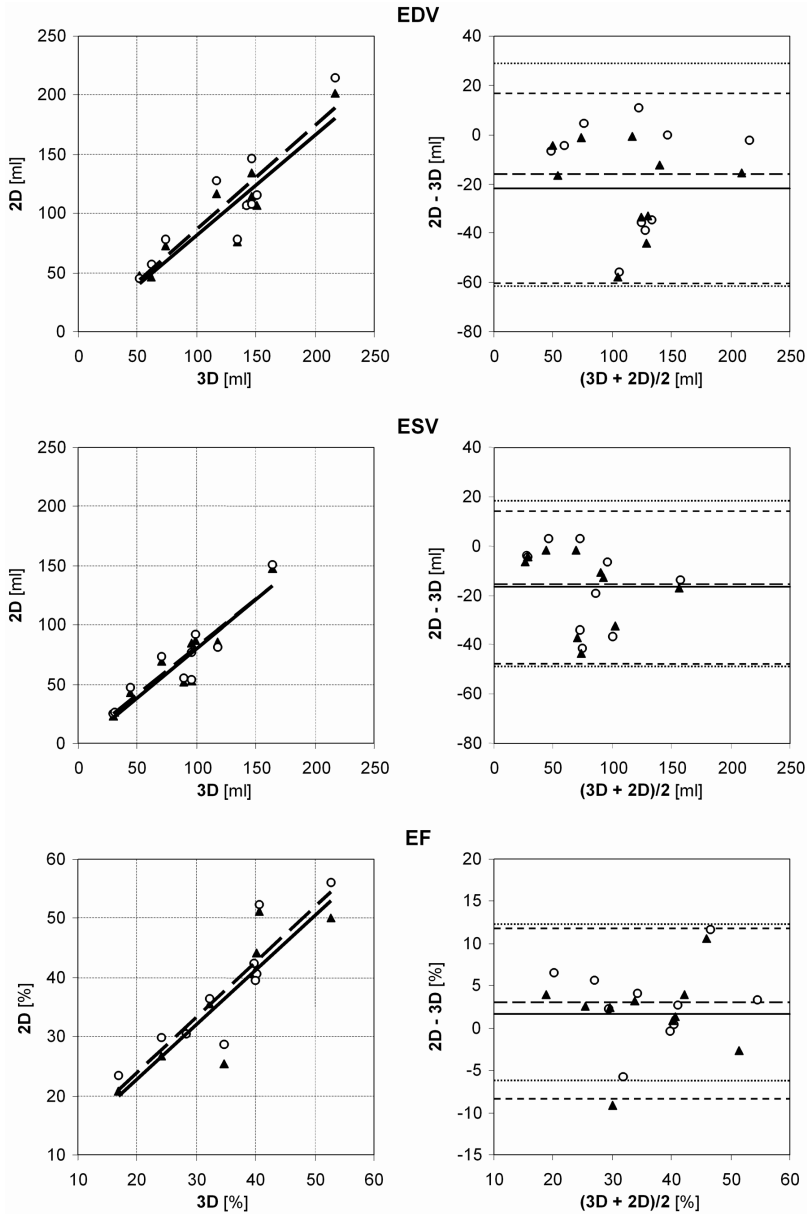
Figure 3:

Relation between 3DE and 2DE measurements of EDV, ESV, and EF. The left panels show the regression analysis between the two methods. Dashed lines delimit 95% confidence interval. (▲, solid line = biplane Simpson method; o, dashed line = single plane area length method). The right panels show plots of the difference between 3DE and 2DE, as a function of the average calculated volumes. Solid and dashed lines represent mean ± 2 SDs of the difference, respectively. (EDV = left ventricular end-diastolic volume; EF = left ventricular ejection fraction; ESV = left ventricular end-systolic volume).

between methods for EDV and ESV were poor with confidence intervals all larger than 30 ml (see Table). ANOVA analysis for EDV, ESV and EF showed significant differences between the different measurement methods (F=8.4, p<0.005). Post-hoc testing showed that both 2DE methods significantly underestimated EDV and ESV compared to 3DE. Limits-of-agreement analysis for EF showed an overestimation for both 2DE methods. However, these differences were not significant compared to 3DE.

Inter- and intra-observer variability:
The limits of agreement analysis of 3DE data from measurements performed by the first observer showed a mean difference of -1.4 ± 6.6 ml for EDV, -0.1 ± 4.4 ml for ESV and -0.3 ± 2.4% for EF. For 2DE using SPM, the results were −1.2 ± 11.4 ml, -3.2 ± 16.0 ml and 1.6 ± 10.6%, respectively. For 2DE using BSR, the results were 3.9 ± 13.9 ml, 1.7 ± 15.2 ml and 0 ± 10.5%, respectively.

The limits of agreement analysis demonstrated a mean difference of -0.1 ± 11.7 ml for LVEDV, 1.3 ± 8.7 ml for LVESV and -0.7 ± 4.8% for LVEF, for 3DE data by two independent observers. For 2DE using SPM, the results were 0.3 ± 8.1 ml, -10.6 ± 22.3 ml and 7.1 ± 14%, respectively. For 2DE using BSR, the results were −3.4 ± 14.7 ml, -2.5 ± 16.4 ml and 1.0 ± 10.3%, respectively.

Discussion

This study demonstrates that image acquisition using 3D-echocardiography is feasible for accurate evaluation of LV function in patients during HD. Previous studies showed that 3D echocardiography calculates LV volume with a precision comparable to cardiac magnetic resonance imaging[11,14,15]. While both techniques are superior to 2D echocardiography, magnetic resonance imaging is not feasible during HD. Tissue Doppler imaging (TDI), a newer Doppler technique advocated as less load-dependent[16,17], can be used during HD[18]. TDI primarily yields information on myocardial contraction and relaxation, but is less used for assessment of overall LV performance, which is usually expressed using the well-known parameters SV and ejection fraction.

The large interval between the limits of agreement and the underestimation of LV volume by 2DE are in line with previous reports[14,19]. 2DE calculations of LV function using the disc-summation method is based on the assumption that a ventricle can be represented by a series of stacked elliptic discs of varying diameters. In patients with regional wall motion abnormalities and deformed ventricles, this assumption may be unjustified and result in an inaccurate and poor reproducibility of 2DE measurements. Using 3DE, however, no assumption is made about the shape of the LV, and LV volume is calculated from a much greater set of data. Therefore, 2DE should be used with caution for LV function analysis when relatively small differences in

LV volume are expected, as during HD. When more image planes are used for LV volume calculation, as in 3DE, an increase in accuracy is observed. Previous studies suggested that at least four to eight image planes are necessary to accurately represent the ventricular volume[20,21]. Nosir et al. showed that a 1% change in LV volume can be observed with a 90% likelihood when 8 image planes are used[22].

To our knowledge, this is the first study to use 3DE during HD. Only one study used 3DE in HD patients for LV function determination[23]. However, this study was not performed in the HD department. Accurately assessing the changes in LV volumes during HD can result in a better insight into the development of dialysis hypotension. Especially the role of the so-called Bezold-Jarisch reflex, which leads to bradycardic hypotension believed to be triggered by a severely underfilled LV, is not well understood. Monitoring changes in LV filling may help predicting the onset of hypotension, and may guide therapeutic strategies such as ultrafiltration profiling. Additionally, more reproducible assessment of LV volumes, function and mass helps cardiovascular risk stratification, which is important not only for managing the dialysis population but also for the work-up of renal transplant candidates among dialysis patients.

Our study is limited by the small number of patients. However, this study was not designed to determine the effect of a single HD session on LV performance. During image acquisition, a partial left lateral decubitus position and 10 sec breath-hold were required. This was well-tolerated by the HD patients in our study. 3DE relies on achieving good endocardial border definition which depends on various factors. As patients in the HD department cannot be positioned in the most optimal way as they are in the echocardiography department (because of interference with blood lines, absence of examination table), this could hamper optimal image quality. Although effort was required by patient and ultrasonographist, we could acquire sufficient image quality in 80% of patients. In only 3 patients, a single acquisition was of insufficient quality. Previous studies have shown an improvement in image quality[24] and, subsequently, smaller limits of agreement in inter- and intraobserver variability when intravenous ultrasound contrast agents are used[25,26]. Further studies are necessary to evaluate the feasibility thereof in this patient population.

Conclusion

We conclude that successful image acquisition for 3D echocardiography is feasible for accurate and reproducible measurement of LV function during HD. This may improve the assessment of the acute effect of HD on cardiac function, and guide therapautic strategies aimed at preventing intradialytic hypotension.

References

1. Chaignon M, Chen WT, Tarazi RC, Nakamoto S, Salcedo E: Acute effects of hemodialysis on echographic-determined cardiac performance: improved contractility resulting from serum increased calcium with reduced potassium despite hypovolemic-reduced cardiac output. Am Heart J 1982;103:374-8.

2. Cohen MV, Diaz P, Scheuer J: Echocardiographic assessment of left ventricular function in patients with chronic uremia. Clin Nephrol 1979;12:156-62.

3. Bornstein A, Gaasch WH, Harrington J: Assessment of the cardiac effects of hemodialysis with systolic time intervals and echocardiography. Am J Cardiol 1983;51:332-5.

4. Zoccali C, Benedetto FA, Mallamaci F, Tripepi G, Giacone G, Cataliotti A, Seminara G, Stancanelli B, Malatino LS: Prognostic value of echocardiographic indicators of left ventricular systolic function in asymptomatic dialysis patients. J Am Soc Nephrol 2004;15:1029-37.

5. Gupta S, Dev V, Kumar MV, Dash SC: Left ventricular diastolic function in end-stage renal disease and the impact of hemodialysis. Am J Cardiol 1993;71:1427-30.

6. Galetta F, Cupisti A, Franzoni F, Carpi A, Barsotti G, Santoro G: Acute effects of hemodialysis on left ventricular function evaluated by tissue Doppler imaging. Biomed Pharmacother 2006;60:66-70.

7. Ie EH, Vletter WB, ten Cate FJ, Nette RW, Weimar W, Roelandt JR, Zietse R: Preload dependence of new Doppler techniques limits their utility for left ventricular diastolic function assessment in hemodialysis patients. J Am Soc Nephrol 2003;14:1858-62.

8. Tomson CR: Echocardiographic assessment of systolic function in dialysis patients. Nephrol Dial Transplant 1990;5:325-31.

9. Monaghan MJ: Role of real time 3D echocardiography in evaluating the left ventricle. Heart 2006;92:131-6.

10. Voormolen MM, Bouakaz A, Krenning BJ, Lancee CT, ten Cate FJ, Roelandt JRTC, van der Steen AFW, de Jong N: A New Transducer for 3D Harmonic Imaging: Proceedings of the IEEE International Ultrasonics Symposium. Munich, 2002, vol 2, pp 1261-1264.

11. Krenning BJ, Voormolen MM, van Geuns RJ, Vletter WB, Lancee CT, de Jong N, Ten Cate FJ, van der Steen AF, Roelandt JR: Rapid and accurate measurement of left ventricular function with a new second-harmonic fast-rotating transducer and semi-automated border detection. Echocardiography 2006;23:447-54.

12. Schiller NB, Shah PM, Crawford M, DeMaria A, Devereux R, Feigenbaum H, Gutgesell H, Reichek N, Sahn D, Schnittger I, et al.: Recommendations for quantitation of the left ventricle by two-dimensional echocardiography. American Society of Echocardiography Committee on Standards, Subcommittee on Quantitation of Two-Dimensional Echocardiograms. J Am Soc Echocardiogr 1989;2:358-67.

13. Bland JM, Altman DG: Statistical methods for assessing agreement between two methods of clinical measurement. Lancet 1986;1:307-10.

14. Gutierrez-Chico JL, Zamorano JL, Perez de Isla L, Orejas M, Almeria C, Rodrigo JL, Ferreiros J, Serra V, Macaya C: Comparison of left ventricular volumes and ejection fractions measured by three-dimensional echocardiography versus by two-dimensional echocardiography and cardiac magnetic resonance in patients with various cardiomyopathies. Am J Cardiol 2005;95:809-13.

15. Corsi C, Lang RM, Veronesi F, Weinert L, Caiani EG, MacEneaney P, Lamberti C, Mor-Avi V: Volumetric quantification of global and regional left ventricular function from real-time three-dimensional echocardiographic images. Circulation 2005;112:1161-70.

16. Sharma R, Pellerin D, Gaze DC, Mehta RL, Gregson H, Streather CP, Collinson PO, Brecker SJ: Mitral peak Doppler E-wave to peak mitral annulus velocity ratio is an accurate estimate of left ventricular filling pressure and predicts mortality in end-stage renal disease. J Am Soc Echocardiogr 2006;19:266-73.

17. Barberato SH, Mantilla DE, Misocami MA, Goncalves SM, Bignelli AT, Riella MC, Pecoits-Filho R: Effect of preload reduction by hemodialysis on left atrial volume and echocardiographic Doppler parameters in patients with end-stage renal disease. Am J Cardiol 2004;94:1208-10.

18. Ie EH, Zietse R: Evaluation of cardiac function in the dialysis patient--a primer for the non-expert. Nephrol Dial Transplant 2006;21:1474-81.

19. Jenkins C, Bricknell K, Hanekom L, Marwick TH: Reproducibility and accuracy of echocardiographic measurements of left ventricular parameters using real-time three-dimensional echocardiography. J Am Coll Cardiol 2004;44:878-86.

20. Tanabe K, Belohlavek M, Jakrapanichakul D, Bae RY, Greenleaf JF, Seward JB: Three-Dimensional Echocardiography: Precision and Accuracy of Left Ventricular Volume Measurement Using Rotational Geometry with Variable Numbers of Slice Resolution. Echocardiography 1998;15:575-580.

21. Siu SC, Rivera JM, Handschumacher MD, Weyman AE, Levine RA, Picard MH: Three-dimensional echocardiography: the influence of number of component images on accuracy of left ventricular volume quantitation. J Am Soc Echocardiogr 1996;9:147-55.

22. Nosir YF, Vletter WB, Kasprzak JD, Boersma E, Lequin MH, Elhendy AA, Yao J, Stoker J, Ten Cate FJ, Roelandt JR: Optimal rotational interval for 3-dimensional echocardiography data acquisition for rapid and accurate measurement of left ventricular function. J Am Soc Echocardiogr 2000;13:715-22.

23. Fathi R, Isbel N, Haluska B, Case C, Johnson DW, Marwick TH: Correlates of subclinical left ventricular dysfunction in ESRD. Am J Kidney Dis 2003;41:1016-25.

24. Kasprzak JD, Paelinck B, Ten Cate FJ, Vletter WB, de Jong N, Poldermans D, Elhendy A, Bouakaz A, Roelandt JR: Comparison of native and contrast-enhanced harmonic echocardiography for visualization of left ventricular endocardial border. Am J Cardiol 1999;83:211-7.

25. Yu EH, Sloggett CE, Iwanochko RM, Rakowski H, Siu SC: Feasibility and accuracy of left ventricular volumes and ejection fraction determination by fundamental, tissue harmonic, and intravenous contrast imaging in difficult-to-image patients. J Am Soc Echocardiogr 2000;13:216-24.

26. Malm S, Frigstad S, Sagberg E, Larsson H, Skjaerpe T: Accurate and reproducible measurement of left ventricular volume and ejection fraction by contrast echocardiography: a comparison with magnetic resonance imaging. J Am Coll Cardiol 2004;44:1030-5.

Chapter 5

Guiding and optimization of resynchronization therapy with dynamic three-dimensional echocardiography and segmental volume-time curves: a feasibility study

BJ Krenning
T Szili-Torok
MM Voormolen
DA Theuns
LJ Jordaens
CT Lancée
N de Jong
AFW van der Steen
FJ ten Cate
JRTC Roelandt

Abstract

Objective
To assess a new approach for guiding and hemodynamic optimization of resynchronization therapy, using three-dimensional (3D) transthoracic echocardiography.

Background
Resynchronization therapy for heart failure provides the greatest hemodynamic benefit when applied to the most delayed left ventricular (LV) site. Currently, the ideal LV pacing site is selected according to acute invasive hemodynamic assessment and/or tissue Doppler imaging.

Methods
A total of 16 patients with advanced heart failure and an implanted biventricular pacemaker were included in this study. Transthoracic apical LV images at equidistant intervals were obtained using a prototype, fast-rotating second harmonic transducer to reconstruct 3D LV datasets during sinus rhythm (SR), right ventricular (RV) apical and biventricular pacing mode. A semi-automated contour analysis system (4D LV analysis, TomTec, Germany) was used for segmental wall motion analysis and identification of the most delayed contracting segment and calculation of global LV function.

Results
Data acquisition duration was 10 s and analyzable 3D images were obtained in 12 patients. Of these patients, data during SR were available in 9 and during biventricular pacing in 11. The greatest contraction delay during SR was found in the anterior and antero-septal segments in five of nine patients. Biventricular pacing resulted in reduction of the contraction delay in seven of eight patients. The global LV function did not change significantly.

Conclusion
3D echocardiography with appropriate analytic software allows detection of the most delayed LV contracting segment and can be used to select the optimal pacing site during resynchronization therapy.

Introduction

Delayed intraventricular depolarization leads to dyssynchrony of ventricular contraction and worsens left ventricle (LV) dysfunction[1-4]. Resynchronization by simultaneous electrical stimulation of both ventricles significantly improves hemodynamics, resulting in increased exercise tolerance and hence quality of life[5-12]. Reduction in morbidity and mortality awaits confirmation from ongoing large-scale studies[5,13]. Recent data indicate that biventricular pacing provides the greatest hemodynamic benefit when applied to the LV segment with the most delayed contraction[14]. Tissue Doppler imaging (TDI) is currently used to identify the most delayed contraction site before the implantation of a resynchronization device[14-16]. This method cannot be used online and the assessment of the hemodynamic effects requires additional studies. It has been demonstrated in previous studies that volume–time curves (VTCs) provide quantitative information on LV performance[17,18]. The aim of the present study was to test the feasibility of 3D echocardiographic VTCs for determining the optimal pacing site. This allows simultaneous hemodynamic evaluation by measuring global LV function.

Table I. Patient characteristics and results for contraction delay measurements

Patients	age	NYHA class	Type of CM	pacing site	FCS	SR		BiV		RV	
						MDS	delay (ms)	MDS	delay (ms)	MDS	delay (ms)
1.	76	III	2	ant	16	9	64	1	69	9	61
2.	56	III	2	pcv	7	10	20	*	*	3	50
3.	56	II	1	plcv	16	2	177	8	80	2	167
4.	71	II	2	lcv	11	7	200	4	143	8	137
5.	64	III	1	plcv	8†	*	*	11	130	8	230
6.	68	III	2	plcv	3†	*	*	6	261	6	198
7.	67	II	2	plcv	10†	*	*	3	53	9	45
8.	62	III	1	plcv	6	2	68	6	66	3	205
9.	63	III	1	plcv	12	7	256	3	128	14	240
10.	59	III	1	pcv	9	11	221	11	113	11	90
11.	61	III	1	plcv	6	9	140	5	88	8	248
12.	53	II	1	ant	12	1	182	11	108	2	228

ant = anterior, CM = cardiomyopathy (1 = dilated cardiomyopathy, 2 = ischemic cardiomyopathy), BiV= biventricular pacing, FCS = first contracting segment, lcv = lateral cardiac vein, MDS= most delayed segment, NYHA = New York Heart Association, pcv = posterior cardiac vein, plcv = posterolateral cardiac vein, RV= right ventricular pacing, SR= sinus rhythm, * = not applicable, † = during biventricular pacing

Methods

Study patients

We studied 16 patients with severe heart failure and a permanent biventricular pacemaker. All patients gave informed consent. Patient characteristics are listed in Table 1. The diagnosis of dilated cardiomyopathy was established according to the classification of cardiomyopathy published previously[19]. Criteria for biventricular pacing were severe heart failure (NYHA II–IV) and dilated cardiomyopathy associated with complete left bundle branch block and a QRS duration of > 125 ms. The LV pacing lead was positioned in the coronary sinus and the right atrial and right ventricular (RV) leads in standard locations. Three acquisitions for 3D reconstruction were performed as follows: The first acquisition was performed in the biventricular pacing mode and the second after the pacemaker was reprogrammed for RV pacing. In patients with intact atrio-ventricular conduction and sinus rhythm (SR), the pacemaker was reprogrammed in order to perform acquisitions during SR. In every patient, the pacemaker was finally reset to the original settings. Acquisitions were performed 5 min after the pacing mode was switched. Data analysis was performed off-line for this feasibility study.

Image acquisition

We used a prototype transthoracic, fast-rotating ultrasound transducer for 3D echocardiographic image acquisition[20] (Fig. 1), which is connected to a commercially available ultrasound system (GE Vingmed Vivid FiVe, Horton, Norway). The 64-element transducer array has a center frequency of 3 MHz and second harmonic capabilities[21]. It continuously rotates inside the transducer assembly at a maximum speed of 8 revolutions/s. The frame rate of the ultrasound system is 100 frames per second. The typical acquisition time is 10 s during a single end-expiratory breath

Figure 1:
Latest prototype of the continuous fast-rotating transducer.

hold. Patients were studied in the left lateral decubitus position with the transducer in the apical position and the image plane rotating around the LV long axis. The depth setting was adjusted to visualize the entire LV and part of the left atrium. Gain and power settings were optimized for endocardial border visualization. The ECG signal was simultaneously recorded for 3D reconstruction.

Image processing

Data are transferred via a network connection to a dedicated workstation for processing and analysis. With self-developed software, using MatLab (The MathWorks, Natick, MA, USA), the original 2D images are post-processed by placing them in their correct spatial and temporal (ECG reference) position using multi beat data fusion[22]. The cardiac cycle is divided in 12 equal intervals, which allows to create 12 3D datasets. Due to the continuous rotation of the transducer array, the original 2D images have a curved shape. However, these are not suited for automated contour analysis with currently available software. Therefore, 20 equidistant plane cross-sectional images (9° interval) are re-sampled from these 12 datasets and used for further analysis.

Image analysis

All the 20 cross-sectional images re-sampled from each of the 12 datasets are subsequently imported into the TomTec® 4D LV-analysis software (TomTec® Imaging Systems, Germany) and displayed (Fig. 2). Their orientation in 3D space is deter-
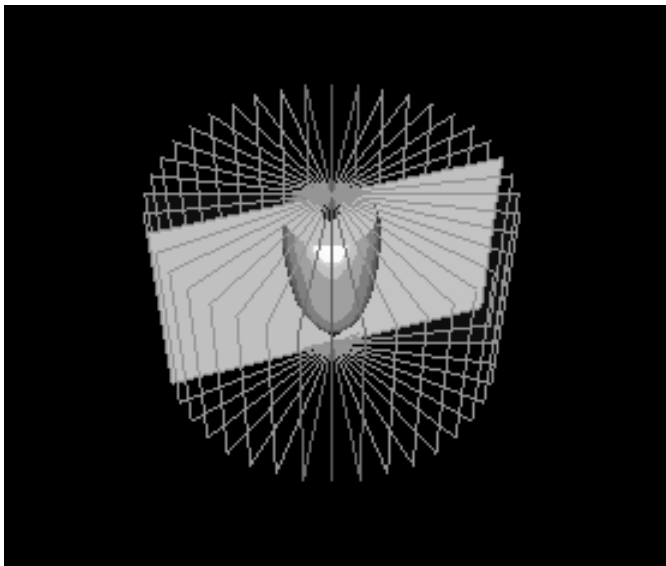
Figure 2:
From each dynamic 3D data set, up to 20 cross-sectional images can be selected. The orientation of each cross-section is shown.

mined by marking the mitral valve, aortic root and apex as landmarks. An elliptical model is placed over one of the images of each cross-sectional position. After this, the software automatically performs endocardial border detection in all images of each cross-sectional position in the 12 datasets. A spatio-temporal spline model is used to generate smooth contours for both the temporal and spatial domain. The long axis of the ventricle is calculated from the center of the mitral annulus to the most distant point in the ventricle, which is the apex.

Two experienced investigators verified and corrected the results from the automated border detection where necessary. This was done blinded, without knowledge of the pacing mode for each analysis. The papillary muscles within the LV cavity are not taken into account for the definition of the contour. After completion of the endocardial border tracing, the program performs a dynamic surface rendered endocardial reconstruction of the LV (Fig. 3A). For each pacing mode, a VTC is plotted from which global LV end-diastolic volume (LVEDV), end-systolic volume (LVESV) and ejection fraction (EF) are calculated applying Gaussian quadrature formulas.

The LV endocardial surface is subdivided in 16 segments, which are colour coded for orientation (Fig. 3B). A segmental volume represents the pyramidal volume
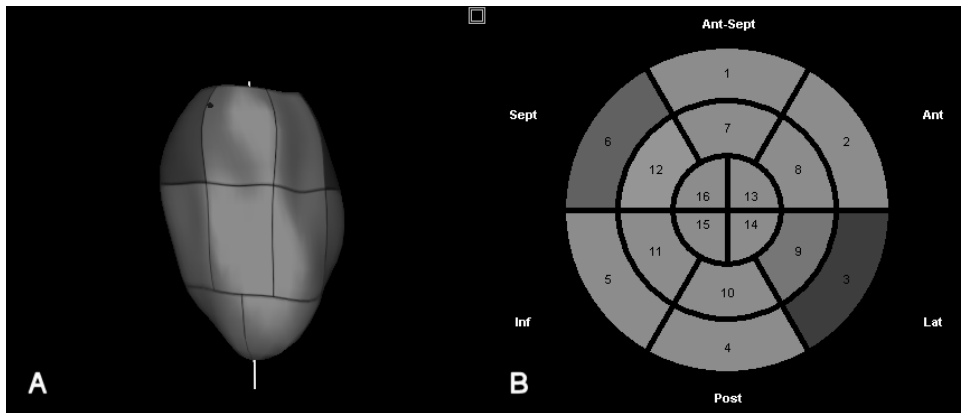
Figure 3:

Three-dimensional reconstruction of the LV (A) and bulls-eye view according to which the endocardial surface is subdivided in 16 colour-coded segments (B).

of a segment to the center of gravity (Fig. 4). The volume change of a segment over the cardiac cycle is plotted in a VTC (Fig. 5), in which time is defined as percentage of the total cardiac cycle. The end-systolic moment, at which a segment has completed maximal myocardial contraction, is represented by the nadir of the segmental volume curve. This moment was extracted from the VTC for every segment in every pacing mode. The difference in time to maximal myocardial contraction between segments was used to assess regional mechanical delay and a measure
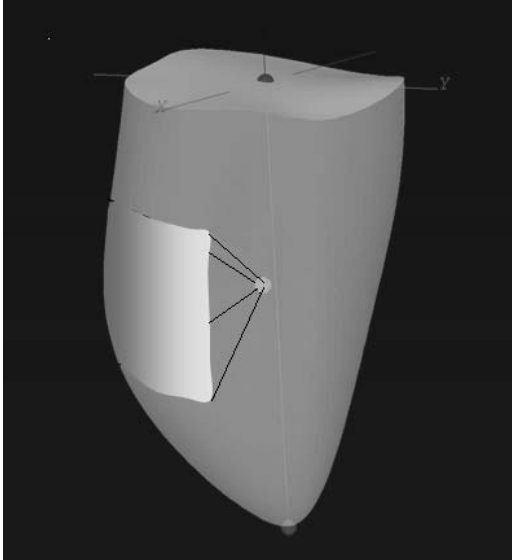
Figure 4:

A segmental volume represents the pyramidal volume of a segment to the center of gravity. The long axis of the ventricle is calculated from the center of the mitral annulus to the apex.

of segmental dyssynergy. From the VTC that represents segmental volume changes in SR, the first contracting segment and the most delayed segment were identified. The delay in contraction was calculated as the difference in time to maximal contraction between these segments and is expressed as percentage of the total cardiac cycle. Using the RR-interval, this was re-calculated in milliseconds. When a segment is hypo- or akinetic, which we defined as a segmental volume change during any part of the cardiac cycle of less then 20%, the segment is not included.
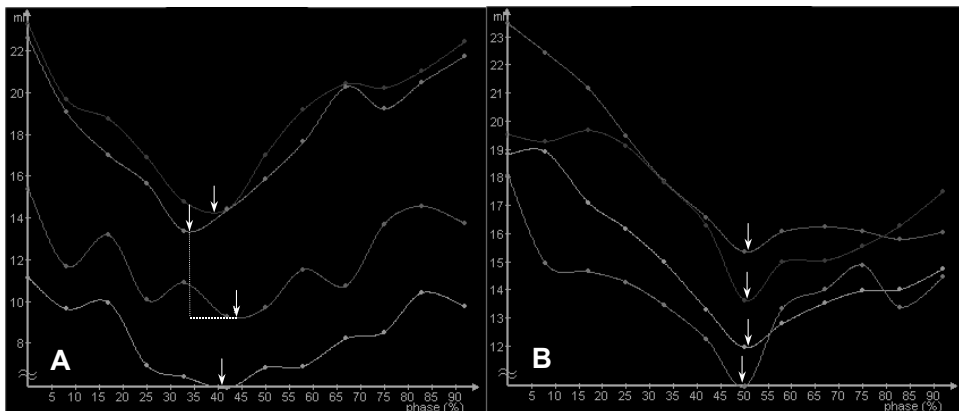
Figure 5:

Example of volume-time curves of four different segments. During sinus rhythm, each segment completes myocardial contraction at a different moment (indicated with an arrow for every segment), causing LV dyssynchrony. From the various delays, the largest delay is shown with a dotted line (A). During biventricular pacing, synchrony in segmental contraction is present (B).

In both biventricular and RV pacing mode, the most delayed segment is determined and the delay between this segment and the first contracting segment calculated.

Statistical analysis
Data are presented as mean ± S.D.. 3D measurements of LV volume were calculated by the analysis software after completion of the endocardial border tracing. To assess accuracy, analysis of VTCs was performed by two observers and analyzed by linear regression and a limits-of-agreement analysis, expressed as the mean difference and 2 S.D. of the difference between the measurements of the two observers. To determine whether the difference in the values between the two observers and between pacing modes was statistically significant, a paired t-test was performed. A probability level of $p < 0.05$ was considered significant.

Results

Of the 16 patients, four were excluded from analysis because of inadequate echocardiographic image quality for faithful automated analysis. In 3 of the remaining 12 patients, no spontaneous sinus rhythm was present and therefore only acquisitions in biventricular and RV pacing mode were performed. In one patient, we did not perform an acquisition in biventricular pacing mode because of LV lead displacement.

Global LV function
The mean ejection fraction of all patients before implantation, by equilibrium radionuclide angiography, was 24 ± 7%. During sinus rhythm, the mean LVEDV, LVESV and LVEF derived from the VTC were 294 ± 85 ml, 230 ± 94 ml and 24 ± 12%, respectively. During RV pacing, these values were 291 ± 97 ml, 225 ± 81 ml and 23 ± 6% and during biventricular pacing, 282 ± 94 ml, 226 ± 86 ml and 21 ± 6%, respectively. No significant difference was present between these values.

Dyssynchrony
The mean heart rate during SR was 69 ± 7 min^{-1}, during biventricular pacing 73 ± 9 min^{-1} and during RV pacing 74 ± 9 min^{-1}. No significant difference was present between these values. In six of eight patients, heart rate was less during SR compared to biventricular pacing. Table 1 shows the most delayed segment for every pacing mode and the delay between the first contracting and most delayed segment. The mean delay was 147 ± 80 ms during SR, 103 ± 34 ms during biventricular pacing ($p < 0.01$; SR vs. biventricular pacing) and 158 ± 78 ms during RV pacing ($p < 0.01$; RV vs. biventricular pacing). In five of nine patients, the anterior or antero-septal segment was most delayed during SR. Biventricular pacing resulted in reduction of

$$y = 0{,}9502x + 1{,}9719$$
$$r = 0{,}9591$$
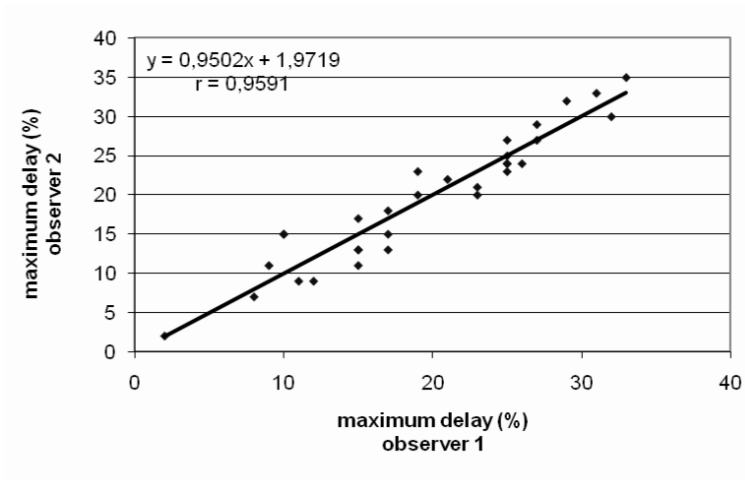
Figure 6:

Regression analysis for measurement of delay between the two most delayed segments by two observers.

the contraction delay in seven patients, compared to SR. Also, in six patients, the contraction delay was less during biventricular pacing compared to RV pacing.

Interobserver agreement

Linear regression analysis indicated a good correlation (r = 0.96) between measurements of delay in contraction between the first contracting segment and the most delayed site by two observers (Fig. 6). The standard error of estimate was 2.42%. The limits-of- agreement analysis demonstrated a small mean difference (0.03 ± 2.50%) between measurements. A paired t-test indicated no significant mean difference between the two observers.

Discussion

This study shows that transthoracic dynamic 3D echocardiography performed with a fast-rotating transducer and combined with semi-automated contour analysis allows to identify LV segments with dyssynchrony together with hemodynamic evaluation. Our data indicate that this method is feasible for the selection of the optimal pacing site during resynchronization therapy.

Rationale for measuring mechanical delay in patients undergoing resynchronization device implantation

A delay in intraventricular conduction leads to dyssynchrony of ventricular contraction which can be corrected by biventricular pacing and subsequently improve

hemodynamics and consequently exercise tolerance and quality of life in patients with severe heart failure. Large-scale trials are ongoing to study long-term effects including morbidity and mortality[5,13,23]. However, a substantial proportion of the patients does not show improvement. This may be partly related to methodological reasons. Indeed, a prolonged QRS complex cannot quantify the degree of dyssynchrony. Clearly, biventricular pacing provides the most benefit when applied to the segment of the LV that is most delayed in contraction. Therefore pacing should be applied to this site but it should be noted that this site will not always be approachable during implantation. While longterm studies showed improvement of LVEF with biventricular pacing, this could not be observed in this study. Possibly, other regulating factors counterbalance the hemodynamic effect of changing pacemaker programming.

The role of improved imaging techniques to guide and evaluate biventricular pacing

Echocardiography has an important role in the evaluation of patients with mechanical dyssynchrony before biventricular pacemaker implantation[24,25]. Sogaard et al.[26] previously used 3D echocardiography for hemodynamic assessment in patients before and after biventricular pacemaker implantation. Currently, TDI is most often used as a guiding tool for the implantation[15,16] and is useful for identifying LV myocardial contraction dyssynchrony at discrete points in patients after ventricular resynchronization[14]. It is suggested that TDI analysis could serve in the future both as a tool for pre-implantation assessment and as a guide to select the most optimal pacing site. However, this approach requires a lengthy echo study and analysis before the implantation, while only the longitudinal function in the basal and mid-segments are studied. Also other diagnostic modalities, such as MRI[18] and gated-SPECT [27], can be used to create volume–time curves and assess regional wall motion. However, MRI cannot be used after device implantation because of its magnetic properties. 3D echocardiography with appropriate software for segmental wall motion analysis allows to determine dyssynchrony between all segments. Obviously, expressing the delay is an issue and requires standardization in the near future. Currently, several parameters are used for describing intra- and interventricular delays during the heart cycle. Using our method, the delay is expressed in relative units (as percentage of the total heart cycle). Actually, this method allows demonstration of shortening of the diastolic period when the heart rate increases. This may play a role in an adverse outcome of this patient population. This phenomenon is clearly demonstrated in Fig. 5. In this particular example, the heart rate in sinus rhythm was lower than in a paced rhythm. This results in relatively longer diastolic period. As the heart rate increases, the systolic period shortens relatively less than the diastolic period, meaning that the systolic periods are almost identical in absolute units (ms), but the diastolic periods become different. Additionally, the position of the RV lead has a significant impact on the LV conduction pattern.

Therefore, the optimal technique should provide the information during the implantation procedure and additional hemodynamic data. This is possible with a fastrotating ultrasound transducer and appropriate software for analysis.

Limitations of the study

We used prototype equipment for this proof-of-principle study requiring further refinements. The post-processing time to obtain a 3D dataset must be shortened to make this technique a practical guiding tool during the intervention. The semi-automated border detection algorithms are userfriendly, but manual interaction remains often a necessity. Real-time 3D echocardiography using a matrix transducer is also appropriate for acquisition of 3D datasets and optimization of resynchronization therapy, using the same border detection and analytic software. Most experience is with the system developed at Duke University[28] (Volumetric Medical Imaging), which makes use of a sparse matrix phased array transducer to scan a 60° x 60° pyramidal volume using parallel processing technology. More recently, Philips Medical Systems has introduced a matrix phased-array transducer with 3000 transmit-receive elements. Development of new border detection algorithms along with technological improvements of 3D echocardiography should be able to improve the accuracy of semi-automated border tracing and eventually provide automatic, even on-line, data analysis in the future.

This was not a prospective study and the patients studied had already their resynchronization device in place. Therefore, we could only study the feasibility of the method and whether dyssynchrony in segmental contraction could be measured.

During image acquisition, a 10-s breath hold was required. We did not find this inconvenient in our patient population with advanced heart failure.

Conclusion

3D echocardiography is a feasible approach for determination of the most delayed LV site with the additional option to assess hemodynamic information, such as LVEDV, LVESV and EF. This preliminary data suggests that 3D echocardiography can be used for selection of the most optimal pacing site before and during resynchronization device implantation. Further studies with prospective study design are required to validate this data against other techniques, e.g. TDI.

References

1. Grines CL, Bashore TM, Boudoulas H, Olson S, Shafer P, Wooley CF. Functional abnormalities in isolated left bundle branch block. The effect of interventricular asynchrony. Circulation 1989;79:845–53.

2. Kerwin WF, Botvinick EH, O'Connell JW, et al. Ventricular contraction abnormalities in dilated cardiomyopathy: effect of biventricular pacing to correct interventricular dyssynchrony. J Am Coll Cardiol 2000;35:1221– 7.

3. Shamim W, Francis DP, Yousufuddin M, et al. Intraventricular conduction delay: a prognostic marker in chronic heart failure. Int J Cardiol 1999;70:171–8.

4. Xiao HB, Lee CH, Gibson DG. Effect of left bundle branch block on diastolic function in dilated cardiomyopathy. Br Heart J 1991;66:443– 7.

5. Mascioli G, Curnis A, Bontempi L, Dei Cas L. Biventricular pacing for patients with severe congestive heart failure: a single center experience. Ital Heart J 2002;3:598 – 602.

6. Abraham WT, Fisher WG, Smith AL, et al. Cardiac resynchronization in chronic heart failure. N Engl J Med 2002;346:1845– 53.

7. Cazeau S, Leclercq C, Lavergne T, et al. Effects of multisite biventricular pacing in patients with heart failure and intraventricular conduction delay. N Engl J Med 2001;344:873–80.

8. Daubert JC, Ritter P, Le Breton H, et al. Permanent left ventricular pacing with transvenous leads inserted into the coronary veins. Pacing Clin Electrophysiol 1998;21:239–45.

9. Gras D, Mabo P, Tang T, et al. Multisite pacing as a supplemental treatment of congestive heart failure: preliminary results of the Medtronic Inc. InSync Study. Pacing Clin Electrophysiol 1998;21:2249– 55.

10. Leclercq C, Cazeau S, Le Breton H, et al. Acute hemodynamic effects of biventricular DDD pacing in patients with end-stage heart failure. J Am Coll Cardiol 1998;32:1825– 31.

11. Leclercq C, Victor F, Alonso C, et al. Comparative effects of permanent biventricular pacing for refractory heart failure in patients with stable sinus rhythm or chronic atrial fibrillation. Am J Cardiol 2000;85:1154– 6 (A9).

12. Kuhlkamp V. Initial experience with an implantable cardioverterdefibrillator incorporating cardiac resynchronization therapy. J Am Coll Cardiol 2002;39:790– 7.

13. Abraham WT. Cardiac resynchronization therapy for heart failure: biventricular pacing and beyond. Curr Opin Cardiol 2002;17:346– 52.

14. Ansalone G, Giannantoni P, Ricci R, Trambaiolo P, Fedele F, Santini M. Doppler myocardial imaging to evaluate the effectiveness of pacing sites in patients receiving biventricular pacing. J Am Coll Cardiol 2002;39:489– 99.

15. Sogaard P, Egeblad H, KimWY, et al. Tissue Doppler imaging predicts improved systolic performance and reversed left ventricular remodeling during long-term cardiac resynchronization therapy. J Am Coll Cardiol 2002;40:723–30.

16. Bax JJ, Molhoek SG, van Erven L, et al. Usefulness of myocardial tissue Doppler echocardiography to evaluate left ventricular dyssynchrony before and after biventricular pacing in patients with idiopathic dilated cardiomyopathy. Am J Cardiol 2003;91:94 – 7.

17. Zeidan Z, Erbel R, Barkhausen J, Hunold P, Bartel T, Buck T. Analysis of global systolic and diastolic left ventricular performance using volume–time curves by real-time three-dimensional echocardiography. J Am Soc Echocardiogr 2003;16:29– 37.

18. Soldo SJ, Norris SL, Gober JR, Haywood LJ, Colletti PM, Terk M. MRI-derived ventricular volume curves for the assessment of left ventricular function. Magn Reson Imaging 1994;12:711– 7.

19. Kuhn H, Beer G, Gietzen F. Definition and classification of cardiomyopathies. Circulation 1996;94:2991–2.

20. Djoa KK, de Jong N, van Egmond FC, et al. A fast rotating scanning unit for real-time three-dimensional echo data acquisition. Ultrasound Med Biol 2000;26:863– 9.

21. Voormolen MM, Bouakaz A, Krenning BJ, et al. A new transducer for 3D harmonic imaging. Proc - IEEE Ultrason Symp 2002. p. 1261– 4.

22. Lancee CT, van Egmond FC, de Jong N, et al. Data processing for a fast rotating phased array real-time 3D acquisition unit. Proc – IEEE Ultrason Symp 2000:1597 – 600.

23. Lozano I, Bocchiardo M, Achtelik M, et al. Impact of biventricular pacing on mortality in a randomized crossover study of patients with heart failure and ventricular arrhythmias. Pacing Clin Electrophysiol 2000;23:1711– 2.

24. Abraham WT. Rationale and design of a randomized clinical trial to assess the safety and efficacy of cardiac resynchronization therapy in patients with advanced heart failure: the Multicenter InSync Randomized Clinical Evaluation (MIRACLE). J Card Fail 2000;6:369– 80.

Chapter 6

Assessment of left ventricular function by three-dimensional echocardiography

BJ Krenning
MM Voormolen
JRTC Roelandt

Abstract

Accurate determination of LV volume, ejection fraction and segmental wall motion abnormalities is important for clinical decision-making and follow-up assessment. Currently, echocardiography is the most common used method to obtain this information. Three-dimensional echocardiography has shown to be an accurate and reproducible method for LV quantitation, mainly by avoiding the use of geometric assumptions. In this review, we describe various methods to acquire a 3D-dataset for LV volume and wall motion analysis, including their advantages and limitations. We provide an overview of studies comparing LV volume and function measurement by various gated and realtime methods of acquisition compared to magnetic resonance imaging. New technical improvements, such as automated endocardial border detection and contrast enhancement, will make accurate on-line assessment with little operator interaction possible in the near future.

Review

Accurate quantification of left ventricular (LV) volume and function is important in clinical decision-making and follow-up assessment. Although various other techniques including invasive angiography, radionuclide angiography and magnetic resonance imaging are used, echocardiography is currently the most commonly applied modality in the practice of cardiology.

M-mode echocardiography, a one dimensional ultrasound scanning of the cardiac structures, was developed in the early 1970s and immediately applied in practice for left ventricular function assessment because of its simple algorithm and non-invasiveness. Ejection fraction was estimated as a percentage derived from the mid left ventricular diameters in end-systole and end-diastole and expressed as fractional shortening. However, serious problems were raised especially in patients with myocardial infarction and asymmetric ventricles.

Two-dimensional sectional echocardiography, with the ability of imaging of the heart in tomographic views, considerably improved the accuracy of left ventricular volume measurement. Of the different mathematical models, modified biplane Simpson's rule provided more accurate data in both symmetric and asymmetric left ventricles.

Software-based algorithms for automatic endocardial border detection and on-line calculation of left ventricular volume and ejection fraction have been developed. As a result, two-dimensional echocardiography has become a routine examination for left ventricular volume and function assessment but the assumptions about LV geometry remain a limitation.

In the past decade, three-dimensional echocardiography has emerged as a more accurate and reproducible approach to LV quantitation mainly by avoiding the use of geometric assumptions of the LV shape. Three methods have been proposed for the acquisition of temporal and positional image data: the use of positional locators (freehand scanning), rotational systems and real-time volumetric scanning. Reconstruction methods using positional locators and rotational scanning systems require additional intervention for respiratory gating (or breathhold) and off-line post-processing of data using specific software. This has limited current routine application in clinical practice. Real-time three-dimensional echocardiography has a great potential for immediate assessment of LV function in various clinical scenarios including stress echocardiography and during interventional procedures.

However, all methods need a stable cardiac rhythm and constant cardiac function during image acquisition.

Freehand scanning (random imaging)

Different devices have been developed for locating the ultrasound transducer and the imaging planes through the ventricles[1,2]. These devices allow free movement of the transducer at one acoustic window or at different acoustic windows. An inter-sectional line or an image plane (usually a longitudinal view of the left ventricle) is used to guide the position and orientation of other imaging planes. The endocardial border of the left ventricle on each cross-sectional view is manually traced. All the traced lines are connected according to their spatial order to form a three-dimensional wire-frame image. The volume of the left ventricle is then calculated by the wedge summation method. Accurate results from this mode of reconstruction have been achieved in both symmetrical and aneurysmatic left ventricles. The limitation of this method is that the spaces between the sampled cross-sectional images are uneven and mistakes may result when interpolating big gaps between imaged planes. Furthermore, the reconstructed three-dimensional images are static and lack tissue depiction, which limits accurate endocardial border identification.

Gated sequential imaging

A. Linear acquisition

Parallel imaging can be performed by computer-controlled movement of the ultrasound transducer in a linear direction (Figure 1). Both a transthoracic and transoesophageal approach were evaluated for this mode of data acquisition.

B. Fan-like scanning

A pyramidal dataset can be obtained by moving the ultrasound transducer in a fan-like arc at prescribed angles (Figure 1). This is accomplished by computer-controlled motors adapted to the transthoracic or transoesophageal probe[3].

C. Stepwise rotational scanning

In this approach, the transducer is rotated around its central axis, resulting in a conical volume dataset (Figure 1). Different algorithms have been developed for computercontrolled sequential image collection of the heart[4]. The endocardial contours of a series of images obtained with a multiplane (omniplane) precordial transducer can be directly traced and used for volume calculation. In three-dimensional reconstruction, a series of images with rotational intervals between 2° and 16° is acquired and a voxel-based three-dimensional dataset is realised. With volume-rendering and various shading techniques, the reconstructed image accurately portrays the tissue characteristics and depth of the cardiac anatomy. Paraplane methods provide multiple equidistant parallel short-axis planes (discs) allowing systematic cross-sectional review of the three-dimensional dataset. It has been shown that slices up to a thickness of 10 mm allow accurate volume determination[5]. By tracing the left ventricular endocardial border in each short-axis image,
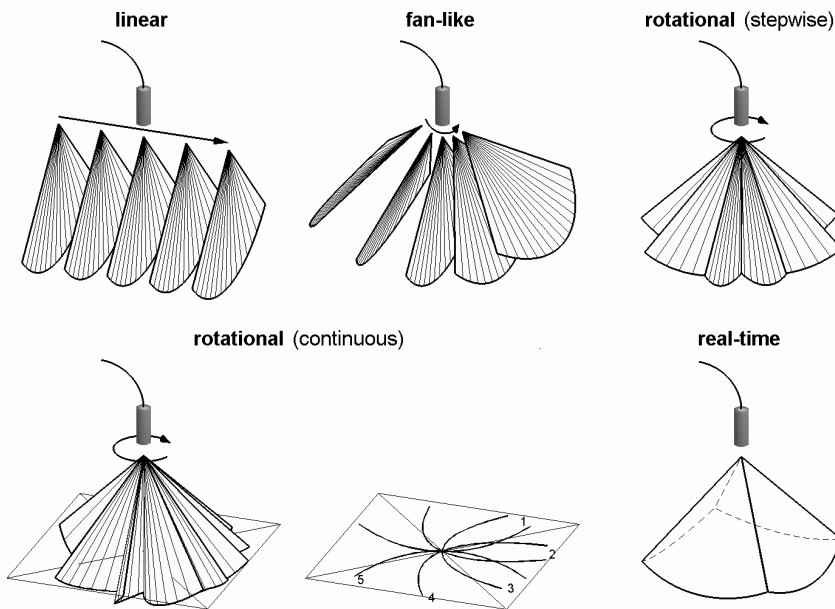
Figure 1:
Different methods of data acquisition for transthoracic 3D-echocardiography. Continuous rotation results, unlike stepwise rotational scanning, in a curved shape of the original images. Real-time imaging provides a pyramidal dataset instantly.

the volume of each slice is calculated by the computer since the slice thickness is known. A summation of the volumes of all slices yields the total volume of the left ventricular cavity at end-diastole or end-systole[4,5]. Subtraction of end-systolic volume from end-diastolic volume results in stroke volume of the left ventricle. The percentage of stroke volume over end-diastolic volume represents left ventricular ejection fraction.

Other algorithms for volume calculation, such as TomTec 4DLV analysis software, are based on the analysis of longaxis views (Figure 2). This software is able to display a dynamic reconstruction of the LV after semi-automated border detection. Not only the sizes and shapes of the left ventricle, but also the regional wall motion of the myocardium can be analysed.

D. Continuous rotational scanning
Various acquisition methods based on continuous rotation with an internally rotating array are reported[6–8]. Some models require inversion of rotation because of cable twisting, thereby making the acquisition less efficient and the reconstruc-
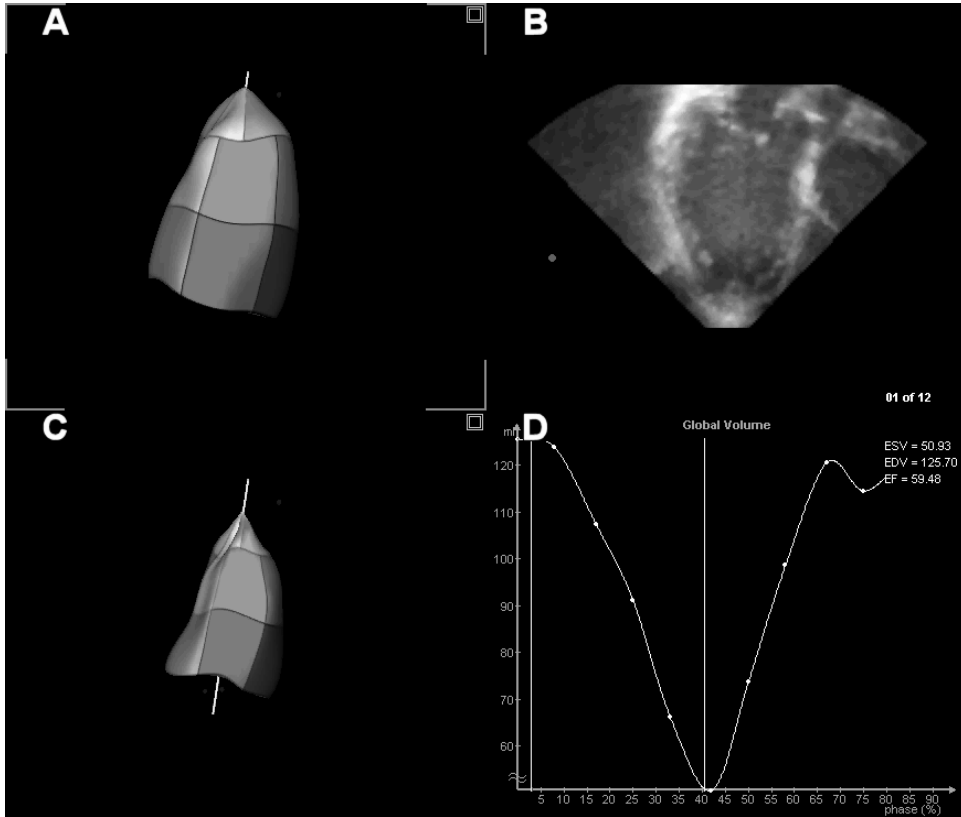
Figure 2:
End-diastolic (A) and End-systolic (C) reconstruction of the left ventricle after semi-automated border analysis of the long-axis views (B). Time volume curve from which ejection fraction can be derived (D).

tion of datasets more complex. Fast continuous rotational scanning of the LV from an apical window can be performed with a newly developed transducer assembly using a standard second-harmonic phased-array transducer and ultrasound system (VingMed Vivid 5) and allows acquisition of 16 volumetric datasets/ sec[9]. The typical acquisition time of 10s makes it possible to acquire all data during a single breath-hold. A slipring, consisting of a static and a rotating part, maintains electrical contact between the rotating array and the static part of the transducer. The original images are transferred to a workstation for reconstruction of the datasets and semi-automated analysis of the LV endocardial contours[10]. This allows rapid calculation of LV volumes, ejection fraction and wall motion analysis. Such a special dedicated system offers advantages for follow-up studies, stress echocardiography and during interventional procedures (e.g. resynchronisation therapy). Initial

experience indicates that this near real-time approach is an alternative to real-time volumetric systems for global and regional wall motion analysis of the LV.

Real-time imaging

The ideal way of three-dimensional echocardiography is on-line acquisition of a three-dimensional dataset of the heart without the need for ECG and respiratory gating avoiding spatial motion artefacts. The first real-time 3D system has been developed by Von Ramm et al.[11] at Duke University and most experience is with

Table 1

Volume and function measurement by reconstruction 3DE in comparison with magnetic resonance imaging

Author/ref.	Object	N	r.	SEE	Mean Diff. ± SD
Gopal et al.[12,14]	LV-EDV	15	0.92	7 ml	
	LV-ESV	--	0.81	4 ml	
Iwase et al.[15]	LV-EDV	30	0.93		-17 ± 23 ml
	LV-ESV	--	0.96		-4 ± 18 ml
	LV-EF	--	0.85		-2 ± 6%
Buck et al.[16]	LV-EDV	23	0.97	14.7 ml	-10.7 ± 14.5 ml
	LV-ESV	--	0.97	12.4 ml	-3.4 ± 12.9 ml
	LV-EF	--	0.74	5.6%	-2.5 ± 6.7%
Altmann et al.[18]	LV-EDV	12	0.98	8.7 ml	-14.2 ± 8.3 ml
	LV-ESV	--	0.98	5.6 ml	-3.4 ± 5.5 ml
	LV-EF	--	0.85	5.3%	-4.4 ± 5.3 %
Nosir et al.[19]	LV-EDV	46	0.98		-1.4 ± 13.5 ml
	LV-ESV	--	0.98		-1.5 ± 10.5 ml
	LV-EF	--	0.98		0.2 ± 2.5%
Kim et al.[20] (patients)	LV-EDV	18			6.4 ± 20 ml
	LV-ESV	--			0.0 ± 13.3 ml
	LV-EF	--			1.4 ± 3.5 %
Kim et al.[20] (volunteers)	LV-EDV	10			-3.1 ± 4.9 ml
	LV-ESV	--			-1.4 ± 2.2 ml
	LV-EF	--			0.5 ± 1.8 %
Poutanen et al.[21] (children)	LV-EDV	30	0.80		4.0 ± 19.6 ml
	LV-ESV	--	0.88		0.4 ± 13.0 ml
	LV-EF	--	0.20		1.7 ± 15.1%
Mannaerts et al.[22]	LV-EDV	17	0.74		-13.5 ± 13.5 %
	LV-ESV	--	0.88		-17.7 ± 23.9 %
	LV-EF	--	0.89		-1.8 ± 5.8 %
Krenning et al. (submitted)	LV-EDV	15	0.98	13.4 ml	-22.7 ± 13.6 ml
	LV-ESV	--	0.99	8.7 ml	-12.6 ± 9.9 ml
	LV-EF	--	0.97		

3DE = three-dimensional echocardiography; N = number of subjects; LV = left ventricle; r = correlation coefficient; SEE = standard error or regression; Diff. = difference; SD = standard differentiation; EDV = end-diastolic volume; ESV = end-systolic volume; EF = ejection fraction.

this system (Volumetric Medical Imaging). This system makes use of a sparse matrix phased array transducer of 512 elements to scan a 60° × 60° pyramidal tissue volume using parallel processing technology which permits the reception of 16 lines for each transmitted signal (16:1) at a rate of 17 volumes/sec with a depth of 16 cm. Image display for analysis consists of 2 independent B-modes or 3 C-mode scans (these are cross-sections parallel to the transducer face which are displayed simultaneously in selected orientations. LV volumes are calculated with dedicated analytic software from either a series of parallel C-scans (short-axis views) or a series of rotated apical long-axis views. More recently, Philips Medical Systems has introduced its live 3D system using a matrix phased-array transducer with 3000 transmit-receive elements. In this transducer, multiple recordings are automatically performed to cover the full left ventricle. This is especially useful in dilated ventricles because of the limited sector angle. The multi-directional beam steering capability enables visualization of two views of the heart simultaneously. Experience is still limited, however, promising results have been reported.

Left ventricular volume measurement by three-dimensional echocardiography

Table 1 and Table 2 provide an overview of studies comparing left ventricular volumes and function by reconstruction and real-time three-dimensional echocardiography, respectively, in comparison with magnetic resonance imaging[12–19]. For the various 3D acquisition methods that have been used, a good correlation can be

Table 2

Volume and function measurement by real-time 3DE in comparison with magnetic resonance imaging

Author/ref.	Object	N	r.	SEE	Mean Diff. ± SD
Shiota et al.[23]	LV-EDV	28	0.97	27 ml	-43 ± 65 ml
	LV-ESV	--	0.94	29 ml	-37 ± 67 ml
	LV-EF	--	0.98	0.04%	0.001 ± 0.04%
Qin et al.[24] (controls)	LV-Vol	16	0.96		-13 ± 18 ml
Qin et al.[24] (aneurysms)	LV-Vol	13	0.99		-28 ± 25 ml
Lee et al.[25]	LV-EDV	25	0.99	11.28 ml	
	LV-ESV	--	0.99	10.21 ml	
	LV-EF	--	0.92	0.06	
Schmidt et al.[26]	LV-EDV	25	0.88		
	LV-ESV	--	0.82		
	LV-EF	--	0.72		
	LV-Vol	--	0.91	28.0 ml	-16 ± 36 ml
Zeidan et al.[27]	LV-EDV	15			-6 ± 11 ml
	LV-ESV	--			-4 ± 9 ml
	LV-EF	--			2 ± 5%

3DE = three-dimensional echocardiography; N = number of subjects; LV = left ventricle; r = correlation coefficient; SEE = standard error or regression; Diff. = difference; SD = standard differentiation; EDV = end-diastolic volume; ESV = end-systolic volume; EF = ejection fraction; Vol = volume

observed. However, most three-dimensional echocardiography studies tend to underestimate ESV and EDV. It should also be noted that large differences in study design were present, including number of patients, LV volumes, image quality and analysis methods. In recent studies, new semi-automated endocardial border detection algorithms replace common methods to measure LV volume, as Simpson's rule and algorithms based on manual border tracing.

Conclusion

Three-dimensional echocardiography is a non-invasive technique which can be performed in many clinical scenarios. It is thus ideal for daily performance and for serial follow-up examinations of left ventricular volume and function.

Regardless of the many improved techniques in three-dimensional echocardiography, time consumption has been the major limitation hampering its routine employment for daily diagnostic echocardiography and for volume and function assessment. Faster data acquisition by reducing the number of cross-sections for reconstruction of the cavity, using a high-speed rotation transducer or a volumetric real-time three-dimensional echocardiographic transducer is being investigated. Data processing and three-dimensional image reconstruction has been accelerated and on-line processing and reconstruction is under investigation. Manual endocardial tracing needed for volume measurement is both laborious and prone for subjective errors. Development of various automatic border detection algorithms along with the improvement of ultrasound spatial resolution and advances in other novel modalities such as harmonic, power-mode Doppler tissue imaging and development of intravenous ultrasound contrast agents that enhance the delineation of endocardium, should be able to avoid the need of manual border tracing and provide automatic, even on-line, volume measurement.

References

1. Handschumacher MD, Lethor JP, Siu SC, Mele D, Rivera JM, Picard MH, Weyman AE and Levine RA: A new integrated system for three-dimensional echocardiographic reconstruction: development and validation for ventricular volume with application in human subjects. *J Am Coll Cardiol* 1993, 21:743-753.

2. Gopal AS, King DL, Katz J, Boxt LM, King DL Jr and Shao MY: Threedimensional echocardiographic volume computation by polyhedral surface reconstruction: in vitro validation and comparison to magnetic resonance imaging. *J Am Soc Echocardiogr* 1992, 5:115-124.

3. Delabays A, Pandian NG, Cao QL, Sugeng L, Marx G, Ludomirski A and Schwartz SL: Transthoracic real-time three-dimensional echocardiography using a fan-like scanning approach for data acquisition: methods, strengths, problems, and initial clinical experience. *Echocardiography* 1995, 12:49-59.

4. Pandian NG, Roelandt J, Nanda NC, Sugeng L, Cao QL, Azevedo J, Schwartz SL, Vannan MA, Ludomirski A and Marx G *et al.*: Dynamic three-dimensional echocardiography: methods and clinical potential. *Echocardiography* 1994, 11:237-259.

5. Nosir YF, Fioretti PM, Vletter WB, Boersma E, Salustri A, Postma JT, Reijs AE, Ten Cate FJ and Roelandt JR: Accurate measurement of left ventricular ejection fraction by three-dimensional echocardiography. A comparison with radionuclide angiography. *Circulation* 1996, 94:460-466.

6. Belohlavek M, Tanabe K, Jakrapanichakul D, Breen JF and Seward JB: Rapid three-dimensional echocardiography : clinically feasible alternative for precise and accurate measurement of left ventricular volumes. *Circulation (Online)* 2001, 103:2882-2884.

7. Nguyen LD and Leger C: Four-dimensional reconstruction of the left ventricle using a fast rotating classical phased array scan head: preliminary results. *J Am Soc Echocardiogr* 2002, 15:593-600.

8. Djoa KK, de Jong N, van Egmond FC, Kasprzak JD, Vletter WB, Lancee CT, van der Steen AF, Bom N and Roelandt JR: A fast rotating scanning unit for real-time three-dimensional echo data acquisition. *Ultrasound Med Biol* 2000, 26:863-869.

9. Voormolen MM, Bouakaz A, Krenning BJ, Lancee CT, ten Cate FJ, Roelandt JRTC, van der Steen AFW and de Jong N: A New Transducer for 3D Harmonic Imaging. In: *Proceedings of the IEEE International Ultrasonics Symposium; Munich* 2002:1261-1264.

10. Lancee CT, van Egmond FC, de Jong N, Mastik F, van der Steen AFW, Roelandt JRTC and Bom N: Data Processing for a Fast Rotating Phased Array Real-time 3D Acquisition Unit. In: *Proceedings of IEEE Ultrasonics Symposium; San Juan* 2000:1597-1600.

11. Sheikh K, Smith SW, von Ramm O and Kisslo J: Real-time, threedimensional echocardiography: feasibility and initial use. *Echocardiography* 1991, 8:119-125.

12. Gopal AS, Keller AM, Rigling R, King DL Jr and King DL: Left ventricular volume and endocardial surface area by threedimensional echocardiography: comparison with twodimensional echocardiography and nuclear magnetic resonance imaging in normal subjects. *J Am Coll Cardiol* 1993, 22:258-270.

13. Gopal AS, Keller AM, Shen Z, Sapin PM, Schroeder KM, King DL Jr and King DL: Three-dimensional echocardiography: in vitro and in vivo validation of left ventricular mass and comparison with conventional echocardiographic methods. *J Am Coll Cardiol* 1994, 24:504-513.

14. King DL, Gopal AS, Keller AM, Sapin PM and Schroder KM: Threedimensional echocardiography. Advances for measurement of ventricular volume and mass. *Hypertension* 1994, 23:I172-179.

15. Iwase M, Kondo T, Hasegawa K, Kimura M, Matsuyama H, Watanabe Y and Hishida H: Three-dimensional echocardiography by semi-automatic border detection in assessment of left ventricular volume and ejection fraction: comparison with magnetic resonance imaging. *J Cardiol* 1997, 30:97-105.

16. Buck T, Hunold P, Wentz KU, Tkalec W, Nesser HJ and Erbel R: Tomographic three-dimensional echocardiographic determination of chamber size and systolic function in patients with left ventricular aneurysm: comparison to magnetic resonance imaging, cineventriculography, and two-dimensional echocardiography. *Circulation* 1997, 96:4286-4297.

17. Vogel M, Gutberlet M, Dittrich S, Hosten N and Lange PE: Comparison of transthoracic three dimensional echocardiography with magnetic resonance imaging in the assessment of right ventricular volume and mass. *Heart* 1997, 78:127-130.

18. Altmann K, Shen Z, Boxt LM, King DL, Gersony WM, Allan LD and Apfel HD: Comparison of three-dimensional echocardiographic assessment of volume, mass, and function in children with functionally single left ventricles with two-dimensional echocardiography and magnetic resonance imaging. *Am J Cardiol* 1997, 80:1060-1065.

19. Nosir YF, Lequin MH, Kasprzak JD, van Domburg RT, Vletter WB, Yao J, Stoker J, Ten Cate FJ and Roelandt JR: Measurements and day-to-day variabilities of left ventricular volumes and ejection fraction by three-dimensional echocardiography and comparison with magnetic resonance imaging. *Am J Cardiol* 1998, 82:209-214.

20. Kim WY, Sogaard P, Kristensen BO and Egeblad H: Measurement of left ventricular volumes by 3-dimensional echocardiography with tissue harmonic imaging: a comparison with magnetic resonance imaging. *J Am Soc Echocardiogr* 2001, 14:169-179.

21. Poutanen T, Ikonen A, Jokinen E, Vainio P and Tikanoja T: Transthoracic three-dimensional echocardiography is as good as magnetic resonance imaging in measuring dynamic changes in left ventricular volume during the heart cycle in children. *Eur J Echocardiogr* 2001, 2:31-39.

22. Mannaerts HF, Van Der Heide JA, Kamp O, Papavassiliu T, Marcus JT, Beek A, Van Rossum AC, Twisk J and Visser CA: Quantification of left ventricular volumes and ejection fraction using freehand transthoracic three-dimensional echocardiography: comparison with magnetic resonance imaging. *J Am Soc Echocardiogr* 2003, 16:101-109.

23. Shiota T, McCarthy PM, White RD, Qin JX, Greenberg NL, Flamm SD, Wong J and Thomas JD: Initial clinical experience of realtime three-dimensional echocardiography in patients with ischemic and idiopathic dilated cardiomyopathy. *Am J Cardiol* 1999, 84:1068-1073.

24. Qin JX, Jones M, Shiota T, Greenberg NL, Tsujino H, Firstenberg MS, Gupta PC, Zetts AD, Xu Y, Ping Sun J, Cardon LA, Odabashian JA, Flamm SD, White RD, Panza JA and Thomas JD: Validation of realtime three-dimensional echocardiography for quantifying left ventricular volumes in the presence of a left ventricular aneurysm: in vitro and in vivo studies. *J Am Coll Cardiol* 2000,36:900-907.

25. Lee D, Fuisz AR, Fan PH, Hsu TL, Liu CP and Chiang HT: Real-time 3-dimensional echocardiographic evaluation of left ventricular volume: correlation with magnetic resonance imaging – a validation study. *J Am Soc Echocardiogr* 2001, 14:1001-1009.

26. Schmidt MA, Ohazama CJ, Agyeman KO, Freidlin RZ, Jones M, Laurienzo JM, Brenneman CL, Arai AE, von Ramm OT and Panza JA: Real-time three-dimensional echocardiography for measurement of left ventricular volumes. *Am J Cardiol* 1999, 84:1434-1439.
27. Zeidan Z, Erbel R, Barkhausen J, Hunold P, Bartel T and Buck T: Analysis of global systolic and diastolic left ventricular performance using volume-time curves by real-time threedimensional echocardiography. *J Am Soc Echocardiogr* 2003, 16:29-37.

Chapter 7

Quantification of left ventricular volumes and function in patients with cardiomyopathies by real-time three-dimensional echocardiography. A head-to-head comparison between two different semi-automated endocardial border detection algorithms

OII Soliman
BJ Krenning
ML Geleijnse
A Nemes
JG Bosch
RJ van Geuns
SW Kirschbaum
AM Anwar
TW Galema
WB Vletter
FJ ten Cate

Abstract

Aim of the study

We evaluated two different commercially available TomTec® real-time three-dimensional echocardiographic (RT3DE) semi-automated border detection algorithms for left ventricular (LV) volume analysis in patients with cardiomyopathy and distorted LV geometry.

Methods

Fifty-three patients in sinus rhythm with various types of cardiomyopathy (mean age 56 ± 11 years, 28 men), and adequate 2D image quality were included. The TomTec RT3DE multiplane interpolation (MI) and full volume reconstruction (FVR) methods were used for LV volume analysis. Magnetic resonance imaging (MRI) was used as the reference method.

Results

A strong correlation (R^2 >0.95) was found for all LV volume and ejection fraction (EF) measurements by either RT3DE method. Analysis time was shorter with the FVR method (6 ± 2 vs. 15 ± 4 min, P <0.01) as compared to the MI method. Bland-Altman analysis showed greater underestimation of end-diastolic volume (EDV) and end-systolic volume (ESV) by MI compared to FVR. For the MI method a bias of –24.0 ml (-15.0% of the mean) for EDV and –11.3 ml (-18.0% of the mean) for ESV was found. For FVR analysis these values were –9.9 ml (-6.0% of the mean) and –5.0 ml (-9.0% of the mean), respectively. EF was similar for the MI and FVR method with a mean difference compared to MRI of 0.6 (1.0%) and 0.8 (1.3%), respectively.

Conclusion

In cardiomyopathic patients with distorted LV geometry and good 2D image quality, the TomTec® FVR method is faster and more accurate than the MI method in assessment of LV volumes.

Introduction

Accurate assessment of left ventricular (LV) volume and systolic function forms a routine part of daily echocardiographic practice.[1] However, the geometric assumptions in motion-mode (1D) and two-dimensional (2D) echocardiography and the poor inter and intra-observer variability limit these techniques.[2,3] The development of real-time three-dimensional echocardiography (RT3DE) with matrix transducer technology made a more reliable analysis of LV function feasible. The increasing accuracy and reproducibility of RT3DE for LV quantification has been shown in many studies.[4-9] Several online and off-line software programs for LV volume quantification by RT3DE are available. However, these programs use a wide spectrum of endocardial contour tracing algorithms, ranging from manual to fully automated algorithms. In previous reports, semi-automated border detection software has been shown to be fast, accurate and less observer-dependent for RT3DE quantification of LV volumes and function.[6] Patients with cardiomyopathy have a distorted LV geometry, which theoretically may preclude accurate LV quantification using semi-automated border detection. The present study sought to assess the accuracy and inter-observer variability of two different TomTec® semi-automated border detection RT3DE analysis programs in patients with cardiomyopathic LVs.

Methods

Patient selection
Fifty-three patients (mean age 56 ± 11 years, 28 men), in sinus rhythm, with a cardiomyopathy and adequate 2D image quality (no more than 2 LV segments not well visualized) were enrolled in the study. These patients represent in image quality terms the best half of our patients seen at the echo laboratory. All patients underwent 3DE and cardiac magnetic resonance imaging (MRI) on the same day, to ensure comparable hemodynamic conditions between the examinations. The etiology of the cardiomyopathy was ischemic in 9 (17%), non-compaction in 11 (21%), hypertrophic in 20 (38%), and idiopathic dilated in 13 (24%) patients. The institutional review board approved the study and all patients gave informed consent.

Transthoracic RT3DE image acquisition
RT3DE was performed using a Sonos 7500 equipped with a X4 matrix-array transducer or an IE33 ultrasound system equipped with a X3-1 transducer (Philips Medical Systems, Best, The Netherlands) with the patient in a left lateral decubitus position. Image acquisition was performed from an apical window with the LV as region of interest. To encompass the complete LV into the 3D data set, a full volume of 93° × 84° scan was acquired in harmonic mode from 4 R-wave triggered subvolumes

(93° × 21°) during an end-expiratory breath-hold. The 3D dataset was stored on CD-ROM and transferred to an off-line analysis workstation.

Data analysis
All data were analysed by a single experienced observer (O.I.I.S.) using the 2 algorithms on two separate occasions to assess intra-observer variability. The first 31 patients were also analyzed by a second observer (A.N.) to assess inter-observer variability. All measurements were performed blinded to both the patient data and results of MRI. MRI data were analyzed by an independent third observer (S.K.) who was also blinded to the patient data and results of RT3DE.

Image analysis: Multiplane interpolation (MI) method
As seen in Figure 1, LV volume analysis using MI was performed off-line using commercially available software (4D LV-Analysis, version 1.2, TomTec®, Unterschleissheim, Germany). The algorithm has been described previously.[6] In brief, the orientation of the 3D dataset is determined by manually marking 3 points in a 5-chamber view: the mitral annulus, aortic valve and apex. Subsequently, the data set is divided into 8 equidistant oblique sagittal (or long-axis) and coronal (or frontal) image planes.[10] In each of the 8 planes, the 3 points are manually marked and end-diastolic and end-systolic still frames are manually defined. An ellipse is then automatically generated by the software and placed in the 8 end-diastolic and
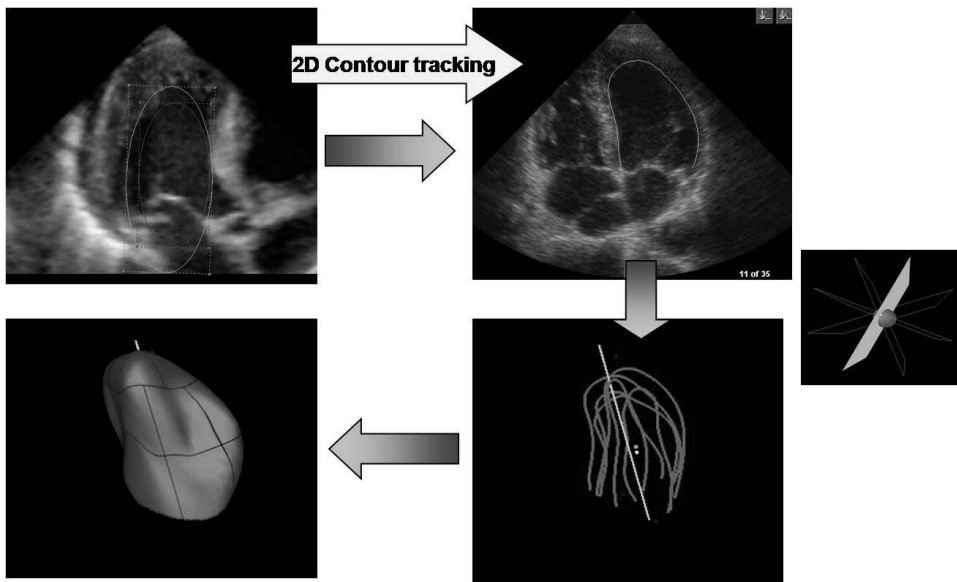
Figure 1
An ellipse is used for initiation of the semi-automatic algorithm in individual cross-sections. After semi automated border detection, an interpolation algorithm is used for LV reconstruction.

end-systolic planes. This ellipse serves for initiation of the semi-automatic algo-rithm by which the software automatically defines the total endocardial border in all frames. A spatio-temporal spline interpolation model is then used to generate a LV model for both the temporal and spatial domain. The analysis program then displays a reconstruction of the LV as a dynamic surface rendered image in which LV wall motion is shown in 3D. At any stage it is possible to revise the ellipse and corresponding endocardial border tracing. LV ejection fraction (EF) is calculated by the software as (EDV – ESV) / EDV × 100%, where EDV = end-diastolic volume and ESV = end-systolic volume.

Image analysis: Full volume reconstruction (FVR) method

As seen in Figure 2, LV volume analysis using FVR was performed off-line using commercially available software (4D LV-Analysis, version 2.0, TomTec®, Unter-schleissheim, Germany). The oblique coronal 4-chamber view and the 60° and
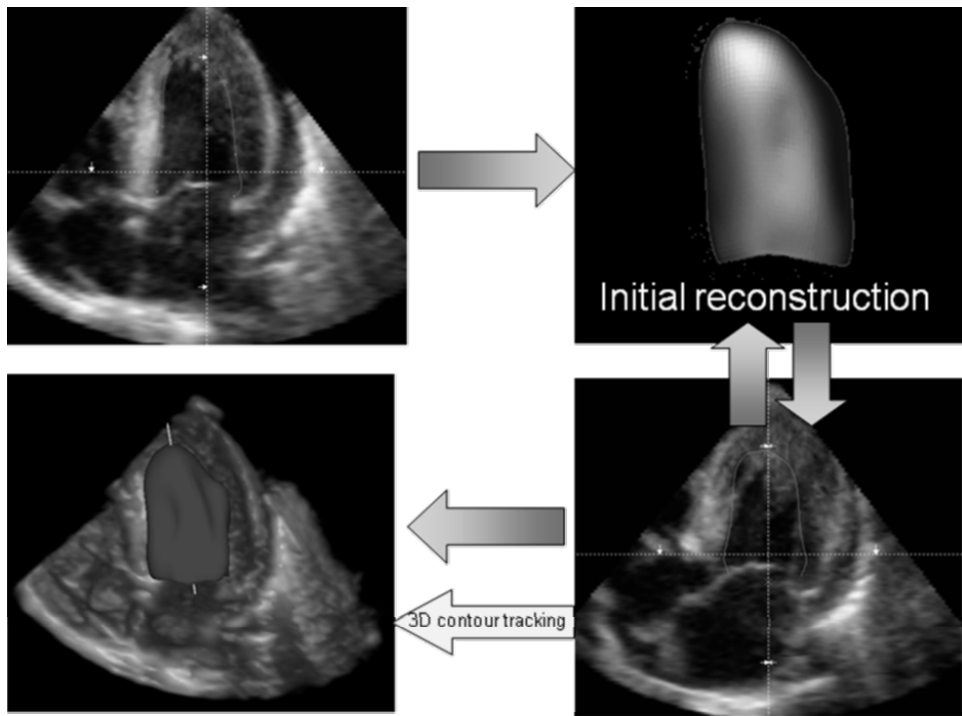
Figure 2

The initial endocardial contour is expanded/rotated 360 degrees and adapted when additional contours are added. According to the initial balloons, the algorithm starts to detect the endocardial border continuously in the entire 4D dataset , e.g. like deforming the balloon in the LV until it best fits the walls in each frame. Adjustments can be made manually after this step and finally a LV reconstruction is created.

120° incremental views are the (tri) planes used for primary analysis. To avoid fore-shortening, the meeting points of the three oblique sagittal and coronal planes are adjusted to meet in the middle of the LV cavity. The end-diastolic and end-systolic frames are identified automatically in this software version. Subsequently, the endocardial border in the three planes is manually traced (LV trabeculations and papillary muscles are included within the LV volume) in both the end-diastolic and end-systolic images for initialization of the algorithm. Based on these 6 initial contours, a spatio-temporal spline interpolation model (like a pulsating balloon) is created by rotational and temporal interpolation of these contours. According to the initial balloons, the algorithm starts to detect the endocardial border continuously in the entire 4D dataset (without large gaps due to interpolation as in the MI method), e.g. like deforming the balloon in the LV until it best fits the walls in each frame. The detection itself employs the same local boundary estimates as the MI method. Adjustments can be made manually after this step in approximately 30 single oblique sagittal and coronal planes. EF is calculated by the software as described in the previous section.

Magnetic resonance imaging
MRI images were acquired using a 1.5 Tesla scanner (GE Signa CV/i, Milwaukee, WI). Patients were positioned in the supine position, with a cardiac eight-element phased-array coil placed over the thorax). Repeated breath holds and electrocardiographic gating were applied to minimize the influence of cardiac and respiratory motion on data collection. Cine MRI was performed using a steady-state free-precession technique (FIESTA). Imaging parameters were; repetition time, 3.5 ms; echotime, 1.3 ms; flip angle, 45°; field of view, 36-40 x 36-40 cm; matrix, 196x160; views per segment, 12, resulting in a temporal resolution of 42 ms. To cover the entire LV 10-12 consecutive slices of 8 mm in the short axis view were planned on the four chambers (gap 2 mm).

To quantify LV volumes, endocardial contours were detected automatically and corrected manually on short-axis cine-MRI images with a dedicated software program using the centerline method (Mass; Medis, Leiden, the Netherlands). Papillary muscles were considered as part of the LV cavity.

Statistical analysis
All data are expressed as mean ± SD. For comparison between the MI and FVR method, and MRI and RT3DE data, linear regression analysis was performed and a Pearson correlation coefficient was calculated. For paired data, the Student's *t* test was used. For agreement between the MI and FVR method, MRI and RT3DE data, the method of Bland and Altman was used.[11] RT3DE inter- and intra-observer variability were calculated for individual patients as an absolute value of difference between the two readings and then mean value from all patients is expressed as a percentage of mean of the two readings. Statistical Package of the Social Science

(SPSS) software version 12.02 (SPSS Inc., Chicago, Illinois) was used for statistical analysis.

Results

The mean time for data analysis was 6 ± 2 minutes for the FVR method compared to 15 ± 5 minutes for the MI method (P <0.001).

Mean LV volumes and EF by the two different RT3DE algorithms and MRI are shown in Table 1. There was an excellent correlation between all values measured by MI, FVR and MRI analysis (Figures 3A to 3I). The lowest values for LV volumes were found by MI analysis; these values were significantly lower than the values found by FVR or MRI analysis. However, FVR still underestimated LV volumes as compared to MRI (Table 2). As seen in Figure 4, Bland-Altman analysis confirmed the greater underestimation of EDV and ESV by MI compared to FVR (when MRI was used as gold standard). As seen in Table 3, a bias of –24.0 ml (-15.0% of the mean) for EDV and –11.3 ml (-18.0% of the mean) for ESV was present with MI analysis compared to –9.9 ml (-6.0% of the mean) and –5.0 ml (-9.0% of the mean) with FVR analysis. As compared to MRI, RT3DE-derived values of EF were similar between the MI and FVR method with mean difference of 0.6 (1.0%) and 0.8 (1.3%), respectively.

Results of intra- and inter-observer variability for MI and FVR analysis are summarized in Table 4.

Table 1. Left Ventricular Volumes and Ejection Fraction by Real-Time Three-Dimensional Echocardiography Using the Full Volume Reconstruction and the Multiplane Interpolation Method for Endocardial Contour Definition

	EDV (range), ml	ESV (range), ml	EF (range), %
Magnetic Resonance Imaging	175 ± 51 (74 to 328)	74 ± 51 (14 to 208)	61 ± 17 (15 to 86)
Full Volume Reconstruction method	165 ± 50 (67 to 308)	69 ± 48 (15 to 194)	61 ± 18 (16 to 85)
Multiplane Interpolation method	150 ± 48 (63 to 301)	63 ± 44 (16 to 182)	61 ± 18 (15 to 86)

Values are expressed in mean ± standard deviation (range), EDV = end-diastolic volume; ESV = end-systolic volume; EF = ejection fraction;

Table 2. Correlation and Comparison Between the Real-Time Three-Dimensional Echocardiographic Methods for Endocardial Contour Definition, and Magnetic Resonance Imaging

	Linear Regression analysis				Paired t-test	
	Regression Equation	R^2	P Value	SEE	Mean Difference ± SD	P Value versus 0
Full Volume Reconstruction Method versus Multiplane Interpolation Method using RT3DE						
EDV, ml	Y = 1.0X + 9.0	0.98	P < 0.001	3.8	14.1 ± 8.4	<0.001
ESV, ml	Y = 1.1X + 0.8	0.99	P < 0.001	1.1	6.4 ± 6.1	<0.001
EF, %	Y = 1.0X - 0.1	0.96	P < 0.001	1.7	0.2 ± 3.3	NS
RT3DE Full Volume Reconstruction method versus MRI						
EDV, ml	Y = 0.98X – 5.7	0.99	P < 0.001	2.2	-9.9 ± 4.7	<0.001
ESV, ml	Y = 0.94X – 0.5	0.99	P < 0.001	1.0	-5.0 ± 4.8	<0.001
EF, %	Y = 0.97X + 2.3	0.98	P < 0.001	1.2	0.6 ± 2.4	NS
RT3DE Multiplane Interpolation method versus MRI						
EDV, ml	Y = 0.92X – 9.9	0.96	P < 0.001	4.3	-24.0 ± 9.7	<0.001
ESV, ml	Y = 0.87X – 0.7	0.98	P < 0.001	1.5	-11.3 ± 8.6	<0.001
EF, %	Y = 0.94X + 4.0	0.95	P < 0.001	2.0	0.8 ± 3.7	NS

Abbreviations as in Table 1. NS = not significant; RT3DE = real-time three-dimensional echocardiography; MRI = magnetic resonance imaging

Table 3. Bland-Altman Analysis and Agreement Between RT3DE Full Volume Reconstruction and Multiplane Interpolation Method and Magnetic Resonance Imaging

	Mean Difference	95% Limits of Agreement
Full Volume Reconstruction Method versus Multiplane Interpolation Method using RT3DE		
EDV, ml	15.4 (9.0%)	-3.1 to 33.9 (-2.0% to 20.0%)
ESV, ml	9.1 (10.0%)	-6.8 to 24.9 (-7.0% to 26.0%)
EF, %	-0.6 (-1.2%)	-6.4 to 5.2 (-13.0% to 10.0%)
RT3DE Full Volume Reconstruction method Versus MRI		
EDV, ml	-9.9 (-6.0%)	-19.1 to -0.9 (-11.0% to 1.0%)
ESV, ml	-5.0 (-9.0%)	-14.4 to -4.4 (-24.0% to 7.0%)
EF, %	0.6 (1.0%)	-4.1 to 5.4 (-7.0% to 9.0%)
RT3DE Multiplane Interpolation method versus MRI		
EDV, ml	-24.0 (-15.0%)	-43.0 to -5.0 (-26.0% to –3.0%)
ESV, ml	-11.3 (-18.0%)	-28.1 to -5.5 (-45.0% to –9.0%)
EF, %	0.8 (1.3%)	-6.5 to 8.1 (-11.0% to 13.0%)

Values between brackets are percentage of the mean of the two measurements; abbreviations as in Tables 1 and 2.

Table 4. Inter- and Intra-Observer Variability of Real-Time Three-Dimensional Echocardiography-Derived Values of Left Ventricular End-Diastolic, End-Systolic and Ejection Fraction Using the TomTec Multiplane Interpolation and the Full Volume Reconstruction Method

	Inter-observer Variability (%)	Intra-observer Variability (%)
EDV		
Full Volume Reconstruction Method	6.4 ± 7.8	4.7 ± 3.2
Multiplane Interpolation Method	8.2 ± 11.4	7.8 ± 8.5
ESV		
Full Volume Reconstruction Method	7.8 ± 9.7	6.1 ± 5.8
Multiplane Interpolation Method	13.5 ± 14.2	9.1 ± 7.2
EF		
Full Volume Reconstruction Method	7.1 ± 6.9	6.6 ± 7.4
Multiplane Interpolation Method	13.1 ± 7.9	11.1 ± 9.3

Abbreviations as in Table 1
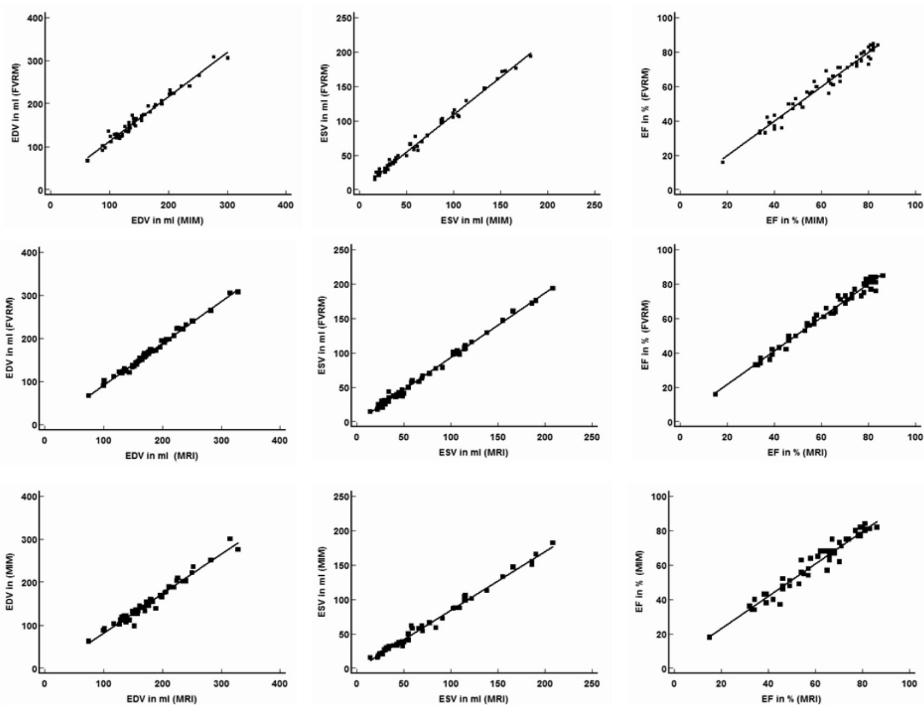
Figure 3

Results of linear regression analysis of real-time three-dimensional echocardiographic values of left ventricular volumes and ejection fraction using the full volume reconstruction method (top) and the multiplane interpolation method (bottom) versus magnetic resonance imaging reference values.
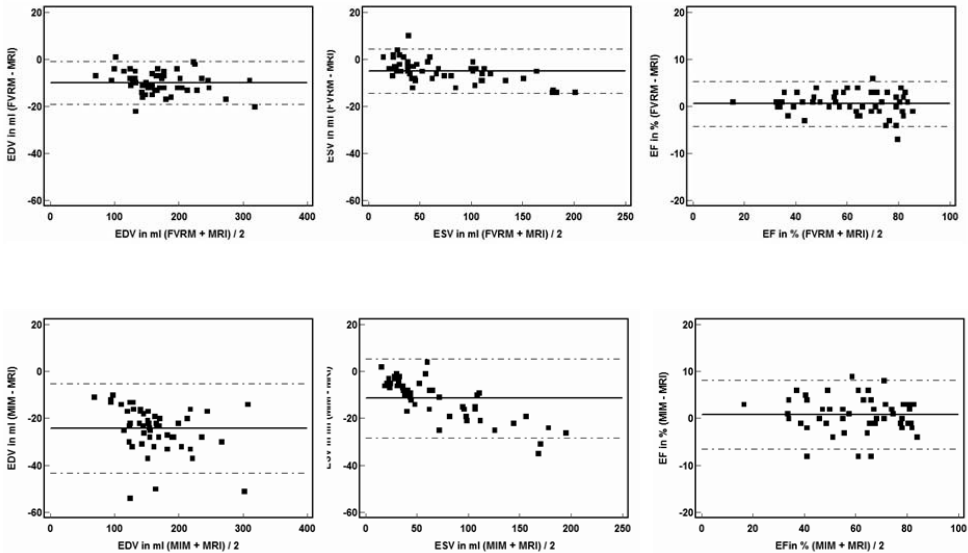
Figure 4

Results of Bland-Altman analysis of real-time three-dimensional echocardiographic values of left ventricular volumes and ejection fraction using the full volume reconstruction method (top) and the multiplane interpolation method (bottom) versus magnetic resonance imaging reference values.

Discussion

The main finding of the present comparative study between two different TomTec® semi-automated border detection algorithms is that the newer FVR method (4D LV Analysis, version 2.0) more accurately estimates LV volumes in patients with cardiomyopathic LVs. Because of the systematic underestimation of all LV volumes by both algorithms (compared to MRI), EF values were similar for both methods. LV volume and EF are important predictors of morbidity and mortality in a wide spectrum of cardiac patients.[12,13]

Recent advances in acquisition and software analysis has made accurate measurements of LV volumes possible with RT3DE in large numbers of patients.[4,6,14,15] Currently, several off-line software programs are available for quantification of LV volumes. The method of endocardial border delineation used in the software algorithm for analysis of a 3D dataset affects accuracy and reproducibility. This is of particular interest in patients with difficult and distorted LVs. In the present study, we compared side-by-side the accuracy and reproducibility of the recently developed FVR algorithm against the previously validated MI algorithm for LV volume quantification in patients with cardiomyopathy and substantially altered LV geometry. The two analysis algorithms used in our study fundamentally differ. In the MI algorithm, the software determines a geometric model for the LV through manual definition of the mitral annulus, aortic valve and apex, and semi-automated border

detection in various LV oblique sagittal (or long-axis) and coronal (or frontal) image planes.[6] This method is limited by boundary detection and contour revision in a limited number of cross-sections. In contrast, the newer FVR algorithm performs automated contour detection in the complete 4D dataset, which can be adjusted anywhere by the reviewer. Besides less (only 6 versus 16 planes) user interaction, faster processing time and better review options, significantly more data is used to estimate the endocardial contour for LV reconstruction. This study shows that this results in higher accuracy and reproducibility as seen from the lower biases and narrower limits of agreement.

Table 5. Comparison of Correlation, Agreement, and Variability Between Real-Time Three-Dimensional Echocardiographic Studies of Left Ventricular Volumes and Function Quantification Using TomTec version 1.2 Software Program

	Author	Year	Pts	MRI analysis	R^2	Biases (units)	Inter-observer (%)	Intra-observer (%)
LV-EDV (ml)	**Soliman**		**53**	**SAX**	**0.96**	**-24.0 ± 9.7**	**8.2 ± 11.4**	**7.8 ± 8.5**
	Jenkins	2006	110	SAX + LAX	0.75	-15.0 ± 28.0		
	Sugeng	2006	31	SAX + LAX	0.94	-5.0 ± 26.0	13.9 ± 2.0	11.2 ± 8.6
	Nikitin	2006	64	SAX	0.96	7.0 ± 28.0	4.0	3.0
	vd Bosch	2006	29	SAX	0.94	-2.9 ± 12.0		
	Kuhl	2004	24	SAX	0.97	-13.6 ± 18.9	0.9 ± 6.9	0.2 ± 6.6
LV-ESV (ml)	**Soliman**		**53**	**SAX**	**0.98**	**-11.3 ± 8.6**	**13.5 ± 14.2**	**9.1 ± 7.2**
	Jenkins	2006	110	SAX + LAX	0.84	-10.0 ± 22.0		
	Sugeng	2006	31	SAX + LAX	0.93	-6.0 ± 26.0	5.6 ± 3.9	14.2 ± 11.8
	Nikitin	2006	64	SAX	0.96	3.0 ± 22.0	6.0	3.0
	vd Bosch	2006	29	SAX	0.96	0.9 ± 10.0		
	Kuhl	2004	24	SAX	0.96	-12.8 ± 20.5	0.7 ± 9.6	-0.0 ± 3.8
LV-EF (%)	**Soliman**		**53**	**SAX**	**0.95**	**-0.8 ± 3.7**	**11.1 ± 9.3**	**13.1 ± 7.9**
	Jenkins	2006	110	SAX + LAX	0.78	1.0 ± 8.0		
	Sugeng	2006	31	SAX + LAX	0.93	0.3 ± 4.0	5.6 ± 3.4	10.5 ± 8.3
	Nikitin	2006	64	SAX	0.89	-1.0 ± 10.0	4.0	4.0
	vd Bosch	2006	29	SAX	0.89	-1.4 ± 7.2		
	Kuhl	2004	24	SAX	0.96	0.9 ± 4.4	-1.5 ± 7.0	-0.6 ± 4.1

Abbreviations as in Table 1

Comparison to previous studies.

Our study is the first to report result for the new FVR method. Therefore, we can only compare the results of the old MI method (4D LV Analysis, version 1.2) with results published by others. As seen in Table 5, the biases described in our paper for ESV and EF are quite comparable to those described by others. Only the biases for EDV seem somewhat higher (but with a small standard deviation), most likely caused by the inclusion of patients with distorted LV geometry in our study.

Limitations.

MRI analysis uses short axis images with a disk summation method to obtain a LV volume. This analysis is not optimal near the apex because of partial-volume artifacts and has limitations in recognizing the mitral valve.[16] Subsequently, a part of the aortic root or left atrium can be included in the volume of the reconstructed disk in the most basal cross-section. This may explain the difference between the measured volumes between RT3DE and MRI. This error can theoretically be reduced by increasing the number of disks (and subsequent decrease of slice thickness) resulting in increased review time. In the future incorporation of long-axis analysis can also improve assessment of LV volumes. However, the short-axis MRI method of analysis is still most widely used for LV volume assessment, both in clinical practice and research.[6,14,17] and does not influence the head-to-head comparison between the two software programs. In should be noted that these results do not necessarily imply a higher accuracy for detection of wall motion abnormalities, which was not the aim of this study.

Conclusion

The newer TomTec® 4D LV Analysis software, version 2.0 that uses the FVR method provides superior assessment of LV volumes compared to the old 1.2 software version using the MI method.

Acknowledgement

References

1. Wang TJ, Evans JC, Benjamin EJ, Levy D, LeRoy EC, Vasan RS. Natural history of asymptomatic left ventricular systolic dysfunction in the community. *Circulation* 2003;108:977-82.
2. Siu SC, Rivera JM, Guerrero JL, Handschumacher MD, Lethor JP, Weyman AE, Levine RA, Picard MH. Three-dimensional echocardiography. In vivo validation for left ventricular volume and function. *Circulation* 1993;88:1715-23.
3. Siu SC, Levine RA, Rivera JM, Xie SW, Lethor JP, Handschumacher MD, Weyman AE, Picard MH. Three-dimensional echocardiography improves noninvasive assessment of left ventricular volume and performance. *Am Heart J* 1995;130:812-22.
4. Jenkins C, Bricknell K, Hanekom L, Marwick TH. Reproducibility and accuracy of echocardiographic measurements of left ventricular parameters using real-time three-dimensional echocardiography. *J Am Coll Cardiol* 2004;44:878-86.
5. Zeidan Z, Erbel R, Barkhausen J, Hunold P, Bartel T, Buck T. Analysis of global systolic and diastolic left ventricular performance using volume-time curves by real-time three-dimensional echocardiography. *J Am Soc Echocardiogr* 2003;16:29-37.
6. Kuhl HP, Schreckenberg M, Rulands D, Katoh M, Schafer W, Schummers G, Bucker A, Hanrath P, Franke A. High-resolution transthoracic real-time three-dimensional echocardiography: quantitation of cardiac volumes and function using semi-automatic border detection and comparison with cardiac magnetic resonance imaging. *J Am Coll Cardiol* 2004;43:2083-90.
7. Simpson IA, Sahn DJ. Adult congenital heart disease: use of transthoracic echocardiography versus magnetic resonance imaging scanning. *Am J Card Imaging* 1995;9:29-37.
8. Bu L, Munns S, Zhang H, Disterhoft M, Dixon M, Stolpen A, Sonka M, Scholz TD, Mahoney LT, Ge S. Rapid full volume data acquisition by real-time 3-dimensional echocardiography for assessment of left ventricular indexes in children: a validation study compared with magnetic resonance imaging. *J Am Soc Echocardiogr* 2005;18:299-305.
9. Gutierrez-Chico JL, Zamorano JL, Perez de Isla L, Orejas M, Almeria C, Rodrigo JL, Ferreiros J, Serra V, Macaya C. Comparison of left ventricular volumes and ejection fractions measured by three-dimensional echocardiography versus by two-dimensional echocardiography and cardiac magnetic resonance in patients with various cardiomyopathies. *Am J Cardiol* 2005;95:809-13.
10. Nanda NC, Kisslo J, Lang R, Pandian N, Marwick T, Shirali G, Kelly G. Examination protocol for three-dimensional echocardiography. *Echocardiography* 2004;21:763-8.
11. Bland JM, Altman DG. Statistical methods for assessing agreement between two methods of clinical measurement. *Lancet* 1986;1:307-10.
12. White HD, Norris RM, Brown MA, Brandt PW, Whitlock RM, Wild CJ. Left ventricular end-systolic volume as the major determinant of survival after recovery from myocardial infarction. *Circulation* 1987;76:44-51.
13. Wong M, Johnson G, Shabetai R, Hughes V, Bhat G, Lopez B, Cohn JN. Echocardiographic variables as prognostic indicators and therapeutic monitors in chronic congestive heart failure. Veterans Affairs cooperative studies V-HeFT I and II. V-HeFT VA Cooperative Studies Group. *Circulation* 1993;87:VI65-70.
14. van den Bosch AE, Robbers-Visser D, Krenning BJ, Voormolen MM, McGhie JS, Helbing WA, Roos-Hesselink JW, Simoons ML, Meijboom FJ. Real-time transthoracic three-dimensional

echocardiographic assessment of left ventricular volume and ejection fraction in congenital heart disease. *J Am Soc Echocardiogr* 2006;19:1-6.

15. Jacobs LD, Salgo IS, Goonewardena S, Weinert L, Coon P, Bardo D, Gerard O, Allain P, Zamorano JL, de Isla LP, Mor-Avi V, Lang RM. Rapid online quantification of left ventricular volume from real-time three-dimensional echocardiographic data. *Eur Heart J* 2006;27:460-8.

16. Sugeng L, Mor-Avi V, Weinert L, Niel J, Ebner C, Steringer-Mascherbauer R, Schmidt F, Galuschky C, Schummers G, Lang RM, Nesser HJ. Quantitative Assessment of Left Ventricular Size and Function. Side-by-Side Comparison of Real-Time Three-Dimensional Echocardiography and Computed Tomography With Magnetic Resonance Reference. *Circulation* 2006;114:654-61.

17. Nikitin NP, Constantin C, Loh PH, Ghosh J, Lukaschuk EI, Bennett A, Hurren S, Alamgir F, Clark AL, Cleland JG. New generation 3-dimensional echocardiography for left ventricular volumetric and functional measurements: comparison with cardiac magnetic resonance. *Eur J Echocardiogr* 2006;7:365-72.

Chapter 8

Comparison of Contrast Versus Non-Contrast Enhanced Real-Time Three-Dimensional Echocardiography For Analysis of Left Ventricular Systolic Function

BJ Krenning
SW Kirschbaum
OII Soliman
A Nemes
RJ van Geuns
WB Vletter
CE Veltman
FJ ten Cate
JRTC Roelandt
ML Geleijnse

Abstract

Ultrasound contrast has shown to improve endocardial border definition. The purpose of this study was to evaluate the value of contrast versus non contrast-enhanced real-time three-dimensional echocardiography (RT3DE) for the assessment of left ventricular (LV) volumes and ejection fraction. Thirty-nine unselected patients underwent RT3DE with and without SonoVue contrast-enhancement and magnetic resonance imaging (MRI) on the same day. An image quality index was calculated by grading all 16 individual LV segments as: 0 = not visible, 1 = poor, 2 = moderate, 3 = good, and 4 = excellent. The 3D data sets were analyzed off-line using dedicated TomTec analysis software. By manual tracing LV end-systolic volume (LV-ESV), LV end-diastolic volume (LV-EDV) and ejection fraction (LV-EF) were calculated. After contrast-enhancement mean image quality index improved from 2.4 ± 1.0 to 3.0 ± 0.9 (P <0.001). Contrast-enhanced RT3DE measurements showed better correlation with MRI (EDV: r = 0.97 vs. 0.86; ESV: r = 0.96 vs. 0.94; EF: r = 0.94 vs. 0.81). The limits of agreement (Bland-Altman analysis) showed a similar bias for RT3DE images with and without contrast but with smaller limits of agreement for contrast-enhanced RT3DE. Also, inter- and intraobserver variability decreased. In a subgroup, patients with poor-to-moderate image quality showed an improvement in agreement after contrast (± 24.4% to ± 12.7%) to the same level as patient with moderate-to-good image quality without contrast (± 10.4%). In conclusion, contrast-enhanced RT3DE is more accurate in assessment of LV function, evidenced by a better correlation and narrower limits of agreement compared to MRI, and lower intra- and interobserver variability.

Accurate assessment of left ventricular (LV) function is important for prognosis and treatment strategy in cardiac patients. Two-dimensional echocardiography (2DE) remains the primary imaging modality for the assessment of cardiac function, besides other techniques such as magnetic resonance imaging[1] (MRI) and radionuclide imaging[2]. The use of these imaging modalities is limited by radiation exposure (for radionuclide imaging), high costs and availability. However, echocardiographic images are sometimes of poor quality that limit LV function assessment. LV opacification with contrast agents has shown to improve image quality and in particular endocardial border delineation[3,4]. Improvement in accuracy has also been shown with real-time three-dimensional echocardiography (RT3DE), because of the absence of geometric assumptions regarding LV shape[5]. Recent advances in three-dimensional cardiac ultrasound imaging technology have made LV function assessment more clinically feasible. The purpose of this study was to evaluate a possible further improvement in accuracy and reproducibility by combing these two major improvements into contrast-enhanced RT3DE.

Methods

Thirty-nine consecutive patients (mean age 58 (15) years, range 24 – 79 years, 34 men) in sinus rhythm were prospectively studied with RT3DE and MRI on the same day. These patients were referred for routine evaluation of cardiac function after myocardial infarction (n = 28), cardiomyopathy (n = 10), and myocarditis (n = 1). No patient was excluded from the study because of echocardiographic image quality. The institutional review board approved the study and all patients gave informed consent.

RT3DE was performed using a Sonos 7500 equipped with a X4 matrix-array transducer (n = 18) or an IE33 ultrasound system equipped with a X3-1 transducer (n = 21) (Philips Medical Systems, Best, The Netherlands) with the patient in a left lateral decubitus position. An apical full volume dataset was acquired in harmonic mode from 4 R-wave triggered subvolumes during an end-expiratory breath-hold. After non-contrast enhanced image acquisition, imaging was repeated with intravenous infusion of SonoVue contrast (Bracco, Milan, Italy). A start bolus injection of 0.5 mL was given, with additional boluses of 0.25 ml when needed. Imaging was performed in harmonic mode at low mechanical index (0.3), and care was taken to record the images at a phase when contrast flow was relatively stable with absent or minimal swirling of contrast in the apex. Both 3D dataset was stored on CD-ROM and transferred to an off-line analysis workstation.

The 3D data sets were analyzed off-line using dedicated analysis software (Echoview© software 5.2, TomTec, Inc., Munich, Germany). In each data set end-systolic (before opening of the mitral valve) and end-diastolic (after closure of the mitral valve) frames were identified. Around a user-defined non-foreshortened LV long axis, the software generated eight uniformly spaced apical images 22.5° apart for each volume. These 8

long-axis end-diastolic and end-systolic images were manually traced with help of mid short-axis evaluations. LV trabeculations and papillary muscles were included within the traced area (LV volume). Subsequently, LV end-systolic volume (LV-ESV), LV end-diastolic volume (LV-EDV) and ejection fraction (LV-EF) were calculated by the software.

Segmental image quality was evaluated by two observers (BJK, OIIS) by grading all 16 individual LV segments[6] as: 0 = not visible, 1 = poor, 2 = moderate, 3 = good, and 4 = excellent. Disagreement was solved by consensus or the evaluation by a third observer (AN). An image quality index was calculated for each acquisition by summation off all segmental scores divided by 16. Also, a separate image quality evaluation of the mid-ventricular short-axis segments was done because these images are used for correction of manual tracings.

To assess intra- and interobserver variability for LV-EDV, LV-ESV and LV-EF measurements, all datasets were re-analyzed by two observers (BJK, OIIS), who were blinded to the results of the previous analysis and the MRI measurements.

MRI images were acquired using a 1.5 Tesla scanner (GE Signa CV/i, Milwaukee, WI). Patients were positioned in the supine position, with a cardiac eight-element phased-array coil placed over the thorax). Repeated breath holds and electrocardiographic gating

Table 1. Comparison between Left Ventricular Volumes and Ejection Fraction by Real-Time Three-Dimensional Echocardiography and Magnetic Resonance Imaging

Variable	MRI	RT3DE	Contrast RT3DE
End-diastolic volume (ml)			
Mean ± SD	218 ± 70	198 ± 60*	200 ± 67*
Range	74 - 364	73 - 340	72 - 340
Correlation (R^2, to MRI)		0.86	0.97
SEE		30.9	17.4
End-systolic volume (ml)			
Mean ± SD	125 ± 69	116 ± 58*	117 ± 65*
Range	26 - 329	23 - 303	18 - 301
Correlation (R^2, to MRI)		0.94	0.96
SEE		19.9	12.5
Ejection fraction (%)			
Mean ± SD	45 ± 15	43 ± 13	44 ± 15
Range	10 - 81	11 - 78	11 - 83
Correlation (R^2, to MRI)		0.81	0.94
SEE		7.7	5.1

MRI = Magnetic Resonance Imaging; RT3DE = Real-Time Three-Dimensional Echocardiography;
*$p < 0.01$ vs MRI
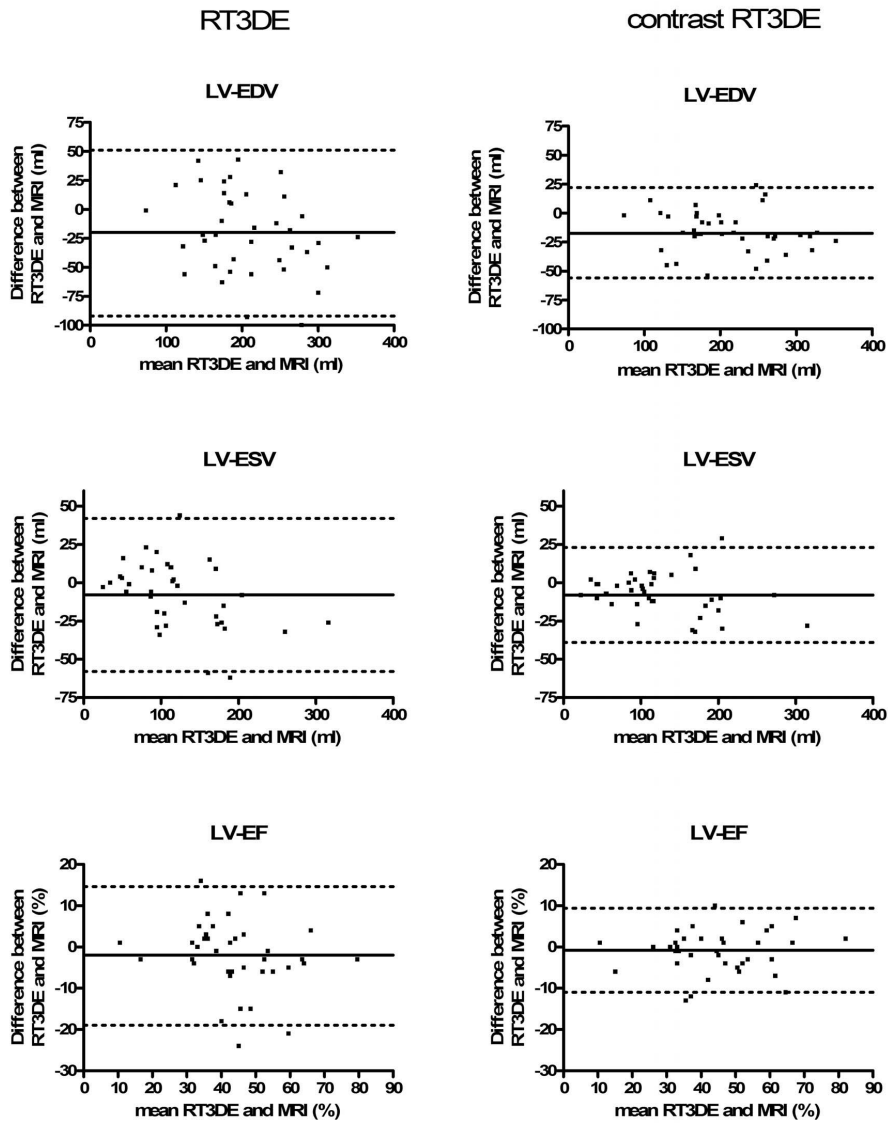
Figure 1:

Plots of the difference between RT3DE (left panels), contrast enhanced RT3DE (right panels) and MRI measurements of LV-EDV, LV-ESV and LV-EF, as a function of the average calculated volumes. Solid and dashed lines represent mean ± 2 SDs of the difference, respectively. (LVEDV = left ventricular end-diastolic volume, LVEF = left ventricular ejection fraction, LVESV = left ventricular end-systolic volume).

were applied to minimize the influence of cardiac and respiratory motion on data collection. Cine MRI was performed using a steady-state free-precession technique (FIESTA). Imaging parameters were; repetition time, 3.5 ms; echotime, 1.3 ms; flip angle, 45°; field of view, 36-40 x 36-40 cm; matrix, 196x160; views per segment, 12, resulting in a temporal resolution of 42 ms. To cover the entire LV 10-12 consecutive slices of 8 mm in the short axis view were planned on the four chambers (gap 2 mm).

To quantify LV volumes, endocardial contours were detected automatically and corrected manually on short-axis cine-MRI images with a dedicated software program using the centerline method (Mass; Medis, Leiden, the Netherlands). Papillary muscles were considered as part of the LV cavity.

Data are presented as mean (SD). A linear regression analysis was performed for the comparison of results obtained by RT3DE and MRI. Limits of agreement were calculated according to the Bland-Altman method[7]. Similarly, inter- and intraobserver variability were calculated and expressed as the mean difference between the two measurements ± 2SD. To determine whether there is a statistically significant difference between comparisons, a paired t-test was performed. A probability level of $p < 0.05$ was considered significant.

Results

The mean time for data analysis ranged from 5 to 20 minutes, depending on image quality. From the total number of 624 segments, 173 segments (28%) had an image quality score <2 without contrast-enhancement, this number decreased to 69 segments (11%) with contrast-enhancement. After contrast-enhancement mean image quality index improved from 2.4 ± 1.0 to 3.0 ± 0.9 (P <0.001). The most profound improvement was seen in the anterior segments (1.9 ± 1.4 to 2.6 ± 1.3). A similar improvement was found for the mid ventricular anterior and anteroseptal short-axis segments (from 1.7 ± 1.5 to 2.6 ± 1.2 after contrast-enhancement).

As seen in Table 1, mean LV-EDV, LV-ESV, and LV-EF values were not different between RT3DE images with and without contrast. Both techniques significantly underestimated LV-EDV and LV-ESV (but not LV-EF) compared to MRI. Better correlations to MRI were found for LV-EDV, ESV and LV-EF with contrast-enhanced RT3DE (see also Table 1). As seen in Figure 1, the limits of agreement (Bland-Altman analysis) showed a similar bias for RT3DE images with and without contrast but with smaller limits of agreement for contrast-enhanced RT3DE.

In a subgroup analysis of patients with poor-to-moderate image quality (image quality index ≤ 2, 14 patients), the 95% limits of agreements for LV-EF narrowed from ± 24.4% to ± 12.7% with contrast-enhanced RT3DE. For moderate-to-good image quality (image quality index ≥ 2.5, 16 patients), the 95% limits of agreements for LV-EF narrowed from ± 10.4% to ± 7.0% with contrast-enhanced RT3DE (See Figure 2).
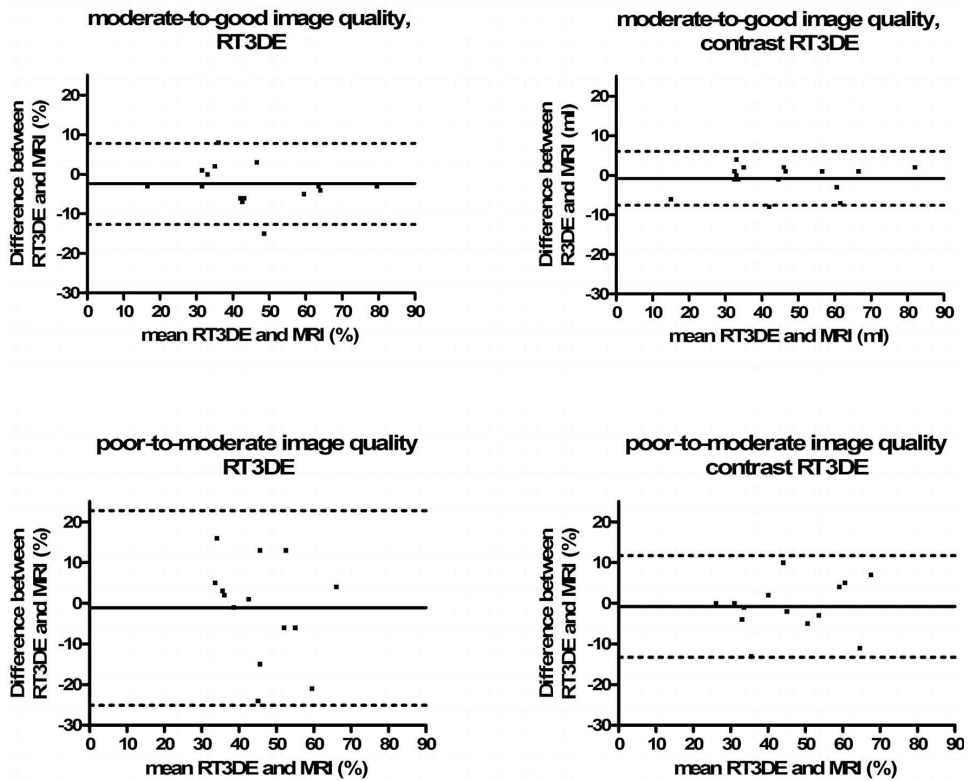
Figure 2:

Subgroup analysis of LV-EF in patients with moderate-to-good (top panels) and poor-to-moderate image quality (bottom panels), with and without contrast enhancement. (abbreviations as in Figure 1)

Interobserver variability for LV-EDV and LV-ESV was lower for contrast-enhanced RT3DE (-3.1 ± 20.0 ml and -0.8 ± 13.9 ml, respectively) compared to non-contrast-enhanced RT3DE (5.6 ± 32.9 ml and 3.0 ± 25.7 ml, respectively). For EF, interobserver variabilities were -0.5 ± 5.8% and 0.7 ± 9.2%, respectively. Intraobserver variability for LV-EDV and LV-ESV was lower for contrast-enhanced RT3DE (1.5 ± 6.6 ml and 0.5 ± 7.3 ml, respectively) compared to non-contrast-enhanced RT3DE (-5.2 ± 21.4 ml and -3.1 ± 19.8 ml, respectively). For EF, intraobserver variabilities were 0.2 ± 3.2% and -0.2 ± 6.2%, respectively.

Discussion

2DE remains the most often used imaging modality to assess LV function, but is limited in accuracy because of geometric assumptions of LV shape and high in-

tra- and interobserver variability[8]. Improvement in accuracy was shown by 3DE, because of the absence of these geometric assumptions[5]. Despite technological improvements, image quality remains less compared to 2DE imaging. Reliable LV contour detection is only possible if the endocardial border is adequately visible during end-systole and end-diastole. Even in good quality echocardiograms, it is sometimes difficult to delineate the endocardium in still frames. In 2DE studies improvement in endocardial border detection with contrast-enhancement resulted in a significant decrease in intra- and interobserver variability for LV function analysis[9,10]. Others and us have shown the value of contrast-enhanced imaging during *stress* RT3DE[11,12].

In the present study the improvement in endocardial border definition during contrast-enhanced RT3DE imaging is confirmed. The number of poor-to-moderate visible segments decreased with 60% after contrast enhancement, in particular the anterior and anteroseptal segments improved in quality. Also, identification of the LV contour improved in the mid-ventricular short-axis, which is important for accurate LV reconstruction. Contrast-enhanced imaging improved the accuracy by means of a higher correlation between RT3DE and MRI. Although the limits of agreement analysis showed a higher agreement, a difference in bias was not observed. In a subgroup analysis, patients with poor-to-moderate image quality showed an improvement in agreement with contrast use to the same level as patients with moderate-to-good image quality studied without contrast. Also, an improvement in reproducibility was found, evidenced by narrower limits of agreement for inter- and intraobserver variability. In a first study, Caiani et al.[13] did not find an improvement in accuracy after use of contrast, and suggested dual end-diastolic and end-systolic gating instead of continuous imaging to reduce bubble destruction and subsequent underestimation of LV volume[14]. We found a similar correlation and limits of agreement using continuous infusion compared to the latter study, without use of dual triggering (see Table 2). We did not experience incomplete visualization of the LV due to bubble destruction while performing continuous acquisition. This may be explained by a different imaging protocol, as we used bolus injections of contrast agent rather than a continuous infusion. Possibly, bolus injections result in a higher LV contrast concentration that is less sensitive to (apical) bubble destruction, at the cost of a period of attenuation[15]. It should be noticed, however, that in our experience well timed bolus injections result in relatively stable LV contrast concentrations during the recording phase. Also, differences in data analysis and baseline image quality may explain different results. However, in both studies patients were not selected for echo quality.

MRI analysis uses short-axis images with a disk summation method to obtain a LV volume. This analysis is not optimal near the apex because of partial-volume artifacts and has limitations in recognizing the mitral valve[16]. Subsequently, a part of the aortic root or left atrium can be included in the volume of the reconstructed disk in the most basal cross-section. This may partially explain the difference in volumes

Table 2. Comparison of Correlation, Agreement, and Variability Between Real-Time Three-Dimensional Echocardiographic Studies of Left Ventricular Volumes and Function Quantification Using Contrast Enhancement.

	Author		Year	Pts	R^2	SEE	Bias (%)	SD (%)
EDV (ml)	Caiani[13]	continuous imaging	2005	14	0.58	31	-34	38
	Caiani[14]	dual triggering	2005	20	0.90	21	-14 (9%)	20 (13%)
	Caiani[14]	continuous imaging	2005	20	0.79	27	-23 (17%)	30 (21%)
	Krenning	continuous imaging	2007	39	0.97	17	-16 (8%)	18 (9%)
ESV (ml)	Caiani[13]	continuous imaging	2005	14	0.72	23	-19	26
	Caiani[14]	dual triggering	2005	20	0.92	14	-5 (6%)	17 (19%)
	Caiani[14]	continuous imaging	2005	20	0.86	18	-15 (19%)	20 (25%)
	Krenning	continuous imaging	2007	39	0.92	13	-7 (6%)	13 (11%)
EF	Caiani[13]	continuous imaging	2005	14	0.50	12	-1	9
	Caiani[14]	dual triggering	2005	20	0.59	11	-4 (10%)	11 (26%)
	Caiani[14]	continuous imaging	2005	20	0.58	10	0 (0%)	11 (23%)
	Krenning	continuous imaging	2007	39	0.88	5	-1 (3%)	5 (11%)

EDV = end-diastolic volume; ESV = end-systolic volume; EF = ejection fraction, RT-3DE = Real-time three-dimensional echocardiography, R^2= Correlation Coefficient, Ref = Reference technique, pts = patients, SEE = Standard error of estimate, SD = Standard deviation

between RT3DE and MRI. This error can theoretically be reduced by increasing the number of disks (and subsequent decrease of slice thickness) resulting in increased review time, or incorporation of long-axis analysis[17-19]. Of note, our main goal was to compare head-to-head the two different RT3DE imaging techniques (with a similar gold standard). To prevent possible error caused by an automated algorithm we used a manual tracing algorithm. Current developments in automated analysis of contrast-enhanced images may improve analysis time and agreement.

References

1. Ioannidis JP, Trikalinos TA, Danias PG: Electrocardiogram-gated single-photon emission computed tomography versus cardiac magnetic resonance imaging for the assessment of left ventricular volumes and ejection fraction: a meta-analysis. *J Am Coll Cardiol* 2002;**39**:2059-2068.

2. Senior R, Sridhara BS, Basu S, Henley M, Handler CE, Raftery EB, Lahiri A: Comparison of radionuclide ventriculography and 2D echocardiography for the measurement of left ventricular ejection fraction following acute myocardial infarction. *Eur Heart J* 1994;**15**:1235-1239.

3. Senior R, Andersson O, Caidahl K, Carlens P, Herregods MC, Jenni R, Kenny A, Melcher A, Svedenhag J, Vanoverschelde JL, Wandt B, Widgren BR, Williams G, Guerret P, la Rosee K, Agati L, Bezante G: Enhanced left ventricular endocardial border delineation with an intravenous injection of SonoVue, a new echocardiographic contrast agent: A European multicenter study. *Echocardiography* 2000;**17**:705-711.

4. Kasprzak JD, Paelinck B, Ten Cate FJ, Vletter WB, de Jong N, Poldermans D, Elhendy A, Bouakaz A, Roelandt JR: Comparison of native and contrast-enhanced harmonic echocardiography for visualization of left ventricular endocardial border. *Am J Cardiol* 1999;**83**:211-217.

5. Krenning BJ, Voormolen MM, Roelandt JR: Assessment of left ventricular function by three-dimensional echocardiography. *Cardiovasc Ultrasound* 2003;**1**:12.

6. Schiller NB, Shah PM, Crawford M, DeMaria A, Devereux R, Feigenbaum H, Gutgesell H, Reichek N, Sahn D, Schnittger I, et al.: Recommendations for quantitation of the left ventricle by two-dimensional echocardiography. American Society of Echocardiography Committee on Standards, Subcommittee on Quantitation of Two-Dimensional Echocardiograms. J Am Soc Echocardiogr 1989;**2**:358-367.

7. Bland JM, Altman DG: Statistical methods for assessing agreement between two methods of clinical measurement. Lancet 1986;**1**:307-310.

8. McGowan JH, Cleland JG: Reliability of reporting left ventricular systolic function by echocardiography: a systematic review of 3 methods. *Am Heart J* 2003;**146**:388-397.

9. Malm S, Frigstad S, Sagberg E, Larsson H, Skjaerpe T: Accurate and reproducible measurement of left ventricular volume and ejection fraction by contrast echocardiography: a comparison with magnetic resonance imaging. *J Am Coll Cardiol* 2004;**44**:1030-1035.

10. Thomson HL, Basmadjian AJ, Rainbird AJ, Razavi M, Avierinos JF, Pellikka PA, Bailey KR, Breen JF, Enriquez-Sarano M: Contrast echocardiography improves the accuracy and reproducibility of left ventricular remodeling measurements: a prospective, randomly assigned, blinded study. *J Am Coll Cardiol* 2001;**38**:867-875.

11. Takeuchi M, Otani S, Weinert L, Spencer KT, Lang RM: Comparison of contrast-enhanced real-time live 3-dimensional dobutamine stress echocardiography with contrast 2-dimensional echocardiography for detecting stress-induced wall-motion abnormalities. *J Am Soc Echocardiogr* 2006;**19**:294-299.

12. Nemes A, Geleijnse ML, Krenning BJ, Soliman OI, Anwar AM, Vletter WB, Ten Cate FJ: Usefulness of ultrasound contrast agent to improve image quality during real-time three-dimensional stress echocardiography. *Am J Cardiol* 2007;**99**:275-278.

13. Caiani EG, Corsi C, Zamorano J, Sugeng L, MacEneaney P, Weinert L, Battani R, Gutierrez JL, Koch R, Perez de Isla L, Mor-Avi V, Lang RM: Improved semiautomated quantification of left ventricular volumes and ejection fraction using 3-dimensional echocardiography

with a full matrix-array transducer: comparison with magnetic resonance imaging. *J Am Soc Echocardiogr* 2005;**18**:779-788.

14. Caiani EG, Coon P, Corsi C, Goonewardena S, Bardo D, Rafter P, Sugeng L, Mor-Avi V, Lang RM: Dual triggering improves the accuracy of left ventricular volume measurements by contrast-enhanced real-time 3-dimensional echocardiography. *J Am Soc Echocardiogr* 2005;**18**:1292-1298.

15. Weissman NJ, Cohen MC, Hack TC, Gillam LD, Cohen JL, Kitzman DW: Infusion versus bolus contrast echocardiography: a multicenter, open-label, crossover trial. *Am Heart J* 2000;**139**:399-404.

16. Sugeng L, Mor-Avi V, Weinert L, Niel J, Ebner C, Steringer-Mascherbauer R, Schmidt F, Galuschky C, Schummers G, Lang RM, Nesser HJ: Quantitative assessment of left ventricular size and function: side-by-side comparison of real-time three-dimensional echocardiography and computed tomography with magnetic resonance reference. *Circulation* 2006;**114**:654-661.

17. Kuhl HP, Schreckenberg M, Rulands D, Katoh M, Schafer W, Schummers G, Bucker A, Hanrath P, Franke A: High-resolution transthoracic real-time three-dimensional echocardiography: quantitation of cardiac volumes and function using semi-automatic border detection and comparison with cardiac magnetic resonance imaging. *J Am Coll Cardiol* 2004;**43**:2083-2090.

18. van den Bosch AE, Robbers-Visser D, Krenning BJ, Voormolen MM, McGhie JS, Helbing WA, Roos-Hesselink JW, Simoons ML, Meijboom FJ: Real-time transthoracic three-dimensional echocardiographic assessment of left ventricular volume and ejection fraction in congenital heart disease. *J Am Soc Echocardiogr* 2006;**19**:1-6.

19. Nikitin NP, Constantin C, Loh PH, Ghosh J, Lukaschuk EI, Bennett A, Hurren S, Alamgir F, Clark AL, Cleland JG: New generation 3-dimensional echocardiography for left ventricular volumetric and functional measurements: comparison with cardiac magnetic resonance. *Eur J Echocardiogr* 2006;**7**:365-372.

Chapter 9

Methodological analysis of diagnostic dobutamine stress echocardiography studies

BJ Krenning
ML Geleijnse
D Poldermans
JRTC Roelandt

Abstract

Background
Dobutamine stress echocardiography (DSE) is an accepted test for the diagnosis of coronary artery disease (CAD), despite its wide diagnostic accuracy.

Aim
Which factors cause test variability of DSE for the diagnosis of CAD.

Methods
In a retrospective analysis of 46 studies in 5,353 patients, the potential causes of diagnostic variability were systematically analyzed, including patient selection, definition of CAD, chest pain characteristics, confounding factors for DSE (left ventricular hypertrophy, left bundle branch block, female gender), work-up bias (present when patient's chance to undergo coronary angiography is influenced by the result of DSE), review bias (present when DSE is interpreted in relation to CAG), DSE protocol and definition of a positive DSE.

Results
Diagnostic variability was related to definition of a positive test, but not related to the definition of CAD or DSE protocol. However, only three of eight methodological standards for research design found general compliance. Differences in the selection of the study population (quality of echocardiographic window, angina pectoris), handling of confounding factors and analysis of disease in individual coronary arteries were observed. Lack of data on analysis of relevant chest pain syndromes and handling of nondiagnostic test results hampered further evaluation of these standards.

Conclusion
Methodologic problems may explain the wide range in diagnostic variability of DSE. An improvement of clinical relevance of DSE testing is possible by stronger adherence to common and new methodologic standards.

Dobutamine stress echocardiography (DSE) is currently a routine and safe test for the diagnosis of coronary artery disease (CAD)[1]. However, reported studies show a wide range of diagnostic sensitivity and specificity[1]. To explain this wide range, we conducted a methodological review of the reported studies in which patients underwent both DSE and coronary arteriography. In analogy to a previous methodological review[2] on exercise testing, we assessed the common causes of diagnostic variability (differences in definition of CAD, the DSE protocol and definition of abnormal DSE). We also used modified methodological criteria for assessing diagnostic accuracy.

Methods

Data sources and data extraction

A MEDLINE search was performed for diagnostic DSE studies in English language between January 1990 and December 2000 that included patients who underwent both DSE and coronary arteriography. The search terms were 'dobutamine stress' and 'coronary artery disease'. We also carefully reviewed all references of the selected articles for additional studies.

Selection criteria

Criteria for the studies to be enrolled in the present analysis were (1) patients, or a subgroup of patients who underwent both DSE and coronary arteriography, (2) data containing calculations of sensitivity and specificity or information that could be used to derive this information. Excluded were studies, which included selected patient populations. In particular patients studied in DSE studies using contrast imaging were excluded because these patients were selected by poor image quality, obviously resulting in low diagnostic sensitivity for conventional DSE. Also excluded were studies including solely patients with left bundle branch block, hypertension, left ventricular hypertrophy or renal transplant recipients. When multiple articles by the same author were identified, only the largest study was included in the present analysis, unless it was clear that different patients were studied.

Data collection

Two investigators (BJK, MLG) independently screened the 44 articles[3-46] that met the inclusion criteria for abstracted variables and the methodological standards described below. Variables abstracted from each report included identifying information (first author, year of publication) and clinical characteristics (number of patients, mean age, percentage of male patients). In addition, we recorded the number of patients without and with CAD and the number of patients with true positive and true negative DSE results.

According to the previously reported common reasons for the wide range of diagnostic accuracy[2], we noted the definition of significant CAD (≥50 or ≥70% reduction in luminal diameter), DSE protocol and definition of positive DSE.

Definition of CAD
When 70% reduction in luminal diameter on a coronary angiogram is used as criterion for significant CAD, the chance of false negative test results is smaller as com-

Table I Methodological standards

standard 1	**adequate selection and identification of patients**
A	adequate selection of patients, information on age and gender available
B	-blockers stopped prior to DSE
standard 2	**adequate analysis of disease in individual coronary arteries**
A	extent of CAD (1,2,3 vessel CAD or single/multi vessel disease) reported
B	location of CAD (at least for single-vessel CAD) reported
C	diagnostic accuracy for extent of CAD available
D	diagnostic accuracy for location of CAD available
E	identification of multi-vessel CAD by multi-region wall motion abnormalities
F	hemodynamic response at ischemic threshold for sub-groups (eg. 1,2,3 vessel CAD) reported
Standard 3	**adequate analysis of relevant chest pain syndromes**
A	information on number of patients with typical angina pectoris
B	diagnostic accuracy in patients with typical angina pectoris available
Standard 4	**avoidance of a limited challenge group**
A	inclusion of patients with possible confounding factors (left ventricular hypertrophy, left bundle branch block, female gender)
B	inclusion of patients with poor thoracic echocardiographic window
standard 5	**avoidance of work-up bias**
	absence of work-up bias (present when patient's chance to undergo coronary angiography is influenced by the result of DSE)
standard 6	**avoidance of diagnostic review bias**
A	DSE interpretation performed blinded to results of coronary angiography
B	coronary angiographic interpretation performed blinded to results DSE
standard 7	**adequate analysis for non-diagnostic DSE tests**
A	number of patients with non-diagnostic test result reported
B	number of patients achieving target heart rate reported
C	average maximum heart rate at peak infusion reported
standard 8	**use of state-of-the-art protocol**
	addition of atropine to dobutamine if target heart rate was not achieved

pared to a 50% reduction. This would cause sensitivity to increase and specificity to decrease.

DSE protocol

Also, addition of atropine to dobutamine and withdrawal of β-blockers has shown to increase diagnostic accuracy[10, 30, 31, 37, 47]. Therefore, the DSE protocol can influence the correlation to angiographic findings.

Definition of positive DSE

Different definitions of abnormal DSE could cause differences in diagnostic accuracy. Studies, in which either at rest or during stress inducible wall motion abnormality is considered indicative of CAD, sensitivity is likely to be higher than in studies in which dobutamine stress-induced wall motion abnormalities are required. Whereas all studies defined DSE positive for significant CAD in case of new or worsening wall motion abnormalities during dobutamine infusion (myocardial ischemia), rest wall motion abnormalities were interpreted differently. Therefore, we introduced three different definitions of positive DSE.

In studies using definition A, DSE was only considered positive in case of new or worsening wall motion abnormalities during dobutamine infusion (myocardial ischemia). In studies using definition B, DSE was considered positive in case of new or worsening wall motion abnormalities or a resting wall motion abnormality without improvement during dobutamine infusion (fixed wall motion abnormality). In studies using definition C, DSE was considered positive in case of new or worsening wall motion abnormalities or a resting wall motion abnormality regardless of change during dobutamine infusion.

According to the previously cited review[2], we also investigated basic differences in research design by using (modified) standards for evaluating DSE (Table I).

Statistical analysis

Statistical tests were performed in a weighted fashion, using the number of diseased patients as the weight for testing of sensitivities and the number of non-diseased patients for testing of specificities. For calculation of 95% confidence intervals, the formula $p \pm 1.96\sqrt{pq/n}$ (p = observed index for either sensitivity or specificity, q = 1-p, n = number of subjects tested) was used. Comparisons of sensitivity and specificity were performed using the standardized normal distribution test. Statistical significance was defined at $p < 0.05$.

Table II Summary of studies and results of methodological review

Reference	Year	Cases (n)	Sub-Group#	men (%)	Sens (%)	Spec (%)	Test protocol*	significant CAD (%) V/Q	Abnormal stress test criterion‡
Cohen[3]	1991	70	N	100	86	95	III	70 V	A
Sawada[4]	1991	55	Y	62	89	85	I	50 Q	A
Epstein[5]	1992	61	N	70	91	57	II	50 V	C
Martin[6]	1992	40	N	95	76	60	II	50 V	A
Salustri[7]	1992	52	N	73	54	80	II	50 Q	A
Marcovitz[8]	1992	141	N	60	96	66	I	50 Q	B
Mazeika[9]	1992	50	N	88	64	93	I	70 V	A
McNeill[10]	1992	80	N	74	70	88	IV	50 V	A
Gunalp[11]	1993	27	N	85	83	89	I	50 V	A
Hoffmann[12]	1993	60	Y	77	79	83	V	70 Q	A
Marwick[13]	1993	217	N	72	72	83	II	50 Q	C
Previtali[14]	1993	80	N	78	79	83	III	50 V	A
Afridi[15]	1994	45	Y	99	71	86	II	70 Q	C
Sahin[16]	1994	65	N	71	79	87	I	50 V	A
Santiago[17]	1994	77	Y	70	79	67	III	70 V	C
Senior[18]	1994	61	N	72	93	94	III	50 V	C
Beleslin[19]	1994	136	N	85	82	76	II	50 Q	A
Daoud[20]	1995	76	N	58	92	73	I	50 V	B
Ho[21]	1995	54	N	85	93	73	II	50 V	A
Sochowski[22]	1995	46	N	67	68	81	II	50 V	A
Dagianti[23]	1995	60	Y	70	72	97	III	70 Q	A
Di Bello[24]	1996	45	N	73	76	86	V	50 V	A
Iwase[25]	1996	96	N	70	79	88	III	70 V	A
Kisacik[26]	1996	69	N	84	94	86	V	50 V	A
San Roman[27]	1996	102	N	56	78	95	IV	50 Q	A
Wu[28]	1996	30	Y	84	94	92	II	50 Q	A
Anthopoulos[29]	1996	120	N	60	87	84	II	50 V	A
Ling[30]	1996	183	Y	35	95	51	IV	70 V	B
Pingitore[31]	1996	110	Y	83	84	89	IV	50 Q	A
Slavich[32]	1996	46	N	0	59	79	V	50 Q	A
Dionisopoulos[33]	1997	288	N	65	87	89	IV	50 Q	C
Hennessy[34]	1997	317	N	72	86	60	V	50 V	B
Ho[35]	1997	223	Y	81	94	79	IV	50 Q	A
Huang[36]	1997	93	N	77	93	77	IV	50 Q	C
Schröder[37]	1997	99	N	80	89	82	V	50 Q	A
Steinberg[38]	1997	120	N	99	87	91	III	70 V	A
Vitarelli[39]	1997	59	N	64	85	82	III	70 V	A

STANDARD

1A	1B	2A	2B	2C	2D	2E	2F	3A	3B	4A	4B	5	6A	6B	7A	7B	7C	8
X	X	X		X		X						X	X	X				
X		X		X		X				X	X		X	X		X		
X		X	X	X	X					X	X		X	X		X		
X		X					X			X	X	X	X	X		X		
X		X		X						X	X	X	X	X		X		
X		X	X	X	X					X	X		X	-				
X	X	X	X	X	X	X						X	X	X	X	X	X	
X		X	X							X	-	X	X	-		X		X
X	X	X	X	X	X	X				X	-	X	X	-		X		
X	X	X		X						X		X	X	X				X
X		X	X	X	X	X			X	X	X	X	X	-		X		
X	X	X		X						X		X	X	X		X		
X		X		X						X			X	X		X		
X	X	X		X			X			X		X	X	X		X		
X	X									X	-		-	-				
X	X	X	X	X	X	X				-		X	X	X		X		
X		X	X	X			X			X	X	X	X	X		X		
X		X		X						X	X		-	-				
X	-	X	X	X	X					X	-	X	X	X				
X		X					X			X	X	X	X	X				
X	X	X		X						X	X	X	X	X				
X	X	X		X			X					X	X	X		X		X
X	X	X		X								X	X	X		X		
X	X	X		X			X			X		X	X	X		X		X
X		X		X			X			X	-	X	X	-		X		X
X		X								X		X	X	X	X	X		
X		X		X			X			-		X	X	X				
X		X								X	-		X	-	X			X
X		X		X						X	-	X	X	X		X		X
X	X	X	X	X						X		X	X	-				X
X		X	X	X	X					X	X	X	X		X	X		X
X	X	X		X			X			X	-	X	X	X				X
X		X	X		X					X		X	X	-				X
X		X	X	X	X						X	X	X	-		X		X
X	X	X		X						X		X	X	-		X		X
X		X		X						X		X	X	X				
X	X	X		X						X	X	-	-			X		

Reference	Year	Cases (n)	Sub-Group#	men (%)	Sens (%)	Spec (%)	Test protocol*	significant CAD (%) V/Q	Abnormal stress test criterion‡
Elhendy[40]	1998	295	Y	67	75	87	IV	50 Q	A
Santoro[41]	1998	60	N	-	61	96	V	70 Q	A
Tackeuchi[42]	1999	178	N	77	84	89	I	50 Q	C
Tackeuchi[42]	1999	249	N	80	85	83	II	50 Q	C
Tackeuchi[42]	1999	511	N	71	85	82	IV	50 Q	C
Lewis[43]	1999	92	N	0	40	94	IV	50 Q	A
Loimaala[44]	1999	60	N	67	95	63	II	50 V	A
Nagel[45]	1999	172	N	71	74	70	V	50 V	A
Smart[46]	2000	183	N	73	87	91	IV	50 Q	C

x standard met by study; - data unavailable; # included patients subgroup of total study population; *see table I; † V/Q: visual estimation or quantitative measurement; ‡A: new or worsening wall motion abnormalities (=myocardial ischemia); B: myocardial ischemia or a resting wall motion abnormality without improvement during dobutamine infusion; C: myocardial ischemia or a resting wall motion abnormality regardless of change during dobutamine infusion.

sens = sensitivity; spec = specificity; MI = myocardial infarction; CAD = coronary artery disease

Results

Overview of studies

In one[42] of the 44 articles, three different DSE protocols were compared and implemented as three different studies in this analysis. The clinical characteristics of the 46 studies including 5,353 patients are outlined in Table II. In some studies, coronary angiography was performed only in a subgroup of patients. In this case, only the results from these latter patients were used for calculation of diagnostic

Table III Variation in sensitivity and specificity

Values of sensitivity or specificity (%)	Sensitivity (number of studies)	Specificity (number of studies)
31-40	1	0
41-50	0	0
51-60	2	4
61-70	4	4
71-80	13	8
81-90	15	21
91-100	11	9
Weighted mean	83%	83%

STANDARD

1A	1B	2A	2B	2C	2D	2E	2F	3A	3B	4A	4B	5	6A	6B	7A	7B	7C	8
x		x		x		x		x		x	−		x	−		x	x	x
	x	x	x	x	x	x		x		x	x		x	−		x	x	x
x		x						x		x	x	x				x		
x		x						x		x	x	x				x		
x		x						x		x	x	x				x		x
x		x						x		x	x	x	x	x	x	x	x	x
x		x					x	x		x	x			−		x		
x	x	x						x		x	x	x	x		x	x		x
x		x	x	x	x		x	x		x	x	x				x		x

Sensitivity and 95%-Confidence Intervals

sensitivity

Reference number
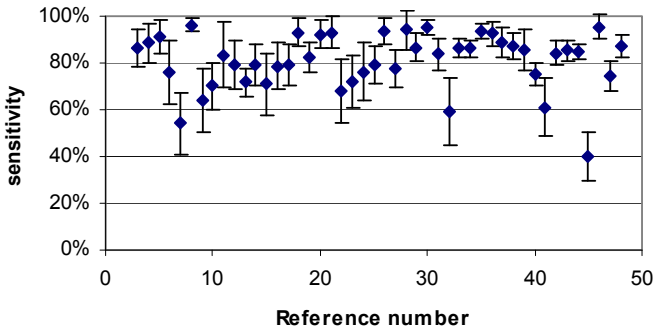
Specificity and 95%-Confidence Intervals

specificity

Reference number
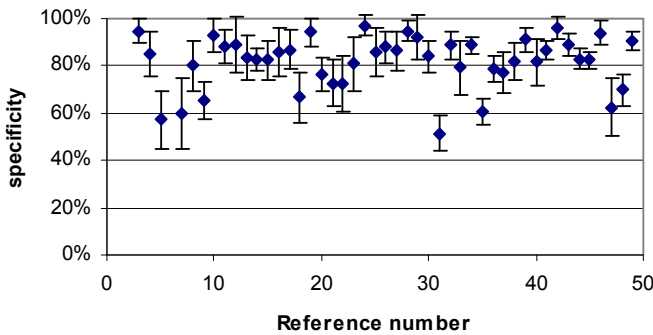
Figure: Sensitivity and specificity with 95%-confidence intervals

accuracy. Baseline patient characteristics were assumed applicable to both the total group and this subgroup with the exception of two studies[4, 28]. In these latter studies, unfortunately patients with resting wall motion abnormalities were only considered to have a positive DSE when dobutamine stress-induced wall motion abnormalities outside the infarction area were present. Therefore, we excluded in these studies patients with a history of myocardial infarction.

Table IV

Sensitivity and specificity according to differences in angiographic definition of coronary artery disease.

Values of sensitivity or specificity (%)	Sensitivity (number of studies)		Specificity (number of studies)	
	50% R	70% R	50% R	70% R
	n=35	n=11	n=35	n=11
31-40	1	0	0	0
41-50	0	0	0	0
51-60	2	0	3	1
61-70	2	2	3	1
71-80	8	5	8	0
81-90	12	3	17	4
91-100	10	1	4	5
Weighted mean	84%	83%	82%	84%

R = reduction in luminal diameter

As seen in Table III, the 46 individual studies had wide variations in sensitivity and specificity, although clustered around higher values. This can also be appreciated from Figure I, which shows the diagnostic accuracy for each study with 95%-confidence intervals.

Definition of CAD
Differences in sensitivity and specificity according to two definitions of CAD remained regardless of which definition is used for CAD (Table IV). In 35 studies, 50% stenosis as criterion for significant CAD was used with a weighted mean sensitivity and specificity of 84% and 82%, respectively. In 11 studies, 70% stenosis was used with a weighted mean sensitivity and specificity of 83% and 84%, respectively.

DSE protocol
Table V gives sensitivity and specificity values separated according to different DSE protocols. Seven studies used a dobutamine dose less then 40 µg/kg/min (protocol I), 12 used ≥ 40 µg/kg/min dobutamine and continued β-blocker (protocol II), 8 used ≥ 40 µg/kg/min dobutamine and stopped β-blocker (protocol III), 11 used addition of atropine, while continuing β-blocker (protocol IV) and 8 used addition of atropine and stopped β-blocker (protocol V). Between individual studies, a wide variation in sensitivity and

specificity can be observed. However, weighted mean sensitivity and specificity were not different.

Table V
Sensitivity and specificity according to differences in stress test protocol.

Values of sensitivity or specificity (%)	Sensitivity (number of studies)					Specificity (number of studies)				
	I	II	III	IV	V	I	II	III	IV	V
	n=7	n=12	n=8	n=11	n=8	n=7	n=12	n=8	n=11	n=8
31-40	0	0	0	1	0	0	0	0	0	0
41-50	0	0	0	0	0	0	0	0	0	0
51-60	0	1	0	0	1	0	2	0	1	1
61-70	1	1	0	1	1	1	1	1	0	1
71-80	1	3	4	2	3	1	4	0	2	1
81-90	3	3	3	4	2	4	4	3	6	4
91-100	2	4	1	3	1	1	1	4	2	1
Weighted mean	87%	81%	83%	84%	82%	83%	80%	88%	84%	76%

I: <40 µg/kg/min,
II: ≥40 µg/kg/min and β-blocker continuation,
III: ≥40 µg/kg/min without β-blocker continuation,
IV: ≥40 µg/kg/min plus atropine addition and β-blocker continuation,
V: ≥40 µg/kg/min plus atropine addition without β-blocker continuation

Table VI
Sensitivity and specificity according to differences in definition of positive DSE.

Values of sensitivity or specificity (%)	Sensitivity (number of studies)			Specificity (number of studies)		
	A	B	C	A	B	C
	n=31	n=11	n=4	n=31	n=11	n=4
31-40	1	0	0	0	0	0
41-50	0	0	0	0	0	0
51-60	2	0	0	1	1	2
61-70	4	0	0	2	1	1
71-80	10	3	0	6	1	1
81-90	9	5	1	14	7	0
91-100	5	3	3	8	1	0
Weighted mean	81%	84%	91%	85%	84%	60%

A: new or worsening wall motion abnormalities (=myocardial ischemia);
B: myocardial ischemia or a resting wall motion abnormality without improvement during dobutamine infusion
C: myocardial ischemia or a resting wall motion abnormality regardless of change during dobutamine infusion

Definition of positive test
Sensitivity and specificity according to three definitions of abnormal DSE described earlier, are presented in Table VI. Criterion A (requiring ischemia) was used in 31 studies, criterion B (requiring ischemia or a fixed wall motion abnormality) in 11 studies and criterion C (requiring a wall motion abnormality at any stage) in 4 studies. The weighted means for sensitivity and specificity regarding these criteria were 81%, 84%, 91% and 85%, 84%, 60%, respectively. Significant differences in sensitivity between protocol A and B (P < 0.02), protocol A and C (P < 0.0001) and protocol B and C (P < 0.0001) were found. Specificity of protocol C versus protocol A and B was significantly different (P<0.0001).

Results for methodological standards

Standard 1: adequate selection and identification of patients
All studies had a reasonably clear description of patient selection, with all but one (98%) giving information about age and gender (standard 1A). Also continued beta-blocker therapy of the population studied may influence the accuracy of the test as a lower heart rate increment, caused by β-blockers, may result in an increased number of non-diagnostic tests and therefore decrease sensitivity. Standard 1B was met by 18 studies (39%), indicating that in these studies β-blocking medication was discontinued before DSE.

Standard 2: adequate analysis of disease in individual coronary arteries
As previously noted[1, 2], the sensitivity for detection of CAD depends on the extent and location of CAD. For example, it is well known that both in patients with single vessel CAD and left circumflex lesions, lower sensitivities are found[1]. Standard 2 was intended to allow evaluation of the test over the full anatomic spectrum of CAD. Almost all studies (98%) described the extent of the coronary lesions in terms of 1,2 or 3-vessel CAD (72%) or single- versus multi-vessel CAD (26%) (standard 2A). Results for the extent of CAD were given in the great majority (87%) of the studies (standard 2C). Fourteen studies (30%) gave sensitivity and specificity for single- and multi vessel CAD only[5, 8, 12, 13, 19, 23-25, 37, 41, 42, 44]. Only 15 studies (33%) reported the location of the involved vessel (standard 2B). From these 15 studies, 12 (26%) met standard 2D by providing DSE results for these individual locations (standard 2D); 5 only gave sensitivity[5, 13, 21, 35, 41] or results for SVD[8, 33]. Although it is essential to differentiate between potential left main or three-vessel CAD versus single-vessel CAD[48], we only found eight studies to determine the number of patients with multi-vessel CAD based on multi-region wall motion abnormalities during DSE (standard 2E). None of the studies mentioned left ventricular cavity dilatation as a marker for multi-vessel CAD. As a low ischemic threshold is also a criterion for more severe and/or extensive CAD[49], we analyzed the number of studies mentioning the dose and heart rate at which new wall motion abnormalities appeared on echocardiography among various sub-groups with CAD. Few studies[3, 14, 23] mentioned ischemic

threshold and only one study[3] (2%) met standard 2F by giving information on ischemic threshold in sub-groups of patients.

Standard 3: adequate analysis for relevant chest pain syndromes
Because both the spectrum of clinical syndromes as well as the anatomical spectrum of CAD should be considered, standard 3 intended to ensure that DSE was performed in patients with the common chest pain syndromes that usually lead to performance of the test. Only 15 studies (33%) provided information on the number of patients with typical angina pectoris (standard 3A). There was a wide variation (17-87%) in number of patients with typical angina. None of the studies provided sensitivity and specificity for chest pain characteristics (standard 3B). Three studies[13, 34, 41] calculated pre-test probability of disease for each patient on the basis of age, gender and chest pain characteristics. In only one study[34], diagnostic accuracy of DSE was assessed according to pre-test probability of disease. In patients with higher pre-test probability of disease DSE sensitivity was higher.

Standard 4: avoidance of a limited challenge group
From exercise testing and thallium scintigraphy, it is known that left bundle branch block[50, 51], left ventricular hypertrophy[52, 53] and female gender[54] can negatively influence the diagnostic accuracy of a stress-test. Therefore, analysis of these patients should be performed in a separate study or performed as a subgroup within a study. Eight studies excluded patients because of left bundle branch block[9, 18, 24, 25, 29, 36], left ventricular hypertrophy[24, 42] or female gender[3], and therefore did not meet standard 4A. The percentage of patients excluded varied from 1% to 14%. One study performed DSE in a female population and showed a low sensitivity in single-vessel CAD[43]. In contrast, most investigations were performed in a predominantly male population. Also, when patients with poor echocardiographic window are excluded, this would reduce the chance of a false-negative result. In 11 studies (24%), information was unavailable concerning the inclusion of patients with poor windows and 22 (48%) excluded patients because of poor basal echocardiographic window. A wide range in number of excluded patients was observed (1-14%). Thirteen studies (28%) met standard 4B, by not excluding patients with poor echo windows.

Standard 5: avoidance of work-up bias
Studies can be designed prospectively and retrospectively. A retrospective study design (in which patients are included who underwent coronary angiography and DSE within a certain time period) may suffer from work-up bias. In these studies it can be assumed that coronary angiography was guided by (usually positive) DSE results. This may obviously increase sensitivity and decrease specificity of DSE. However, most prospective study designs are also sub optimal. Patients recruited from a coronary angiography waiting list are likely to have undergone some other stress test with positive result and thus some sort of work-up bias is still pres-

ent. Patient prospectively scheduled for coronary angiography and DSE usually do not represent the whole spectrum of disease as encountered in clinical practice (i.e. consecutive patients with non-anginal chest pain, atypical and typical angina) but usually represent the most diseased part of the spectrum. Thirty-six studies (78%) had a prospective study-design and thereby fulfilled standard 5, avoidance of work-up bias.

Standard 6: avoidance of diagnostic review bias
Interpreting DSE with knowledge of the results of coronary angiography can lead to an overestimate of a test's accuracy, especially because DSE is open to subjective interpretation. In contrast to previous published reviews on exercise testing[2] and thallium-201 imaging[55], 43 studies (93%) met standard 6A by clearly stating that DSE scoring was performed blinded. Thirty studies (65%) noted the blinding of the readers of the coronary angiogram. Both standard 6A and 6B were met by 30 studies (65%).

Standard 7: adequate analysis for non-diagnostic DSE tests
If non-diagnostic tests are included as a negative test in the results, sensitivity is artificially decreased and specificity increased. The frequency of non-diagnostic results in a (new) diagnostic test is important because a test will have a low clinical effectiveness if its results cannot be interpreted in a substantial number of patients. Common causes for a non-diagnostic DSE are a protocol that is unable to achieve target heart rate or side effects resulting in premature termination of the test. Only three studies[13, 43, 45] (7%) gave explicit information about the number of patients with a diagnostic test or this could be deducted from a table with individual patient data in two studies[7, 9] (4%). In one study[45], these patients were excluded and in the other four the DSE results were included as normal. Seven studies (15%) mentioned the number of patients reaching target heart rate (standard 7B) and 32 studies (70%) reported the mean maximum heart rate (standard 7C). However, this can only give an indication of stress induced by dobutamine. For instance, in a severely diseased study population, the number of patients achieving target heart rate may be limited because ischemia was observed prior and mean maximum heart rate is strongly dependent on the mean age of the study population.

Standard 8: use of state-of-the-art protocol
The last standard intended to analyze the number of studies using atropine. Several reports have shown that addition of atropine to dobutamine is safe[56] and beneficial in patients who do not reach target heart rate and have no echocardiographic signs and symptoms of ischemia[10, 30, 31, 37, 47]. In our analysis, only 19 studies (41%) used a maximum dose of 40 or 50 μg/kg/min of dobutamine and additional atropine if necessary, although a clear trend is seen to the use in more recent years.

Discussion

The main finding of this study is that the diagnostic variability of DSE for the diagnosis of CAD is related to the definition of a positive test, and not to the definition of CAD by coronary angiography nor by the DSE protocol used. However, because this cannot sufficiently explain the wide variation in diagnostic accuracy, we performed a complete and unbiased evaluation of research design. This methodological analysis showed reasonable compliance with only three of eight standards. Differences were observed in the selection of the study population (quality of echocardiographic window, presence of angina pectoris), handling of confounding factors and analysis of disease in individual coronary arteries. Lack of data on analysis of relevant chest pain syndromes and handling of non-diagnostic test results hampered further evaluation of these standards. The variations in methodology described in this review could produce highly variable results for diagnostic accuracy. Many suggestions have already been described to improve study design for diagnostic tests[2, 55]. We can add several recommendations for improving study design for DSE.

Recommendations for diagnostic DSE studies.
   Study design. DSE studies should be prospectively designed to minimize the influence of work-up (post-test) bias. Information on numbers, and reasons, of excluded patients should be provided. In particular, it should be stated in how many patients poor echo window quality precluded DSE analysis. Patients with potential false positive or negative test results should not be excluded but analysed separately.
   Patients. Patient data should preferably be presented in a table with individual data on gender, age, risk factors for CAD, clinical history and chest pain type. Such a table will make it possible for a reader to assess the pre-test probability of CAD for each patient and the study population[57].
   DSE protocol. Beta-blockers should preferably be stopped before diagnostic DSE since these drugs lower peak cardiac work load[58] and thus have the potential to lower DSE sensitivity. Current state-of-the-art (dobutamine-atropine) protocols, including use of the biphasic response, should be used[1]. Analysis of echo segments and correlation with coronary territories should be performed following standardized guidelines[59], blinded for clinical and coronary angiographic information. DSE should be considered positive in case of stress-induced abnormalities in one or more segments[60]. A possible exception are isolated stress-induced abnormalities in basal inferior-posterior segments, because these are well known for their tendency toward false positive results[61, 62]. The stress protocol should probably (more safety data are needed) not be terminated because of the induction of minor wall motion abnormalities, as the chance to identify multi-vessel CAD increases when maximal stress testing is pursued. DSE results should be obligatory analysed for the

presence of significant CAD (DSE positivity defined as stress-induced wall motion abnormality). In patients without a clinical history of myocardial infarction, analysis for the presence of CAD (DSE positivity defined as rest and/or stress-induced wall motion abnormality) may be reported in addition. Most importantly, all above mentioned elements of the protocol should be clearly described.

Coronary angiographic protocol. Coronary angiography should be scored blinded for clinical and DSE information. Stenosis should preferably be scored quantitatively with 50% diameter stenosis as cut off point for hemodynamic significance[63].

Description of results. As important as knowledge about the number of patients excluded because of a poor echo window is the number, and reason, of non-diagnostic DSE studies. These two sets of data determine, together with diagnostic accuracy, the clinical efficacy of DSE in real clinical practice. As with patient data, test results should be preferably presented in a table with individual data on peak heart rate, test end-point, ischemic threshold, and localisation (coronary territory) of ischemia and coronary stenosis. Such a table will make it possible for a reader to assess overall diagnostic accuracy and in various subgroups.

Clinical interpretation of results. Clinicians must be aware of differences in clinical characteristics between their patient population and the population in which a diagnostic test was evaluated. Differences in study groups and work-up bias may change diagnostic sensitivity and specificity.

Conclusion

Compared to earlier methodological reviews on exercise electrocardiography[2, 64] and stress thallium scintigraphy[55, 65], an increase in conformation to methodological standards can be observed. However, a stronger adherence to, and addition of important methodological standards can still improve the clinical relevance of DSE research.

References

1. Geleijnse ML, Fioretti PM, Roelandt JR. Methodology, feasibility, safety and diagnostic accuracy of dobutamine stress echocardiography. J Am Coll Cardiol 1997; 30:595-606.
2. Philbrick JT, Horwitz RI, Feinstein AR. Methodologic problems of exercise testing for coronary artery disease: groups, analysis and bias. Am J Cardiol 1980; 46:807-12.
3. Cohen JL, Greene TO, Ottenweller J, Binenbaum SZ, Wilchfort SD, Kim CS. Dobutamine digital echocardiography for detecting coronary artery disease. Am J Cardiol 1991; 67:1311-8.
4. Sawada SG, Segar DS, Ryan T, et al. Echocardiographic detection of coronary artery disease during dobutamine infusion. Circulation 1991; 83:1605-14.
5. Epstein M, Gin K, Sterns L, Pollick C. Dobutamine stress echocardiography: initial experience of a Canadian centre. Can J Cardiol 1992; 8:273-9.
6. Martin TW, Seaworth JF, Johns JP, Pupa LE, Condos WR. Comparison of adenosine, dipyridamole, and dobutamine in stress echocardiography. Ann Intern Med 1992; 116:190-6.
7. Salustri A, Fioretti PM, Pozzoli MM, McNeill AJ, Roelandt JR. Dobutamine stress echocardiography: its role in the diagnosis of coronary artery disease. Eur Heart J 1992; 13:70-7.
8. Marcovitz PA, Armstrong WF. Accuracy of dobutamine stress echocardiography in detecting coronary artery disease. Am J Cardiol 1992; 69:1269-73.
9. Mazeika PK, Nadazdin A, Oakley CM. Dobutamine stress echocardiography for detection and assessment of coronary artery disease. J Am Coll Cardiol 1992; 19:1203-11.
10. McNeill AJ, Fioretti PM, el-Said SM, Salustri A, Forster T, Roelandt JR. Enhanced sensitivity for detection of coronary artery disease by addition of atropine to dobutamine stress echocardiography. Am J Cardiol 1992; 70:41-6.
11. Gunalp B, Dokumaci B, Uyan C, et al. Value of dobutamine technetium-99m-sestamibi SPECT and echocardiography in the detection of coronary artery disease compared with coronary angiography. J Nucl Med 1993; 34:889-94.
12. Hoffmann R, Lethen H, Kleinhans E, Weiss M, Flachskampf FA, Hanrath P. Comparative evaluation of bicycle and dobutamine stress echocardiography with perfusion scintigraphy and bicycle electrocardiogram for identification of coronary artery disease. Am J Cardiol 1993; 72:555-9.
13. Marwick T, D'Hondt AM, Baudhuin T, et al. Optimal use of dobutamine stress for the detection and evaluation of coronary artery disease: combination with echocardiography or scintigraphy, or both? J Am Coll Cardiol 1993; 22:159-67.
14. Previtali M, Lanzarini L, Fetiveau R, et al. Comparison of dobutamine stress echocardiography, dipyridamole stress echocardiography and exercise stress testing for diagnosis of coronary artery disease. Am J Cardiol 1993; 72:865-70.
15. Afridi I, Quinones MA, Zoghbi WA, Cheirif J. Dobutamine stress echocardiography: sensitivity, specificity, and predictive value for future cardiac events. Am Heart J 1994; 127:1510-5.
16. Sahin M, Karakelleoglu S, Alp N, Atesal S, Senocak H. Diagnostic value of dobutamine stress echocardiography in coronary artery disease. Thorac Cardiovasc Surg 1994; 42:285-9.
17. Santiago P, Vacek JL, Rosamond TL. Dobutamine stress echocardiography: clinical utility and predictive value at various infusion rates. Am Heart J 1994; 128:804-8.
18. Senior R, Sridhara BS, Anagnostou E, Handler C, Raftery EB, Lahiri A. Synergistic value of simultaneous stress dobutamine sestamibi single- photon-emission computerized tomography and echocardiography in the detection of coronary artery disease. Am Heart J 1994; 128:713-8.

19. Beleslin BD, Ostojic M, Stepanovic J, et al. Stress echocardiography in the detection of myocardial ischemia. Head- to-head comparison of exercise, dobutamine, and dipyridamole tests. Circulation 1994; 90:1168-76.

20. Daoud EG, Pitt A, Armstrong WF. Electrocardiographic response during dobutamine stress echocardiography. Am Heart J 1995; 129:672-7.

21. Ho FM, Huang PJ, Liau CS, et al. Dobutamine stress echocardiography compared with dipyridamole thallium- 201 single-photon emission computed tomography in detecting coronary artery disease. Eur Heart J 1995; 16:570-5.

22. Sochowski RA, Yvorchuk KJ, Yang Y, Rattes MF, Chan KL. Dobutamine and dipyridamole stress echocardiography in patients with a low incidence of severe coronary artery disease. J Am Soc Echocardiogr 1995; 8:482-7.

23. Dagianti A, Penco M, Agati L, Sciomer S, Rosanio S, Fedele F. Stress echocardiography: comparison of exercise, dipyridamole and dobutamine in detecting and predicting the extent of coronary artery disease. J Am Coll Cardiol 1995; 26:18-25.

24. Di Bello V, Bellina CR, Gori E, et al. Incremental diagnostic value of dobutamine stress echocardiography and dobutamine scintigraphy (technetium 99m-labeled sestamibi single-photon emission computed tomography) for assessment of presence and extent of coronary artery disease. J Nucl Cardiol 1996; 3:212-20.

25. Iwase M, Fukui M, Tamagaki H, et al. Advantages and disadvantages of dobutamine stress echocardiography compared with treadmill exercise electrocardiography in detecting ischemia. Jpn Circ J 1996; 60:954-60.

26. Kisacik HL, Ozdemir K, Altinyay E, et al. Comparison of exercise stress testing with simultaneous dobutamine stress echocardiography and technetium-99m isonitrile single-photon emission computerized tomography for diagnosis of coronary artery disease. Eur Heart J 1996; 17:113-9.

27. San Roman JA, Vilacosta I, Castillo JA, et al. Dipyridamole and dobutamine-atropine stress echocardiography in the diagnosis of coronary artery disease. Comparison with exercise stress test, analysis of agreement, and impact of antianginal treatment. Chest 1996; 110:1248-54.

28. Wu CC, Ho YL, Kao SL, et al. Dobutamine stress echocardiography for detecting coronary artery disease. Cardiology 1996; 87:244-9.

29. Anthopoulos LP, Bonou MS, Kardaras FG, et al. Stress echocardiography in elderly patients with coronary artery disease: applicability, safety and prognostic value of dobutamine and adenosine echocardiography in elderly patients. J Am Coll Cardiol 1996; 28:52-9.

30. Ling LH, Pellikka PA, Mahoney DW, et al. Atropine augmentation in dobutamine stress echocardiography: role and incremental value in a clinical practice setting. J Am Coll Cardiol 1996; 28:551-7.

31. Pingitore A, Picano E, Colosso MQ, et al. The atropine factor in pharmacologic stress echocardiography. Echo Persantine (EPIC) and Echo Dobutamine International Cooperative (EDIC) Study Groups. J Am Coll Cardiol 1996; 27:1164-70.

32. Slavich GA, Guerra UP, Morocutti G, et al. Feasibility of simultaneous Tc99m sestamibi and 2D-echo cardiac imaging during dobutamine pharmacologic stress. Preliminary results in a female population. Int J Card Imaging 1996; 12:113-8.

33. Dionisopoulos PN, Collins JD, Smart SC, Knickelbine TA, Sagar KB. The value of dobutamine stress echocardiography for the detection of coronary artery disease in women. J Am Soc Echocardiogr 1997; 10:811-7.

34. Hennessy TG, Codd MB, Kane G, McCarthy C, McCann HA, Sugrue DD. Dobutamine stress echocardiography in the detection of coronary artery disease: importance of the pretest likelihood of disease. Am Heart J 1997; 134:685-92.

35. Ho YL, Wu CC, Lin LC, et al. Assessment of the functional significance of coronary artery stenosis by dobutamine-atropine stress echocardiography. Cardiology 1997; 88:386-92.

36. Huang PJ, Ho YL, Wu CC, et al. Simultaneous dobutamine stress echocardiography and thallium-201 perfusion imaging for the detection of coronary artery disease. Cardiology 1997; 88:556-62.

37. Schroder K, Agrawal R, Voller H, Kursten B, Dissmann R, Schultheiss HP. Factors influencing the diagnostic accuracy of dobutamine stress echocardiography. Int J Card Imaging 1997; 13:493-8.

38. Steinberg EH, Madmon L, Patel CP, Sedlis SP, Kronzon I, Cohen JL. Long-term prognostic significance of dobutamine echocardiography in patients with suspected coronary artery disease: results of a 5-year follow-up study. J Am Coll Cardiol 1997; 29:969-73.

39. Vitarelli A, Luzzi MF, Penco M, Fedele F, Dagianti A. On-line quantitative assessment of left ventricular filling during dobutamine stress echocardiography: a useful addition to conventional wall motion scoring. Int J Cardiol 1997; 59:57-69.

40. Elhendy A, van Domburg RT, Poldermans D, et al. Safety and feasibility of dobutamine-atropine stress echocardiography for the diagnosis of coronary artery disease in diabetic patients unable to perform an exercise stress test. Diabetes Care 1998; 21:1797-802.

41. Santoro GM, Sciagra R, Buonamici P, et al. Head-to-head comparison of exercise stress testing, pharmacologic stress echocardiography, and perfusion tomography as first-line examination for chest pain in patients without history of coronary artery disease. J Nucl Cardiol 1998; 5:19-27.

42. Takeuchi M, Miura Y, Sonoda S, Kuroiwa A. Comparison of Three Different Protocols for Dobutamine Stress Echocardiography: Does the Addition of Atropine Increase Complications, and Does It Improve Diagnostic Accuracy? Echocardiography 1999; 16:347-355.

43. Lewis JF, Lin L, McGorray S, et al. Dobutamine stress echocardiography in women with chest pain. Pilot phase data from the National Heart, Lung and Blood Institute Women's Ischemia Syndrome Evaluation (WISE). J Am Coll Cardiol 1999; 33:1462-8.

44. Loimaala A, Groundstroem K, Pasanen M, Oja P, Vuori I. Comparison of bicycle, heavy isometric, dipyridamole-atropine and dobutamine stress echocardiography for diagnosis of myocardial ischemia. Am J Cardiol 1999; 84:1396-400.

45. Nagel E, Lehmkuhl HB, Bocksch W, et al. Noninvasive diagnosis of ischemia-induced wall motion abnormalities with the use of high-dose dobutamine stress MRI: comparison with dobutamine stress echocardiography. Circulation 1999; 99:763-70.

46. Smart SC, Bhatia A, Hellman R, et al. Dobutamine-atropine stress echocardiography and dipyridamole sestamibi scintigraphy for the detection of coronary artery disease: limitations and concordance. J Am Coll Cardiol 2000; 36:1265-73.

47. Fioretti PM, Poldermans D, Salustri A, et al. Atropine increases the accuracy of dobutamine stress echocardiography in patients taking beta-blockers. Eur Heart J 1994; 15:355-60.

48. Califf RM, Harrell FE, Jr., Lee KL, et al. The evolution of medical and surgical therapy for coronary artery disease. A 15-year perspective. Jama 1989; 261:2077-86.

49. Panza JA, Curiel RV, Laurienzo JM, Quyyumi AA, Dilsizian V. Relation between ischemic threshold measured during dobutamine stress echocardiography and known indices of poor prognosis in patients with coronary artery disease. Circulation 1995; 92:2095-101.

50. Orzan F, Garcia E, Mathur VS, Hall RJ. Is the treadmill exercise test useful for evaluating coronary artery disease in patients with complete left bundle branch block? Am J Cardiol 1978; 42:36-40.

51. Hirzel HO, Senn M, Nuesch K, et al. Thallium-201 scintigraphy in complete left bundle branch block. Am J Cardiol 1984; 53:764-9.

52. Senior R, Basu S, Handler C, Raftery EB, Lahiri A. Diagnostic accuracy of dobutamine stress echocardiography for detection of coronary heart disease in hypertensive patients. Eur Heart J 1996; 17:289-95.

53. Schulman DS, Francis CK, Black HR, Wackers FJ. Thallium-201 stress imaging in hypertensive patients. Hypertension 1987; 10:16-21.

54. Chae SC, Heo J, Iskandrian AS, Wasserleben V, Cave V. Identification of extensive coronary artery disease in women by exercise single-photon emission computed tomographic (SPECT) thallium imaging. J Am Coll Cardiol 1993; 21:1305-11.

55. Detrano R, Lyons KP, Marcondes G, Abbassi N, Froelicher VF, Janosi A. Methodologic problems in exercise testing research. Are we solving them? Arch Intern Med 1988; 148:1289-95.

56. Poldermans D, Fioretti PM, Boersma E, et al. Safety of dobutamine-atropine stress echocardiography in patients with suspected or proven coronary artery disease. Am J Cardiol 1994; 73:456-9.

57. Diamond GA, Forrester JS. Analysis of probability as an aid in the clinical diagnosis of coronary-artery disease. N Engl J Med 1979; 300:1350-8.

58. Weissman NJ, Levangie MW, Newell JB, Guerrero JL, Weyman AE, Picard MH. Effect of beta-adrenergic receptor blockade on the physiologic response to dobutamine stress echocardiography. Am Heart J 1995; 130:248-53.

59. Schiller NB, Shah PM, Crawford M, et al. Recommendations for quantitation of the left ventricle by two-dimensional echocardiography. American Society of Echocardiography Committee on Standards, Subcommittee on Quantitation of Two-Dimensional Echocardiograms. J Am Soc Echocardiogr 1989; 2:358-67.

60. Elhendy A, van Domburg RT, Bax JJ, et al. Optimal criteria for the diagnosis of coronary artery disease by dobutamine stress echocardiography. Am J Cardiol 1998; 82:1339-44.

61. Carstensen S, Ali SM, Stensgaard-Hansen FV, et al. Dobutamine-atropine stress echocardiography in asymptomatic healthy individuals. The relativity of stress-induced hyperkinesia. Circulation 1995; 92:3453-63.

62. Bach DS, Muller DW, Gros BJ, Armstrong WF. False positive dobutamine stress echocardiograms: characterization of clinical, echocardiographic and angiographic findings. J Am Coll Cardiol 1994; 24:928-33.

63. Baptista J, Arnese M, Roelandt JR, et al. Quantitative coronary angiography in the estimation of the functional significance of coronary stenosis: correlations with dobutamine- atropine stress test. J Am Coll Cardiol 1994; 23:1434-9.

64. Hlatky MA, Pryor DB, Harrell FE, Jr., Califf RM, Mark DB, Rosati RA. Factors affecting sensitivity and specificity of exercise electrocardiography. Multivariable analysis. Am J Med 1984; 77:64-71.

65. Detrano R, Janosi A, Lyons KP, Marcondes G, Abbassi N, Froelicher VF. Factors affecting sensitivity and specificity of a diagnostic test: the exercise thallium scintigram. Am J Med 1988; 84:699-710.

Chapter 10

Factors affecting sensitivity and specificity of dobutamine stress echocardiography

ML Geleijnse
BJ Krenning
A Nemes
E Boersma
JG Bosch
TW Galema
FJ ten Cate

Abstract

Aim
Clinical characteristics of patients, angiographic referral bias and several technical factors may all affect the reported diagnostic accuracies of tests. This study aims to assess their influence on the diagnostic accuracy of dobutamine stress echocardiography (DSE).

Methods and results
The medical literature from 1991 to 2006 was searched for diagnostic DSE studies and meta-analysis was applied to the 62 studies thus retrieved, including 6,881 patients. These studies were analyzed for year of publication, direct comparison with newer technologies, gender and mean age of patients, inclusion of patients with prior myocardial infarction, multi-vessel coronary disease, typical angina or beta-blocking medication, blinding of tests, definition of angiographic disease, angiographic referral bias, addition of atropine, definition of positive DSE and use of the biphasic response. DSE sensitivity was significantly related to the inclusion of patients with prior myocardial infarction (0.834 vs. 0.740, P <0.0006) and defining DSE already positive in case of resting wall motion abnormalities rather than obligatory myocardial ischemia (0.786 vs 0.864, P=0.01). Specificity tended to be lower when patients with resting wall motion abnormalities were included in the study (0.812% vs. 0.877, P=0.08). The presence of referral bias adversely affected DSE specificity (0.771 vs. 0.842, P=0.01).

Conclusion
This analysis suggests that the reported sensitivity of DSE is higher and the specificity lower than that expected in clinical practice because of the inappropriate inclusion of patients with prior myocardial infarction, definition of positive DSE and the presence of referral bias.

Dobutamine stress echocardiography (DSE) has been extensively studied as a diagnostic test for the prediction of coronary artery disease (CAD). However, sensitivities and specificities differ greatly from one report to another. In one, often cited, review sensitivities ranged from 54% to 96% and specificities ranged from 62% to 93% [1]. Recently, controversy has also arisen regarding the inter-institutional stability of sensitivity and specificity and the wisdom of applying DSE results reported in the literature to other clinical laboratories [2]. Clinical characteristics of patients, angiographic referral bias and several technical factors have all been implicated as causes of differences in reported diagnostic accuracies for other stress modalities such as exercise electrocardiography [3] and thallium scintigraphy [4]. Therefore, we analyzed which factors influenced the sensitivity and specificity of DSE by applying meta-analysis on published diagnostic studies.

Methodology

Literature review
A Medline search for diagnostic DSE studies published up to 2006 using the terms "dobutamine stress" and "coronary artery disease" was performed. In addition, we reviewed the reference lists of review articles and eligible studies to complete the data search. Excluded from this search were reports solely reporting on patients with poor echocardiographic windows, left bundle branch block, hypertension and/or left ventricular hypertrophy or prior myocardial infarction. To avoid duplication of data only the largest report from an institution was considered, unless it was clear that different patients were included. Occasionally, reports were excluded because of clear mistakes in presentation of data[5]. The remaining 60 reports were retained for review [6-65]. One of these reports [61] described results of three separate study samples that had been based on different DSE protocols and these samples were treated as independent observations. For reports describing the value of atropine addition to DSE [32,39,45] only the dobutamine-atropine results were considered for analysis. For reports describing the value of second harmonic imaging [43,59] only the fundamental imaging data were used for analysis.

Statistical analysis
Sensitivity was defined as the number of true-positive tests divided by the total number of patients with angiographically significant CAD. *Specificity* was defined as the number of true-negative tests divided by the total number of patients without angiographically significant CAD. Sensitivity and specificity were first calculated for each study separately. The overall estimate of these test performance characteristics was then determined as the weighed average of the study specific values. The weighting factor was the square root of the number of patients on which the study specific sensitivity and specificity were based. Differences in the overall sensitivity

and specificity between groups of patients according to clinically relevant patient- and test characteristics were evaluated by Student's t-tests. Statistical significance for all tests was defined at the $P < 0.05$ level.

Univariable and multivariable linear meta-regression was applied to identify the relation between the variables that are listed in Table 4 and overall sensitivity/ specificity. All variables entered the multivariable stage, irrespective of the results in univariable analysis. The final regression model was constructed via a backward selection method, and variables with a P-value < 0.05 were maintained.

Recording the variables
The values of the variables were noted before recording the reported sensitivity and specificity. Two investigators (MLG and BJK) read the reports independently and recorded the variables listed in the tables. When a disagreement occurred between the two investigators issues were resolved by consensus or a third investigator.

Discrete variables
These included the following: direct comparison with newer technologies (magnetic resonance imaging, three-dimensional echocardiography, tissue Doppler imaging, myocardial contrast echocardiography, fractional area changes, rapid beta-blocker injection, or second harmonic imaging), inclusion of patients with prior myocardial infarction, inclusion of patients with beta-blocking medication (for analysis no avail- able information on beta-blocking medication was interpreted as present), blind interpretation of DSE and coronary angiography (for analysis no available informa- tion regarding blinding was interpreted as not blinded), definition of angiographic disease (50% versus 70% reduction in luminal diameter), presence of angiograph- ic referral bias (DSE results influencing the decision to undergo coronary angio- graphy), addition of atropine, echocardiographic imaging technique (fundamental or second harmonic), definition of positive DSE (dobutamine stress-induced or any wall motion abnormality), number of wall motion abnormalities required for a posi- tive test (one or two segments, for analysis no available information on the number of segments or statements like 'a wall motion abnormality' were interpreted as one segment), and use of the biphasic response (improvement of wall motion at low- dose followed by worsening of wall motion at high-dose, for analysis no available information on use of the biphasic response was interpreted as not used).

Continuous variables
These included the following: year of publication, mean age, percentage of men, percentage of patients with prior myocardial infarction, percentage of patients with CAD ("a priori CAD probability"), and percentage of patients receiving beta-block- ing medication.

Table 1. Group Characteristics Variables and Diagnostic Accuracies.

Author	Year	Patients	Mean Age	Men (%)	Typical Angina (%)	CAD (%)	MVD CAD (%)	Beta-blocker	Beta-blocker (%)	MI	MI (%)	Sensitivity (%)	Specificity (%)
Afridi[6]	1994	45	62	99	-	84	69	Yes	27	Yes	29	71	86
Ahmad[7]	2001	90	-	47	32	64	41	Yes	40	Yes	25	59	81
Anthopoulos[8]	1996	120	75	60	43	74	58	Yes	46	Yes	40	87	84
Beleslin[9]	1994	136	50	85	36	88	8	Yes	43	Yes	57	82	76
Cain[10]	2001	114	62	75	-	74	47	Yes	52	Yes	8	88	80
Carstensen[11]	2002	68	56	84	-	75	73	Yes	38	Yes	46	73	71
Chiou[12]	2004	132	67	75	32	64	58	-	-	No	0	84	81
Cohen[13]	1991	70	62	100	-	73	50	Stopped	0	Yes	27	86	95
Dagianti[14]	1995	60	55	70	-	42	25	Stopped	0	No	0	72	97
Daoud[15]	1995	76	60	58	-	86	55	Yes	12	Yes	37	92	73
Di Bello[16]	1996	45	53	73	87	84	42	Stopped	0	No	0	76	86
Dionisopoulos[17]	1997	288	61	65	-	73	42	Yes	31	Yes	-	87	89
Elhendy[18]	1998	295	60	67	32	77	48	Yes	35	Yes	52	75	87
Elhendy[19]	2004	170	60	58	-	75	75	Stopped	0	Yes	23	70	74
Epstein[20]	1992	61	59	70	-	89	48	Yes	34	Yes	-	91	57
Eroglu[21]	2006	36	63	84	72	78	57	Yes	44	Yes	14	93	75
Fathi[22]	2001	77	61	74	-	71	47	Yes	32	Yes	42	98	59
Gunalp[23]	1993	27	47	85	-	67	33	Stopped	0	No	0	83	89
Hennessy[24]	1997	317	60	72	57	86	62	Stopped	0	Yes	39	86	60
Ho[25]	1995	54	58	85	-	80	67	-	-	Yes	41	93	73
Ho[26]	1997	223	58	81	-	73	56	Yes	-	Yes	39	94	79
Hoffmann[27]	1993	60	57	77	-	80	35	Stopped	0	No	0	79	83
Huang[28]	1997	93	61	77	-	72	52	Yes	58	Yes	39	93	77
Iwase[29]	1996	96	59	70	-	66	29	Stopped	0	Yes	30	79	88
Kisacik[30]	1996	69	51	84	45	68	45	Stopped	0	Yes	30	94	86
Lewis[31]	1999	92	58	0	-	27	16	Yes	22	Yes	10	40	94
Ling[32]	1996	183	69	35	-	81	60	Yes	23	Yes	32	95	51
Loimaala[33]	1999	60	55	67	65	73	30	Yes	20	Yes	15	95	63
Marcovitz[34]	1992	141	60	60	-	77	33	Yes	-	Yes	11	96	66

Author	Year	N											
Martin [35]	1992	40	50	95	30	63	0	Yes	33	Yes	35	76	60
Marwick [36]	1993	217	58	72	65	65	34	Yes	19	No	0	72	83
Mathias [37]	2003	101	58	60	-	63	59	Yes	46	Yes	16	84	92
Mazeika [38]	1992	50	54	88	-	72	48	Stopped	0	Yes	26	64	93
McNeill [39]	1992	80	59	74	-	59	19	Yes	80	Yes	35	70	88
Mishra [40]	2002	44	53	0	-	59	38	No	-	No	0	73	94
Ángel [41]	1999	172	60	71	-	63	41	No	0	No	0	74	70
Nedeljkovic [42]	2006	117	54	78	59	59	17	Yes	34	Yes	27	96	92
Nixdorf [43]	2001	50	62	80		20	10	stopped	0	yes	34	60	93
Peteiro [44]	2001	41	63	78	-	78	49	-	-	Yes	41	81	89
Pingitore [45]	1996	110	60	83	-	84	46	Yes	5	Yes	27	84	89
Previtali [46]	1993	80	53	78	-	71	41	Stopped	0	Yes	19	79	83
Rollan [47]	1999	236	63	58	75	61	51	Yes	-	No	0	72	89
Sahin [48]	1994	65	58	71	71	65	40	Stopped	0	Yes	23	79	87
Salustri [49]	1992	52	58	73	-	71	33	Yes	69	Yes	27	54	80
San Román [50]	1996	102	62	56	25	62	33	Yes	21	No	0	78	95
Santiago [51]	1994	77	67	70	-	69	0	Stopped	0	Yes	-	79	67
Santoro [52]	1998	60	-	-	17	55	35	No	0	No	0	61	96
Sawada [53]	1991	55	59	62	19	64	25	Yes	51	No	0	89	85
Schröder [54]	1997	99	57	80	-	89	41	Stopped	0	Yes	53	89	82
Senior [55]	1994	61	63	72	-	72	49	Stopped	0	Yes	21	93	94
Slavich [56]	1996	46	59	0	-	48	26	Stopped	0	No	0	59	79
Smart [57]	2000	183	60	73	26	65	32	Yes	27	Yes	-	87	91
Sochowski [58]	1995	46	58	67	48	54	28	Yes	37	No	0	68	81
Sozzi [59]	2001	64	59	70	-	77	55	Yes	50	Yes	55	78	73
Steinberg [60]	1997	120	67	99	-	72	46	Stopped	0	Yes	23	87	91
Takeuchi [61]	1999	178	63	77	-	65	31	Yes	16	Yes	55	84	89
Takeuchi [61]	1999	249	64	80	-	55	33	Yes	18	Yes	48	85	83
Takeuchi [61]	1999	511	63	71	-	53	25	Yes	16	Yes	50	85	82
Vitarelli [62]	1997	59	52	64	-	81	44	Stopped	0	Yes	-	85	82
Wu [63]	1996	30	58	84	-	57	40	Yes	-	No	0	94	92
Xie [64]	2005	27	56	35	-	78	48	-	-	No	0	33	83
Yuda [65]	2002	161	61	65	-	66	57	Yes	39	No	0	66	38

CAD = Coronary Artery Disease. MI = Myocardial Infarction. MVD = Multi Vessel Disease. - = Not Available

Results

Sensitivities and specificities (Table 1)
For the 62 unique study groups in the 60 reports, 6,881 patients were studied with DSE and coronary angiography with sufficient data to record sensitivity and specificity. Of these, 4,718 had angiographic CAD whereas 2,163 did not. A total of 3,882 patients had true positive DSE resulting in a sensitivity of 0.812. There were 1,790 true negatives, allowing for a specificity of 0.822. Sensitivities and specificities for each of the 62 study groups are reported in Table 1.

Effect of patient characteristics (Tables 1 and 4)
Extend of CAD. In 48 studies sensitivity for single-vessel and multi-vessel CAD could be calculated separately (mean sensitivity and specificity in these 5,581 patients was 0.814 and 0.836, respectively). In the 1,663 patients with single-vessel CAD sensitivity was 0.728. In the 2.156 patients with multi-vessel CAD sensitivity was 0.877.

Prior myocardial infarction. The mean reported sensitivity and specificity from the 45 studies that included patients with prior myocardial infarction were 0.834 and 0.811, respectively. For the 17 studies that excluded patients with prior myocardial infarction sensitivity and specificity were 0.740 (P <0.01) and 0.852, respectively. In the 780 myocardial infarction patients whose angiographic disease status and DSE result could be inferred from the available data, sensitivity was 0.820 and specificity was 0.745. In the 2,161 non-myocardial infarction patients whose angiographic disease status and DSE result could be inferred, sensitivity was 0.756 (P <0.05) and specificity was 0.868 (P <0.01). In the 12 studies in which patients with resting wall motion abnormalities were excluded, sensitivity tended to be lower compared to the 50 studies in which also patients with resting wall motions were included (0.756 vs. 0.821, P = 0.14) and specificity was higher (0.877 vs. 0.812, P <0.01). Of the continuous variables, the a priori CAD probability and the percentage of patients with resting wall motion abnormalities showed the highest correlation with DSE sensitivity (r = 0.376, P <0.01 and r = 0.254, P <0.01, respectively) and specificity (r = -0.352, P <0.01 and r = -0.224, P <0.01, respectively).

Other patient characteristics. Mean age, percentage of men and continuation of beta-blocking medication during DSE did not significantly affect DSE sensitivity or specificity.

Effect of publication factors (Table 1)
The years that studies were published were not correlated to DSE sensitivity or specificity.

Table 2. Referral bias and other Angiographic Factors.

Author	Referral Bias	Angiography Blinded	Angiography CAD% cut off	Angiography Quantitative
Afridi [6]	Yes	Yes	70	Yes
Ahmad [7]	Yes	No	50	No
Anthopoulos [8]	No	Yes	50	No
Beleslin [9]	No	Yes	50	Yes
Cain [10]	Yes	Yes	50	Yes
Carstensen [11]	No	Yes	50	Yes
Chiou [12]	No	Yes	50	Yes
Cohen [13]	No	Yes	70	No
Dagianti [14]	No	Yes	70	Yes
Daoud [15]	Yes	No	50	No
Di Bello [16]	No	Yes	50	No
Dionisopoulos [17]	Yes	Yes	50	Yes
Elhendy [18]	Yes	No	50	Yes
Elhendy [19]	Yes	Yes	50	Yes
Epstein [20]	Yes	Yes	50	No
Eroglu [21]	No	No	50	No
Fathi [22]	Yes	Yes	50	Yes
Gunalp [23]	No	No	50	No
Hennessy [24]	No	Yes	50	No
Ho [25]	No	Yes	50	No
Ho [26]	No	No	50	Yes
Hoffmann [27]	No	Yes	70	Yes
Huang [28]	No	No	50	Yes
Iwase [29]	No	Yes	70	No
Kisacik [30]	No	Yes	50	No
Lewis [31]	No	Yes	50	Yes
Ling [32]	Yes	No	70	No
Loimaala [33]	No	No	50	No
Marcovitz [34]	Yes	No	50	Yes
Martin [35]	No	Yes	50	No
Marwick [36]	No	No	50	Yes
Mathias [37]	Yes	Yes	50	Yes
Mazeika [38]	No	Yes	70	No
McNeill [39]	No	No	50	No
Mishra [40]	Yes	Yes	70	No
Nagel [41]	No	Yes	50	No

Nedeljkovic [42]	No	Yes	50	Yes
Nixdorff [43]	No	yes	70	Yes
Peteiro [44]	No	Yes	50	No
Pingitore [45]	No	Yes	50	Yes
Previtali [46]	No	Yes	50	No
Rollan [47]	No	No	70	No
Sahin [48]	No	Yes	50	No
Salustri [49]	No	Yes	50	Yes
San Román [50]	No	No	50	Yes
Santiago [51]	No	No	70	No
Santoro [52]	Yes	No	70	Yes
Sawada [53]	Yes	Yes	50	Yes
Schröder [54]	No	No	50	Yes
Senior [55]	No	Yes	50	No
Slavich [56]	No	No	50	Yes
Smart [57]	No	Yes	50	Yes
Sochowski [58]	No	Yes	50	No
Sozzi [59]	Yes	No	70	Yes
Steinberg [60]	No	Yes	70	No
Takeuchi [61]	No	Yes	50	Yes
Takeuchi [61]	No	Yes	50	Yes
Takeuchi [61]	No	Yes	50	Yes
Vitarelli [62]	Yes	No	70	No
Wu [63]	No	Yes	50	Yes
Xie [64]	No	No	50	Yes
Yuda [65]	Yes	Yes	50	Yes

Abbreviation see Table 1.

Effect of angiographic referral bias (Tables 2 and 4)

The presence of referral bias, present in 18 studies, negatively affected test specificity (0.771 vs. 0.842, P <0.01).

Effect of technical angiographic factors (Tables 2 and 4)

Definition of stenosis. There was no difference in sensitivity between the 47 studies in which 50% diameter stenosis was used as cut off for significant CAD compared to the 15 studies in which 70% diameter stenosis was used as cut off for significant CAD.

Blinding of reading. Blinding of the coronary angiogram, present in 41 studies, did not significantly affect sensitivity.

Quantitative scoring of stenosis. Quantitative scoring of the coronary angiogram, present in 34 studies, did not significantly affect sensitivity and specificity. In the 28

Table 3. Stress Echocardiographic Factors.

Author	Comparison with New Technology	Stress Echo Blinded	Dobu-tamine Dose	Atropine Addition	Definition of Positive Test	Segments Required	Biphasic Response
Afridi [6]	No	Yes	40	No	Rest or Stress	-	No
Ahmad [7]	Yes	Yes	40	Yes	Stress	-	-
Anthopoulos [8]	No	Yes	40	No	Stress	1	No
Beleslin [9]	No	Yes	40	No	Stress	1	-
Cain [10]	Yes	Yes	40	Yes	Rest or Stress	-	Yes
Carstensen [11]	Yes	Yes	40	Yes	Stress	1	No
Chiou [12]	Yes	Yes	40	Yes	Stress	2	NA
Cohen [13]	No	Yes	40	No	Stress	-	No
Dagianti [14]	No	Yes	40	No	Stress	1	NA
Daoud [15]	No	-	30	No	Rest or Stress	1	No
Di Bello [16]	No	Yes	40	Yes	Stress	1	NA
Dionisopoulos [17]	No	Yes	40	Yes	Rest or Stress	2	Yes
Elhendy [18]	No	Yes	40	Yes	Stress	1	Yes
Elhendy [19]	Yes	Yes	50	Yes	Stress	2	No
Epstein [20]	No	Yes	50	No	Rest or Stress	1	-
Eroglu [21]	Yes	Yes	40	Yes	Stress	1	Yes
Fathi [22]	Yes	Yes	40	Yes	Stress	-	Yes
Gunalp [23]	No	Yes	30	No	Stress	1	No
Hennessy [24]	No	Yes	50	Yes	Rest or Stress	2	-
Ho [25]	No	Yes	40	No	Stress	1	No
Ho [26]	No	Yes	40	Yes	Stress	2	No
Hoffmann [27]	No	Yes	40	Yes	Stress	-	NA
Huang [28]	No	Yes	40	Yes	Rest or Stress	-	Yes
Iwase [29]	No	Yes	40	No	Stress	-	No
Kisacik [30]	No	Yes	40	Yes	Stress	1	No
Lewis [31]	No	Yes	40	Yes	Stress	1	Yes
Ling [32]	No	Yes	40	Yes	Rest or Stress	1	-
Loimaala [33]	No	Yes	40	No	Stress	1	-
Marcovitz [34]	No	Yes	30	No	Rest or Stress	-	No
Martin [35]	No	Yes	40	No	Stress	2	No
Marwick [36]	No	Yes	40	No	Rest or Stress	1	No
Mathias [37]	Yes	Yes	40	Yes	Stress	1	Yes
Mazeika [38]	No	Yes	20	No	Stress	1	No
McNeill [39]	No	Yes	40	Yes	Stress	1	No
Mishra [40]	Yes	-	40	Yes	Stress	1	NA
Nagel [41]	Yes	Yes	40	Yes	Stress	1	Yes
Nedeljkovic [42]	No	Yes	40	Yes	Stress	1	NA
Nixdorff [43]	Yes	yes	40	yes	Stress	2	Yes
Peteiro [44]	Yes	Yes	40	Yes	Rest or Stress	-	Yes
Pingitore [45]	No	Yes	40	Yes	Stress	1	No
Previtali [46]	No	Yes	40	No	Stress	1	No
Rollan [47]	No	Yes	40	Yes	Stress	1	No

Sahin [48]	No	Yes	30	No	Stress	1	No
Salustri [49]	No	Yes	40	No	Stress	1	No
San Román [50]	No	Yes	40	Yes	Stress	1	No
Santiago [51]	No	-	40	No	Rest or Stress	1	-
Santoro [52]	No	Yes	40	Yes	Stress	-	NA
Sawada [53]	No	Yes	30	No	Stress	-	NA
Schröder [54]	No	Yes	40	Yes	Stress	2	-
Senior [55]	No	Yes	40	No	Rest or Stress	-	-
Slavich [56]	No	Yes	40	Yes	Stress	1	NA
Smart [57]	No	Yes	40	Yes	Rest or Stress	2	No
Sochowski [58]	No	Yes	40	No	Stress	-	-
Sozzi [59]	Yes	Yes	40	Yes	Stress	1	-
Steinberg [60]	No	Yes	40	No	Stress	1	No
Takeuchi [61]	No	Yes	30	No	Rest or Stress	1	-
Takeuchi [61]	No	Yes	40	No	Rest or Stress	1	-
Takeuchi [61]	No	Yes	40	Yes	Rest or Stress	1	-
Vitarelli [62]	No	-	50	No	Stress	1	Yes
Wu [63]	No	Yes	40	No	Stress	1	NA
Xie [64]	Yes	-	40	Yes	Stress	1	NA
Yuda [65]	No	Yes	40	Yes	Stress	1	NA

Abbreviation see Table 1. NA = not applicable because no patients with rest wall motion abnormalities were included in that studies.

Table 4: Sensitivity and specificity according to different variables

Variable	Sensitivity			Specificity		
	Yes	No	P-value	Yes	No	P-value
Categorical variables						
History of myocardial infarction	0.834	0.740	<0.01	0.811	0.852	0.17
Rest wall motion abnormalities included	0.821	0.756	0.14	0.812	0.877	<0.10
Referral bias present	0.831	0.804	0.40	0.771	0.842	<0.01
Stenosis cut-off 50%	0.781	0.821	0.28	0.855	0.813	0.19
Blind reading of CAG	0.817	0.804	0.69	0.834	0.797	0.18
Blind reading of DSE	0.816	0.763	0.39	0.824	0.792	0.59
Quantitative scoring of CAG	0.805	0.820	0.62	0.839	0.797	0.13
Comparison with newer technologies	0.764	0.824	<0.10	0.795	0.829	0.30
Ischemia for test positivity needed	0.786	0.864	<0.01	0.838	0.789	<0.10
Use of beta-blocker	0.829	0.791	0.21	0.813	0.841	0.35
Use of atropine	0.803	0.827	0.43	0.823	0.821	0.97
Use of biphasic response	0.816	0.822	0.87	0.832	0.806	0.47
Second harmonic imaging	0.811	0.813	0.97	0.803	0.825	0.57
>1 segments for positive test required	0.840	0.806	0.38	0.800	0.827	0.45
Continuous variables	R		P-value	R		P-value
Age, year	0.004		0.20	-0.002		0.47
% Beta-Blocker	-0.050		0.46	-0.075		0.27
% Wall motion abnormalities	0.254		<0.01	-0.224		<0.01
% Men	0.079		0.14	-0.025		0.57
A priori CAD probability	0.376		<0.01	-0.352		<0.01

CAG = coronary angiography; DSE = dobutamine stress echocardiography; R = regression coefficient

studies in which reading of the coronary angiogram was not blinded non-quantitative (visual) scoring did also not significantly affect sensitivity and specificity.

Effect of technical stress echocardiographic factors (Tables 3 and 4)
Blinding of reading. Because DSE was in all but five studies blinded the effect of blinding could not be established reliably (no effects were seen).

Comparison with newer technologies
In the 14 studies assessing the value of newer technologies in direct comparison with DSE, no significant difference in diagnostic accuracy was observed, although in particular sensitivity tended to be lower in these studies (0.764 vs. 0.824, P <0.10)

DSE protocol
In the 17 studies in which resting wall motion abnormalities already constituted a positive DSE, sensitivity was higher compared to the 45 studies in which a dobu-

tamine stress-induced wall motion abnormality (myocardial ischemia) was necessary to define DSE positive (0.864 vs. 0.786, P <0.01) and specificity tended to be lower (0.789 vs. 0.838, P <0.10). Second harmonic imaging, beta-blocker patients' exclusion, addition of atropine, use of the biphasic response and the requirement of only one (versus two) ischemic segment for a positive DSE did not increase DSE sensitivity. When only the 45 studies that required myocardial ischemia for a positive DSE were included, atropine did also not increase sensitivity.

Multivariable analysis
In multivariable analysis, the definition of a positive test was the only independent factor influencing DSE sensitivity. When dobutamine stress-induced ischemia was necessary for a positive test, sensitivity was significantly lower (P = 0.02)

Discussion

This meta-analytical review indicates that patient characteristics, referral bias and technical factors (such as the definition of positive DSE) all significantly affect the reported sensitivity and specificity of DSE.

The inclusion of patients with prior myocardial infarction significantly increased the sensitivity of DSE. This may be the result of more extensive and/or severe CAD or the definition of positive DSE (see later). Since the diagnosis of CAD in patients with known prior myocardial infarction is nearly certain, the inclusion of such patients in investigations purporting to predict CAD seems inappropriate.

Ischemia during DSE is more likely in patients with more extensive CAD. The significant relation between the number of diseased vessels and the likelihood of dobutamine-stress induced wall motion abnormalities confirmed this. This finding confirms earlier reports [1] and support the use of DSE to identify patients at higher risk of multi-vessel CAD. The value of other CAD characteristics such as lesion severity [66,67], lesion type [68,69] or the presence of collaterals [68,70] could not be assessed because information concerning these variables was lacking in virtually all included diagnostic DSE studies.

We had expected that in studies which included patients on beta-blocking medication DSE sensitivity would be lower because dobutamine effects (predominantly mediated by beta-receptors) are obviously limited, resulting in a lesser increase in rate-pressure product [71,72]. Surprisingly, in these studies peak mean heart rate (uncorrected for age) was almost identical to studies that not included patients on beta-blocker (122 vs.124 beats per minute) and consequently beta-blocker use did not affect DSE sensitivity. This latter finding may also be explained by more extensive and/or severe CAD in patients on beta-blockers [73] and the use of atropine in most of the studies including patients on beta-blockers [72]. However, in studies

in which atropine was not used, inclusion of patients on continued beta-blocker medication also did not result in a markedly lower peak mean heart rate (108 vs.110 beats per minute) and consequently did not affect DSE sensitivity.

Unlike exercise electrocardiography [3] and exercise thallium scintigraphy [4], female gender did not affect DSE sensitivity or specificity. This finding is consistent with other publications focusing on the role of DSE in women [74].

Referral bias

Referral bias is present when angiography is guided by results of the stress test under investigation. Because patients are predominantly send for coronary angiography with positive DSE this may increase sensitivity and decrease specificity of DSE. Unfortunately, regardless of study design it is almost impossible to completely avoid referral bias. Clearly, diagnostic DSE studies based on patients who are retrospectively selected because they underwent coronary angiography and DSE within a certain time frame (usually 6-12 weeks) will suffer severely from referral bias. However, prospective studies based on patients recruited from a coronary angiography waiting list are also not free from referral bias. These patients are usually listed because of some other positive stress test and thus are more likely to have a positive DSE. Finally, chest pain patients prospectively scheduled for coronary angiography and DSE usually represent those with more serious complaints (typical angina rather than non-anginal chest pain) and are therefore not truly representative for the whole spectrum of patients encountered at the outpatient clinic. Nevertheless these limitations, those studies that attempted to avoid referral bias by not allowing the results of DSE to affect the decision to perform coronary angiogram had significantly higher specificities than studies that did not. Therefore, specificity in normal control patients will be somewhat higher than that obtained in most DSE studies.

Publication factors

We expected that technical advances would make sensitivity and specificity increase with time. However, we found no significant increase in test sensitivity between 1991 and 2006. Also, specificity was unaffected by time although this may be caused by the influence of referral bias in more recently published studies.

Stress echocardiographic technical factors

In studies in which rest wall motion abnormalities defined DSE already positive sensitivity was significantly higher. The criterion for a positive DSE was in fact the only independent factor related to sensitivity. As mentioned before, since the diagnosis of CAD in patients with rest wall motion abnormalities is nearly certain, the inclusion of such patients in investigations purporting to predict CAD seems inappropriate.

Previous studies have shown that addition of atropine to dobutamine by increasing heart rate significantly increased DSE sensitivity without a loss in specificity

[32,39,45]. In our analysis, despite a very significant higher peak mean heart rate (131 vs. 109 beats per minute), the addition of atropine did not affect DSE sensitivity. Also, use of the biphasic response did not affect test sensitivity. Previous studies have shown that in patients with rest wall motion abnormalities use of the biphasic response significantly increased DSE sensitivity [75,76]. With respect to the biphasic response one problem is to determine exactly in which studies it was used. In one third of all studies it was unclear whether or not the biphasic response was used (Table 3). We assumed that the biphasic response was only used when it was clearly reported or could clearly be deducted. The validity of our conclusion that the biphasic response did not affect test sensitivity rests on this assumption. Another problem is that in some studies none of the patients had rest wall motion abnormalities and that in some studies including patients with rest wall motion abnormalities these latter already constituted a positive DSE. However, exclusion of these latter studies did not change our analysis.

Also, defining DSE positive in case of dobutamine stress-induced wall motion abnormality in one rather than two segments did not increase sensitivity of DSE. A previous study has shown that in particular in patients with prior myocardial infarction the use of at least two segments reduces sensitivity without a significant improvement in specificity [77]. Our results may be different by our assumption that studies in which the description was unclear, the usual definition of the requirement of only one segment for a positive test was used.

Sensitivity and specificity of DSE tended to be lower when the test was directly compared in the same patients with newer technologies. It is an intriguing finding that for many stress modalities (i.e. stress radionuclide angiography) initially excellent results are reported, whereas in comparisons with newer tests results of the previously considered state-of-the-art test are not comparable to the initial reported results.

Other technical factors
When the result of one test influences the interpretation of another, a higher concordance between the two is expected. Since DSE reading was not blinded in only five studies we could not reliably assess the effect of non-blinding DSE. With respect to blinding of the coronary angiogram one problem is to determine exactly in which studies authors were blinded. Since the authors never reported the non-blinding of test analysis, we therefore assumed that studies used blinded analysis only when it was reported as such. In contradiction to reports on exercise thallium scintigraphy [4], blind reading of the coronary angiogram did not affect DSE sensitivity. Again, the validity of our conclusion that blinding does not affect DSE sensitivity significantly rests on this assumption.

Clinical and research applications

Clinicians should be aware of the expected diagnostic sensitivity and specificity of DSE. A large amount of data on this topic is available in the medical literature. However, one should always question whether these diagnostic accuracies obtained in top centers by experts in the field can be applied to your own clinical laboratory. Moreover, clinical characteristics of the patients studied, referral bias and several technical factors may all cause differences in diagnostic accuracies in real life. Our results indicate that the reported sensitivity of DSE is higher and the specificity lower than that expected in clinical practice because of the inappropriate inclusion of patients with prior myocardial infarction, definition of positive DSE and the presence of referral bias, although only the definition of positive DSE independently influenced diagnostic sensitivity.

As stated many years ago by Detrano *et al.* [4] and later by us [78], investigators in the field of diagnostic testing should more conform to methodological standards in conducting research and reporting their results [4,79-81]. Inappropriate patients such as those with prior myocardial infarction should be excluded or treated separately. Study groups should be explicitly defined; with careful description of patients characteristics and patients should not be excluded because they are expected to give false-positive or false-negative results. All tests (DSE and coronary angiography) should be analyzed blindly, and referral bias should be avoided. Reviewers should use these standards in their criticisms and publication decisions. No report should be refused solely because the results are negative or disappointing since this practice has probably inflated the diagnostic accuracy of many tests.

References

1. Geleijnse ML, Fioretti PM, Roelandt JR. Methodology, feasibility, safety and diagnostic accuracy of dobutamine stress echocardiography. *J Am Coll Cardiol* 1997;**30**:595-606.
2. Hoffmann R, Lethen H, Marwick T, Arnese M, Fioretti P, Pingitore A, Picano E, Buck T, Erbel R, Flachskampf FA, Hanrath P. Analysis of interinstitutional observer agreement in interpretation of dobutamine stress echocardiograms. *J Am Coll Cardiol* 1996;**27**:330-6.
3. Hlatky MA, Pryor DB, Harrell FE, Jr., Califf RM, Mark DB, Rosati RA. Factors affecting sensitivity and specificity of exercise electrocardiography. Multivariable analysis. *Am J Med* 1984;**77**:64-71.
4. Detrano R, Janosi A, Lyons KP, Marcondes G, Abbassi N, Froelicher VF. Factors affecting sensitivity and specificity of a diagnostic test: the exercise thallium scintigram. *Am J Med* 1988;**84**:699-710.
5. Karagiannis SE, Bax JJ, Elhendy A, Feringa HH, Cokkinos DV, van Domburg R, Simoons M, Poldermans D. Enhanced sensitivity of dobutamine stress echocardiography by observing wall motion abnormalities during the recovery phase after acute beta-blocker administration. *Am J Cardiol* 2006;**97**:462-5.
6. Afridi I, Quinones MA, Zoghbi WA, Cheirif J. Dobutamine stress echocardiography: sensitivity, specificity, and predictive value for future cardiac events. *Am Heart J* 1994;**127**:1510-5.
7. Ahmad M, Xie T, McCulloch M, Abreo G, Runge M. Real-time three-dimensional dobutamine stress echocardiography in assessment stress echocardiography in assessment of ischemia: comparison with two-dimensional dobutamine stress echocardiography. *J Am Coll Cardiol* 2001;**37**:1303-9.
8. Anthopoulos LP, Bonou MS, Kardaras FG, Sioras EP, Kardara DN, Sideris AM, Kranidis AI, Margaris NG. Stress echocardiography in elderly patients with coronary artery disease: applicability, safety and prognostic value of dobutamine and adenosine echocardiography in elderly patients. *J Am Coll Cardiol* 1996;**28**:52-9.
9. Beleslin BD, Ostojic M, Stepanovic J, Djordjevic-Dikic A, Stojkovic S, Nedeljkovic M, Stankovic G, Petrasinovic Z, Gojkovic L, Vasiljevic-Pokrajcic Z, et al. Stress echocardiography in the detection of myocardial ischemia. Head- to-head comparison of exercise, dobutamine, and dipyridamole tests. *Circulation* 1994;**90**:1168-76.
10. Cain P, Baglin T, Case C, Spicer D, Short L, Marwick TH. Application of tissue Doppler to interpretation of dobutamine echocardiography and comparison with quantitative coronary angiography. *Am J Cardiol* 2001;**87**:525-31.
11. Carstensen S, Host U, Saunamaki K, Kelbaek H. Quantitative analysis of dobutamine-atropine stress echocardiography by fractional area change. *Eur J Echocardiogr* 2002;**3**:220-8.
12. Chiou KR, Huang WC, Lin SL, Hsieh PL, Liu CP, Tsay DG, Chiang HT. Real-time dobutamine stress myocardial contrast echocardiography for detecting coronary artery disease: correlating abnormal wall motion and disturbed perfusion. *Can J Cardiol* 2004;**20**:1237-43.
13. Cohen JL, Greene TO, Ottenweller J, Binenbaum SZ, Wilchfort SD, Kim CS. Dobutamine digital echocardiography for detecting coronary artery disease. *Am J Cardiol* 1991;**67**:1311-8.
14. Dagianti A, Penco M, Agati L, Sciomer S, Rosanio S, Fedele F. Stress echocardiography: comparison of exercise, dipyridamole and dobutamine in detecting and predicting the extent of coronary artery disease. *J Am Coll Cardiol* 1995;**26**:18-25.
15. Daoud EG, Pitt A, Armstrong WF. Electrocardiographic response during dobutamine stress echocardiography. *Am Heart J* 1995;**129**:672-7.

16. Di Bello V, Bellina CR, Gori E, Molea N, Talarico L, Boni G, Magagnini E, Matteucci F, Giorgi D, Lazzeri E, Bertini A, Romano MF, Bianchi R, Giusti C. Incremental diagnostic value of dobutamine stress echocardiography and dobutamine scintigraphy (technetium 99m-labeled sestamibi single-photon emission computed tomography) for assessment of presence and extent of coronary artery disease. *J Nucl Cardiol* 1996;**3**:212-20.

17. Dionisopoulos PN, Collins JD, Smart SC, Knickelbine TA, Sagar KB. The value of dobutamine stress echocardiography for the detection of coronary artery disease in women. *J Am Soc Echocardiogr* 1997;**10**:811-7.

18. Elhendy A, van Domburg RT, Poldermans D, Bax JJ, Nierop PR, Geleijnse ML, Roelandt JR. Safety and feasibility of dobutamine-atropine stress echocardiography for the diagnosis of coronary artery disease in diabetic patients unable to perform an exercise stress test. *Diabetes Care* 1998;**21**:1797-802.

19. Elhendy A, O'Leary EL, Xie F, McGrain AC, Anderson JR, Porter TR. Comparative accuracy of real-time myocardial contrast perfusion imaging and wall motion analysis during dobutamine stress echocardiography for the diagnosis of coronary artery disease. *J Am Coll Cardiol* 2004;**44**:2185-91.

20. Epstein M, Gin K, Sterns L, Pollick C. Dobutamine stress echocardiography: initial experience of a Canadian centre. *Can J Cardiol* 1992;**8**:273-9.

21. Eroglu E, D'Hooge J, Herbots L, Thijs D, Dubois C, Sinnaeve P, Dens J, Vanhaecke J, Rademakers F. Comparison of real-time tri-plane and conventional 2D dobutamine stress echocardiography for the assessment of coronary artery disease. *Eur Heart J* 2006;**27**:1719-24.

22. Fathi R, Cain P, Nakatani S, Yu HC, Marwick TH. Effect of tissue Doppler on the accuracy of novice and expert interpreters of dobutamine echocardiography. *Am J Cardiol* 2001;**88**:400-5.

23. Gunalp B, Dokumaci B, Uyan C, Vardareli E, Isik E, Bayhan H, Ozguven M, Ozturk E. Value of dobutamine technetium-99m-sestamibi SPECT and echocardiography in the detection of coronary artery disease compared with coronary angiography. *J Nucl Med* 1993;**34**:889-94.

24. Hennessy TG, Codd MB, Kane G, McCarthy C, McCann HA, Sugrue DD. Dobutamine stress echocardiography in the detection of coronary artery disease: importance of the pretest likelihood of disease. *Am Heart J* 1997;**134**:685-92.

25. Ho FM, Huang PJ, Liau CS, Lee FK, Chieng PU, Su CT, Lee YT. Dobutamine stress echocardiography compared with dipyridamole thallium- 201 single-photon emission computed tomography in detecting coronary artery disease. *Eur Heart J* 1995;**16**:570-5.

26. Ho YL, Wu CC, Lin LC, Liu YB, Chen WJ, Chen MF, Liau CS, Lee YT. Assessment of the functional significance of coronary artery stenosis by dobutamine-atropine stress echocardiography. *Cardiology* 1997;**88**:386-92.

27. Hoffmann R, Lethen H, Kleinhans E, Weiss M, Flachskampf FA, Hanrath P. Comparative evaluation of bicycle and dobutamine stress echocardiography with perfusion scintigraphy and bicycle electrocardiogram for identification of coronary artery disease. *Am J Cardiol* 1993;**72**:555-9.

28. Huang PJ, Ho YL, Wu CC, Chao CL, Chen MF, Chieng PU, Lee YT. Simultaneous dobutamine stress echocardiography and thallium-201 perfusion imaging for the detection of coronary artery disease. *Cardiology* 1997;**88**:556-62.

29. Iwase M, Fukui M, Tamagaki H, Kimura M, Hasegawa K, Matsuyama H, Nomura M, Watanabe Y, Hishida H. Advantages and disadvantages of dobutamine stress echocardiogra-

phy compared with treadmill exercise electrocardiography in detecting ischemia. *Jpn Circ J* 1996;**60**:954-60.

30. Kisacik HL, Ozdemir K, Altinyay E, Oguzhan A, Kural T, Kir M, Kutuk E, Goksel S. Comparison of exercise stress testing with simultaneous dobutamine stress echocardiography and technetium-99m isonitrile single-photon emission computerized tomography for diagnosis of coronary artery disease. *Eur Heart J* 1996;**17**:113-9.

31. Lewis JF, Lin L, McGorray S, Pepine CJ, Doyle M, Edmundowicz D, Holubkov R, Pohost G, Reichek N, Rogers W, Sharaf BL, Sopko G, Merz CN. Dobutamine stress echocardiography in women with chest pain. Pilot phase data from the National Heart, Lung and Blood Institute Women's Ischemia Syndrome Evaluation (WISE). *J Am Coll Cardiol* 1999;**33**:1462-8.

32. Ling LH, Pellikka PA, Mahoney DW, Oh JK, McCully RB, Roger VL, Seward JB. Atropine augmentation in dobutamine stress echocardiography: role and incremental value in a clinical practice setting. *J Am Coll Cardiol* 1996;**28**:551-7.

33. Loimaala A, Groundstroem K, Pasanen M, Oja P, Vuori I. Comparison of bicycle, heavy isometric, dipyridamole-atropine and dobutamine stress echocardiography for diagnosis of myocardial ischemia. *Am J Cardiol* 1999;**84**:1396-400.

34. Marcovitz PA, Armstrong WF. Accuracy of dobutamine stress echocardiography in detecting coronary artery disease. *Am J Cardiol* 1992;**69**:1269-73.

35. Martin TW, Seaworth JF, Johns JP, Pupa LE, Condos WR. Comparison of adenosine, dipyridamole, and dobutamine in stress echocardiography. *Ann Intern Med* 1992;**116**:190-6.

36. Marwick T, D'Hondt AM, Baudhuin T, Willemart B, Wijns W, Detry JM, Melin J. Optimal use of dobutamine stress for the detection and evaluation of coronary artery disease: combination with echocardiography or scintigraphy, or both? *J Am Coll Cardiol* 1993;**22**:159-67.

37. Mathias W, Jr., Tsutsui JM, Andrade JL, Kowatsch I, Lemos PA, Leal SM, Khandheria BK, Ramires JF. Value of rapid beta-blocker injection at peak dobutamine-atropine stress echocardiography for detection of coronary artery disease. *J Am Coll Cardiol* 2003;**41**:1583-9.

38. Mazeika PK, Nadazdin A, Oakley CM. Dobutamine stress echocardiography for detection and assessment of coronary artery disease. *J Am Coll Cardiol* 1992;**19**:1203-11.

39. McNeill AJ, Fioretti PM, el-Said SM, Salustri A, Forster T, Roelandt JR. Enhanced sensitivity for detection of coronary artery disease by addition of atropine to dobutamine stress echocardiography. *Am J Cardiol* 1992;**70**:41-6.

40. Mishra MB, Lythall DA, Chambers JB. A comparison of wall motion analysis and systolic left ventricular long axis function during dobutamine stress echocardiography. *Eur Heart J* 2002;**23**:579-85.

41. Nagel E, Lehmkuhl HB, Bocksch W, Klein C, Vogel U, Frantz E, Ellmer A, Dreysse S, Fleck E. Noninvasive diagnosis of ischemia-induced wall motion abnormalities with the use of high-dose dobutamine stress MRI: comparison with dobutamine stress echocardiography. *Circulation* 1999;**99**:763-70.

42. Nedeljkovic I, Ostojic M, Beleslin B, Djordjevic-Dikic A, Stepanovic J, Nedeljkovic M, Stojkovic S, Stankovic G, Saponjski J, Petrasinovic Z, Giga V, Mitrovic P. Comparison of exercise, dobutamine-atropine and dipyridamole-atropine stress echocardiography in detecting coronary artery disease. *Cardiovasc Ultrasound* 2006;**4**:22.

43. Nixdorff U, Matschke C, Winklmaier M, Flachskampf FA, Ludwig J, Pohle K, Land M, Gefeller O, Daniel WG. Native tissue second harmonic imaging improves endocardial and epicardial border definition in dobutamine stress echocardiography. *Eur J Echocardiogr* 2001;**2**:52-61.

44. Peteiro J, Monserrat L, Fabregas R, Manuel Vazquez J, Calvino R, Castro-Beiras A. Comparison of two-dimensional echocardiography and pulsed Doppler tissue imaging during dobutamine-atropine stress testing to detect coronary artery disease. *Echocardiography* 2001;**18**:275-84.

45. Pingitore A, Picano E, Colosso MQ, Reisenhofer B, Gigli G, Lucarini AR, Petix N, Previtali M, Bigi R, Chiaranda G, Minardi G, de Alcantara M, Lowenstein J, Sclavo MG, Palmieri C, Galati A, Seveso G, Heyman J, Mathias W, Jr., Casazza F, Sicari R, Raciti M, Landi P, Marzilli M. The atropine factor in pharmacologic stress echocardiography. Echo Persantine (EPIC) and Echo Dobutamine International Cooperative (EDIC) Study Groups. *J Am Coll Cardiol* 1996;**27**:1164-70.

46. Previtali M, Lanzarini L, Fetiveau R, Poli A, Ferrario M, Falcone C, Mussini A. Comparison of dobutamine stress echocardiography, dipyridamole stress echocardiography and exercise stress testing for diagnosis of coronary artery disease. *Am J Cardiol* 1993;72:865-70.

47. Rollan MJ, San Roman JA, Vilacosta I, Ortega JR, Serrador A, Pastor G, Medina A, Bratos JL, Fernandez-Aviles F. [The influence of sex on the performance of dobutamine echocardiography for the diagnosis of ischemic cardiopathy]. *Rev Esp Cardiol* 1999;**52**:1060-5.

48. Sahin M, Karakelleoglu S, Alp N, Atesal S, Senocak H. Diagnostic value of dobutamine stress echocardiography in coronary artery disease. *Thorac Cardiovasc Surg* 1994;42:285-9.

49. Salustri A, Fioretti PM, Pozzoli MM, McNeill AJ, Roelandt JR. Dobutamine stress echocardiography: its role in the diagnosis of coronary artery disease. *Eur Heart J* 1992;**13**:70-7.

50. San Roman JA, Vilacosta I, Castillo JA, Rollan MJ, Peral V, Sanchez-Harguindey L, Fernandez-Aviles F. Dipyridamole and dobutamine-atropine stress echocardiography in the diagnosis of coronary artery disease. Comparison with exercise stress test, analysis of agreement, and impact of antianginal treatment. *Chest* 1996;**110**:1248-54.

51. Santiago P, Vacek JL, Rosamond TL. Dobutamine stress echocardiography: clinical utility and predictive value at various infusion rates. *Am Heart J* 1994;**128**:804-8.

52. Santoro GM, Sciagra R, Buonamici P, Consoli N, Mazzoni V, Zerauschek F, Bisi G, Fazzini PF. Head-to-head comparison of exercise stress testing, pharmacologic stress echocardiography, and perfusion tomography as first-line examination for chest pain in patients without history of coronary artery disease. *J Nucl Cardiol* 1998;**5**:19-27.

53. Sawada SG, Segar DS, Ryan T, Brown SE, Dohan AM, Williams R, Fineberg NS, Armstrong WF, Feigenbaum H. Echocardiographic detection of coronary artery disease during dobutamine infusion. *Circulation* 1991;**83**:1605-14.

54. Schroder K, Agrawal R, Voller H, Kursten B, Dissmann R, Schultheiss HP. Factors influencing the diagnostic accuracy of dobutamine stress echocardiography. *Int J Card Imaging* 1997;**13**:493-8.

55. Senior R, Sridhara BS, Anagnostou E, Handler C, Raftery EB, Lahiri A. Synergistic value of simultaneous stress dobutamine sestamibi single- photon-emission computerized tomography and echocardiography in the detection of coronary artery disease. *Am Heart J* 1994;**128**:713-8.

56. Slavich GA, Guerra UP, Morocutti G, Fioretti PM, Fresco C, Orlandi C, Orsolon PG, Forster T, Feruglio GA. Feasibility of simultaneous Tc99m sestamibi and 2D-echo cardiac imaging during dobutamine pharmacologic stress. Preliminary results in a female population. *Int J Card Imaging* 1996;**12**:113-8.

57. Smart SC, Bhatia A, Hellman R, Stoiber T, Krasnow A, Collier BD, Sagar KB. Dobutamine-atropine stress echocardiography and dipyridamole sestamibi scintigraphy for the detection

of coronary artery disease: limitations and concordance. *J Am Coll Cardiol* 2000;**36**:1265-73.

58. Sochowski RA, Yvorchuk KJ, Yang Y, Rattes MF, Chan KL. Dobutamine and dipyridamole stress echocardiography in patients with a low incidence of severe coronary artery disease. *J Am Soc Echocardiogr* 1995;**8**:482-7.

59. Sozzi FB, Poldermans D, Bax JJ, Boersma E, Vletter WB, Elhendy A, Borghetti A, Roelandt JR. Second harmonic imaging improves sensitivity of dobutamine stress echocardiography for the diagnosis of coronary artery disease. *Am Heart J* 2001;**142**:153-9.

60. Steinberg EH, Madmon L, Patel CP, Sedlis SP, Kronzon I, Cohen JL. Long-term prognostic significance of dobutamine echocardiography in patients with suspected coronary artery disease: results of a 5-year follow-up study. *J Am Coll Cardiol* 1997;**29**:969-73.

61. Takeuchi M, Miura Y, Sonoda S, Kuroiwa A. Comparison of Three Different Protocols for Dobutamine Stress Echocardiography: Does the Addition of Atropine Increase Complications, and Does It Improve Diagnostic Accuracy? *Echocardiography* 1999;**16**:347-355.

62. Vitarelli A, Luzzi MF, Penco M, Fedele F, Dagianti A. On-line quantitative assessment of left ventricular filling during dobutamine stress echocardiography: a useful addition to conventional wall motion scoring. *Int J Cardiol* 1997;**59**:57-69.

63. Wu CC, Ho YL, Kao SL, Chen WJ, Lee CM, Chen MF, Liau CS, Lee YT. Dobutamine stress echocardiography for detecting coronary artery disease. *Cardiology* 1996;**87**:244-9.

64. Xie F, Tsutsui JM, McGrain AC, Demaria A, Cotter B, Becher H, Lebleu C, Labovitz A, Picard MH, O'Leary EL, Porter TR. Comparison of dobutamine stress echocardiography with and without real-time perfusion imaging for detection of coronary artery disease. *Am J Cardiol* 2005;**96**:506-11.

65. Yuda S, Khoury V, Marwick TH. Influence of wall stress and left ventricular geometry on the accuracy of dobutamine stress echocardiography. *J Am Coll Cardiol* 2002;**40**:1311-9.

66. Arnese M, Salustri A, Fioretti PM, Cornel JH, Boersma E, Reijs AE, de Feyter PJ, Roelandt JR. Quantitative angiographic measurements of isolated left anterior descending coronary artery stenosis. Correlation with exercise echocardiography and technetium-99m 2-methoxy isobutyl isonitrile single-photon emission computed tomography. *J Am Coll Cardiol* 1995;**25**:1486-91.

67. Baptista J, Arnese M, Roelandt JR, Fioretti P, Keane D, Escaned J, Boersma E, di Mario C, Serruys PW. Quantitative coronary angiography in the estimation of the functional significance of coronary stenosis: correlations with dobutamine- atropine stress test. *J Am Coll Cardiol* 1994;**23**:1434-9.

68. Beleslin BD, Ostojic M, Djordjevic-Dikic A, Babic R, Nedeljkovic M, Stankovic G, Stojkovic S, Marinkovic J, Nedeljkovic I, Stepanovic J, Saponjski J, Petrasinovic Z, Nedeljkovic S, Kanjuh V. Integrated evaluation of relation between coronary lesion features and stress echocardiography results: the importance of coronary lesion morphology. *J Am Coll Cardiol* 1999;**33**:717-26.

69. Heyman J, Salvade P, Picano E, Varga A, Gliozheni E, Sicari R, Previtali M, Rovelli G. The elusive link between coronary lesion morphology and dobutamine stress echocardiography results. The EDIC (Echo Dobutamine International Cooperative) Study Group. *Int J Card Imaging* 1997;**13**:395-401.

70. Elhendy A, Cornel JH, Roelandt JR, Nierop PR, van Domburg RT, Geleijnse ML, Trocino G, Bax JJ, Ibrahim MM, Fioretti PM. Impact of severity of coronary artery stenosis and the collateral circulation on the functional outcome of dyssynergic myocardium after revasculariza-

tion in patients with healed myocardial infarction and chronic left ventricular dysfunction. *Am J Cardiol* 1997;**79**:883-8.

71.   Weissman NJ, Levangie MW, Guerrero JL, Weyman AE, Picard MH. Effect of beta-blockade on dobutamine stress echocardiography. *Am Heart J* 1996;**131**:698-703.

72.   Fioretti PM, Poldermans D, Salustri A, Forster T, Bellotti P, Boersma E, McNeill AJ, el-Said ES, Roelandt JR. Atropine increases the accuracy of dobutamine stress echocardiography in patients taking beta-blockers. *Eur Heart J* 1994;**15**:355-60.

73.   Salustri A, Fioretti PM, McNeill AJ, Pozzoli MM, Roelandt JR. Pharmacological stress echocardiography in the diagnosis of coronary artery disease and myocardial ischaemia: a comparison between dobutamine and dipyridamole. *Eur Heart J* 1992;**13**:1356-62.

74.   Geleijnse ML, Krenning BJ, Soliman OI, Nemes A, Galema TW, ten Cate FJ. Dobutamine stress echocardiography for the detection of coronary artery disease in women. *Am J Cardiol* 2007;**99**:714-7.

75.   Senior R, Lahiri A. Enhanced detection of myocardial ischemia by stress dobutamine echocardiography utilizing the "biphasic" response of wall thickening during low and high dose dobutamine infusion. *J Am Coll Cardiol* 1995;**26**:26-32.

76.   Elhendy A, Cornel JH, Roelandt JR, van Domburg RT, Nierop PR, Geleynse ML, El-Said GM, Fioretti PM. Relation between contractile response of akinetic segments during dobutamine stress echocardiography and myocardial ischemia assessed by simultaneous thallium-201 single-photon emission computed tomography. *Am J Cardiol* 1996;**77**:955-9.

77.   Elhendy A, van Domburg RT, Bax JJ, Poldermans D, Nierop PR, Kasprzak JD, Roelandt JR. Optimal criteria for the diagnosis of coronary artery disease by dobutamine stress echocardiography. *Am J Cardiol* 1998;**82**:1339-44.

78.   Krenning BJ, Geleijnse ML, Poldermans D, Roelandt JR. Methodological analysis of diagnostic dobutamine stress echocardiography studies. *Echocardiography* 2004;**21**:725-36.

79.   Philbrick JT, Horwitz RI, Feinstein AR, Langou RA, Chandler JP. The limited spectrum of patients studied in exercise test research. Analyzing the tip of the iceberg. *Jama* 1982;**248**:2467-70.

80.   Wasson JH, Sox HC, Neff RK, Goldman L. Clinical prediction rules. Applications and methodological standards. *N Engl J Med* 1985;**313**:793-9.

81.   Diamond GA. Monkey business. *Am J Cardiol* 1986;**57**:471-5.

Chapter 11

Current Status of Real-Time Three-Dimensional Stress Echocardiography

A Nemes
BJ Krenning
JG Bosch
OII Soliman
KYE Leung
WB Vletter
FJ ten Cate
ML Geleijnse

## Abstract

Two-dimensional stress echocardiography is a non-invasive imaging stress modality with a continuously evolving spectrum of indications. Although the diagnostic and prognostic roles of stress echocardiography are well established, it is widely known that stress echocardiography suffers from a number of limitations. Real-time three-dimensional echocardiography has been advocated to solve some of these problems. The aim of the present state-of-the-art paper is to discuss the benefits and current limitations of this new stress methodology.

Two-dimensional (2D) stress echocardiography is a non-invasive stress modality with a continuously evolving spectrum of indications. One of the most important indications is the identification of patients with coronary artery disease (CAD)[1]. For this purpose, wall motion of left ventricular (LV) segments is compared between rest, low-dose, and peak stress on several standardized LV views. The rationale for the use of stress echocardiography is that cardiovascular stress will in the presence of significant CAD result in myocardial ischemia, manifested as a regional wall motion abnormality. Although the diagnostic and prognostic roles of 2D stress echocardiography are well established[1,2], it is widely known that stress echocardiography suffers from a number of limitations. Suboptimal diagnostic accuracy may be caused by inadequate image quality, comparisons of non-identical LV wall segments at rest, low-dose, and peak stress, and smaller ischemic areas that may be missed in the limited available LV cross sections. Also, interpretation of 2D stress echocardiography is subjective with different existing definitions of abnormality and considerable inter-observer and inter-institutional diagnostic variability[3]. Stress real-time three-dimensional echocardiography (RT3DE) may be one of the ways to shorten acquisition times and/or to improve the suboptimal diagnostic accuracy of stress echocardiography.

## Acquisition and analysis of 3D images

From one single apical window the full LV volume data set can be acquired. This process may be facilitated by use of two displayed reference 2D images, such as an apical four-chamber and an orthogonal view. Full LV volume is acquired by scanning 4 to 7 subvolumes during consecutive, electrocardiographically triggered beats (Philips iE33, GE Healthcare Vivid 7 Dimension) or 4 subvolumes during 7 (Philips Sonos) consecutive, electrocardiographically triggered, heartbeats. These LV subvolumes are automatically integrated by the system into one pyramidal data set of ~80° x 80°, incorporating full LV volume (Figure 1). All desired LV anatomical images can be cropped out of the pyramidal volumetric data set after which regional LV wall motion can be assessed. Analysis of LV wall segments can be done according to the 17-segment model recommended by the American Society of Echocardiography[4], but with 3D more detailed models (incorporating for example short axis views) can also be designed. For off-line analysis, the TomTec 4D Echo-View system (TomTec GmbH, Unterschleissheim, Germany), the Qlab system (Philips Medical Systems, Andover, Massachussets, USA), or the EchoPAC Dimension Workstation (GE Healthcare, Milwaukee, USA) can be used.
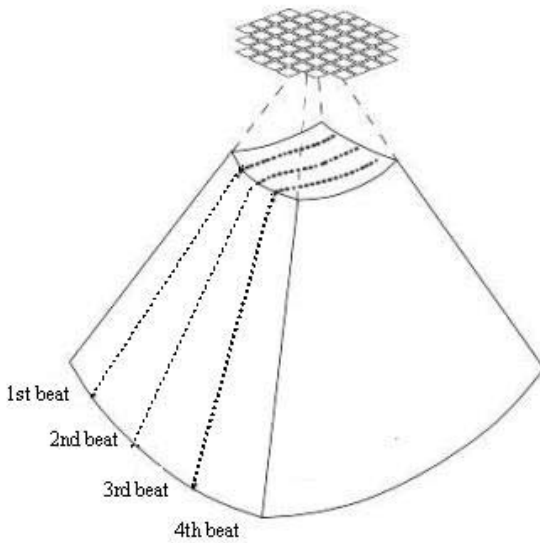
Figure 1:
During 3D data acquisition four 20° x 80° sectors are scanned during four consecutive heartbeats that are integrated automatically into a 80° x 80° pyramid.

Benefits of RT3DE imaging

The introduction of new generation RT3DE systems has improved 3D data acquisition and LV volume analysis to a great extent. Importantly, compared to other 3D imaging modalities such as magnetic resonance imaging or computed tomography,
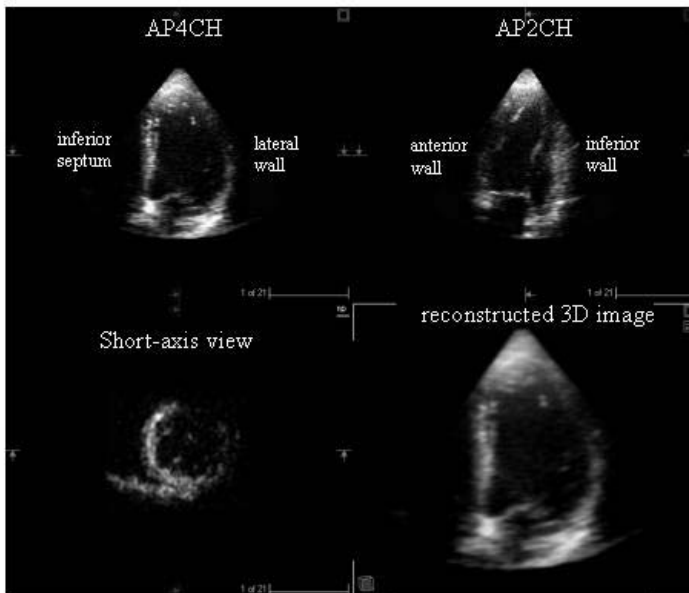
Figure 2:
Overview of wall motion produced automatically from a 3D dataset at rest showing apical 4-chamber view (AP4CH, left, top), apical 2-chamber (AP2CH, right, top), cross-sectional short-axis (left, bottom) and reconstructed 3D image (right, bottom).

RT3DE is easy to learn and a less time consuming imaging modality. As pointed out on earlier, RT3DE has excellent correlation with cardiac magnetic resonance imaging for evaluation of LV volume, mass and ejection fraction with comparable reproducibility[5-7].

With stress RT3DE, at each stress level only one 3D data acquisition from one window is needed instead of multiple 2D data acquisitions from multiple windows. This makes a 3D examination faster than conventional 2D stress imaging. This allows for faster acquisition protocols and/or repeated acquisitions to optimize image quality (although this will obviously eliminate the recording speed advantage to some extent). Fast image acquisition is very beneficial since stress-induced myocardial ischemia may resolve quickly and the time between peak stress and image acquisition influences test sensitivity[8]. From the acquired 3D volumetric data sets, matching views at baseline and at different levels of stress can be selected for a precise comparison of identical segments. Importantly, foreshortened acquired LV walls can be corrected by rotating the 3D data set. RT3DE allows analysis of similar segments in more detail from different planes simply by cropping and rotating the 3D volumetric data set helping the identification of small ischemic LV regions[9] (Figures 2 and 3). Some investigators have suggested that stress RT3DE identifies more readily wall motion abnormalities in the apical region compared to 2D imaging due to non-foreshortened acquisition and analysis resulting in a trend towards better diagnosing myocardial ischemia in the left anterior descending coronary territory[9,10]. However, this potential benefit becomes only reality after off-line adjustments. In this respect it should also be noticed that modern 2D machines, but not the RT3DE systems, allow direct comparisons on-line of the 2D images at the different stress levels. Thereby, ischemia may be detected (although potentially
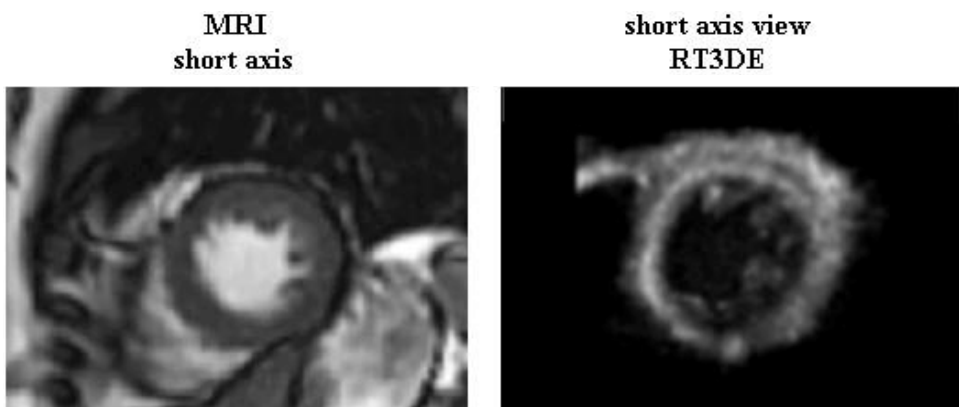
Figure 3:

Comparison of left ventricular short axis images at the papillary muscle level in a patient who underwent stress magnetic resonance imaging (MRI) and stress real-time three-dimensional echocardiography (RT3DE). Observe the great similarity in images between RT3DE and MRI.
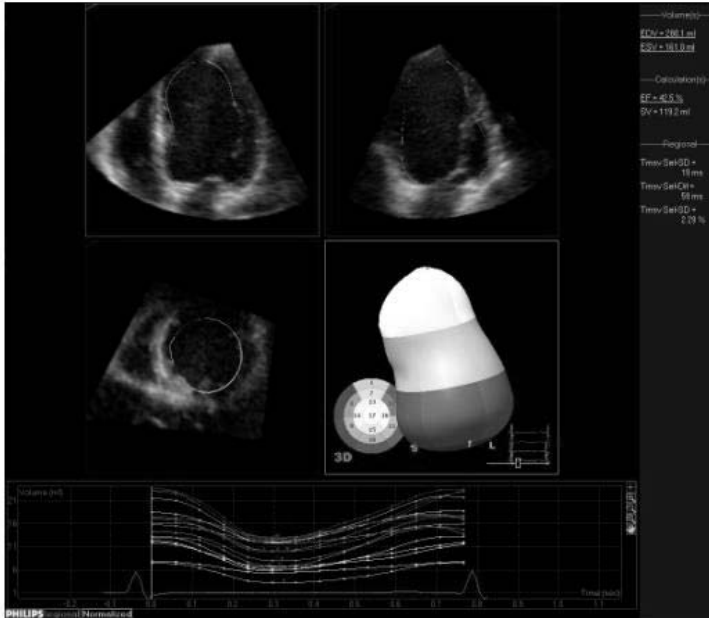
Figure 4:

Real-time three-dimensional echocardiography allows the analysis of regional (segmental) wall motion and calculation of volume/time curve of the left ventricle based on semi-automated contour tracings. The volume/time curves of each colour-coded segment in the bull`s eye view (right bottom) are represented in the volume/time curve (bottom)

inferior) more convenient during 2D stress echocardiography, which could have implications for test safety.

In addition, changes in LV volumes during stress have been shown to be helpful for the diagnosis of CAD and estimation of prognosis in stress 2D echocardiography[11]. RT3DE also allows a more accurate measurement of LV volumes compared to 2D echocardiography[12]. Another advantage of RT3DE can be that after the identification of some anatomical landmarks, RT3DE allows automatic calculation of regional volumes that can be another indicator for a wall motion abnormality (Figure 4). Finally, RT3DE allows anyplane evaluation of the LV helping to create short-axis views at different LV levels that may be easier to understand by other (non-cardiologists) physicians.

Current limitations of RT3DE imaging

Notwithstanding its great opportunities, at this moment stress RT3DE has a number of technical limitations. In this section, we report on the most important limitations that others and us encountered.

Spatial volume and spatio-temporal resolution

The primary restriction for RT3DE is the limited spatial volume coverage, or actually the trade-off between spatial volume, spatial resolution and temporal resolution (3D frame rate). In analogy to 2D echo, there is a trade-off between frame rate, image depth and number of beams. This limitation is directly related to a physical constant: the speed of sound in human tissue (~1450 m/s). It takes 0.14 msecs to transmit an ultrasound pulse and receive its echoes from a depth of 10 cm. Therefore, only approximately 7500 beams can be acquired per second. With specialized beam forming, multiple beams can be acquired simultaneously, but this goes at the cost of additional artefacts and is bound to practical limits[13]. For practical use in echocardiography, the temporal and spatial resolution should satisfy certain minimum requirements. This means that the 3D volume imaged within a time frame is limited. This is the volume we see in the 'live 3D' mode, which is the true real-time 3D mode of the system.

In real practice, to cover the whole LV, four complete heartbeats containing four LV subvolumes have to be recorded. These four LV subvolumes are stitched together to form the total pyramidal LV volume (Figure 1). Of note, 3D image acquisition with the older Philips Sonos 7500 system takes seven heart cycles to complete, because some processing is required before the next beat can be acquired. Slice stitching may give rise to discontinuities at the slice edges (Figure 5). 3D image slice discontinuities may be aggravated by transducer or patient motion (prominent breathing motion at peak stress), variations in heart rate (during stress the latest recorded beat may be shorter in duration), arrhythmias and imperfect electrocardiographic triggering. Unfortunately, irregular heart rhythms (extra-systolic beats, atrial fibrillation) are not seldom encountered during dobutamine stress[1].
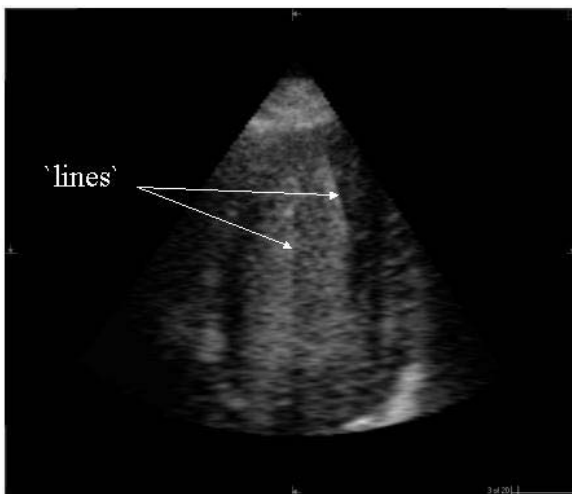
Figure 5:
Slice stitching may give rise to discontinuities at the slice edges.

Poor anterior wall visualization

Visualization of the LV anterior wall can sometimes be difficult even during 2D echocardiography. Unfortunately, the anterior wall is inadequately visualized in a considerable number of our stress 3D examinations[14], although others have reported better results for imaging of the anterior wall[10,15], probably related to patient selection[16]. In addition, acquisition of a full-volume dataset in patients with severely dilated ventricles can be problematic. As shown in Figure 6, in particular visualization problems of the LV anterior wall may be related to the relatively large footprint of the RT3DE transducers, in particular the older Philips X4 matrix transducer, compared to a standard transducer (24 x 20 vs. 24 x 15 mm), leading to rib shadowing. One could try to make an additional recording from a parasternal window to cover the basal and mid anterior wall (distal segments will usually not be visible from this window) with even a somewhat higher frame rate (due to less depth), but this would eliminate the advantageous short recording time of RT3DE[17,18]. In addition, parasternal-acquired myocardial segments will suffer at some extent from right ventricular contrast shielding. Better results may be expected with newer, smaller adult transducers such as the Philips X3-1 transducer that has a size comparable to a standard transducer or (currently only available in paediatrics) single crystal transducers (Philips X7-2 with PureWave crystal technology) with improved electromechanical properties (transducer bandwidth and sensitivity).

Quad-screen display

A practical obstacle for the use of stress RT3DE is the lacking possibility of TomTec and Qlab software to display the different stress stages simultaneously in a quad-screen display. Recently, we developed a simple extension program (Stress4Qlab) that allows simultaneous, synchronized viewing of multiple 3D datasets. Information on this program is available upon request. It is to be expected that built-in support for 3D stress echo will be available soon.
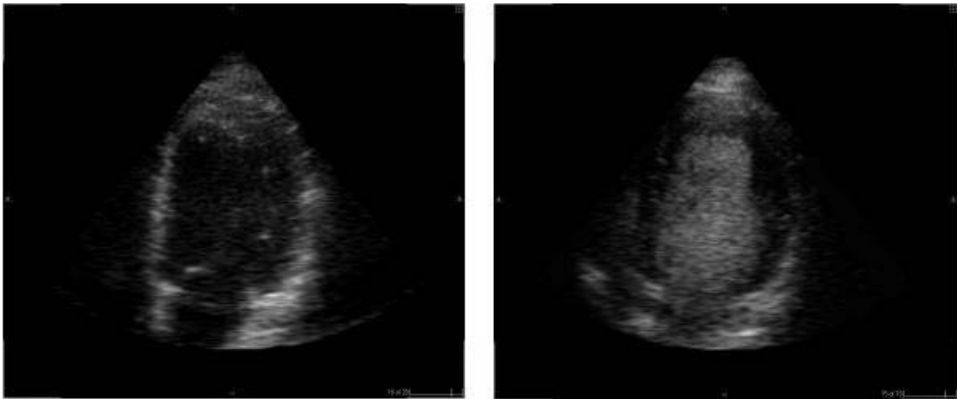

Figure 6:
Size of the different Philips transducers, from left to right: 3D-X3-1 (24 x 15 mm), 3D-X4 (24 x 20 mm) and 2D-S3 (24 x 15 mm).

Contrast imaging

It has been demonstrated that echo contrast improves endocardial border visualization during stress 2D echocardiography[19]. Because of the earlier described more problematic spatial resolution of 3D images contrast may be an essential part of stress RT3DE[18,20] (Figure 7). However, with contrast LV opacification, stitching artefacts (visible sharp transitions at the slice edges) may become aggravated and some additional artefacts may appear[21]. In particular, during the seven-beat acquisition period used in the older Philips Sonos system contrast opacification of the LV may decay significantly because of microbubble insonification. This problem may be less when the contrast agent is continuously infused rather than given as repeated boluses or when the acquisition period is shortened to four beats, as is possible with the newer Philips iE33 system. Furthermore, the differentiation between contrast and tissue is not as good as in standard 2D harmonic imaging, because the matrix transducer has a limited relative bandwidth, and is therefore less suitable for harmonic imaging.

A minor additional problem with the is the brighter appearance of the first frame of a beat compared to the next frames. This is attributable to the fact that there is no acquisition at the second, fourth and sixth heartbeat, so the first frame of each beat is acquired after a period without insonification. In later frames some contrast will be progressively destroyed by the ultrasound pulse and contrast brightness will be lower.

Figure 7:

Improvement of endocardial delineation by the use of contrast agent (compare unenhanced (left side) and contrast-enhanced (right side) left ventricular long-axis planes).

Clinical 3D stress echocardiography studies

Three-dimensional echocardiography has been available for several years using time-consuming reconstruction techniques. However, recent advances in transducer technology and front-end data processing have brought real-time 3D echocardiography (RT3DE) into clinical practice. In several studies, resting RT3DE was as accurate as magnetic resonance imaging (MRI) in the evaluation of LV morphology and function[5-7, 22].

At this moment, only a few centers have reported data on the clinical value of *stress* RT3DE (see Table 1). Several general conclusions can be drawn from these reports. The percentage of LV segments visible at peak stress ranges in studies from approximately 75% to 90% [9, 17, 18, 20]. Apart from improvements in transducer technology there are two major ways to improve this number. Inclusion of paraster-

Table 1. Real-Time Three-Dimensional Stress Echocardiographic Studies.

Authors	Stress	RT3DE system	Windows	Segments visible at peak stress (conventional imaging)	Segments visible at peak stress (contrast imaging)	Sensitivity in detecting ischemia (3D vs. 2D)
Zwas (17)	Treadmill	VMI / 2.5 MHz	AP + PS	89% (98%*)	-	-
Ahmad (24)	Dob.	VMI / 2.5 MHz	AP + PS	-	-	78% vs. 59%#
Matsumura (9)	Dob.	Sonos 7500 / 2-4 MHz	AP	89%	-	75% vs. 75%$
Takeuchi (15)	Dob.	Sonos 7500 / 2-4 MHz	AP	-	97%	-
Pulerwitz (20)	Dob.	Sonos 7500 / 2-4 MHz	AP	75% (87%@)	97% (99%@)	-
Nemes (14)	Dob.	Sonos 7500 / 2-4 MHz	AP	76%	90%	-
Nemes (25)	Dob.	Sonos 7500 / 2-4 MHz	AP + PS	-	91% (96%*)	-
Krenning	Dob.	Sonos 7500 / 2-4 MHz or iE33 / 1-3 MHz	AP	78%	90%	61% vs. NA
Agelli (10)	Dob.	iE33 / 1-3 MHz	AP	-	-	84% vs. 72%#
Yang (26)	Dob.	Sonos 7500 / 2-4 MHz or iE33 / 1-3 MHz	AP	-	100%&	-

* including parasternal view analysis. AP = apical. Dop = dobutamine. PS = parasternal. VMI = Volumetrics Medical Imaging. Gold standard = # coronary angiography, $ Tl-201 reversible defects, @ including short-axes analysis. & Contrast given in patients with >1 segment not adequately visualised.

Table 2. Benefits of RT3DE compared to 2D echocardiography

	2D echocardiography	RT3DE
Wall motion	+	++
Contrast	++	+
Volumes	+	++
Regional volumes	-	+

+ means clinically available, - means clinically not available

nal-acquired images into the data set will increase the percentage of visible LV segments by approximately 5 to 10%, but at the cost of the advantageous fast recording time of RT3DE[17, 20]. On the other hand it has been shown by several authors that contrast-enhancement can increase the visibility of LV segments with at least a similar value, at the cost of a lower frame rate and some artifacts[18, 20]. Despite these limitations, contrast-enhancement has been shown to improve interobserver agreement for myocardial ischemia[18], and may therefore improve the diagnostic accuracy of stress RT3DE.

It has been shown that stress RT3DE requires significant shorter acquisition times compared to stress 2D imaging[9, 10, 23]. In these head-to-head comparative studies between stress 2D and 3D, equal[9] or at least equal[10,23], diagnostic sensitivities for stress RT3DE were reported, mainly due to the aforementioned more readily interpretation of wall motion abnormalities in the apical region with RT3DE imaging due to non-foreshortened acquisition and analysis.

Conclusions and future developments

Although stress RT3DE may be well clinical feasible according to some studies[9, 17, 20, 23], in our opinion this imaging modality is currently still hampered by some major technical limitations. However, most of these limitations may be handled with or may be overcome in the near future. Analysis software will be adapted to support stress RT3DE with proper choice of corresponding viewing planes in rest, low-dose and stress with simultaneous synchronized viewing. In addition, future transducers will have larger bandwidth and thus will be more suitable for harmonic imaging and contrast and the transducer footprint size will be further reduced. The X3-1 transducer on the new iE33 system already has a much smaller footprint that may circumvent rib shadowing.

Multibeat frame composition and limited spatial resolution actually form the major technical limitations[18]. To overcome this, more ultrasound beams have to be processed in parallel. This requires technological innovation, but it will ultimately

result in true RT3DE LV visualization. This will seriously extend the possibilities and clinical value of RT3DE, not just for stress RT3DE.

Ultimately, the inherent advantages of stress RT3DE will eliminate some of the current limitations of stress 2D echocardiography, and may result in an improved diagnostic technique (Table 2). Moreover, with the development of more advanced automated border detection software, we can also expect a decrease in inter-observer variability associated with the visual scoring of segmental wall motion. Also the learning curve to interpret wall motion analysis may become easier because of the 3D nature of the images. If 3D image quality can be brought to a comparable level as 2D image quality, stress RT3DE may be more suitable for such automated analysis than stress 2D echo because 3D images offer higher information content with complete LV visualization. Provided that all these technical improvements will occur stress RT3DE may become an important diagnostic test of the future.

References

1. Geleijnse ML, Fioretti PM, Roelandt JR. Methodology, feasibility, safety and diagnostic accuracy of dobutamine stress echocardiography. J Am Coll Cardiol 1997;30(3):595-606.

2. Armstrong WF, Zoghbi WA. Stress echocardiography: current methodology and clinical applications. J Am Coll Cardiol 2005;45(11):1739-47.

3. Smart SC, Bhatia A, Hellman R, Stoiber T, Krasnow A, Collier BD, et al. Dobutamine-atropine stress echocardiography and dipyridamole sestamibi scintigraphy for the detection of coronary artery disease: limitations and concordance. J Am Coll Cardiol 2000;36(4):1265-73.

4. Cerqueira MD, Weissman NJ, Dilsizian V, Jacobs AK, Kaul S, Laskey WK, et al. Standardized myocardial segmentation and nomenclature for tomographic imaging of the heart: a statement for healthcare professionals from the Cardiac Imaging Committee of the Council on Clinical Cardiology of the American Heart Association. Circulation 2002;105(4):539-42.

5. van den Bosch AE, Robbers-Visser D, Krenning BJ, McGhie JS, Helbing WA, Meijboom FJ, et al. Comparison of real-time three-dimensional echocardiography to magnetic resonance imaging for assessment of left ventricular mass. Am J Cardiol 2006;97(1):113-7.

6. van den Bosch AE, Robbers-Visser D, Krenning BJ, Voormolen MM, McGhie JS, Helbing WA, et al. Real-time transthoracic three-dimensional echocardiographic assessment of left ventricular volume and ejection fraction in congenital heart disease. J Am Soc Echocardiogr 2006;19(1):1-6.

7. Bu L, Munns S, Zhang H, Disterhoft M, Dixon M, Stolpen A, et al. Rapid full volume data acquisition by real-time 3-dimensional echocardiography for assessment of left ventricular indexes in children: a validation study compared with magnetic resonance imaging. J Am Soc Echocardiogr 2005;18(4):299-305.

8. Hecht HS, DeBord L, Sotomayor N, Shaw R, Dunlap R, Ryan C. Supine bicycle stress echocardiography: peak exercise imaging is superior to postexercise imaging. J Am Soc Echocardiogr 1993;6(3 Pt 1):265-71.

9. Matsumura Y, Hozumi T, Arai K, Sugioka K, Ujino K, Takemoto Y, et al. Non-invasive assessment of myocardial ischaemia using new real-time three-dimensional dobutamine stress echocardiography: comparison with conventional two-dimensional methods. Eur Heart J 2005;26(16):1625-32.

10. Aggeli C, Giannopoulos G, Misovoulos P, Roussakis G, Christoforatou E, Kokkinakis C, et al. Real-time three-dimensional dobutamine stress echocardiography for coronary artery disease diagnosis - validation with coronary angiography. Heart 2006.

11. Olson CE, Porter TR, Deligonul U, Xie F, Anderson JR. Left ventricular volume changes during dobutamine stress echocardiography identify patients with more extensive coronary artery disease. J Am Coll Cardiol 1994;24(5):1268-73.

12. Arai K, Hozumi T, Matsumura Y, Sugioka K, Takemoto Y, Yamagishi H, et al. Accuracy of measurement of left ventricular volume and ejection fraction by new real-time three-dimensional echocardiography in patients with wall motion abnormalities secondary to myocardial infarction. Am J Cardiol 2004;94(5):552-8.

13. Hergum T, Bjastad T, Torp H. Parallel beamforming using Synthetic Transit Beams. In: proceedings IEEE Ultrasonics symposium; 2004; 2004. p. 1401-1404.

14. Nemes A, Geleijnse ML, Krenning BJ, Soliman OII, Anwar AM, Vletter WB, et al. Usefulness of Ultrasound Contrast Agen to Improve Image Quality During Real-Time Three-Dimensional Stress Echocardiography. Am J Cardiol 2006:(in press).

15. Takeuchi M, Otani S, Weinert L, Spencer KT, Lang RM. Comparison of contrast-enhanced real-time live 3-dimensional dobutamine stress echocardiography with contrast 2-dimensional echocardiography for detecting stress-induced wall-motion abnormalities. J Am Soc Echocardiogr 2006;19(3):294-9.

16. Geleijnse ML, Nemes A, Vletter WB. Contrast-enhanced Real-time 3-Dimensional Dobutamine Stress Echocardiography. J Am Soc Echocardiogr 2006;19(8):1076.

17. Zwas DR, Takuma S, Mullis-Jansson S, Fard A, Chaudhry H, Wu H, et al. Feasibility of real-time 3-dimensional treadmill stress echocardiography. J Am Soc Echocardiogr 1999;12(5):285-9.

18. Nemes A, Geleijnse ML, Krenning BJ, Soliman OI, Anwar AM, Vletter WB, et al. Usefulness of ultrasound contrast agent to improve image quality during real-time three-dimensional stress echocardiography. Am J Cardiol 2007;99(2):275-8.

19. Dolan MS, Riad K, El-Shafei A, Puri S, Tamirisa K, Bierig M, et al. Effect of intravenous contrast for left ventricular opacification and border definition on sensitivity and specificity of dobutamine stress echocardiography compared with coronary angiography in technically difficult patients. Am Heart J 2001;142(5):908-15.

20. Pulerwitz T, Hirata K, Abe Y, Otsuka R, Herz S, Okajima K, et al. Feasibility of Using a Real-time 3-Dimensional Technique for Contrast Dobutamine Stress Echocardiography. J Am Soc Echocardiogr 2006;19(5):540-5.

21. Voormolen MM, Bouakaz A, Krenning BJ, Lancee CT, ten Cate FJ, de Jong N. Feasibility of 3D harmonic contrast imaging. Ultrasonics 2004;42(1-9):739-43.

22. Jenkins C, Bricknell K, Hanekom L, Marwick TH. Reproducibility and accuracy of echocardiographic measurements of left ventricular parameters using real-time three-dimensional echocardiography. J Am Coll Cardiol 2004;44(4):878-86.

23. Ahmad M, Xie T, McCulloch M, Abreo G, Runge M. Real-time three-dimensional dobutamine stress echocardiography in assessment stress echocardiography in assessment of ischemia: comparison with two-dimensional dobutamine stress echocardiography. J Am Coll Cardiol 2001;37(5):1303-9.

24. Ahmad M, Xie T, McCulloch M, Abreo G, Runge M. Real-time three-dimensional dobutamine stress echocardiography in assessment stress echocardiography in assessment of ischemia: comparison with two-dimensional dobutamine stress echocardiography. J Am Coll Cardiol 2001;37(5):1303-9.

25. Nemes A, Geleijnse ML, Vletter WB, Krenning BJ, Soliman OI, ten Cate FJ. Role of parasternal data acquisition during contrast enhanced real-time three-dimensional echocardiography. Echocardiography 2007 (in press).

26. Yang HS, Pellikka PA, McCully RB, Oh JK, Kukuzke JA, Khandheria BK, et al. Role of biplane and biplane echocardiographically guided 3-dimensional echocardiography during dobutamine stress echocardiography. J Am Soc Echocardiogr 2006;19(9):1136-43.

Chapter 12

Real-time three-dimensional contrast stress echocardiography: a bridge too far?

BJ Krenning
WB Vletter
A Nemes
ML Geleijnse
JRTC Roelandt

Two-dimensional stress echocardiography is a non-invasive diagnostic and prognostic imaging modality with a wide spectrum of indications [1, 2]. Although its clinical value is well established, it is recognized that stress echocardiography has a number of limitations. The method is highly operator dependent, as it requires multiple, successive acquisitions. These successive acquisitions at rest, low-dose, and peak stress may contain non-identical left ventricular (LV) wall segments that may limit optimal comparison of wall motion and diagnostic accuracy. In addition, the limited number of cross-sections available for interpretation may limit the identification of smaller ischemic areas. Real-time three-dimensional echocardiography (RT3DE) has the potential to eliminate these limitations (Table 1). Some critical considerations, however, are appropriate. Good image quality is a prerequisite for stress echocardiography but the spatial resolution of RT3DE is still limited. This is likely to improve with the evolution of transducer and processing technology. RT3DE systems have a number of options for optimization of spatial resolution. Depending on the size of the LV, the sector angle can be narrowed resulting in a higher line density and better image resolution. The Extreme Resolution setting (Xres) is an image-processing technique for improved visualization of tissue patterns, but has a negative effect on the frame-rate and should therefore not be used for LV function analysis.

A high temporal resolution is as important as spatial resolution for the diagnostic accuracy of stress RT3DE. In two-dimensional stress echocardiography lower frame rates negatively influence the identification of significant coronary artery dis-

Table 1. Benefits of real-time three-dimensional echocardiography

Rapid image acquisition
Less operator dependent
Reproducible views for analysis
Unlimited number of cross-sections
Absent left ventricular foreshortening

Table 2. Philips iE33 ultrasound system settings for real-time three-dimensional echocardiography at a depth of 13 cm influencing frame rate.

Contrast enhancement	Number of transmitted pulses	Second harmonics	Power modulation	Number of subvolumes for full volume reconstruction	Frame-rate	Number of volumes per cardiac cycle at peak stress[#]
	1	X		4	20 Hz	10
	1	X		7	35 Hz	18
X	1	X		7	30 Hz	15
X	2	X	X	7	14 Hz	7
X	3		X	7	9 Hz	5

Peak stress defined as 120 beats per minute

ease[3]. The number of available frames per heart cycle depends both on the frame-rate and heart rate of the patient. When the heart rate of the patient increases, fewer volumes per heart cycle are available for analysis. The frame-rate is further affected by several machine settings (Table 2). The scanning depth should always be minimized to a depth that just includes the entire LV. Also, the frame-rate is affected by the number of heart cycles used for full LV volume reconstruction. For analysis, a full LV volume is acquired by automated fusion of multiple subvolumes during several consecutive electrocardiographically triggered heart cycles. On the latest ultrasound systems, it is possible to choose 4 or 7 heart cycles for LV volume reconstruction. The latter has the advantage of a higher temporal resolution, but with a greater chance of artifacts due to motion, respiration and beat-to-beat variability.

Contrast enhancement is recommended to improve endocardial border visualization in stress RT3DE [4, 5]. Specific imaging functions are used to improve the detection of ultrasound contrast agents, such as pulse inversion (with 2D) and power modulation (with RT3DE), which are integrated in preset functions. In pulse inversion imaging, the frame-rate is lowered because a sequence of two ultrasound pulses must be transmitted instead of only a single pulse. In power modulation, a multi-pulse technique is used whereby the acoustic amplitude of the transmitted pulses is changed. Although these methods improve contrast-imaging quality, both functions nearly halve the frame rate. It appears that when a heart rate of 120 beats per minute is reached during the stress test, the number of volumes per heart cycle may be too low for diagnostic testing (Table 2). Therefore, only second harmonic imaging should be used during contrast-enhanced stress RT3DE.

In conclusion, several settings are available on current high-end ultrasound systems that have an important influence on spatial and temporal resolution, and subsequently on diagnostic accuracy of stress RT3DE. Information on these settings is currently lacking in the published reports on stress RT3DE. Specific contrast imaging methods such as pulse inversion and power modulation seem unsuitable for stress RT3DE because of the major limitation on frame-rate. With current technology, it may therefore be too early to use RT3DE as a reliable diagnostic test as the temporal and spatial resolutions are too low. Future studies will have to show consistency in the currently available data on diagnostic accuracy[6, 7]. However, before any objective comparison can be made, the machine settings should always be available in publications in order to compare data between studies.

References

1. Geleijnse ML, Fioretti PM, Roelandt JR. Methodology, feasibility, safety and diagnostic accuracy of dobutamine stress echocardiography. J Am Coll Cardiol. 1997;30(3):595-606.

2. Armstrong WF, Zoghbi WA. Stress echocardiography: current methodology and clinical applications. J Am Coll Cardiol. 2005;45(11):1739-1747.

3. Bjornstad K, Aakhus S, Torp HG. How does computer-assisted digital wall motion analysis influence observer agreement and diagnostic accuracy during stress echocardiography? Int J Card Imaging. 1997;13(2):105-114.

4. Nemes A, Geleijnse ML, Krenning BJ, Soliman OI, Anwar AM, Vletter WB, et al. Usefulness of ultrasound contrast agent to improve image quality during real-time three-dimensional stress echocardiography. Am J Cardiol. Jan 15 2007;99(2):275-278.

5. Pulerwitz T, Hirata K, Abe Y, Otsuka R, Herz S, Okajima K, et al. Feasibility of using a real-time 3-dimensional technique for contrast dobutamine stress echocardiography. J Am Soc Echocardiogr. 2006;19(5):540-545.

6. Aggeli C, Giannopoulos G, Misovoulos P, Roussakis G, Christoforatou E, Kokkinakis C, et al. Real-time three-dimensional dobutamine stress echocardiography for coronary artery disease diagnosis - validation with coronary angiography. Heart. 2007;93(6):672-5.

7. Ahmad M, Xie T, McCulloch M, Abreo G, Runge M. Real-time three-dimensional dobutamine stress echocardiography in assessment stress echocardiography in assessment of ischemia: comparison with two-dimensional dobutamine stress echocardiography. J Am Coll Cardiol. 2001;37(5):1303-1309.

Chapter 13

Usefulness of ultrasound contrast agent to improve image quality during real-time three-dimensional stress echocardiography

A Nemes
ML Geleijnse
BJ Krenning
OII Soliman
AM Anwar
WB Vletter
FJ ten Cate

Abstract

Dobutamine stress echocardiography is an accepted tool for the diagnosis of coronary artery disease. Some investigators have claimed that three-dimensional imaging improves the diagnostic accuracy of dobutamine stress echocardiography. The purpose of the present investigation was to examine the role of echo contrast in the improvement of segmental quality and inter-observer agreement during stress real-time 3D echocardiography (RT3DE). The study comprised 36 consecutive patients with stable chest pain referred for routine stress testing. The 3D images were acquired with a RT3DE system with X4 matrix array transducer. All available reconstructed 2D segments were graded as optimal, good, moderate and poor. Wall motion was scored as normal, mild hypokinesia, severe hypokinesia, akinesia and dyskinesia. At peak stress, 466 of the 612 segments (76%) could be analysed during conventional RT3DE. With contrast-enhanced RT3DE, the number of available segments increased to 553 (90%). The image quality index during conventional RT3DE was 2.2, while with contrast-enhanced RT3DE 3.1. With conventional RT3DE, the two independent observers agreed on the diagnosis of myocardial ischaemia in 85 of 108 coronary territories (79%, κ = 0.26). With contrast-enhanced RT3DE, it increased to 95 of 108 coronary territories (88%, κ = 0.59). Study agreement on myocardial ischaemia was present in 26 of 36 studies (72%, κ = 0.43) with conventional RT3DE, and in 32 of 36 studies (89%, κ = 0.77) with contrast-enhanced RT3DE. In conclusion, during stress RT3DE contrast-enhanced imaging significantly decreases the number of poorly visualized myocardial segments and improves inter-observer agreement for the diagnosis of myocardial ischemia.

Dobutamine stress echocardiography is an accepted tool for the diagnosis of coronary artery disease [1]. The interpretation of the echocardiographic images, however, is critically dependent on the quality of the recordings and the experience of the observer [2]. Some investigators have claimed that three-dimensional imaging improves the diagnostic accuracy of dobutamine stress echocardiography [3-5]. However, one of the main limitations of three-dimensional imaging is the inherently lower image quality compared to two-dimensional imaging. Left ventricular (LV) opacificating contrast agents have been successfully applied during 2-dimensional dobutamine stress echocardiography to improve endocardial border delineation [6]. The use of intravenous ultrasound contrast improves endocardial border visualization, leading to a more accurate interpretation of wall motion abnormalities [6]. The purpose of the present investigation was to examine the role of echo contrast in the improvement of LV segmental quality and interobserver agreement during stress real-time three-dimensional echocardiography (RT3DE).

Patients and Methods

Patient population

The study comprised 36 consecutive patients in sinus rhythm with chest pain referred for stress testing. Baseline clinical characteristics of the patients are presented in Table 1. Beta-blockers were used in 22 patients (61%). The study was approved by the institutional review board and all patients gave informed consent.

Table 1 Clinical and demographic characteristics (n = 36)

Variable	Subjects
Age (years)	57 ± 13
Men	24 (67%)
Diabetes mellitus	9 (25%)
Hypertension *	18 (50%)
Hypercholesterolemia †	14 (39%)
Current smoker	4 (11%)
Prior acute myocardial infarction	10 (28%)
Prior coronary bypass surgery	2 (6%)
Prior coronary angioplasty	7 (19%)

* Defined as systolic blood pressure ≥140 mm Hg and/or diastolic blood pressure ≥90 mm Hg and/or the use of antihypertensive medication.

† Defined as total serum cholesterol ≥230 mg/dl and/or serum triglycerides ≥200 mg/dl or the use of a lipid-lowering agent.

Dobutamine-atropine stress protocol

Dobutamine was administered through a peripheral vein by three-minute stages of 10, 20, 30 and 40 µg/kg/min, respectively. The infusion was stopped when 85% of age-predicted heart rate was reached. Otherwise, dobutamine infusion was continued and supplemented by 0.25 mg doses of atropine (to a maximal dose of 1 mg). The stress test was terminated when severe angina, shortness of breath, symptomatic decrease in systolic blood pressure (>40 mm Hg), arterial hypertension (> 240/120 mm Hg), severe arrhythmias or other serious adverse effects occurred.

The contrast examination

Sonovue (Bracco, Milan, Italy) was used at baseline conditions, low-dose and peak stress. The contrast agent was given as a bolus of 0.5 ml with additional boluses of 0.25 ml when needed. A low mechanical index (0.3) was used. Care was taken to record the images at a phase when contrast flow was relatively stable with absent or minimal swirling of contrast in the apex.

Real-time three-dimensional dobutamine stress echocardiography

The RT3DE images were acquired from an apical window with a Sonos 7500 echo system (Philips Medical Systems, Best, The Netherlands) equipped with a 3D data acquisition software package. X4 matrix array transducer was attached to the echocardiograph. After visualizing the reference images (the apical four-chamber and orthogonal views) a full volume data set of the LV was acquired. With electrocardiographic gating four pyramidal subvolumes of ~20x80° were acquired during the first, third, fifth, and seventh cardiac cycle. These four conical subvolumes were automatically integrated into a pyramidal data set of ~80x80° incorporating full LV volume. Regional LV wall motion was evaluated using cropped planes representative of the 4-chamber, 2-chamber, and 3-chamber view.

Off-line data analysis

The digitally stored RT3DE data set was analysed off-line with assistance of 4D TomTec Echo-View 5.3 software (TomTec Inc., Unterschleissheim, Germany). The RT3DE data set was judged on the basis of the absence of artefacts throughout the cardiac cycle. All at peak stress available reconstructed segments were graded as optimal (excellent quality without possibility to improve - 4), good (good quality without artefacts - 3), moderate (sufficient quality without artefacts or good quality with artefact - 2) or poor (poor or moderate quality with artefacts - 1). An image quality index was calculated for each segment by summation of all scores in that particular segment divided by the number of analysed segments. Wall motion was assessed using the standard 17-segment LV model of the 3 reconstructed apical views by two independent observers who were blinded to the patient's clinical data [7]. Wall motion was scored as normal, mild hypokinesia, severe hypokinesia, akinesia and dyskinesia. A test was considered positive in case of new or worsening wall

motion abnormalities at any stage during stress. Segmental wall motion abnormalities were assigned to coronary artery territories as described before [1].

Statistical analysis

All values were expressed as a mean ± SD. The Student *t* test was used to compare the difference between tests. The kappa (κ) coefficient was calculated to determine interobserver agreement. A kappa value <0.4 was considered poor, 0.4 to 0.7 moderate, and >0.7 good. Data were analyzed using standard statistical software (SPSS, version 12.0, Chicago, Illinois).

Results

Dobutamine stress data

Heart rate increased from 71 ± 13 to 124 ± 23 bpm and systolic blood pressure from 128 ± 21 to 140 ± 29 mm Hg. No significant side effects were encountered during the dobutamine stress contrast study.

Myocardial segmental visibility

At peak stress, 466 of the 612 segments (76%) could be analysed during conventional stress RT3DE. With contrast-enhanced stress RT3DE, the number of available LV segments increased to 553 (90%). Non-visualized LV segment distribution during conventional and contrast-enhanced stress RT3DE is depicted in Figure 1. -studies (agreement 72%, κ = 0.43) with conventional stress RT3DE, and in 32 of 36 studies (agreement 89%, κ = 0.77) with contrast-enhanced stress RT3DE.

Myocardial segment image quality

The image quality index of the 466 analysable segments during conventional stress RT3DE was 2.2. With contrast-enhanced stress RT3DE the image quality index in the 553 analysable segments was 3.1. The quality index distribution of the visualized segments during conventional and contrast-enhanced stress RT3DE is depicted in Figure 2.

Interobserver agreement for ischaemia

As seen in Figure 3, with conventional stress RT3DE the two observers agreed on the diagnosis of myocardial ischaemia in 85 of 108 coronary territories (agreement 79%, κ = 0.26). With contrast-enhanced stress RT3DE, the two observers agreed on the diagnosis of myocardial ischaemia, in 95 of 108 coronary territories (agreement 88%, κ = 0.59). Study agreement on myocardial ischaemia was present in 26 of 36 studies (agreement 72%, κ = 0.43) with conventional stress RT3DE, and in 32 of 36 studies (agreement 89%, κ = 0.77) with contrast-enhanced stress RT3DE.

Not available segments at peak stress (%)
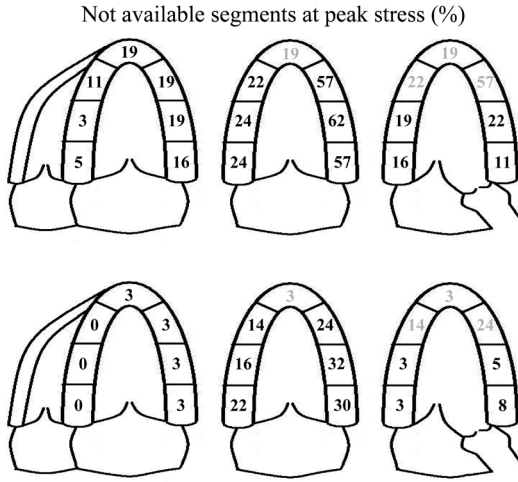
Figure 1:
Left ventricular 17-segments model showing the percentage of non-visualized segments during peak stress with conventional (top) and contrast-enhanced (bottom) three-dimensional echocardiography.

Not available segments at peak stress (%)
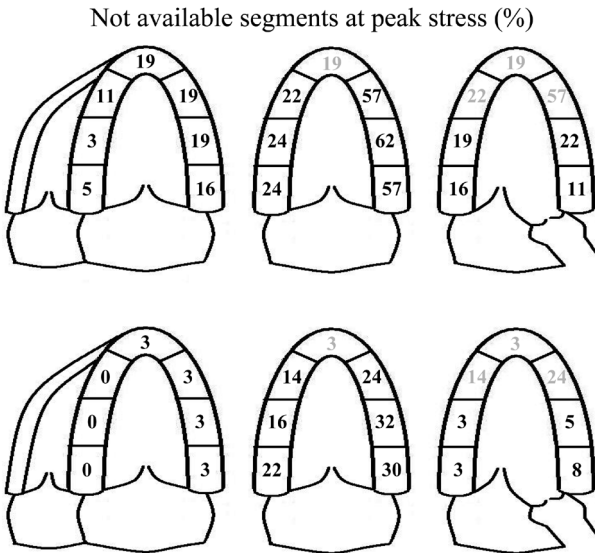
Figure 2:
Left ventricular 17-segments model showing the segmental quality index in the visualized segments during peak stress with conventional (top) and contrast-enhanced (bottom) at peak stress three-dimensional echocardiography.

Discussion

The major findings in this study are: [1] a relatively high number of myocardial segments are poorly visualized with conventional stress RT3DE, [2] contrast-enhanced imaging significantly decreases the number of poorly visualized myocardial segments and [3] contrast-enhanced imaging improves interobserver agreement for diagnosis of myocardial ischemia.

	Conventional			**Contrast**	
	+	-		+	-
All Territories +	7	15	+	13	6
(n = 108) -	8	78	-	7	82
	Kappa 0.26			Kappa 0.59	

	+	-		+	-
Ischemic study +	8	9	+	12	3
(n = 36) -	1	18	-	1	20
	Kappa 0.43			Kappa 0.77	

Figure 3:

Interobserver agreement with conventional (left) and contrast-enhanced (right) three-dimensional stress echocardiography for the diagnosis of myocardial ischemia for all coronary territories (top) and the overall study result (bottom).

Two-dimensional dobutamine stress echocardiography is based on the detection of stress-induced wall motion abnormalities and is an important clinical tool for the detection of coronary artery disease [1]. For the detection of wall motion abnormalities endocardial border visualization is essential. However, an important number of patients have suboptimal echo windows [6]. Second harmonic imaging [8,9] and contrast echocardiography [6,10] are known to enhance LV endocardial visualization during 2-dimensional dobutamine stress echocardiography. Because of the trade off between frame rate, image depth and number of beams, RT3DE image quality is inherently lower compared to two-dimensional imaging. Therefore, contrast imaging may be expected to play a major role in improvement of RT3DE image quality.

Table 2. Segments visible at peak stress with apical real-time three-dimensional stress echocardiography.

Authors	Patients	Stress	RT3DE system	Segments visible with conventional imaging	Segments visible with contrast imaging
Zwas et al. [5]	20	Treadmill	Volumetrics MI	89% - 98%*	NA
Ahmad et al. [4]	253	Dobutamine	Volumetrics MI	92%*	NA
Matsumura et al. [3]	56	Dobutamine	Sonos 7500 / X4 probe	89%	NA
Takeuchi et al. [12]	78	Dobutamine	Sonos 7500 / X4 probe	NA	97%
Pulerwitz et al. [11]	14	Dobutamine	Sonos 7500 / X4 probe	75% - 87%#	97% - 99%#
Present study	36	Dobutamine	Sonos 7500 / X4 probe	76%	90%

* Segment visible when also the parasternal window was used. MI = Medical Imaging. NA = not available. # short axis views were used

In our non-selected patients 24% of LV wall segments could not be visualized at conventional peak stress RT3DE. In particular, anterior wall segments were poorly visualized. Obviously, this is an important limitation for conventional stress RT3DE because this wall is crucial for the diagnosis of left anterior descending disease. Apart from an inherently lower quality of three-dimensional imaging, the large X4 transducer footprint (24x20 mm) may be responsible for this limitation. As seen in Table 2, our results of conventional RT3DE imaging look unfavourable compared to other published studies [3-5,11,12]. It should, however, be noticed that we studied non-selected patients whereas in other studies patients with poor two-dimensional image quality were excluded from analysis [4,11].

Contrast stress RT3DE substantially decreased the number of non-visualized LV segments and the quality of the visible LV segments was markedly higher. These results confirm the value of contrast use for stress RT3DE recently published by Pulerwitz *et al.* in a very small group of 14 patients [11]. Importantly, our study is the first in which it is shown that the improved visibility of segments at peak RT3DE stress improves interobserver agreement for the diagnosis of myocardial ischemia in coronary territories with κ-values that improved from poor to moderate and for the overall diagnosis of myocardial ischemia with κ-values that improved from moderate to good. Notwithstanding our promising results on contrast stress RT3DE new, better transducer technology seems necessary to bring stress RT3DE into clinical practice.

References

1. Geleijnse ML, Fioretti PM, Roelandt JR. Methodology, feasibility, safety and diagnostic accuracy of dobutamine stress echocardiography. *J Am Coll Cardiol* 1997;30:595-606.

2. Picano E, Lattanzi F, Orlandini A, Marini C, L'Abbate A. Stress echocardiography and the human factor: the importance of being expert. *J Am Coll Cardiol* 1991;17:666-669.

3. Matsumura Y, Hozumi T, Arai K, Sugioka K, Ujino K, Takemoto Y, Yamagishi H, Yoshiyama M, Yoshikawa J. Non-invasive assessment of myocardial ischaemia using new real-time three-dimensional dobutamine stress echocardiography: comparison with conventional two-dimensional methods. *Eur Heart J* 2005;26:1625-1632.

4. Ahmad M, Xie T, McCulloch M, Abreo G, Runge M. Real-time three-dimensional dobutamine stress echocardiography in assessment stress echocardiography in assessment of ischemia: comparison with two-dimensional dobutamine stress echocardiography. *J Am Coll Cardiol* 2001;37:1303-1309.

5. Zwas DR, Takuma S, Mullis-Jansson S, Fard A, Chaudhry H, Wu H, Di Tullio MR, Homma S. Feasibility of real-time 3-dimensional treadmill stress echocardiography. *J Am Soc Echocardiogr* 1999;12:285-289.

6. Dolan MS, Riad K, El-Shafei A, Puri S, Tamirisa K, Bierig M, St Vrain J, McKinney L, Havens E, Habermehl K, Pyatt L, Kern M, Labovitz AJ. Effect of intravenous contrast for left ventricular opacification and border definition on sensitivity and specificity of dobutamine stress echocardiography compared with coronary angiography in technically difficult patients. *Am Heart J* 2001;142:908-915.

7. Cerqueira MD, Weissman NJ, Dilsizian V, Jacobs AK, Kaul S, Laskey WK, Pennell DJ, Rumberger JA, Ryan T, Verani MS. Standardized myocardial segmentation and nomenclature for tomographic imaging of the heart: a statement for healthcare professionals from the Cardiac Imaging Committee of the Council on Clinical Cardiology of the American Heart Association. *Circulation* 2002;105:539-542.

8. Senior R, Soman P, Khattar RS, Lahiri A. Improved endocardial visualization with second harmonic imaging compared with fundamental two-dimensional echocardiographic imaging. *Am Heart J* 1999;138:163-168.

9. Sozzi FB, Poldermans D, Bax JJ, Boersma E, Vletter WB, Elhendy A, Borghetti A, Roelandt JR. Second harmonic imaging improves sensitivity of dobutamine stress echocardiography for the diagnosis of coronary artery disease. *Am Heart J* 2001;142:153-159.

10. Falcone RA, Marcovitz PA, Perez JE, Dittrich HC, Hopkins WE, Armstrong WF. Intravenous albunex during dobutamine stress echocardiography: enhanced localization of left ventricular endocardial borders. *Am Heart J* 1995;130:254-258.

11. Pulerwitz T, Hirata K, Abe Y, Otsuka R, Herz S, Okajima K, Jin Z, Di Tullio MR, Homma S. Feasibility of Using a Real-time 3-Dimensional Technique for Contrast Dobutamine Stress Echocardiography. *J Am Soc Echocardiogr* 2006;19:540-545.

12. Takeuchi M, Otani S, Weinert L, Spencer KT, Lang RM. Comparison of contrast-enhanced real-time live 3-dimensional dobutamine stress echocardiography with contrast 2-dimensional echocardiography for detecting stress-induced wall-motion abnormalities. *J Am Soc Echocardiogr* 2006;19:294-299.

Chapter 14

Contrast enhanced three-dimensional dobutamine stress echocardiography: between Scylla and Charybdis?

BJ Krenning
A Nemes
OII Soliman
WB Vletter
JG Bosch
FJ ten Cate
JRTC Roelandt
ML Geleijnse

Abstract

Real-time three-dimensional echocardiography (RT3DE) allows quick volumetric scanning of the left ventricle (LV). We evaluated the diagnostic accuracy of contrast-enhanced stress RT3DE for the detection of CAD in comparison with coronary arteriography as the reference technique. Forty-five consecutive patients (age 59 ± 10, 31 males) referred for coronary angiography were examined by contrast-enhanced RT3DE. Wall motion analysis was performed off-line by dedicated software. New or worsening wall motion abnormalities were detected in 17 of 28 patients with significant CAD (sensitivity 61%), and in 2 of 17 patients without significant CAD (specificity 88%). The sensitivity for detection of single vessel CAD was 8/15 patients (53%), for two-vessel CAD 4/6 (67%) and for three-vessel CAD 5/7 (71%). In 35 patients, comparison with conventional RT3DE was available. The image quality index at rest improved from 2.5 ± 1.2 to 3.2 ± 1.0 (P<0.001) with contrast and at peak stress from 2.3 ± 1.2 to 3.1 ± 1.0 (P<0.001). Interobserver agreement on the diagnosis of myocardial ischemia improved from 26 of 35 studies (74%, κ = 0.44) with conventional stress RT3DE to 30 of 35 studies (86%, κ = 0.69) with contrast-enhanced stress RT3DE. Sensitivity increased from 50% to 55% and specificity from 69% to 85% with contrast-enhanced stress RT3DE in these patients. In conclusion, despite some important practical and theoretical benefits, contrast-enhanced stress RT3DE currently has only moderate diagnostic sensitivity due to several technical limitations as temporal and spatial resolution.

Introduction

Dobutamine stress echocardiography (DSE) is a well-established method for the diagnosis of coronary artery disease (CAD)[1]. Although standard two-dimensional echocardiography (2DE) has acceptable temporal and spatial resolution for assessment of wall motion abnormalities, the technique is limited by the necessity of sequentially acquiring 2DE images from multiple precordial windows for analysis. This is overcome by real-time three-dimensional echocardiography (RT3DE), by obtaining quick volumetric datasets of the left ventricle (LV)[2]. Previously, we showed that the use of ultrasound contrast agent during stress RT3DE improves LV cavity border delineation and thus decreases interobserver variability for identifying wall motion abnormalities[3]. The aim of this study was to evaluate the diagnostic accuracy of contrast-enhanced stress RT3DE for the detection of CAD in comparison with the results of coronary arteriography as the reference method.

Methods

Study patients

We studied 45 consecutive patients in sinus rhythm with suspected CAD referred for diagnostic coronary arteriography. No selection based on image quality was made. Baseline clinical characteristics of the patients are listed in Table 1. Beta-blockers were used in 27 patients (60%). The institutional review board approved the study and all patients gave informed consent.

Table 2. Myocardial image quality at rest and peak stress with and without contrast enhancement.

	Rest		Peak stress	
	Contrast -	Contrast +	Contrast -	Contrast +
Number of invisible segments	63 (11%)	55 (9%)	123 (21%)	60 (10%)
Overall visibility index	2.5 ± 1.2	3.2 ± 1.0	2.3 ± 1.2	3.1 ± 1.0
Apical segments	2.7 ± 1.2	3.2 ± 0.9	2.5 ± 1.1	3.2 ±0.9
Mid ventricular segments	2.5 ± 1.2	3.2 ± 1.0	2.3 ± 1.2	3.1 ± 1.0
Basal segments	2.3 ± 1.2	3.1 ± 1.0	2.1 ± 1.2	3.0 ± 1.1

Dobutamine–atropine stress protocol

Dobutamine was administered through a peripheral vein in 3-minute stages of 10, 20, 30, and 40 µg/kg/min. The infusion was aborted when 85% of age-predicted heart rate was reached. Otherwise, dobutamine infusion was continued and supplemented by 0.25-mg doses of atropine (to a maximal dose of 1 mg). The infusion was stopped when severe angina, shortness of breath, a symptomatic decrease in systolic blood pressure (>40 mm Hg), arterial hypertension (>240/120 mmHg), severe arrhythmias, or other serious adverse effects occurred [1].

Contrast examination
SonoVue (Bracco Imaging, Milan, Italy) was used at baseline conditions, low dose, and peak stress as a bolus of 0.5 ml with additional boluses of 0.25 ml when needed[4]. A low mechanical index (0.3) was used. Care was taken to record the images at a phase when contrast flow was relatively stable, with absent or minimal swirling of contrast in the apex.

Dobutamine stress RT3DE
The RT3DE images were acquired from an apical window with a Sonos 7500 echocardiographic system (Philips Medical Systems, Best, The Netherlands) with a X4 matrix-array transducer (n = 36) or iE33 system with a X3-1 transducer (n = 9), using second harmonic imaging. After visualizing the reference images (in the apical 4-chamber and orthogonal views), a full-volume data set of the LV was acquired. With electrocardiographic gating, 4 (using the X4-transducer) or 7 pyramidal subvolumes (using the X3-1 transducer) were acquired which were automatically integrated into a pyramidal data set of 80° x 80° incorporing full LV volume.

Off-line data analysis
The RT3DE datasets were analyzed off-line with the assistance of 4D TomTec Echoview 5.3 software (TomTec Inc., Unterschleissheim, Germany). Two-dimensional long-axis and short-axis cross-sections were reconstructed for analysis. These images were judged on the basis of the absence of artifacts throughout the cardiac cycle. All at peak stress available reconstructed segments were graded as optimal (4 = excellent quality without possibility to improve), good (3 = good quality without artifacts), moderate (2 = sufficient quality without artifacts or good quality with artifacts), or poor (1 = poor or moderate quality with artifacts). An image quality index was calculated by the summation of all scores of each analyzed segment divided by the number of analyzed segments. Wall motion was assessed using the standard 17-segment LV model of the 3 reconstructed apical views by 2 independent observers who were blinded to the patients' clinical data[5]. Wall motion was scored as normal, mild hypokinesia, severe hypokinesia, akinesia, or dyskinesia. Test results were considered positive in case of new or worsening wall motion abnormalities at any stage during stress. Segmental wall motion abnormalities were assigned to coronary artery territories as previously described[5]. Because of the known limitations of stress imaging in distinguishing the right coronary artery and the left circumflex artery territory, the data were analyzed according to the anterior and common posterior circulation[1].

Coronary arteriography
Coronary angiography was performed within 2 weeks in all patients. Significant coronary artery disease was defined as a diameter stenosis ≥ 50% in a major epicardial artery including major side branches at quantitative angiography.

Statistical analysis

All values are expressed as mean ± SD. Continuous variables were compared by use of the paired Student's t-test. The   coefficient was calculated to determine interobserver agreement. Sensitivity was defined as the number of true positive tests divided by the total number of patients with a positive angiogram. Specificity was defined as the number of true negative tests divided by the total number of patients with a negative angiogram. Data were analyzed using standard statistical software (SPSS version 12.0; SPSS, Inc., Chicago, Illinois).

Results

Coronary angiography
Coronary angiography showed significant CAD in 28 (62%) patients, 15/28 (54%) patients had single vessel CAD, 6/28 (21%) two-vessel CAD and 7/28 (25%) three-vessel CAD. Coronary artery stenoses involved the left anterior descending artery in 17 (38%) patients, the right coronary artery in 17 (38%) patients and the left circumflex artery in 14 (31%) patients. The posterior circulation was involved in 23 (51%) patients.

DSE results
DSE increased heart rate (from 73 ± 14 to 130 ± 21 beats per minute, P <0.001) and systolic blood pressure (from 125 ± 19 to 143 ± 25 mmHg, P <0.001). Atropine was administered in 13 patients (29%) at a mean dose of 0.6 ± 0.2 mg. Chest pain occurred in 10 patients (22%) and ST-segment depression (>0.1 mV horizontal or down sloping) in 5 (11%) patients. Reasons for termination of the test were target heart rate in 34 (76%), maximal dose of dobutamine-atropine in 4 (9%), angina in 5 (11%), and ST-segment changes in 2 (4%). New or worsening wall motion abnormalities during contrast-enhanced RT3DE occurred in 19 (42%) patients.

Diagnostic accuracy of contrast-enhanced RT3DE
New or worsening wall motion abnormalities were detected in 17 of 28 patients with significant CAD (sensitivity 61%), and in 2 of 17 patients without significant CAD (specificity 88%). The sensitivity for detection of single vessel CAD was 8/15 patients (53%), for two-vessel CAD 4/6 (67%) and for three-vessel CAD 5/7 (71%). The sensitivity and specificity for detection of significant CAD in the anterior circulation was 9/17 (53%) and 26/28 (93%), respectively. The sensitivity for detection of significant CAD in the posterior circulation was 10/23 (43%), with a specificity of 19/22 (86%).

Comparison between conventional and contrast-enhanced RT3DE

In 35 (78%) patients, a comparison between acquisition using unenhanced second harmonic imaging and contrast-enhanced RT3DE was available. During conventional RT3DE, 532 segments (89%) could be analyzed at rest and 472 segments (78%) at peak stress. With contrast-enhanced stress RT3DE, the number of available LV segments at peak stress increased to 535 (90%) (P <0.001). The image quality index of the analyzable segments is depicted in Table 2. The global LV myocardial segment visibility index at rest improved from 2.5 ± 1.2 to 3.2 ± 1.0 (P <0.001) with contrast and at peak stress from 2.3 ± 1.2 to 3.1 ± 1.0 (P <0.001). There were no regional differences in improvement with contrast.

As shown in the Figure, the 2 observers agreed on the diagnosis of myocardial ischemia in 26 of 35 studies (74%, κ = 0.44) with conventional stress RT3DE and in 30 of 35 studies (86%, κ = 0.69) with contrast-enhanced stress RT3DE. In these 35 patients, sensitivity increased from 50% to 55% and specificity from 69% to 85% with contrast-enhanced stress RT3DE.

Table 2. Myocardial image quality at rest and peak stress with and without contrast enhancement.

	Rest		Peak stress	
	Contrast -	Contrast +	Contrast -	Contrast +
Number of invisible segments	63 (11%)	55 (9%)	123 (21%)	60 (10%)
Overall visibility index	2.5 ± 1.2	3.2 ± 1.0	2.3 ± 1.2	3.1 ± 1.0
Apical segments	2.7 ± 1.2	3.2 ± 0.9	2.5 ± 1.1	3.2 ±0.9
Mid ventricular segments	2.5 ± 1.2	3.2 ± 1.0	2.3 ± 1.2	3.1 ± 1.0
Basal segments	2.3 ± 1.2	3.1 ± 1.0	2.1 ± 1.2	3.0 ± 1.1

Interobserver agreement with conventional (left) and contrast-enhanced (right) 3-dimensional stress echocardiography for the diagnosis of myocardial ischemia for all territories (top) and the overall study result (bottom).

Discussion

Stress RT3DE has the potential to become the new standard in stress echocardiography, because of the shorter acquisition time, elimination of off-axis acquisition and/or analysis, the ability to obtain multiple cross-sections of any desired LV segment, and more precise comparison of identical segments.

In this study we confirm our previous results on image quality improvement in regional endocardial wall delineation with contrast-enhanced imaging resulting in a better interobserver agreement for the diagnosis of myocardial ischemia[3]. Contrast-enhanced stress RT3DE also increased diagnostic accuracy, although non-significantly due to the relatively small number of patients. The sensitivity of 61% and specificity of 88% for contrast-enhanced stress RT3DE reported in our study is in the range of those reported in 2DE stress studies[1]. However, it should be noted that in two earlier stress RT3DE studies higher sensitivities of 78% to 84% were reported[6, 7].

Several patient and technical characteristics may explain the relatively low diagnostic sensitivity found in our study. Most of our patients with CAD had single-vessel disease and in particular left circumflex stenosis. Patients with such characteristics are very difficult to identify with any stress test[1, 8, 9]. This is in agreement with the low sensitivity (65% and 63%, respectively) for stenosis in the left circumflex territory by Aggeli *et al.*[7] and Matsumura *et al.*[10]. Also, the vast majority of our patients did not have a history of prior myocardial infarction or rest wall motion abnormalities. Such characteristics are also known to negatively affect the diagnostic sensitivity of DSE[11].

Also, several technical issues limit the accuracy of stress RT3DE in its current form compared to 2DE. In earlier studies, others and us have shown that in particular anterior wall segments may be poorly visualized because of ribs interfering with the large foot print of the X4 transducer[3, 12]. Both Aggeli *et al.* and Matsumura *et al.* suggested that stress RT3DE identifies more readily wall motion abnormalities in the apical region compared to 2D imaging due to non-foreshortening acquisition and/or analysis[7, 10]. However, in our study approximately 10% of the distal segments could not be visualized due to the earlier described interfering ribs and prominent near-field artifacts. It should be noted that all patients in the study of Aggeli *et al.* were studied with the smaller X3-1 transducer, whereas in our study only a minority were studied with this newer transducer. Moreover, different methods for data analysis are used. Aggeli *et al.* and Matsumura *et al.* used the integrated software of the ultrasound system to analyze cropped planes from apex to base along the long axis of the LV. We used TomTec off-line analysis software to visualize identical two-dimensional cross-sections of the LV at baseline and peak stress. Both methods take advantage of the full volumetric dataset, but quantify wall-motion abnormalities only in a limited number of cropped planes. Further investigations are necessary to develop a semi-automated approach to endocardial border delineation and

subsequent wall motion analysis. This may result in less observer dependent analysis and more quantitative determination of myocardial ischemia.

Both spatial and temporal resolution are still the Achilles heel of stress RT3DE. The spatial resolution of RT3DE is less compared to 2DE, which can partially be circumvented by contrast enhancement. Additionally, it is known from 2D stress echocardiography that lower frame rates negatively influence the identification of significant CAD[13]. The number of available frames per heart cycle for analysis depends on several machine settings and the heart rate of the patient. When the heart rate of the patient increases, fewer volumes per heart cycle are available for analysis. Specific imaging methods may be used to improve the detection of ultrasound contrast agents, such as power modulation. In this multi-pulse technique, the acoustic amplitude of the transmitted pulses is changed. Although this method improves contrast-imaging quality, unfortunately, this technique significantly decreases frame rate. During a typical full-volume acquisition of the LV with second harmonic imaging, frame-rate decreases from 30 to 9 Hz when power modulation is activated[14]. Therefore, an improvement in image quality is followed by a lower temporal resolution, as in navigating between 'Scylla and Charybdis'.

Conclusions

Despite some important practical and theoretical benefits, contrast-enhanced stress RT3DE currently has only moderate diagnostic sensitivity due to several technical limitations. Further developments in transducer technology (e.g. with single crystal technology[15]) seem necessary to really profit from these benefits and bring (contrast-enhanced) stress RT3DE into clinical practice. Specific imaging functions to improve the detection of ultrasound contrast agents, such as power modulation, should not be used because of the negative effect on frame-rate.

References

1.   Geleijnse ML, Fioretti PM, Roelandt JR. Methodology, feasibility, safety and diagnostic accuracy of dobutamine stress echocardiography. J Am Coll Cardiol 1997;30(3):595-606.
2.   Krenning BJ, Voormolen MM, Roelandt JR. Assessment of left ventricular function by three-dimensional echocardiography. Cardiovasc Ultrasound 2003;1:12.
3.   Nemes A, Geleijnse ML, Krenning BJ, Soliman OI, Anwar AM, Vletter WB, et al. Usefulness of ultrasound contrast agent to improve image quality during real-time three-dimensional stress echocardiography. Am J Cardiol 2007;99(2):275-8.
4.   Bezante GP, Girardi N, Agosti S, Barsotti A. Contrast echocardiography: the role of sulfur hexafluoride in achieving optimal results. Eur J Echocardiogr 2006;7 Suppl 2:S2-7.
5.   Cerqueira MD, Weissman NJ, Dilsizian V, Jacobs AK, Kaul S, Laskey WK, et al. Standardized myocardial segmentation and nomenclature for tomographic imaging of the heart: a statement for healthcare professionals from the Cardiac Imaging Committee of the Council on Clinical Cardiology of the American Heart Association. Circulation 2002;105(4):539-42.
6.   Ahmad M, Xie T, McCulloch M, Abreo G, Runge M. Real-time three-dimensional dobutamine stress echocardiography in assessment stress echocardiography in assessment of ischemia: comparison with two-dimensional dobutamine stress echocardiography. J Am Coll Cardiol 2001;37(5):1303-9.
7.   Aggeli C, Giannopoulos G, Misovoulos P, Roussakis G, Christoforatou E, Kokkinakis C, et al. Real-time three-dimensional dobutamine stress echocardiography for coronary artery disease diagnosis: validation with coronary angiography. Heart 2007;93(6):672-5.
8.   Geleijnse ML, Elhendy A, Fioretti PM, Roelandt JR. Dobutamine stress myocardial perfusion imaging. J Am Coll Cardiol 2000;36(7):2017-27.
9.   van Rugge FP, van der Wall EE, Spanjersberg SJ, de Roos A, Matheijssen NA, Zwinderman AH, et al. Magnetic resonance imaging during dobutamine stress for detection and localization of coronary artery disease. Quantitative wall motion analysis using a modification of the centerline method. Circulation 1994;90(1):127-38.
10. Matsumura Y, Hozumi T, Arai K, Sugioka K, Ujino K, Takemoto Y, et al. Non-invasive assessment of myocardial ischaemia using new real-time three-dimensional dobutamine stress echocardiography: comparison with conventional two-dimensional methods. Eur Heart J 2005;26(16):1625-32.
11. Geleijnse ML, Krenning BJ, Nemes A, Soliman OI, Galema TW, ten Cate FJ. Diagnostic value of dobutamine stress echocardiography in patients with normal wall motion at rest. Echocardiography 2007;24(5):553-7.
12. Pulerwitz T, Hirata K, Abe Y, Otsuka R, Herz S, Okajima K, et al. Feasibility of using a real-time 3-dimensional technique for contrast dobutamine stress echocardiography. J Am Soc Echocardiogr 2006;19(5):540-5.
13. Bjornstad K, Aakhus S, Torp HG. How does computer-assisted digital wall motion analysis influence observer agreement and diagnostic accuracy during stress echocardiography? Int J Card Imaging 1997;13(2):105-14.
14. Krenning BJ, Vletter WB, Nemes A, Geleijnse ML, Roelandt JR. Real-time 3-Dimensional Contrast Stress Echocardiography: A Bridge Too Far? J Am Soc Echocardiogr 2007.
15. Marin-Franch P, Cochran S, Kirk K. Progress towards ultrasound applications of new single crystal materials. Journal of Material Science 2004;15:715-720.

Chapter 15

Summary and Conclusion

We evaluated the use of three-dimensional echocardiography for quantification of left ventricular function. For this purpose, we used different acquisition systems for three-dimensional echocardiography in several different patient populations.

In the introduction to this thesis, the methodology and the outline of the thesis are brought to attention.

Chapter 2 provides the technical background of the fast rotating ultrasound transducer. This transducer has several advantages, such as the capability of using standard high-resolution two-dimensional ultrasound techniques, such as second harmonic imaging. Also, a high frame rate at a wide sector angle of 90° can be chosen, which is necessary to capture the full left ventricle in most patients. The validation study (Chapter 3) shows a high diagnostic accuracy for measurement of left ventricular function using the fast rotating ultrasound transducer when using magnetic resonance imaging as the reference method.

The acute effects of volume changes due to hemodialysis on cardiac function remain poorly understood due to conflicting results in earlier studies. These studies, mainly using M-mode echocardiography and two-dimensional echocardiography, may be hampered by low accuracy of measurements. Previous studies showed that smaller changes in volume are more accurately detected by three-dimensional echocardiography, and therefore may improve the assessment of the acute effect of hemodialysis on left ventricular performance. In chapter four, we show that three-dimensional echocardiography using the fast-rotating ultrasound transducer is feasible for image acquisition in patients undergoing hemodialysis. Successful image acquisition was achieved in 10/12 patients (83%). We found a significant difference between measurements using two- and three-dimensional echocardiography. However, no significant difference in volumes was observed at different time intervals during hemodialysis, probably due to the small number of patients included in our study. The correlation between measurements of volume and ejection fraction using two- and three-dimensional echocardiography were moderate, but the limits of agreement between these methods was poor (for volume measurements larger than 30 ml). This study shows that the fast-rotating ultrasound transducer is applicable in a complex patient population for accurate and reproducible measurement of left ventricular function.

We used three-dimensional echocardiography using the fast rotating ultrasound transducer for diagnosis of left ventricular dyssynchrony in patients with severe heart failure. Currently, patients are selected for biventricular pacemaker implantation based on standard electrocardiographic and echocardiographic criteria, but additional selection criteria are needed because 20 to 30% of patients do not respond. Tissue Doppler imaging is mostly used for demonstration of left ventricular dyssynchrony and other echocardiographic methods are also explored. We demonstrated that dyssynchronic segments can be identified and biventricular pacing resulted in reduction of dyssynchrony in seven of eight patients using the fast rotating

ultrasound transducer. Thus, this technique could be used as a new approach for diagnosis and guidance of pacemaker implantation for achieving optimal results.

In *part 2*, an overview of studies using three-dimensional echocardiography for assessment of left ventricular function in comparison with magnetic resonance imaging is given. We evaluated two different semi-automated border detection algorithms for assessment of left ventricular function using a novel real-time three-dimensional echocardiographic instrument. The older method is limited by endocardial contour detection and revision in a limited number of cross-sections and subsequent interpolation for left ventricular cavity reconstruction and analysis. The most recently developed algorithm, however, takes advantage of the full three-dimensional dataset for left ventricular volume calculation. The main finding of this comparative study is that the new method more accurately estimates left ventricular volumes. Bland-Altman analysis showed greater underestimation of end-diastolic volume and end-systolic volume by the interpolation algorithm. Larger biases for end-diastolic (-24.0 vs. -9.9 ml, respectively) and end-systolic volumes (-11.3 vs. -5.0 ml, respectively) were found. It is suggested that a higher accuracy is achieved by automated contour detection in the complete three-dimensional dataset, using significantly more data for reconstruction of the endocardial contour and avoiding errors due to interpolation. Besides less user interaction, this new method is faster (6 ± 2 vs. 15 ± 4 min, P <0.01) and has better review options.

The study presented in chapter 8 shows that the use of contrast enhancement during real-time three-dimensional echocardiography results in more accurate assessment of left ventricular function, evidenced by a better correlation and smaller limits of agreement compared to magnetic resonance imaging, and lower intra- and interobserver variability. Interestingly, patients with poor-to-moderate image quality showed an improvement in agreement in left ventricular ejection fraction measurement after contrast (± 24.4% to ± 12.7%) to the same level as patient with moderate-to-good image quality without contrast (± 10.4%).

In the reviews presented in chapters 9 and 10, the factors affecting sensitivity and specificity of dobutamine stress echocardiography are described. The analysis shows that methodologic problems may explain the wide range in diagnostic variability of dobutamine stress echocardiography. An improvement of clinical relevance of dobutamine stress echocardiography testing is possible by stronger adherence to common and new methodologic standards. Also, the reported sensitivity of dobutamine stress echocardiography is higher and the specificity lower than that expected in clinical practice because of the inappropriate inclusion of patients with prior myocardial infarction, definition of positive dobutamine stress echocardiography and the presence of referral bias. Chapter 11 provides an overview of the current status of real-time three-dimensional stress echocardiography, describing its advantages over two-dimensional dobutamine stress echocardiography, such as a faster and easier image acquisition, and reconstruction of matching views from baseline and different stress levels for a precise comparison of identical segments.

However, this imaging method is still hampered by several technical limitations, such as multibeat frame composition and limited spatial and temporal resolution. Also, several settings are available on current ultrasound systems that have an important influence on the spatial and temporal resolution, and subsequently on diagnostic accuracy of real-time three-dimensional stress echocardiography. The latter is described in further detail in chapter 12. It is expected that most of these limitations will be overcome in the near future by new ultrasound transducer technology and faster processors.

Our results in chapter 13 indicate that an important number of left ventricular segments are insufficiently visualized during unenhanced real-time three-dimensional stress echocardiography. Contrast-enhancement significantly decreases the number of non-interpretable segments and improves interobserver agreement for the diagnosis of myocardial ischemia. Finally, we performed a diagnostic study comparing contrast-enhanced real-time three-dimensional stress echocardiography with coronary arteriography as the reference standard. We found a sensitivity of 61% for detection of coronary artery disease, and a specificity of 88%. In a subgroup of 35 patients, an acquisition using second harmonic imaging and contrast-enhanced real-time three-dimensional echocardiography was available for comparison. Sensitivity increased from 50% to 55% and specificity from 69% to 85% with contrast-enhanced real-time three-dimensional stress echocardiography. Thus, despite some important practical and theoretical benefits, contrast-enhanced real-time three-dimensional stress echocardiography currently has only moderate diagnostic sensitivity due to above-mentioned technical limitations.

In conclusion, the fast-rotating ultrasound transducer combines ultrasound imaging properties of a standard phased array transducer with a fast acquisition time and is easily integrated into existing ultrasound systems. Together with appropriate analytic reconstruction software, it forms an accurate and reproducible method for assessment of left ventricular function. For several daily clinical referral questions, such as patient follow-up and guidance of resynchronization therapy, this method can be used without the need for an expensive high-end ultrasound system or magnetic resonance imaging. Despite above-mentioned advantages and favorable results, the fast-rotating ultrasound transducer has not been taken into commercial production so far. Several ultrasound companies offer products for three-dimensional echocardiography, but most of the current research and development focus on (expensive) matrix transducer technology. Despite its cost effectiveness, practical disadvantages such as maintenance issues and possible defects from moving mechanical parts, may be an important drawback for the production of a mechanical transducer.

   In general, newer algorithms for automated border detection will decrease analysis time with a higher diagnostic accuracy. In patients with suboptimal image qual-

ity, the use of ultrasound contrast-enhancement is necessary for accurate assessment of left ventricular volume and function.

Real-time three-dimensional stress echocardiography has several theoretical advantages, such as less operator dependency. However, we found a lower diagnostic accuracy compared to two-dimensional echocardiography caused by a lower spatial and temporal resolution. Contrast enhanced real-time three-dimensional stress echocardiography has shown to improve image quality, but several technical limitations remain. Future improvements in transducer technology will likely solve these issues and improve its diagnostic accuracy, and make it a practical test to detect ischemia .

Samenvatting en conclusie

Dit proefschrift richt zich op de toepassing van driedimensionale echocardiografie voor het kwantificeren van de linker ventrikelfunctie. Hiertoe werden verschillende echo systemen toegepast bij diverse patiënten populaties.

In de introductie wordt de methodologie beschreven en een overzicht van dit proefschrift weergegeven.

In hoofdstuk twee wordt de technische achtergrond van de snel roterende ultrageluidstransducer beschreven. Deze transducer heeft verschillende voordelen, zoals toepassing van de tweedimensionale 'second harmonic imaging' echocardiografie techniek. Voorts wordt gebruik gemaakt van een hoge 'frame rate' en brede sector hoek van 90^0, hetgeen bij de meeste patiënten nodig is om de linker ventrikel volledig te omvatten. De validatie studie (hoofdstuk 3) toont een hoge nauwkeurigheid voor metingen van de linker ventrikelfunctie met de snel roterende ultrageluidstransducer, waarbij MRI werd gebruikt als referentie methode.

De acute effecten van volume veranderingen in het lichaam als gevolg van hemodialyse op de cardiale functie zijn nog steeds niet volledig bekend. Eerdere onderzoeken werden beperkt door een lagere nauwkeurigheid van de metingen door het gebruik van M-mode echocardiografie en tweedimensionale echocardiografie. Studies hebben uitgewezen dat kleine volume veranderingen nauwkeuriger kunnen worden gedetecteerd door driedimensionale echocardiografie. In hoofdstuk vier tonen we aan dat driedimensionale echocardiografie met de snel roterende transducer geschikt is voor beeldvorming bij patiënten gedurende hemodialyse. Bij 10/12 patiënten (83%) konden analyseerbare beelden worden verkregen. Er werd een significant verschil aangetoond tussen metingen met twee- en driedimensionale echocardiografie. Echter, er kon geen significant verschil met echocardiografie worden vastgesteld op verschillende tijdsintervallen gedurende de hemodialyse, waarschijnlijk door de kleine studie populatie. De correlaties van volume en ejectie fractie, gemeten met twee- en driedimensionale echocardiografie, waren matig. Echter, de mate van overeenstemming (methode van Bland-Altman) was slecht. Concluderend toont deze studie toont aan dat de snel roterende ultrageluidstransducer bruikbaar is bij een complexe patiënten populatie voor nauwkeurige en reproduceerbare meting van de linker ventrikelfunctie.

Wij gebruikten driedimensionale echocardiografie met gebruikmaking van de snel roterende ultrageluidstransducer voor de diagnose van linker ventrikel dissynchronie bij patiënten met ernstig hartfalen. Op dit moment worden patiënten geselecteerd voor biventriculaire resynchronisatie therapie op basis van standaard electrocardiografische criteria. Echter, aanvullende criteria zijn nodig om de 20-30% van de patiënten te identificeren die niet op deze therapie reageren. Echocar-

diografische 'tissue Doppler' metingen worden frequent gebruikt voor het aantonen van linker ventrikel dissynchronie, maar ook andere methoden worden momenteel onderzocht. Onze studie met driedimensionale echocardiografie toont aan dat dissynchrone segmenten kunnen worden gedetecteerd en biventriculaire stimulatie resulteerde in reductie van dissynchronie bij zeven van de acht patiënten. De voorspellende waarde van driedimensionale echocardiografie voor resynchronisatie uitkomst is momenteel een belangrijk onderwerp van onderzoek in ons centrum.

Deel twee van het proefschrift toont een overzicht van studies die gebruik maken van driedimensionale echocardiografie voor de bepaling van linker ventrikelfunctie, met MRI als referentiemethode. Wij vergeleken twee verschillende deels automatische contour detectie algoritmen voor de bepaling van linker ventrikel volumes. De oudere methode wordt beperkt door endocardiale contour detectie en revisie in een gelimiteerd aantal doorsneden. Vervolgens vindt interpolatie plaats voor linker ventrikel reconstructie en analyse. Het meest recente algoritme gebruikt de volledige driedimensionale dataset voor linker ventrikel volume calculaties, hetgeen resulteerde in nauwkeurigere resultaten. Bland-Altman analyse toonde een grotere onderschatting van het eind-diastolisch (-24.0 vs -9.9 ml, respectievelijk) en eindsystolisch volume (-11.3 vs. -5.0 ml, respectievelijk) door het interpolatie algoritme. Het is aannemelijk dat een hogere nauwkeurigheid wordt verkregen door automatische contourdetectie in de volledige driedimensionale dataset, doordat aanzienlijk meer data worden gebruikt voor reconstructie van de endocardiale contour en fouten als gevolg van interpolatie worden vermeden. Voorts is deze nieuwe methode sneller (6 ± 2 vs. 15 ± 4 min, P <0.01) en heeft het betere revisie mogelijkheden.

De studie gepresenteerd in hoofdstuk 8 toont aan dat het toepassen van contrast gedurende 'real-time' driedimensionale echocardiografie resulteert in een nauwkeuriger bepaling van linker ventrikel volumes en functie. Interessant is dat bij patiënten met een verminderde beeld kwaliteit, het gebruik van contrast bij driedimensionale echocardiografie resulteert in een verbetering in de overeenstemming van de gemeten linker ventrikel ejectiefracties ten opzichte van MRI (± 24.4% naar ± 12.7%) tot hetzelfde niveau als bij patiënten met redelijk tot goede beeldkwaliteit zonder contrast (± 10.4%).

In de overzichtartikelen gepresenteerd in hoofdstuk 9 en 10 worden de factoren beschreven die de sensitiviteit en specificiteit van dobutamine stress echocardiografie beïnvloeden. Analyse toont aan dat methodologische problemen de grote verschillen in de gepubliceerde diagnostische variabiliteit zouden kunnen verklaren. Een verbetering van klinische relevantie van diagnostische dobutamine stress echocardiografie studies is mogelijk door gebruikmaking van de huidige en nieuwe methodologische standaarden. De gerapporteerde sensitiviteit van dobutamine stress echocardiografie is hoger en de specificiteit lager dan verwacht in de klinische praktijk door de onterechte inclusie van patiënten met een myocard infarct in

de voorgeschiedenis, verschillende definities van een positieve dobutamine stress test en de aanwezigheid van 'referral bias'.

Hoofdstuk 11 toont een overzicht van de huidige status van 'real-time' driedimensionale stress echocardiografie. De voordelen boven tweedimensionale echocardiografie worden belicht, zoals snellere en eenvoudiger acquisitie, en nauwkeuriger vergelijking van identieke segmenten van verschillende stadia gedurende de test. Er zijn echter nog verschillende technische beperkingen, zoals de beperkte ruimtelijke en temporele resolutie. Voorts zijn er diverse instellingen beschikbaar op de huidige echocardiografie systemen die een belangrijke invloed hebben op de resolutie en derhalve ook op de diagnostische nauwkeurigheid van 'real-time' driedimensionale stress echocardiografie. Dit laatste wordt in detail beschreven in hoofdstuk 12. Het is de verwachting dat de meeste technische beperkingen binnen afzienbare tijd door nieuwe transducer technologie en snellere processoren zullen verbeteren.

Onze resultaten in hoofdstuk 13 maken duidelijk dat een belangrijk aantal linker ventrikel segmenten onvoldoende wordt gevisualiseerd gedurende 'real-time' driedimensionale stress echocardiografie. Toepassing van contrast verlaagt het aantal niet-interpreteerbare segmenten significant en verbetert de overeenstemming tussen gebruikers voor de diagnose van myocard ischemie. Ten slotte voerden wij een diagnostische studie uit ter vergelijking van 'real-time' driedimensionale echocardiografie met toepassing van contrast en met coronair angiografie als de referentie methode. Wij vonden een sensitiviteit van 61% en een specificiteit van 88% voor de detectie van coronairlijden. In een subgroep van 35 patiënten beschikten wij over een opname met en zonder toepassing van contrast, waardoor vergelijking mogelijk was. In deze groep nam de sensitiviteit toe van 50 naar 55% en de specificiteit van 69 tot 85% bij gebruik van contrast 'real-time' driedimensionale stress echocardiografie. Dus, ondanks diverse belangrijke praktische en theoretische voordelen, is de huidige diagnostische sensitiviteit van contrast 'real-time' driedimensionale stress echocardiografie beperkt.

Concluderend combineert de snel roterende ultrageluidstransducer eigenschappen van een standaard 'phased array' transducer met een snelle acquisitie tijd en is eenvoudig integreerbaar op bestaande ultrageluid systemen. Indien gebruikt met geschikte analytische reconstructie software vormt dit een nauwkeurige en reproduceerbare methode voor de bepaling van de linker ventrikelfunctie. Voor diverse gebruikelijke klinische verwijzingen, zoals vervolgcontroles en resynchronisatie therapie, kan deze methode worden gebruikt zonder de noodzaak van een duur en geavanceerd echocardiografie systeem of MRI. Ondanks bovenstaande voordelen en gunstige resultaten is de snel roterende ultrageluidstransducer tot op heden niet in commerciële productie genomen. Diverse bedrijven bieden producten voor driedimensionale echocardiografie, maar het meeste onderzoek en ontwikkeling richt zich op (dure) matrix technologie. Ondanks de kosteneffectiviteit, zouden

praktische nadelen zoals onderhoud en mogelijke defecten van bewegende me-
chanische onderdelen een argument kunnen zijn om af te zien van de productie van
een mechanische transducer.

In het algemeen zullen nieuwe algoritmes voor automatische endocardiale con-
tour detectie de analyse tijd verminderen met een hoge nauwkeurigheid. Bij patiën-
ten met suboptimale beeldkwaliteit is het gebruik van echografie contrast noodza-
kelijk voor een nauwkeurige bepaling van linker ventrikelvolume en functie.

'Real-time' driedimensionale stress echocardiografie heeft diverse theoretische
voordelen, zoals minder afhankelijkheid van de echografist. Echter, wij vonden een
lagere diagnostische nauwkeurigheid vergeleken met tweedimensionale echocardi-
ografie door een lagere ruimtelijke en temporele resolutie. Contrast 'real-time' drie-
dimensionale stress echocardiografie verhoogt de beeldkwaliteit, maar technische
beperkingen blijven aanwezig. Het is aannemelijk dat ontwikkelingen op het gebied
van transducer technologie deze problemen zullen oplossen en de diagnostische
waarde verbeteren, zodat het een praktische test vormt om ischemie de detecte-
ren.

Dankwoord

Dit proefschrift is tot stand gekomen met hulp en inspanningen van velen, die ik hiervoor veel dank verschuldigd ben.

Als eerste wil ik mijn dank betuigen aan mijn eerste promotor, Professor Roelandt. Beste Jos, bij mijn sollicitatie voor een opleidingsplaats in de Cardiologie greep je al snel naar je notebook om een presentatie te tonen over driedimensionale echocardiografie en de mogelijkheden hiervan. Ik was erg geïnteresseerd in en onder de indruk van de technische aspecten, waarna een verdere oriëntatie op de 23ste etage (de experimentele echocardiografie) volgde. Jouw enthousiasme voor het vak, alswel de vele verhalen en anecdotes over de 'early years' van de cardiologie en je verre reizen hebben mij altijd geboeid.

Dr. Ir. C.T. Lancee, beste Charles, jij was de eerste die mij op de afdeling experimentele echocardiografie met veel enthousiasme verwelkomde. De roterende ultrageluidstransducer heeft dankzij jou een grote ontwikkeling doorgemaakt in het Thoraxcentrum. Dank voor alle technische know-how en oplossingen.

Mijn tweede promotor, Professor van der Steen, beste Ton, dank voor alle steun in de afgelopen jaren. Onder jouw leiding en met jouw visie blijft de experimentele echocardiografie een afdeling vol innovatieve ontwikkelingen.
Professor de Jong, beste Nico, dank voor alle uitleg over echocardiografie en de hulp om technische details helder op papier te krijgen.
Professor Bom en dr. Kamp, hartelijk dank voor het plaatsnemen in de leescommissie en uw bereidheid om dit proefschrift te beoordelen.
Tevens gaat mijn dank uit naar Professor Simoons voor het creëren van de mogelijkheden om dit proefschrift te kunnen afronden gedurende mijn opleidingstijd.
Professor de Feyter en Professor Jordaens, hartelijk dank voor het zitting willen nemen in de grote commissie.

Beste Marco, van collegae op hetzelfde 3D project tot goede vrienden. Ik benijd je om je relativerende vermogen, niet alleen op onderzoeksgebied. Door jouw inzet is de roterende 3D transducer verder geperfectioneerd en klinisch toepasbaar geworden. Zonder deze ontwikkeling en jouw hulp was dit proefschrift nooit tot stand gekomen. Wij (of alleen ik?) wisten niet hoeveel werk er op technisch gebied verzet moest worden om tot deze ontwikkeling te komen. Met grote interesse zie ik uit naar de verdere ontwikkeling op dit gebied door de huidige 3D-groep met Marijn van Stralen, Gerard van Burken en Esther Leung. Veel dank aan dr. Hans Bosch voor de bereidheid om altijd op zeer korte termijn technische aspecten in manuscripten helder te verwoorden.

Uiteraard dank aan mijn co-promotor, dr. Geleijnse. Beste Marcel, met jouw ondersteuning kon ik dit proefschrift afronden. Het corrigeren van manuscripten op de sportschool, of tijdens een rondje Kralingse Plas moeten we eigenlijk weer gaan oppakken.

Dr. ten Cate, beste Folkert, dank voor de ondersteuning, zowel in praktische zin om alle studies op de afdeling uit te voeren, als wetenschappelijk om dit onderzoek te voltooien.

Ook wil ik dr. Han-Yo Ie bedanken voor zijn hulp bij het uitvoeren van de hemodialyse studie. Beste Han-Yo, zonder jouw input had deze publicatie zeker niet de huidige wetenschappelijke waarde gehad. Ook dank aan dr. Tamas Szili-Torok voor zijn hulp bij het uitvoeren van de studie bij patiënten met resynchronisatie therapie.

Zonder het werk van Attila Nemes en Osama Soliman zou het onderzoek met de real-time driedimensionale echocardiografie niet een vogelvlucht hebben genomen in het Thoraxcentrum. Dear Attila and Osama, although the analysis time decreases with newer 3D reconstruction software, many hours were still necessary to analyze the hundreds of datasets. Your help and advice was most valuable. I enjoyed the three months of cooperation in the first quarter of this year!

Robert-Jan van Geuns, Sharon Kirschbaum en Timo Baks, ik dank jullie voor de vele MRI acquisities bij de studie patiënten.

Wim Vletter, door jouw jarenlange ervaring en deskundigheid op het gebied van echocardiografie konden we gebruik maken van echobeelden van sublieme kwaliteit. Ook voor je hulp om die betere beeldkwaliteit te krijgen wanneer mij dat niet lukte, ben ik je erg dankbaar. Ook dank aan de overige (oud)medewerkers van de echo afdeling, Jacky, Debbie, Marjan, Dieny en Hans. René, bedankt voor de technische ondersteuning bij de diverse artikelen.

Door de grote gastvrijheid van de maatschap (dr. Leenders, dr. Ilmer en dr. Neumann) en het secretariaat cardiologie van het Havenziekenhuis kon ik ook lang na mijn vooropleiding interne geneeskunde op zoek naar patiënten om in een studie te includeren. Veel dank hiervoor!

Tot slot gaat mijn grote dank uit naar mijn ouders voor de ondersteuning, vooral wanneer de weg wat hobbelig werd. Uiteraard ben ik ook veel dank aan mijn aanstaande schoon-ouders verschuldigd, met name voor alle goede zorg voor Mijntje als het thuis te druk werd. Lieve Annemien, jij wist al dat promoveren tijd kost, maar kon dit zelfs combineren met de geboorte van Mijntje. Nu we opnieuw een promotie hebben afgerond rondom de komst van Vittoria, ben ik benieuwd wat onze volgende stap zal zijn.......dank je wel voor alle steun!

Curriculum Vitae

Boudewijn Jurriaan Krenning werd op 21 augustus 1975 geboren in het Dijkzigt Ziekenhuis te Rotterdam. Na het eindexamen te hebben afgelegd in 1993 aan het Rotterdamsch Lyceum, studeerde hij geneeskunde aan de Erasmus Universiteit Rotterdam. Na het doctoraal examen in 1998 deed hij gedurende een jaar onderzoek aan de University of New-Mexico (New Mexico, V.S.), naar de behandeling van neuro-endocriene tumoren met verschillende radioactief gelabelde peptiden. Hierna werden de co-schappen doorlopen, en het arts-examen met lof behaald in 2001. Vervolgens startte hij als onderzoeker op de afdeling experimentele echocardiografie van het Thoraxcentrum (onder leiding van Prof. Dr. Ir. N. Bom, later Prof. Dr. Ir. A.F.W. van der Steen) met het promotie-onderzoek waarvan dit proefschrift het eindresultaat is. In januari 2004 werd aangevangen met de vooropleiding Interne Geneeskunde in het Havenziekenhuis te Rotterdam (opleider dr. P.J. Wismans). In januari 2006 startte hij met de opleiding Cardiologie in het ErasmusMC (opleider: Prof. Dr. M.L. Simoons). Hij en Annemien van den Bosch hebben twee dochters, Mijntje (2005) en Vittoria (2007).